UNIVERSITÉ DE STRASBOURG

ÉCOLE DOCTORALE 182

ICPMS UMR 7504

THÈSE présentée par :

Vincent HARDEL

Soutenue le : **14 novembre 2024**

Pour obtenir le grade de : **Docteur de l'université de Strasbourg**

Discipline/ Spécialité : Physique

CLASSICAL ANALOGS
OF
QUANTUM DYNAMICS

THÈSE dirigée par :

Mr Giovanni MANFREDI	Directeur de Recherches, CNRS

RAPPORTEURS :

Mr David GUERY-ODELIN	Professeur, Université Toulouse III - Paul Sabatier
Mr Thomas DURT	Professeur, Centrale Méditerranée

AUTRES MEMBRES DU JURY :

Mr Cyriaque GENET	Directeur de Recherches, CNRS
Mme Sabine KLAPP	Professeur, Technische Universität Berlin

To my parents, family, and friends.

Acknowledgements

First and foremost, I express my deepest gratitude to my supervisor, Giovanni Manfredi, for his unwavering support and insightful critiques throughout my research journey. His guidance has been invaluable in shaping this work. I am also profoundly grateful to Paul-Antoine Hervieux, whose scientific curiosity sparked enriching discussions that significantly contributed to the development of this manuscript.

I extend my sincere appreciation to my reviewers, Thomas Durt and David Guéry-Odelin, for their dedicated efforts in evaluating my PhD thesis. Their detailed comments have been instrumental in refining my research, and I am truly grateful for their engagement during the defense, which led to a stimulating and constructive discussion. Additionally, I would like to thank Sabine Klapp for her participation in this jury and for making the journey from Berlin to Strasbourg for the occasion. Finally, I am deeply thankful to Cyriaque Genet for graciously assuming the role of jury president.

I would also like to express my gratitude to Rémi Goerlich, with whom I thoroughly enjoyed working on quantum-classical analogies and discussing the experimental aspects of our research.

Completing this work would have been far more challenging without the supportive and welcoming environment of the QDyno group. For that, I am immensely thankful to all its members: Denis, Adrien, and Jean-Gabriel, the pioneers of the team, as well as Benjamin, Sébastien, Yannick, and Pierre, who joined later. This group has been more than just colleagues—we have become friends, and I will cherish the unforgettable memories we have created together over the years. I would also like to extend my thanks to Paul-Louis and Andrea, who joined the team just a few months ago, as well as to Damien and Lorry. And, of course, a special mention to the team's coffee machine, which was undoubtedly a key player in the success of my PhD.

J'aimerais remercier mes amis de Nouvelle-Calédonie, Max, Jason, Bastien, Julien, Pablo et Killian—qui ont traversé la France pour assister à ma présentation. Je suis également reconnaissant envers les amis que j'ai rencontrés à Strasbourg, en particulier Yona et Anaëlle, pour leur soutien et leur amitié.

Enfin, il m'est impossible de ne pas exprimer ma profonde gratitude envers ma famille pour leur soutien indéfectible au cours de ces dernières années, et bien au-delà. Je remercie de tout cœur ma mère et mon père, qui n'ont pas hésité à traverser le monde pour être présents lors de ma soutenance. Je suis également reconnaissant envers ma sœur Émilie et son compagnon Clément qui m'ont donné mes neveux Ky-Mani et Noa, qui m'apportent tant de joie malgré la distance qui nous sépare. Je tiens aussi à exprimer toute ma gratitude à ma grand-mère Huguette, pour l'amour qu'elle m'a donné tout au long de ces années. J'aurais aimé que mon grand-père Jean puisse lire cet ouvrage ; je le remercie de m'avoir permis de devenir la personne que je suis aujourd'hui.

PUBLICATION AND CONFERENCE LIST

LIST OF PUBLICATIONS

Quantum Equilibrium:

- V. Hardel, P.-A. Hervieux and G. Manfredi. Relaxation to quantum equilibrium and the Born rule in Nelson's stochastic dynamics, November 2023

  DOI: `https://doi.org/10.1007/s10701-023-00730-w`

Classical analogues of quantum dynamics:

- V. Hardel, G. Manfredi, P.-A. Hervieux, and R. Goerlich. Shortcuts to adiabaticity in harmonic traps : A quantum-classical analog, May 2024

  DOI: `https://doi-org.scd-rproxy.u-strasbg.fr/10.1103/PhysRevE.110.054138`

POSTER SESSIONS AND CONFERENCES

- **2021**: Summer School, *From the first to the second quantum revolution : Theory and applications* (Peyresq): oral presentation
- **2022**: Conference, (Institut Charles Sadron et Institut de Physique et de Chimie des Matériaux de Strasbourg): oral presentation
- **2023**: Conference, *Centenaire de Louis de Broglie* (Sorbonne, Paris): poster session
- **2024**: Conference, *Out of equilibrium nanothermodynamics with levitated particles* (Saclay): Poster session

CONTENTS

QUOTE

Solving a particular physical problem has many similarities with making a trip. First, we have to decide which route to take. Most of the times getting the one recommended by a prestigious guide is enough. Sometimes other routes are even faster or allow us to see beautiful views of the countryside while driving. Eventually, we can find unexpected roadblocks in the selected route and alternatives are mandatory. A good knowledge of a particular territory implies that we are able to use different routes. When we know many routes (and the connections between them), traveling along this particular region has no mystery to us. In classical mechanics, for example, most of the times the recommended route is taking the Newtonian one. In other occasions, because of the specific characteristics of the trip, it is better to take the Lagrangian, the Hamiltonian or the Hamilton-Jacobi routes. Quantum mechanics is not different. Many times practical problems are solved with the formalisms associated to the so-called standard route, also known as the orthodox or Copenhagen route. The standard route itself has many subroutes. For example, the quantum harmonic oscillator problem is cleanly and easily studied with the raising and lowering operators of the (Heisenberg) matrix formulation, while many other problems are better addressed directly with the (Schrödinger) wave function formalism. Another relevant route is the Feynman path integral formulation which is rarely the easiest way to approach a nonrelativistic quantum problem, but which has innumerable and very successful applications in quantum statistics and quantum field theory. Certainly, having a good knowledge of all possible routes (and their connections) in the quantum territory is very helpful when facing a particular quantum problem. However, there are routes that do not appear usually in the guides. One of these unexplained routes is Bohmian mechanics.

ALBERT BENSENY, in Applied Bohmian mechanics [1].

[1] Benseny, A.; Albareda, G., et al. *The European Physical Journal D* **2014**, *68*, 286.

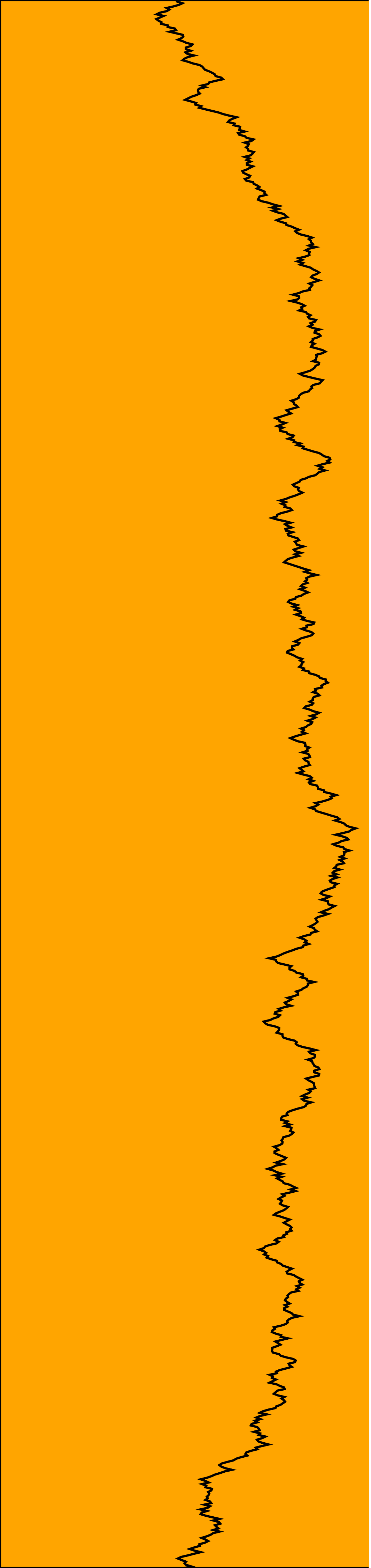

INTRODUCTION

INTRODUCTION

La science remplace du visible compliqué par de l'invisible simple.
— J. Perrin

CONTEXT

The boundary between classical and quantum systems has long been a topic of interest for physicists, offering deep insights into the fundamental nature of physical reality. Classical mechanics, governed by deterministic laws such as Newton's law, has been highly successful in describing macroscopic phenomena, where objects follow predictable, well-defined trajectories.

However, when studying systems involving a large number of particles, such as gases or liquids, the deterministic approach of classical mechanics becomes inadequate due to the sheer number of particles involved, of the order of Avogadro's number.

As a result, scientists developed new approaches to model these types of systems, where the description is no longer based on the motion of a single particle but on the statistical behavior of a large number of particles. This led to the development of statistical mechanics, which incorporates uncertainty into the description of physical systems. The system is then characterized by a probability distribution that provides the chances of finding a particle in a particular state. This probabilistic framework offers a more practical way to describe the behavior of systems with many particles. In theory, with an infinitely powerful computer, it would be possible to track the motion of every particle in the system and to achieve a deterministic description. However, in practice, this is not feasible, making the probabilistic description provided by statistical mechanics the best available approach.

In the early years of university, one important course is statistical mechanics, which is generally taught for systems in equilibrium where the probability distribution is stationary. Later in their studies, students learn that the world is not always in equilibrium and that the probability distribution can change over time. This introduces non-equilibrium statistical mechanics, where the goal is to describe the behavior of systems that are not in equilibrium. It is a very active field of research, aiming to understand how systems evolve over time, how they reach equilibrium, and even how to control this process. This field is usually introduced within the framework of stochastic mechanics, where the system's evolution is described by a stochastic process, incorporating randomness. Consequently, a single trajectory is not sufficient to describe the system; instead, one must consider a distribution of trajectories, which provides the probability of finding the system in a specific state at a given time.

We transition from a purely deterministic description of systems to a probabilistic one. This probabilistic nature arises from our limited knowledge of the state of every particle in the system and our inability to track the motion of each particle.

At the same time, another crucial course is quantum mechanics, the theory describing the behavior of matter at microscopic scales. In this course, students learn that the description of particles departs from the concept of trajectories, as the state of a particle is fully described by an object called the wavefunction. According to the Copenhagen interpretation, the wavefunction is a mathematical tool that provides the ampitude of probability of finding a particle in a particular state (Born's rule). Thus, quantum mechanics is inherently a probabilistic theory, where the outcome of an experiment is not deterministic but probabilistic.

While the same term *probability* is used in both statistical mechanics and quantum mechanics, the interpretation is different. In statistical mechanics, probability arises from our lack of knowledge about the state of the system and is a tool used to simplify modeling. In contrast, in quantum mechanics, probability is intrinsic to the nature of particles. This distinction is fundamental to the two theories. Quantum theory does not provide the origin of this probability; it is assumed to be a fundamental property of particles.

Despite these differences, there are some similarities in the way probabilities are treated in both contexts. In both cases, the probability is the solution of a first-order differential equation, the diffusion equation in statistical mechanics and the Schrödinger equation in quantum mechanics (for a free particle):

$$\frac{\partial P}{\partial t} = D\nabla^2 P \qquad \text{and} \qquad \frac{\partial \psi}{\partial t} = i\frac{\hbar}{2m}\nabla^2\psi.$$

However, a key difference is that in quantum mechanics, the diffusion coefficient[1] is imaginary, while in statistical mechanics, it is real. This difference is fundamental because, in quantum mechanics, the wavefunction represents the probability amplitude, and the actual probability is the square of this wavefunction. This distinction leads to interference effects in quantum mechanics, which are absent in statistical mechanics.

However, there are formulations of quantum mechanics that offer alternative interpretations of probabilities. Notably, Bohmian mechanics, developed by Louis de Broglie and later David Bohm, provides a deterministic description of quantum mechanics, but at the cost of making it non-local in space. This formulation reintroduces the concept of trajectories for quantum particles, guided by the wavefunction. These trajectories obey deterministic equations of motion, with the probability arising from the uncertainty of the initial conditions of the system. The particle trajectories are distributed randomly according to the probability distribution given by the square of the wavefunction. This perspective closely resembles the Newtonian viewpoint, where particles are described by deterministic trajectories.

There is another formulation, similar in concept to Bohmian mechanics but with a different set of axioms, which introduces probability in yet another way. This is the Nelsonian formulation, where particles are still described by trajectories, but these trajectories are stochastic. Here, probabilities emerge not only due to the lack of knowledge of the initial conditions but also from the intrinsic randomness of the trajectories themselves. However, this formulation does not provide an origin for these fluctuations; they are simply assumed to exist. Nelson suggested that, similar to the Langevin description of Brown-

---

[1] In fact, the Laplacian term in the Schrödinger equation is dispersive, as the diffusion coefficient is imaginary. Rather than damping the amplitude of the wavefunction, as a real coefficient would, it instead induces dispersion.

ian motion, the Nelsonian theory could be an effective theory, pointing toward a deeper underlying theory of quantum mechanics.
These approaches are generally not often used in current research, as the standard formulation of quantum mechanics is highly effective and provides an excellent description of physical phenomena. Many authors discuss these alternative formulations from a philosophical perspective, but since they are equivalent to the standard formulation, they are rarely applied in practice. However, although ontological questions may be interesting to explore, we will see throughout this thesis that changing the point of view can lead to powerful tools for describing quantum systems, which might not naturally emerge from the standard formulation. The ability to derive new techniques for controlling quantum systems would add value to these alternative formulations of quantum mechanics and offer practical benefits. Clearly, this does not aim to replace the standard formulation but to complement it and provide new insights into quantum systems.
This thesis will specifically explore such potential advancements by applying one of these alternative frameworks: the Nelson formalism.

Objectives and challenges

The main goal of this thesis is to develop new tools for understanding, controlling, and manipulating quantum systems, both for fundamental research and practical applications. We will explore powerful optimization methods for classical systems and see how they can be adapted for quantum systems using the Nelsonian formalism, which helps establish classical analogues of quantum systems.

The problematics we will address are:

- What is the Nelsonian formulation of quantum mechanics, and how does it differ from the standard approach?
- How can its mathematical similarity to stochastic mechanics help to xestablish a quantum - classical analogy?
- How does this analogy allow us to transfer classical optimization methods to the quantum domain?
- How can we extend these methods to control open quantum systems?

A key challenge in this work is to create a solid mathematical connection between classical and quantum systems, ensuring that methods developed for classical systems can be effectively applied to quantum ones. This requires a strong grasp of both classical and quantum mechanics, as well as the mathematical tools used to describe them.

We will primarily focus on the control of the quantum harmonic oscillator, a simple and fundamental system in quantum mechanics that can be easily manipulated. The optimization methods we develop will be particularly useful for controlling such systems. We aim to design protocols for the harmonic potential parameters that allow us to reach a target state faster than adiabatic processes while minimizing a specific cost, depending on the desired optimization. The effectiveness of our methods will be demonstrated by comparing them to other control techniques across different cost functions, illustrating the versatility and efficiency of our approach. To our knowledge, no other technique has proven optimal for a general cost function.

Controlling the dynamics of quantum systems opens up numerous practical applications. For instance, it can improve the performance of quantum computers, enhance the efficiency of quantum sensors, and aid in the development of new quantum technologies. Such control is essential for the progress of quantum technologies, and the methods introduced in this thesis could serve as valuable tools for achieving this goal.

The final step of this work will be to extend these control methods to open quantum systems, a challenging task due to their complexity compared to closed systems. These methods could lay the groundwork for new ways to control open quantum systems, with implications for a variety of applications, from thermal machines to quantum information processing. As technology advances and devices like nano-process chips and nano-thermal engines become miniaturized, understanding thermodynamic relationships at the microscopic level—such as heat dissipation and work efficiency—becomes crucial due to quantum effects. Quantum heat engines (QHEs), which convert thermal energy into mechanical work using quantum systems like single particles or qubits, play a significant role in quantum thermodynamics and nanotechnology. A key open question is whether quantum effects can enhance QHE performance, and the development of new control protocols for open quantum systems could provide initial insights into this problem.

STRUCTURE OF THE MANUSCRIPT

The manuscript is structured into two main parts. Part. I provides the theoretical foundation by presenting the Langevin and Nelson theories, which are central to understanding the dynamics of classical and quantum particles, respectively. Part. II then applies these theories to study quantum systems in various contexts, covering both foundational questions and practical applications.

Part. I is organized into two chapters. In Chap. 1, we introduce classical Brownian motion, starting with its historical background from Brown to Einstein and Langevin. We then develop the necessary mathematical framework, focusing on the Langevin and Fokker-Planck equations, which describe the stochastic dynamics of particles. A detailed analysis of the overdamped regime of Brownian motion and the role of Wiener processes, which are key in stochastic calculus, sets the stage for exploring quantum analogs in Part. II.
In Chap. 2, we shift our focus to quantum mechanics and introduce Nelson's stochastic formalism, which describes quantum particles through well-defined stochastic trajectories. We derive the formalism used to describe quantum systems within the Nelsonian framework, highlighting the similarities and differences with the standard formulation of quantum mechanics. Examples of quantum systems described by the Nelsonian formalism are then provided, demonstrating its advantages, particularly in describing tunneling phenomena, where it offers an intuitive perspective on the time required for a particle to cross a barrier.

With these theoretical tools in place, Part II, consisting of three chapters, aims to apply Nelson's theory from two perspectives: a fundamental one and a practical one.
Chap. 3 explores one of the foundational assumptions of quantum mechanics: Born's rule. We show that this assumption is not necessary within the Nelsonian formalism, where the probability density is not necessarily tied to the squared modulus of the wavefunction. We then introduce the concept of quantum equilibrium, a state where Born's rule is satisfied, and demonstrate that if a system is initially not in quantum equilibrium, it will

eventually reach it over time. We investigate the convergence of a quantum system to quantum equilibrium and calculate the time required to reach this state for three different quantum systems, comparing it to the characteristic times of each system. The goal is to estimate the order of magnitude of the convergence time to determine whether it might be possible to observe this process experimentally, assuming an initial state that is out of equilibrium.

Following this theoretical discussion, Chap. 4 shifts the focus to practical applications. Highlighting the mathematical similarities between the Nelson equation and the overdamped Langevin equation, we demonstrate that the Nelsonian formalism can be used to develop a new technique for the control of quantum systems, leveraging classical analogues of the quantum system. Specifically, this technique enables the efficient transition of a quantum system from an initial to a final stationary state in less time than required by an adiabatic (quasi-static) process. We apply this method to control the stiffness of a harmonic potential and derive the optimal protocol to reach a target stiffness, minimizing both the duration of the process and an arbitrary cost function, which is kept general in the derivation. We then apply the technique to two different cost functions: the cumulative energy over the protocol and the evolution of the dynamical phase of the wavefunction during the protocol. Finally, we compare our protocols to those derived from other techniques to demonstrate the efficiency of our approach.

Finally, in Chap. 5, we explore the extension of the Nelsonian formalism to open quantum systems. Our goal is to apply the techniques from the previous chapter to control open quantum systems, with the aim of creating optimal cycles for quantum engines. To achieve this, we examine three different effective theories of open quantum systems and derive the corresponding Nelson equations for each. We demonstrate that these approaches are promising and could potentially be used for the control of open quantum systems.

We conclude the thesis by summarizing the main results and discussing potential future research directions in this field.

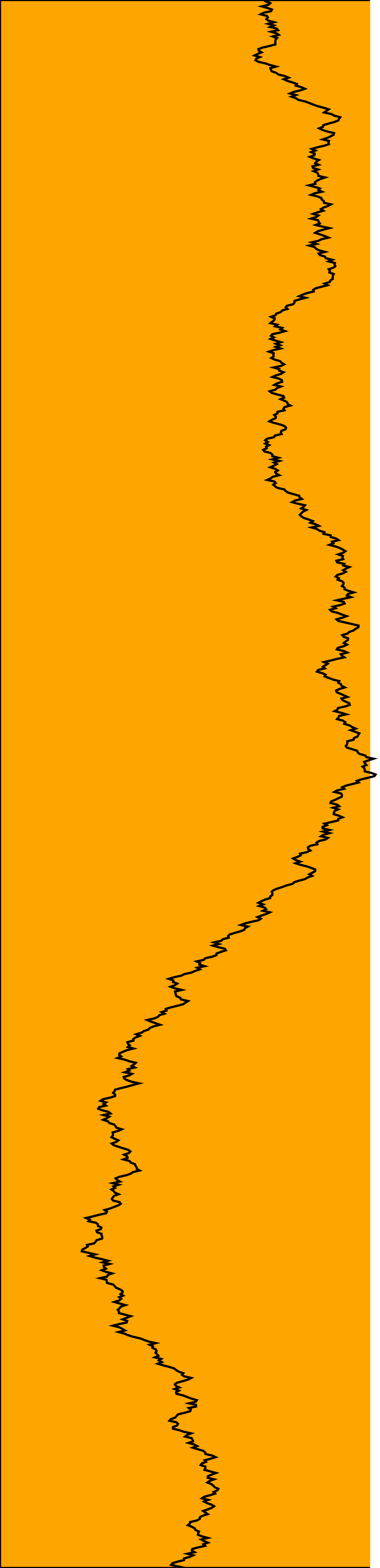

PART I

Theoretical background in stochastic mechanics

PREFACE OF PART I

> *Since traveling was onerous (and expensive), and eating, hunting, and wenching generally did not fill the 17th century gentleman's day, two possibilities remained to occupy the empty hours, praying and gambling; many preferred the latter.*
>
> — E. W. Montroll

Although calculations of probability were undertaken in Roman times, according to Libri [2], it was in Dante's Divine Comedy, written at the beginning of the 14th century, that one of the earliest explicit enumerations of the different probabilities associated with the result of throwing three dice was presented [3]. The theory of probability was born from the need to understand the games of chance and the first book on probability theory was written by Cardano [4] in 1526. It was not until the 17th century that the first mathematical foundations of probability theory were laid in the exchange of letters between Pascal and Fermat [5]. Since then, the theory of probability has been developed and has become a fundamental tool in many fields of science, including physics. In physics, the concept of probability has two distinct origins. Firstly, in statistical mechanics, probabilities are employed due to the lack of complete knowledge about all the degrees of freedom within a system. This approach is necessary because it is practically impossible to track every particle's position and momentum in a macroscopic system. Consequently, statistical mechanics uses probabilities to describe the average behaviour of a large number of particles, providing a statistical understanding of thermodynamic properties such as temperature and pressure. A classic example is that of Boltzmann [6] in the 1870s, who employed the Maxwell-Boltzmann distribution to describe the probability of finding a molecule with a certain speed in a perfect gas. Secondly, probabilities emerge from the intrinsic uncertainty inherent in quantum systems. These are governed by the principles of standard quantum mechanics, where particles exhibit wave-like behaviour and their properties, such as position and momentum, are fundamentally uncertain. This intrinsic uncertainty is quantified by probability distributions derived from the wavefunction, as articulated by the Heisenberg uncertainty principle. These distributions reflect a fundamental aspect of nature. In this part, we will consider both situations. In Chapter 1, we will provide an overview of statistical mechanics, particularly the stochastic mechanics through the Langevin equation and the Fokker-Planck equation. In Chapter 2, we will examine the foundations of quantum mechanics and demonstrate how it is possible to derive the Schrödinger equation from Nelson's mechanics, a stochastic approach to quantum mechanics.

BIBLIOGRAPHY

[2] Libri, G., *Histoire des sciences mathématiques en Italie : depuis la renaissance des lettres jusqu'à la fin du XVIIe siècle*; Renouard: 1838–1841; Vol. 2; 188-189.

[3] Samueli, J.-J., *Une histoire des probabilités: des origines à 1900*; Ellipses: Paris, 2008; 7-8.

[4] Moyer, A. E. *Renaissance Quarterly* **2007**, *60*, 1419–1420.

[5] Smith, D. E. *The American Mathematical Monthly* **1928**, *35*, 280–282.

[6] Ludwig Boltzmann, *Lectures on Gas Theory*; Univ of California Press: 2022; 500 pp.

CHAPTER 1

BROWNIAN MOTION AND LANGEVIN EQUATION

These motions were such as to satisfy me, after frequently repeated observation, that they arose neither from currents in the fluid, nor from its gradual evaporation, but belonged to the particle itself

— R. Brown

In this chapter, we introduce the fundamental concepts of Brownian motion, tracing its historical development and mathematical modeling. We begin in Sec. 1.1 by providing an overview of Brown's observations and the significance of Brownian motion in physics. In Sec. 1.2, we discuss Einstein's theoretical explanation of Brownian motion, deriving the diffusion equation and introducing the Einstein relation that connects the diffusion coefficient to measurable physical quantities. Langevin's dynamical approach is presented in Sec. 1.3, where we formulate the Langevin equation and discuss the coarse-graining technique used to model the random forces acting on a Brownian particle. In Sec. 1.4, we solve the Langevin equation for a free Brownian particle, analyzing the behavior of velocity and position momenta over time. The overdamped limit of the Langevin equation is explored in Sec. 1.5, leading to a simplified description focusing on the particle's position. We then introduce the Fokker-Planck equation in Sec. 1.6, discussing its derivation from the Langevin equation and its role in describing the temporal evolution of the probability density. Finally, in Sec. 1.8, we summarize the key findings of the chapter, emphasizing the equivalence between the Langevin and Fokker-Planck approaches and their importance in the study of stochastic processes and Brownian motion.

Contents

1.1 INTRODUCTION TO THE BROWNIAN MOTION

1.1.1 Historical approach to the Brownian motion

Brownian motion, also known as pedesis, is a fundamental physical phenomenon first observed in 1827 by the botanist Robert Brown [7]. It describes the erratic and random motion of microscopic particles when suspended in a fluid (liquid or gas). These seemingly chaotic motions result from collisions with the much smaller, fast-moving molecules of the fluid, which are themselves in constant thermal motion. Brownian motion represents a fundamental concept within the field of statistical mechanics, and plays a pivotal role in numerous scientific disciplines, including physics, chemistry, biology, and finance. The concept of stochastic modelling, which forms the basis of our understanding of Brownian motion, emerged at the end of the 18th century, primarily in the field of economics. The prediction of financial market risks necessitated a probabilistic description of economic processes and the control of risks and odd outcomes in gambling games, as elucidated in [8]. A notable contribution to this field was made by Louis Bachelier in his 1900 Ph.D. thesis [9], which was completed under the supervision of the renowned mathematician Henri Poincaré. Bachelier's thesis included numerous results pertaining to stochastic processes, notably providing an early solution to the Brownian motion problem, although this was not recognised as such at the time. The theoretical foundation for Brownian motion was subsequently reinforced by Albert Einstein in 1905 [10] and independently by Marian Smoluchowski. They provided the first mathematical models for this physical system, which explained that the random motion of particles like pollen grains in a fluid is due to unpredictable collisions with solvent molecules. Although each collision is individually insignificant, collectively they result in the macroscopic random motion observed. In 1908, Jean Perrin, a French physicist, played a pivotal role in experimentally validating Einstein's theoretical predictions [11]. His meticulous experiments provided empirical evidence for the molecular-kinetic theory of heat, thereby supporting the existence of atoms and molecules. Perrin's work not only validated the existence of Brownian motion but also led to his receipt of the Nobel Prize in Physics in 1926. Paul Langevin [12] made a significant contribution to the field of physics by developing a more comprehensive description of Brownian motion. In 1908, he introduced the Langevin equation, which describes the evolution of the velocity of a particle under the influence of frictional and random forces. This equation provides a more detailed understanding of the dynamics involved in Brownian motion and is a cornerstone in the field of stochastic processes. It was in 1920 that Norbert Wiener [13], an American mathematician, provided a precise mathematical description of Brownian motion, which led to the eponymous Wiener process being named after him.

The phenomenon of Brownian motion offers profound insights into the behaviour of particles in diverse systems and contributes to advancements across multiple scientific and mathematical disciplines. In the following sections, we will present a mathematical description of Brownian motion and present the Langevin equation in detail.

1.1.2 Brown's observations

During its experimental observation, Brown noted several properties about the motion of the pollen particles. The most important ones are listed:

- *While continuous, the motion is erratic, irregular and appears to be not differentiable so that non global velocity can be defined.*

- *Even when particles are close to each other, they move independently, the interaction between them looks purely elastic.*
- *The motion is universal, i.e. neither the molecular composition of the fluid nor the nature of particles affect the existance of the motion.*
- *When the temperature of the fluid increases, its viscosity decreases or the mass of the particle decreases, the motion of the particles becomes more intense.*
- *The motion of the particle nerver stops, the system is out-of-equilibrium.*

These observations only form a qualitative description of the Brownian motion. For a quantitative description, we need to introduce a mathematical framework, as Einstein and Langevin did in the early 20th century.

1.2 EINSTEIN'S APPROACH TO THE BROWNIAN MOTION

As previously mentioned, Einstein provided the first mathematical model for Brownian motion in one of his historical articles published in 1905. He did not directly explain Brown's observations but suggested that the phenomenon could be related to the kinetic theory of heat and the incessant collisions of fluid molecules with the suspended particles. Einstein considered an ensemble of particles suspended in a liquid, suggesting that water might be a suitable medium. He postulated that the particles perform an irregular motion due to the collision with the molecules of the liquid. He did not want to treat each particle individually, but to describe the particles globally with a probabilistic approach. With this article, he sought to address two questions: *how far does a Brownian particle travel in a given time interval* and *how Brownian motion is related to other physical quantities*? Indeed, if the theoretical predictions of Einstein were to be verified, it would suggest that the classical thermodynamic approach may not be entirely valid on a microscopic level. As its approach was based on hypotheses involving the atomic nature of matter, it would provide strong evidence for the existence of atoms and molecules. He then wanted to express the parameters of its approach to physical and measurable quantities, so that his theory could be tested experimentally.

1.2.1 Diffusion of particles suspended in a fluid

For the sake of simplicity, we will suppose that the system is in a one-dimensional space, so that the positions of the particles are described by a single variable x. Let us denote by $p(x,t)$ the probability density of finding a particle at position x at time t. Under certain assumptions, such as the Markovian nature of the process—a concept that will be defined later—Einstein demonstrated that the probability density satisfies a partial differential equation, which is a deterministic equation. This equation is a diffusion equation of the form

$$\frac{\partial}{\partial t}p(x,t) = D\frac{\partial^2}{\partial x^2}p(x,t) \tag{1.1}$$

where D is the diffusion coefficient, having the dimension $[D] = \mathrm{L}^2\ \mathrm{T}^{-1}$. This last parameter is a direct measure of the intensity of the Brownian motion *i.e.* the greater it is, the more intense the motion is. This result establishes a clear link between the Brownian motion and the diffusion of particles in a fluid. If we assume that all particles are initially at the same position x_0, with $p(x,0) = \delta(x - x_0)$, then the solution to the diffusion equation at times $t > t_0$ is given by the Gaussian distribution

$$p(x,t) = \frac{1}{\sqrt{2\pi\sigma^2(t)}} \exp\left(-\frac{(x-x_0)^2}{2\sigma^2(t)}\right). \tag{1.2}$$

The variance of the distribution is represented by the equation $\sigma^2 = \left\langle (x(t) - x_0)^2 \right\rangle = 2Dt$, which denotes the spread of particles in space. This spread increases linearly over time, a characteristic of diffusive motion. The variance essentially measures the extent to which particles undergoing Brownian motion disperse over time. This dispersion is monitored by the diffusion constant D. Moreover, the variance of the distribution is the average value of $(x - x_0)^2$, which signifies the average squared distance from the initial position x_0. Thus, the diffusion coefficient D directly correlates with the expectation value over all possible particle trajectories. Furthermore, the variance provides insight into the distance a Brownian particle can travel over a given time interval t. This relationship highlights the interconnection between the diffusion process, which is inherently irreversible, and Brownian motion, which arises from random collisions of particles. The irreversibility of diffusion is directly linked to the random forces exerted on the Brownian particle due to collisions with water molecules. In summary, the variance in the distribution offers a comprehensive view of particle spread in diffusive motion, bridging the gap between microscopic random collisions and macroscopic diffusion characteristics.

1.2.2 Heuristic derivation of Fokker-Planck equation

Let us consider a simple model that describes the random motion of a Brownian particle in a one-dimensional space and that allows to derive the Fokker-Planck equation: the random walker. We discretize the space in a lattice with a spacing Δx and the time in discrete steps of Δt. The probability of finding a particle at position $x_i = i\Delta x$ at time $t^n = n\Delta t$ is denoted by $P(x_i, t^n) = P_i^n$, for $i \in \mathbb{Z}$ and $t \in \mathbb{N}$. The random walker model is based on the following assumptions:

- *Markovian assumption*: the probability of the particle moving from x_i to x_j at time t^{n+1} depends only on the position of the particle at time t^n and not on its previous positions.
- *Locality assumption*: The particle can jump to adjacent positions or stay at the same position between two successive time steps (nearest neighbours).
- *Homogeneity assumption*: the transition probabilities are constant in space and time.

The probabilities associated with these movements between time t^n and t^{n+1} are defined as follows. The probability that:

- the particle remains at x_i is a,
- the particle moves from x_{i-1} to x_i is b,
- the particle moves from x_{i+1} to x_i c.

The system is represented in Fig. 1.1. Given that the total probability must sum to one, we have:

$$a + b + c = 1. \tag{1.3}$$

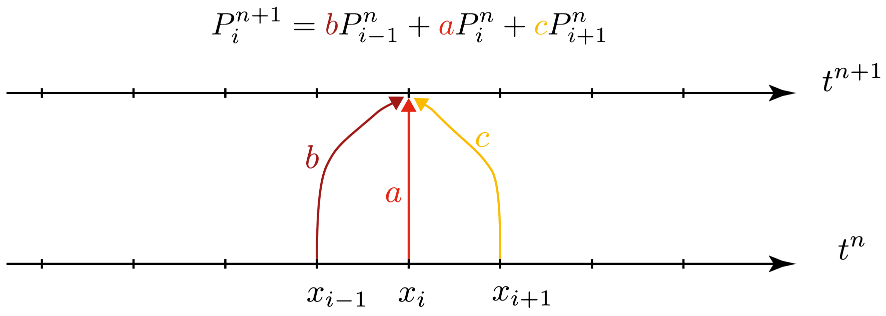

Figure 1.1: The random walker model.

Additionally, we assume symmetry in the transition probabilities, such that

$$b = c. \tag{1.4}$$

To derive the equation governing the evolution of $P(x_i, t^n)$, we consider the probability balance at position x_i^n. The probability of finding the particle at x_i at time t^{n+1} is given by the sum of the probabilities of the particle arriving at x_i from x_{i-1}, x_{i+1}, and remaining at x_i:

$$P_i^{n+1} = aP_i^n + bP_{i-1}^n + cP_{i+1}^n. \tag{1.5}$$

Using Eq. (1.3) and Eq. (1.4), we can rewrite the probability balance equation as

$$P_i^{n+1} - P_i^n = c\big[P_{i-1}^n + P_{i+1}^n - 2P_i^n\big] \tag{1.6}$$

We recognise the finite difference expression of the time derivative (left-hand side) and the Laplacian (right-hand side) of P. Dividing by Δt and taking the limit $\Delta t \to 0$ and $\Delta x \to 0$, assuming $c\,(\Delta x)^2/\Delta t$ remains finite, we obtain the Fokker-Planck equation

$$\frac{\partial P(x,t)}{\partial t} = D\frac{\partial^2 P(x,t)}{\partial x^2} \tag{1.7}$$

where

$$D = c\frac{\Delta x^2}{\Delta t} \tag{1.8}$$

is the diffusion coefficient. This equation describes the time evolution of the probability distribution $P(x,t)$ for finding a particle at position x at time t in a diffusive process.

1.2.3 Einstein's relation

The second objective of Einstein was to relate the Brownian motion to other physical quantities in order to test experimentally his theory. To achieve this, he needed to express the parameters of the system, knowing the diffusion coefficient, in terms of macroscopic quantities. These are the fluid temperature T, its viscosity η, the mass m of the particle and the radius of the particles a. It is common to introduce the friction coefficient, defined as $\gamma = 6\pi\eta a$, which is a measure of the resistance of the fluid to the motion of the particles. Einstein began by assuming that, despite the particles being large molecules, they can be described by applying statistical mechanics. It is also supposed that the particles are not interacting with each other, as they are so few in the experiments that they can be considered isolated from each other. Consequently, if one considers an ensemble of Brownian particles in suspension in water, it is then possible to treat them as an ideal gas that exerts a partial pressure of $P = nk_\mathrm{B}T$, with n being the number of particles per unit volume and k_{B} the Boltzmann constant. It can then be assumed that a force F causes a gradient of pressure, with the equilibrium condition being that $Fn = k_{\mathrm{B}}T\partial_x n$. Furthermore, the Stock's law states that when a particle is in motion in a liquid, it is subject to a friction force proportional to its velocity, that is to say $f = -m\gamma v$, where the velocity is noted v. By combining these two equations, one can write the Newton's equation of motion as $ma = -m\gamma v + F$. If we suppose a steady state, then it turns out that $v = F/m\gamma = k_{\mathrm{B}}T\partial_x n/\gamma$. The final step consists of a flux balance. The force F generates a flux of particles $J_F = nv$, where n is the particle number density and v is the particle velocity. According to Fick's law, the pressure gradient generates another flux $F_P = -D\partial_x n$, where D is the diffusion coefficient. Because equilibrium is assumed, both fluxes compensate each other, so that $J_F + J_P = 0$. By identification, one obtains the Einstein relation.

$$D = \frac{k_{\mathrm{B}}T}{M\gamma} = \frac{RT}{6\pi\eta a\mathcal{N}_{\mathrm{a}}}, \tag{1.9}$$

where $R = k_{\mathrm{B}}\mathcal{N}_{\mathrm{a}}$ is the ideal gas constant and $\mathcal{N}_{\mathrm{a}}$ the Avogadro number. It is clear that D represents a balance between the fluctuations in particle motion due to random forces (through κT) and the frictional forces that tend to impede particle motion (through γ). The Einstein relation represents a specific instance of the more general fluctuation-dissipation theorem, which was derived approximately fifty years later. With the expression of the diffusion coefficient, we can now rewrite the expression of the variance of the distribution of the particles as $\sigma^2(t) = 2Dt = 2RTt/6\pi a\eta\mathcal{N}_{\mathrm{a}}$. As the σ^2 is a quantity that can be measured in an experiment, it is possible to determine the Avogadro constant, which was not known at the time. Finally, Einstein's theory provides the value of the diffusion coefficient and an initial understanding of the nature of the erratic motion of Brownian particles. However, it does not provide information about the dynamics of the particles. If one considers the typical displacement $\sqrt{\sigma^2}$ of the particles after a time interval Δt, then one can write that $\frac{\sqrt{\sigma^2}}{\Delta t} \sim \frac{1}{\sqrt{\Delta t}}$. In the limit of zero time interval, the displacement of the particles becomes infinite. Consequently, in order to describe the motion of the particles, it is necessary to consider non-differentiable trajectories, as is the case with stochastic processes. This is the objective of the Langevin equation, which will be presented in the subsequent section.

1.3 LANGEVIN'S APPROACH TO THE BROWNIAN MOTION

In 1908, Paul Langevin proposed a model of Brownian motion based on the dynamics of the macroscopic Brownian particle. However, given that the interactions with the fluid's particles are microscopic and that a significant number of collisions occur before a macroscopic displacement of the Brownian particle, it is necessary to model the motion of the Brownian particle using a probabilistic approach.

1.3.1 Coarse-graining of the system

In modelling the motion of a Brownian particle (BP) in a fluid, it is assumed that the BP's degrees of freedom change slowly over time in comparison to the rapid microscopic motion of the fluid particles. The force exerted on the Brownian particle (BP) by the fluid can be approximated as an average force derived from the collisions between the fluid particles and the BP. This process is known as coarse-graining, whereby the fast-moving interactions of the fluid particles are averaged out to provide a simplified, mesoscopic description of the BP's motion. This averaging process occurs over a specific time interval,

denoted as τ_{Bath}, which represents the characteristic time scale of the microscopic motion of the fluid particles. The selection of this value is of great consequence. It is essential that the chosen time interval is sufficiently long to allow for the averaging out of the rapid degrees of freedom of the fluid particles, while still ensuring that the motion of the BP is not significantly affected. In most cases, the shortest time scale, denoted as τ_{s}, is associated with the solvent particles colliding with the BP. This typically occurs around 10^{-12} seconds. The average velocity of the BP reaches its equilibrium value over a time scale, denoted as τ_{B}, which is inversely proportional to the damping coefficient, γ, of the BP in the fluid. The system can be described in different ways, depending on the value of τ_{Bath} selected. If τ_{Bath} is selected to be larger than τ_{B}, the motion of the BP can be described in terms of its position only, as proposed by Einstein. Conversly, if $\tau_{\mathrm{Bath}} < \tau_{\mathrm{B}}$, the Brownian particle's motion is described by both its position and velocity. This is the principle of coarse-graining, which results in the appearance of a random force in the Langevin equation.
The relevant time scales in the system are then:

- the time scale of the fluid particles' degrees of freedom, that is represented by τ_{s},
- the time scale of the BP's velocity relaxation, denoted as τ_{B}, that is defined as the inverse of the damping coefficient γ,
- the coarse-graining time scale, denoted as $\tau^{\mathrm{E}}_{\mathrm{Bath}}$, that is employed for the description of the BP by its positional data alone (Einstein's approach or overdamped regime),
- the coarse-graining time scale, denoted as $\tau^{\mathrm{L}}_{\mathrm{Bath}}$, that is employed to describe the BP by its position and velocity, (Langevin's approach or underdamped/inertial regime).

For accurate modeling, one has $\tau_{\mathrm{s}} \ll \tau^{\mathrm{L}}_{\mathrm{Bath}} \ll \tau_{\mathrm{B}} = 1/\gamma \ll \tau^{\mathrm{E}}_{\mathrm{Bath}}$. A visual representation of these different time scales is shown in Fig. 1.2.
The following section will present the Langevin equation, which describes the motion of the Brownian particle in a fluid. The action of the fluid particle is modelled by a random force, which is the result of the coarse-graining of the system. The Langevin equation is employed in numerous fields of physics, as it can be utilized to describe a diverse range of systems, from colloidal particles to biomolecules [14]. A straightforward derivation of the Langevin equation is provided in Appendix A, where the coupling of the Brownian particle with the fluid is treated in a manner analogous to that of the Caldeira-Leggett model [15, 16].

1.3.2 Langevin equation

As previously stated, the collision between the BP and the fluid particles results in an ever-changing and random force acting on the BP, even when the fluid is in equilibrium. It follows that the position x and velocity v of the BP should be modelled by a stochastic process [17] whose dynamics is driven by the random force emerging from the coarse-graining of the system. The equation of motion for the one-dimensional BP will be derived herewith; the generalisation to three-dimensional space is straightforward. As is the case with any classical system, the equation of motion is obtained by means of Newton's second law. In order to do so, it is necessary to express all the different forces acting on the BP.

- Let us suppose that a force $F(x, t)$, deriving from a potential $V(x, t)$ that depends on the position of the BP and possibly on time, acts on the BP.

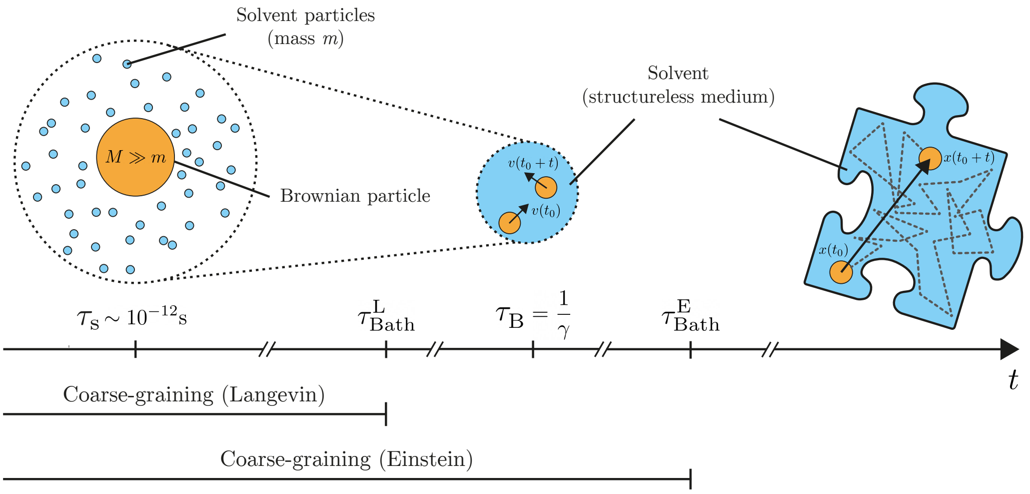

Figure 1.2: The above visual representation depicts the various time scales involved in the coarse-graining process of a Brownian particle (BP) of mass M in a fluid composed of particles of mass m. The degrees of freedom of the fluid particles change over a time interval, designated as τ_{S}, which is exceedingly small in comparison to the time scale of the BP's degrees of freedom, represented by τ_{B} for the velocity. The averaging of the fluid particles' motion is realised over a time interval, designated as τ_{Bath}, which is dependent upon the desired level of detail required to describe the motion of the Brownian particle. If the time scale of the bath is equal to the Langevin time scale, $\tau^{\mathrm{L}}_{\mathrm{Bath}}$, then the Brownian particle (BP) is described by both its velocity and its position. This is known as the Langevin description. Conversely, if $\tau_{\mathrm{Bath}} = \tau^{\mathrm{E}}_{\mathrm{Bath}}$, then only the position of the BP is relevant, and the description is known as the Einstein description. Note that as $\gamma \to \infty$, only the Einstein description remains.

- If the BP has a velocity v relative to the fluid, it encounters a larger number of fluid particles coming from the direction of its motion than from the opposite direction. Moreover, this imbalance is amplified as the velocity v, increases. It is therefore necessary to introduce a friction force that acts against the direction of motion and increases in magnitude with the velocity. The simplest assumption is that this force is proportional to the velocity. This is the same force as the viscous force $-M\gamma v$ exerted by a Newtonian fluid on a moving particle. This expression is proportional to the viscosity, resistance, of the fluid, which is precisely the relationship observed in Sec. 1.2.3.

- The last force is the fluctuating random force that arises from the coarse-graining of the collisions between the BP and the fluid particles. This force is known as the Langevin force $F_{\mathrm{L}}(t)$, and it is assumed to be independent of the position and velocity of the BP.

It should be noted that as the friction force and the random force originate from the same microscopic phenomenon, a relationship between them is to be expected. The equation of motion of the BP is then given by

$$\begin{cases} M\dot{v}(t) = \overset{\text{Newton}}{F(x(t),t)} - \overset{\text{friction}}{M\gamma v(t)} + \overset{\text{random}}{F_{\mathrm{L}}(t)}\,, \\ \dot{x}(t) = v(t), \end{cases} \tag{1.10}$$

where the dot denotes the derivative with respect to time. This is the Langevin equation, which is a linear random differential equation. It should be noted that the solutions x

and v will also be stochastic processes. Consequently, each realisation of the Langevin approach, even with the same initial conditions, will result in a different solution. Then, the general behaviour of the BP is not given by one stochastic trajectory, but rather by averaged quantities obtained by averaging over a multitude of realisations of the Langevin equation Eq. (1.10). These include the mean position and the mean velocity, the mean square displacement, the mean square velocity, the correlation functions, and so forth. In the following, the mean values over the possible fluid's microscopic configuration will be denoted by the symbol $\langle\cdot\rangle$. At this point, it is necessary to specify the statistical properties of the Langevin force F_L.

1.3.3 Statistical properties of the Langevin force

Given that the position and velocity of the BP are measured in the frame of the fluid, which is assumed to be at rest, the BP must be motionless on average when no external force acts on it. In this case, it is necessary that the average value of the Langevin force, denoted by $F_\mathrm{L}(t)$, vanishes. Additionally, since it is assumed that the Langevin force is independent of the BP's position and velocity, this must hold true even if the particle is moving. Thus, we have

$$\langle F_\mathrm{L}(t)\rangle = 0 \tag{1.11}$$

in all cases. Moreover, the stochastic process must be stationary, that is to say, its statistical properties must remain the same when subjected to time translation. This consequently implies that the autocorrelation function of the Langevin force is solely dependent on the time difference,

$$\left\langle F_\mathrm{L}(t+\tau)F_\mathrm{L}(t'+\tau)\right\rangle = \left\langle F_\mathrm{L}(t)F_\mathrm{L}(t')\right\rangle. \tag{1.12}$$

There are numerous potential autocorrelation functions, but the most prevalent is the white noise, which is a Gaussian process with a Dirac distribution as its autocorrelation function. The term Gaussian process denotes that at each time point, $F_\mathrm{L}(t)$ follows a normal distribution. The term white noise signifies that the Langevin force is uncorrelated in time, that is to say, the correlation function is a Dirac distribution.

$$\left\langle F_\mathrm{L}(t)F_\mathrm{L}(t')\right\rangle = 2D\delta(t-t') \tag{1.13}$$

where D represents the intensity of the Langevin force. In some cases, it is more appropriate to work with an autocorrelation function that is correlated in time, with a finite correlation time τ_c. In this case, the autocorrelation function is given by

$$\left\langle F_\mathrm{L}(t)F_\mathrm{L}(t')\right\rangle = 2D\delta_{\tau_\mathrm{c}}(t-t') \tag{1.14}$$

where $\delta_{\tau_\mathrm{c}}(t-t')$ is a function peaked around $t=t'$ with a width τ_c and has an integral equal to one. We call this type of noise coloured noise, $1/\tau_\mathrm{c}$ corresponding to the frequence of colour. Generally, δ_{τ_c} is taken as a Gaussian function. Note that if $\tau_\mathrm{c}\to 0$, we recover the limit of the white noise. In the following, we will restrict to the case of the white noise.

In summary, the Langevin force that we will consider is fully characterized by the following properties:

- *Stationarity*: The stochastic process is stationary, meaning that its statistical properties, such as the mean and variance, are invariant under time translation.

- *Gaussianity*: The process is Gaussian, meaning that at each time point, $F_{\mathrm{L}}(t)$ follows a normal distribution, and all moments of order higher than two are zero.
- *Markovianity*: The process is Markovian, where the future evolution of the system depends only on its current state, not on its history.
- *White Noise*: The Langevin force is uncorrelated in time, with an autocorrelation function represented by a Dirac delta function, $\langle F_{\mathrm{L}}(t) F_{\mathrm{L}}(t')\rangle = 2D\delta(t-t')$.

1.4 SOLUTIONS FOR THE FREE BROWNIAN PARTICLE

Let us assume that the BP is not subjected to any forces other than friction and the random force, *i.e.* $F(x,t) = 0$. It is interesting to study the relaxation of the velocities and positions of the BP in this case, as it will give us information about the diffusion process of the BP. The Langevin equation Eq. (1.10) becomes

$$\begin{cases} M\dot{v}(t) = -M\gamma v(t) + F_{\mathrm{L}}(t), \\ \quad \dot{x}(t) = v(t). \end{cases} \tag{1.15}$$

and the velocity is, in this case, an Ornstein-Uhlenbeck process [18], as the only forces are the friction, linear in v, and the white noise. Then, the process is stationary, Markovian and Gaussian.

1.4.1 Solution for the velocity momenta

If we denote the initial velocity of the BP by v_0, the solution of the first equation of Eq. (1.15) is given by

$$v(t) = v_0 e^{-\gamma t} + \frac{1}{M}\int_0^t \mathrm{d}\tau\; e^{-\gamma(t-\tau)} F_{\mathrm{L}}(\tau). \tag{1.16}$$

and it is possible to compute the mean velocity $\langle v(t)\rangle$ and the mean square velocity $\left\langle v^2(t)\right\rangle$. As the mean of the random force is zero, we have

$$\langle v(t)\rangle = v_0 e^{-\gamma t} \tag{1.17}$$

and it is clear that the mean velocity relaxes exponentially to zero with a characteristic time $\tau_{\mathrm{B}} = 1/\gamma$. It corresponds to the time needed by the BP to forgets its initial velocity. The velocity variance is given by

$$\sigma_v^2(t) = \left\langle \left[v(t) - \langle v(t)\rangle\right]^2 \right\rangle = \frac{D}{M^2\gamma}\left(1 - \mathrm{e}^{-2\gamma t}\right). \tag{1.18}$$

Initially it is zero, since the velocity of the BP is perfectly known at $t = 0$. At very small times (with respect to τ_{B}) it increases linearly with time, indicating that D is a diffusion coefficient in the velocity space, until it reaches a plateau at $D/M\gamma$ for large times. Since the mean velocity is also zero at large times, the variance of the velocity is equal to the mean square velocity. It follows that the mean kinetic energy of the BP at large time is

$$\langle E_{\mathrm{K}}(t)\rangle := \frac{1}{2}M\left\langle v^2(t)\right\rangle = \frac{D}{2M\gamma}. \tag{1.19}$$

When the system is in equilibrium, according to the equipartition of energy, the average kinetic energy must be equal to $k_\mathrm{B}T/2$, where k_B is the Boltzmann constant and T is the temperature of the fluid. Thus we have a definition of D as

$$D = M\gamma k_\mathrm{B}T. \tag{1.20}$$

This relation connects the amplitude of the random force, represented by the diffusion coefficient, to the damping coefficient, γ, which accounts for the friction with the fluid. This is an example of the fluctuation-dissipation theorem.

1.4.2 Solution for the position momenta

If we now consider the second equation of Eq. (1.15), we can calculate the mean position $\langle x(t)\rangle$ and the mean square displacement $\langle x^2(t)\rangle$, or the variance $\left\langle [x - \langle x(t)\rangle]^2\right\rangle$. The solution of the equation is given by

$$x(t) = x_0 + \frac{v_0}{\gamma}\left(1 - \mathrm{e}^{-\gamma t}\right) + \frac{1}{M\gamma}\int_0^t \mathrm{d}\tau\, \left(1 - e^{-\gamma(t-\tau)}\right) F_\mathrm{L}(\tau). \tag{1.21}$$

From this equation, it is clear that the position of the BP is also a stochastic process. The mean position is given by

$$\langle x(t)\rangle = x_0 + \frac{v_0}{\gamma}\left(1 - \mathrm{e}^{-\gamma t}\right). \tag{1.22}$$

For small times we get $\langle x(t)\rangle = x_0 + v_0 t$, which is the expected behaviour of a free particle, a ballistic motion. For large times, it converges exponentially to $x_0 + v_0/\gamma$. Another interesting quantity is the variance of the position with respect to its initial position. This is given by $\left\langle [x(t) - x_0]^2\right\rangle$. We know that $\dot{x} = v$, so integrating this equation over time gives $x(t) - x_0 = \int_0^t \mathrm{d}\tau\ v(\tau)$. The mean square displacement is then given by

$$\left\langle [x(t) - x_0]^2\right\rangle = \int_0^t \mathrm{d}\tau_1 \int_0^t \mathrm{d}\tau_2\ \langle v(\tau_1)v(\tau_2)\rangle \tag{1.23}$$

$$= 2t\int_0^t \mathrm{d}\tau\, \left(1 - \frac{\tau}{t}\right) \langle v(\tau)v(0)\rangle \tag{1.24}$$

where we used that the velocity process is stationary, and integrated by part. The quantity $\langle v(\tau)v(0)\rangle$ is the autocorrelation of the velocities. Since we are considering the case of the free particle, it is possible to have an explicit expression for the mean square displacement. Using Eq. (1.16) in this expression, or Eq. (1.21), it is given by

$$\left\langle [x(t) - x_0]^2\right\rangle = \frac{2k_\mathrm{B}T}{M\gamma^2}\left[\gamma t - \left(1 - \mathrm{e}^{-\gamma t}\right)\right]. \tag{1.25}$$

In the short time limit, still with respect to τ_B, the mean square displacement increases as a second order polynomial, $\left\langle [x(t) - x_0]^2\right\rangle = k_\mathrm{B}Tt^2/M$. We observe the ballistic motion of a free particle, as the BP does not have the time to undergo a collision with the fluid particle. At large times, the mean square displacement (MSD) increases linearly with time, $\left\langle [x(t) - x_0]^2\right\rangle = 2k_\mathrm{B}Tt/M\gamma = 2D_x t$. This is a purely diffusive regime, signature of a diffusive motion in the position space associated with a diffusion coefficient $D_x = k_\mathrm{B}T/M\gamma$, which is no more than the Einstein relation. Note that the MSD has no finite limit as time goes to infinity, so the position process is not stationary. Finally, by combining Eq. (1.24) and Eq. (1.25) in the large time limit, one can write the well-known Green-Kubo relation

$$D_x = \lim_{t\to+\infty} \frac{\left\langle [x(t)-x_0]^2 \right\rangle}{2t} = \int_0^{+\infty} \mathrm{d}\tau \ \left\langle v(\tau)v(0) \right\rangle . \tag{1.26}$$

This is another example of fluctuation-dissipation theorem, since at equilibrium it relates the diffusion of the BP to a response function, which is the autocorrelation function of the velocities, *i.e.* a measure of the dissipation. Finally, the position process is a Gaussian and Markovian process, but it is not stationary.
We have seen that the Einstein relation can be recovered from the Langevin equation by considering the processus in position space. However, the Langevin approach is based on a description of the BP in phase space, where both position and velocity are considered. We have seen in Sec. 1.2 that Einstein only considered the position of the BP and not the velocity. We will see below that the Langevin equation is more general than Einstein's approach, and that it is possible to recover Einstein's description from the Langevin equation.

1.5 OVERDAMPED LIMIT OF THE LANGEVIN EQUATION

If a stochastic equation of motion for the position only is desired, it is necessary to eliminate the velocity derivative from the Langevin equation, which corresponds to suppressing the second derivative of the position. This is possible by considering the overdamped limit, where the inertia of the BP is negligible compared to the frictional force. This is the case when the mass of the BP is small or when the damping coefficient is very large. In fact, $M\dot{v}$ is the term that takes into account the inertia of the BP in the Langevin equation. As mentioned after Eq. (1.17), $1/\gamma$ is the time scale over which the BP loses information about its initial velocity. Then, for $\gamma t \gg 1$, the velocity of the BP has reached a quasi-steady state and its variation is negligible[1] compared to its amplitude, $\dot{v}/\gamma \ll v$. Neglecting the inertia term in the Langevin equation Eq. (1.10), we obtain the overdamped Langevin equation

$$M\gamma\dot{x}(t) = F(x(t),t) + F_{\mathrm{L}}(t). \tag{1.27}$$

which is a random differential equation of the first order in the position. This changes the time scale used to coarse-grain the system from $\tau_{\mathrm{B}}^{\mathrm{L}}$ to $\tau_{\mathrm{B}}^{\mathrm{E}}$, which is much bigger. This allows us to focus only on the position of the BP and not on the speed, the latter being ill-defined. Eq. (1.27) is called the overdamped Langevin equation because we made the approximation of large damping coefficient. Dividing Eq. (1.27) by $M\gamma$ and introducing the diffusion coefficient $D_{\mathrm{E}} = D/(M\gamma)^2$, the overdamped Langevin equation has the form

$$\dot{x}(t) = \frac{1}{M\gamma} F(x(t),t) + F_{\mathrm{E}}(t). \tag{1.28}$$

where F_{E} is still a Gaussian white noise, but whose intensity is

$$D_{\mathrm{E}} = \frac{k_{\mathrm{B}}T}{M\gamma} \tag{1.29}$$

so that the diffusion coefficient is the same as in the Einstein approach.

---

[1] If the force is time-dependent, its characteristic frequency also needs to be small compared to γ.

1.6 FOKKER-PLANCK EQUATION

As mentioned in 1.3, the Langevin equation gives the dynamics of a single BP using random forces, leading to a stochastic and non-deterministic equation of motion: if we solve the Langevin equation many times with exactly the same initial conditions, we will not get the same time evolution. There is another approach to treat the BM, closer to Einstein's approach, where the BP is described by a probability density function. The equation desribing the temporal evolution of the probability density is called the Fokker-Planck equation, named after Adriaan Fokker [19] and Max Planck [20], when the dynamics of the BP is assumed to be Markovian. This is a linear partial differential equation, of the first order in time, and it can be derived in many ways, in particular it is a special case of the Kramers-Moyal expansion [21, 22]. In the following, we will not give the derivation of the Fokker-Planck equation, but we will give its form and concentrate on the overdamped approximation.

1.6.1 Temporal evolution of the probability density

The probability of finding the BP in position in the interval $[x, x + \mathrm{d}x]$ and velocity in the interval $[v, v + \mathrm{d}v]$, at time t, is given by $P(x, v, t)\mathrm{d}x\mathrm{d}v$. It can be shown that the probability density $P(x, v, t)$ satisfies the Fokker-Planck equation

$$\partial_t P(x,v,t) = -v\partial_x P(x,v,t) + \partial_v\left[\left(\gamma v - \frac{F(x,t)}{M}\right)P(x,v,t)\right] + D\partial_v^2 P(x,v,t) \tag{1.30}$$

as long as the random force F_L of the Langevin, equation is a white noise, since the process is then Markovian. In this special case of a dynamics in the phase space (x, v), this equation is also called the Klein-Kramers equation. If we consider the overdamped limit, the probability density no longer depends on v and the Fokker-Planck equation becomes

$$\partial_t P(x,t) = -\partial_x\left[\frac{F(x,t)}{M\gamma}P(x,t)\right] + D_\mathrm{E}\partial_x^2 P(x,t) \tag{1.31}$$

which is called the Smoluchowski equation [23]. See [24–26] for a rigorous mathematical proof of the convergence of the Klein-Kramers equation to the Smoluchowski equation. This equation is equivalent to the convection-diffusion equation without source term. Note that, for both Eq. (1.30) and Eq. (1.31), in the limit of no diffusion, we recover the continuity equation, with the first-order derivative terms of the right-hand sides being the associated probability current. If we consider the special case where the BP is free, *i.e.* $F(x, t) = 0$, we then recover exactly the diffusion Eq. (1.1) obtained in Einstein's approach.

1.6.2 Stationary solution of Smoluchowski equation

If we write the force F as the gradient of a potential, $F(x, t) = -\partial_x V(x, t)$, it is straightforward to see that a stationary solution of the Smoluchowski , given by Eq. (1.31), is nothing more than the Boltzmann distribution

$$P_\mathrm{eq}(x) = \frac{1}{Z}\mathrm{e}^{-V(x)/k_\mathrm{B}T} \tag{1.32}$$

where Z is the partition function that is computed by normalising the probability density to unity. This distribution is the one we would get if we solved the Langevin equation for a very long time for many independent BPs and realised a histogram of the positions of the different BPs, since both approaches, Langevin and Fokker-Planck, are equivalent [27]. They use a different point of view on the system but the macroscopic quantities that they provide are the same.

1.7 STOCHASTIC DIFFERENTIAL EQUATION

Throughout this chapter, we have referred to the Langevin equation as a random differential equation (RDE). We derived it by starting from the standard differential equation of motion for a particle, *i.e.*, Newton's law, and introducing a random force. In the overdamped limit, the position of the Brownian particle (BP) is described by

$$\dot{x}(t) = b(x(t), t) + \zeta(t), \tag{1.33}$$

where $b(x(t), t)$ and $\zeta(t)$ represent the deterministic and random contributions, respectively. We identified $\zeta(t)$ as Gaussian white noise, characterized by its autocorrelation function:

$$\langle \zeta(t)\zeta(t') \rangle = 2D\delta(t - t'), \tag{1.34}$$

where D denotes the noise amplitude. This traditional approach assumes that it is mathematically valid to express the derivative of the position in this form. However, from a rigorous mathematical standpoint, the derivative of the position is not well-defined. The appropriate mathematical framework to address such processes is Itô calculus [28]. It can be shown that the Langevin equation can be associated to a stochastic differential equation (SDE), which involves the increment of the position rather than its derivative. The SDE corresponding to the overdamped Langevin equation is

$$\mathrm{d}x(t) = b(x(t), t)\mathrm{d}t + \mathrm{d}W(t), \tag{1.35}$$

where $\mathrm{d}x(t) = x(t + \mathrm{d}t) - x(t)$ represents the position increment over the time interval $\mathrm{d}t$, and $W(t)$ is a Wiener process. The Wiener process is a stochastic process that can be interpreted as the integral of white noise, with increments that are Gaussian random variables with zero mean and variance $\mathrm{d}t$. Specifically, we have

$$\langle \mathrm{d}W(t) \rangle = 0, \tag{1.36}$$

and

$$\langle \mathrm{d}W(t)^2 \rangle = 2D\mathrm{d}t. \tag{1.37}$$

The SDE provides a more rigorous framework for handling stochastic processes and is widely adopted in the field of stochastic analysis. This approach is more general than the RDE formulation, as, according to the Wong-Zakai theorem [29], it is possible to associate an SDE with an RDE under certain conditions (though the converse is not always true). Finally, the probability density associated with Eq. (1.35) is governed by the Fokker-Planck equation:

$$\partial_t P(x, t) = -\partial_x \left[b(x, t)P(x, t) \right] + D\partial_x^2 P(x, t), \tag{1.38}$$

which is identical to the Smoluchowski equation given by Eq. (1.31). The Fokker-Planck equation derived from an SDE is always equivalent to the probability density associated with the corresponding RDE. In the subsequent chapters, we will use the SDE framework.

1.8 CONCLUSION

In this chapter, we have explored the phenomenon of Brownian motion from its historical origins to the mathematical models that describe it. Brownian motion, initially observed by Robert Brown in 1827, is a fundamental process characterized by the random, erratic motion of particles suspended in a fluid. This motion arises from collisions between the particles and the fast-moving molecules of the surrounding fluid, a concept that has been foundational in various scientific disciplines, including physics, chemistry, biology, and finance.

The historical development of the theory behind Brownian motion involved significant contributions from several key figures. Louis Bachelier provided an early probabilistic approach in his 1900 thesis, and Albert Einstein's 1905 work offered the first quantitative explanation, linking the phenomenon to the molecular theory of heat. Einstein's model established the relationship between Brownian motion and diffusion, culminating in the derivation of the diffusion equation and the Einstein relation, which connects the diffusion coefficient to measurable physical quantities. Paul Langevin further advanced the understanding of Brownian motion by introducing a dynamical approach in 1908. His Langevin equation provides a random differential equation that describes the velocity and position of a Brownian particle under the influence of random forces. This approach captures the probabilistic nature of the system, accounting for the random collisions with fluid molecules that drive the motion. We have also discussed the coarse-graining technique, which simplifies the description of Brownian motion by averaging out the fast degrees of freedom of the fluid particles. The resulting Langevin equation describes the system's behavior over a more extended time scale and is essential in fields such as statistical mechanics and stochastic processes. Moreover, we explored the solutions of the Langevin equation, both for the velocity and position of the Brownian particle, and introduced the concept of the overdamped limit, where the inertia of the particle is negligible. This leads to the overdamped Langevin equation, which focuses on the position of the particle alone and is closely related to Einstein's approach. Finally, we introduced the Fokker-Planck equation, which describes the time evolution of the probability density function of the particle's position and velocity. In the overdamped limit, this equation reduces to the Smoluchowski equation, which further simplifies the description of the system. We showed that both the Langevin and Fokker-Planck approaches are equivalent and lead to the same macroscopic predictions.

In conclusion, the study of Brownian motion has provided profound insights into the behavior of particles at the microscopic level, establishing a crucial link between random molecular collisions and macroscopic diffusion processes. The mathematical frameworks developed to describe this phenomenon, including the Einstein relation, Langevin equation, and Fokker-Planck equation, continue to be fundamental tools in the study of stochastic processes and statistical mechanics. These models do not only enhance our understanding of physical systems but also find applications in a wide range of scientific and engineering disciplines.

In the following chapter, we aim to extend this mathematical formalism to describe quantum systems, which requires us to explore modifications that render the formalism time-reversible, in contrast to the inherently irreversible nature of classical Brownian motion, as it is an open system.

KEY TAKEAWAYS

This chapter has been devoted to introducing the basic tool of the mathematical description of Brownian motion. We have seen that the Brownian particle can be described in two different but equivalent ways. The first is based on the Langevin equation, which is a random differential equation describing the motion of the BP in phase space. The second is based on the Fokker-Planck equation, which is a partial differential equation describing the time evolution of the probability density of the BP.

The Langevin equation includes a random force, the Langevin force, which we will consider as Gaussian white noise. It is possible to neglect the inertial effect of the BP, leading to an overdamped Langevin equation

$$\dot{x}(t) = \frac{1}{M\gamma} F(x(t), t) + F_{\mathrm{E}}(t)$$

with F_{E} is a Gaussian white noise with intensity

$$D_{\mathrm{E}} = k_{\mathrm{B}} T / M\gamma$$

and satisfying

$$\langle F_{\mathrm{E}}(t) \rangle = 0 \qquad \text{and} \qquad \langle F_{\mathrm{E}}(t) F_{\mathrm{E}}(t') \rangle = 2 D_{\mathrm{E}} \delta(t - t').$$

The associated Fokker-Planck equation is the Smoluchowski equation, which is a partial differential equation describing the temporal evolution of the probability density of the BP in the position space

$$\partial_t P(x, t) = -\partial_x \left[\frac{F(x, t)}{M\gamma} P(x, t) \right] + D_{\mathrm{E}} \partial_x^2 P(x, t).$$

It is possible to rewrite the Langevin equation in the form of a stochastic differential equation, which is more rigorous from a mathematical point of view. The SDE associated with the overdamped Langevin equation is

$$\mathrm{d}x(t) = \frac{1}{M\gamma} F(x(t), t) \mathrm{d}t + \mathrm{d}W(t),$$

where the W is a Wiener process satisfying to

$$\langle \mathrm{d}W(t) \rangle = 0 \qquad \text{and} \qquad \langle \mathrm{d}W(t)^2 \rangle = 2 D_{\mathrm{E}} \mathrm{d}t.$$

These equations are the basic tools for describing the Brownian motion of a particle in a fluid. They are the starting point for the study of the dynamics of Brownian particles, and will be used below in the case of the quantum dynamics of a particle in a potential.

REFERENCES

[7] Brown, R. *The Philosophical Magazine* **1828**, *4*, 161–173.

[8] Paul, W.; Baschnagel, J., *Stochastic Processes*; Springer International Publishing: Heidelberg, 2013.

[9] Bachelier, L. *Annales scientifiques de l'École Normale Supérieure* **1900**, *17*, 21–86.

[10] Einstein, A. *Annalen der physik* **1905**, *17*, 549–560.

[11] Perrin, J. *Le Radium* **1909**, *6*, 353–360.

[12] Langevin *C. R. Hebd. Séances Acad. Sci.* **1908**, *146*, 530.

[13] Wiener *Ann. of Math* **1920**, *22*, 66–72.

[14] Purcell, E. M. *American Journal of Physics* **1977**, *45*, 3–11.

[15] Caldeira, A. O.; Leggett, A. J. *Annals of Physics* **1983**, *149*, 374–456.

[16] Leggett, A. J.; Chakravarty, S., et al. *Reviews of Modern Physics* **1987**, *59*, 1–85.

[17] Lemons, D. S.; Gythiel, A. *American Journal of Physics* **1997**, *65*, 1079–1081.

[18] Uhlenbeck, G. E.; Ornstein, L. S. *Physical Review* **1930**, *36*, 823–841.

[19] Fokker, A. D. *Annalen der Physik* **1914**, *348*, 810–820.

[20] Der Wissenschaften zu Berlin., D. A.; zu Berlin, D. A. d. W., *Sitzungsberichte Der Königlich Preussischen Akademie Der Wissenschaften Zu Berlin*; Deutsche Akademie der Wissenschaften zu Berlin: Berlin, 1917; Vol. Jan-Dec 1917, pp 1–912; 912 pp.

[21] Kramers, H. A. *Physica* **1940**, *7*, 284–304.

[22] Moyal, J. E. *Journal of the Royal Statistical Society: Series B (Methodological)* **1949**, *11*, 150–210.

[23] Smoluchowski *Ann. Phys* **1906**, *21*, 756–780.

[24] Wilemski, G. *Journal of Statistical Physics* **1976**, *14*, 153–169.

[25] Titulaer, U. M. *Physica A: Statistical Mechanics and its Applications* **1978**, *91*, 321–344.

[26] Bocquet, L. *American Journal of Physics* **1997**, *65*, 140–144.

[27] Risken, H., *The Fokker-Planck Equation: Methods of Solution and Applications*; Haken, H., red.; Springer Series in Synergetics, Vol. 18; Springer: Berlin, Heidelberg, 1996.

[28] Ito, K. On Stochastic Differential Equations American Mathematical Society.

[29] Wong, E.; Zakai, M. *The Annals of Mathematical Statistics* **1965**, *36*, 1560–1564.

CHAPTER 2

STOCHASTIC QUANTUM MECHANICS

> *In science one tries to tell people, in such a way as to be understood by everyone, something that no one ever knew before. But in the case of poetry, it's the exact opposite!*
>
> — Paul Dirac

In this chapter, we introduce the Nelson formalism in quantum mechanics, which provides a stochastic approach to describe quantum systems using time-reversible stochastic processes. We begin in Sec. 2.1 by discussing the challenges of applying stochastic methods to closed quantum systems and introducing the concept of time-reversible stochastic processes, leading to Nelson's stochastic mechanics. In Sec. 2.2, we define forward and backward processes and their associated derivatives, establishing the foundation for time-reversible stochastic descriptions. Next, in Sec. 2.3, we introduce an acceleration law in configuration space, analogous to Newton's second law, which incorporates dynamics into the stochastic framework. Applying these concepts to quantum systems in Sec. 2.4, we derive the Schrödinger equation from the acceleration law and establish the connection to standard quantum mechanics. In Sec. 2.5, we discuss numerical methods for solving the Nelson equation, focusing on the second-order Helfand-Greenside method and outlining the computational methodology. We illustrate the application of the Nelson formalism in Sec. 2.6 with numerical examples involving a free Gaussian wavepacket and a particle encountering a potential barrier, demonstrating how the approach can reproduce key quantum phenomena such as tunneling and the Heisenberg uncertainty principle. Finally, in Sec. 2.7, we summarize the key points and discuss the implications of the Nelson formalism in quantum mechanics.

Contents

2.1 INTRODUCTION

In the previous chapter, we introduced the basic concepts needed to describe the dynamics of a system influenced by randomness. The goal of this study is to apply these mathematical ideas to describe a closed quantum system. At first, it might seem unusual to use a stochastic approach for a quantum system because quantum mechanics is usually time-reversible. This means that the Schrödinger equation, which governs quantum mechanics, remains unchanged when time is reversed, as long as the time reversal operator[1] and the system's Hamiltonian commute. On the other hand, the stochastic approach, often used to describe systems like Brownian motion, typically does not have this time-reversibility. This is because it includes random elements in the equations and is usually applied to systems that are not in equilibrium. However, as Schrödinger suggested in 1931 [30], it is possible to make a stochastic description of a system that is time-reversible at the level of probability density. This idea is the foundation of Nelson stochastic mechanics [31]. This quantum theory is related to the de Broglie-Bohm interpretation of quantum mechanics, as discussed in Refs.[32–34]. In the de Broglie-Bohm theory, quantum particles are thought to have definite positions and are guided by the wave function. Louis de Broglie first presented these ideas at the Solvay Conference in 1927, as detailed in Ref.[35]. Before we go deeper into Nelson's formalism, it is helpful to look at the de Broglie-Bohm pilot-wave theory since it is closely related to Nelson's mechanics. Understanding this theory will give us a better grasp of Nelson's approach. In both theories, particles are assumed to have well-defined positions, with each particle being guided by the wavefunction ψ, which is why it is called a pilot wave. In the de Broglie-Bohm theory, it is assumed that the wave function ψ satisfies the Schrödinger equation

$$i\hbar\partial_t\psi(x,t) = \hat{H}\psi(x,t), \tag{2.1}$$

where $\hbar$ is the reduced Planck constant and $\hat{H}$ is the Hamiltonian of the system considered. However, as we will see, this is not the case in the Nelson approach. In this approach, the wave function alone is not sufficient to fully describe a quantum system. To complete the description, the positions of the particles, considered hidden from the observer's point of view, must also be specified. Therefore, it is essential to write the equation for the trajectories. This can be done by introducing the probability current associated with the wave function, defined as

$$j(x,t) = \frac{\hbar}{m}\,\mathrm{Im}\left[\bar{\psi}(x,t)\partial_x\psi(x,t)\right], \tag{2.2}$$

where m is the mass of the quantum particle, Im refers to the imaginary part, and $\bar{\psi}$ denotes the complex conjugate of ψ. It can be shown from the Schrödinger equation that ψ and j satisfy the continuity equation

$$\partial_t|\psi(x,t)|^2 + \partial_x j(x,t) = 0. \tag{2.3}$$

The probability current allows us to define a velocity, similar to how it is done in fluid dynamics. This velocity is simply the ratio of the current to the density:

$$v(x,t) = \frac{j(x,t)}{|\psi(x,t)|^2}. \tag{2.4}$$

If we express the wave function in polar form

$$\psi(x,t) = R(x,t)\mathrm{e}^{iS(x,t)/}, \tag{2.5}$$

---

[1] The operator that changes t into $-t$ and conjugates the wavefunction.

where $R(x,t) = \sqrt{|\psi(x,t)|^2}$ is the amplitude and $S(x,t)$ is the phase, then the current becomes

$$j(x,t) = \frac{\hbar}{m}|\psi(x,t)|^2\partial_x S. \tag{2.6}$$

and the velocity field is

$$v(x,t) = \frac{\hbar}{m}\partial_x S(x,t). \tag{2.7}$$

To find the particle's trajectory $x(t)$, we can evaluate the velocity field at $x(t)$ and integrate Eq. (2.7) with respect to time, given an initial condition x_0. The velocity is the time derivative of the position, leading to the de Broglie guiding equation:

$$\mathrm{d}x = \frac{\hbar}{m}\partial_x S \; \mathrm{d}t, \tag{2.8}$$

which describes the change in position $\mathrm{d}x$ over a time interval $\mathrm{d}t$. Here, the phase S of the wave function serves as a guiding principle for the trajectories. Thus, to calculate the particle's path, the wave function must first be determined. It should be noted that de Broglie-Bohm's theory is deterministic: if the initial position is known, the particle's future position can be predicted. The probabilistic nature of quantum mechanics arises from our uncertainty about the initial position. Now that we have explained the concept of a well-defined trajectory, we will present the stochastic version of the de Broglie-Bohm theory, known as Nelson's theory of quantum mechanics. As we will see, there are many similarities between the two theories. A comparison of the guiding equation Eq. (2.8) with Nelson's equation will highlight them in the following sections.

2.2 TIME REVERSIBILITY FOR STOCHASTIC PROCESSES

We aim to describe the dynamics of a quantum system in terms of stochastic processes. We have seen that the de Broglie equation describes the evolution of the positions of quantum particles, similar to how the overdamped Langevin equation describes classical Brownian particles (where the equation of the motion describes the change of position over time). We might expect to obtain a *generalization*[2] of the guiding equation that includes a stochastic term, turning the position into a random process whose probability distribution follows a Fokker-Planck equation, assuming no memory effects as is typical for closed quantum systems. Along the chapter, we will focus on the dynamics of a single quantum particle in configuration space, *i.e.*, considering only the particle's position and not its velocity. The goal is to construct a stochastic process whose probability density is time-reversible, then to develop the Nelson formalism from it and verify that it reproduces the results of quantum mechanics.

2.2.1 Forward and backward processes

Let us write the equation of motion for the particle as

$$\mathrm{d}x(t) = b(x(t),t)\mathrm{d}t + \mathrm{d}W(t), \tag{2.9}$$

where x is the position of the particle. This equation consists of two terms: a deterministic term $b(x,t)$, which can be interpreted as the mean velocity of the particle and acts as the force applied to the particle, and a stochastic term $\mathrm{d}W(t) = W(t+\mathrm{d}t) - W(t)$, which

---

[2] Nelson approach is not a generalization of de Broglie-Bohm theory as both theories do not share the same initial axiomatic.

is a Gaussian process, meaning its distribution is Gaussian. Here, $W(t)$ is a Wiener process with the same properties as the one mentioned in Chap. 1. This equation gives the increment of position $\mathrm{d}x = x(t+\mathrm{d}t) - x(t)$ corresponding to a time interval $\mathrm{d}t$. In the case of the de Broglie guiding equation, b is proportional to the gradient of the phase of the wavefunction, and the Wiener process is null. As we are dealing with a random process, we can average over the realizations of the Wiener process. We still have that $\langle \mathrm{d}W(t)\rangle = 0$ and $\langle \mathrm{d}W(t)\mathrm{d}W(t')\rangle = 2D_{\mathrm{Q}}\mathrm{d}t$, where D_{Q} is the diffusion coefficient, which will be discussed later. These considerations apply to a positive time increment $\mathrm{d}t$, and Eq. (2.9) is referred to as the forward process. We can also consider the associated backward process, defined as

$$\mathrm{d}x^*(t) = b^*(x(t),t)\mathrm{d}t + \mathrm{d}W^*(t), \tag{2.10}$$

with the * referring to the backward process. The difference here is that $\mathrm{d}x^*(t) = x(t) - x(t-\mathrm{d}t)$, meaning that we approach $x(t)$ from the future. In this case, b^*, the backward mean velocity or drift, is evaluated at $x(t)$. The Wiener process W^* shares the same properties as W. To ensure time reversibility, we need to impose that the probability density of the forward process is the same as that of the backward process, making it a solution to both the forward and backward Fokker-Planck equations. Imposing this condition implies that the drifts b and b^* are not independent but are related by an equation that we will need to derive.

2.2.2 Forward and backward derivatives

The drifts b and b^* are analogous to the mean velocity of the particle in the forward and backward processes, respectively. However, since the position is not differentiable with respect to time, we need to introduce a new type of derivative to define the concept of velocity. Similar to the material derivative in fluid mechanics[3], we can define the forward derivative [36] of a function of the position x and the time t as

$$\mathcal{D}f(x,t) = \lim_{\Delta t\to 0}\frac{1}{\Delta t}\left\langle f(x(t+\Delta t), t+\Delta t) - f(x(t),t) \mid x(t) = x\right\rangle, \tag{2.11}$$

where we introduced the conditional expectation notation $\langle \cdot \mid x(t) = x\rangle$ to indicate that the expectation is taken over the realizations of the Wiener process that satisfy $x(t) = x$. Similarly, the backward derivative is defined as

$$\mathcal{D}^*f(x,t) = \lim_{\Delta t\to 0}\frac{1}{\Delta t}\left\langle f(x(t),t) - f(x(t-\Delta t), t-\Delta t) \mid x(t) = x\right\rangle. \tag{2.12}$$

The computation of the conditional expectation is done using the conditional probability density $P(x,t \mid x',t')$, which gives the probability of finding the particle at position x at time t, given that it was at position x' at time t'. The conditional expectation is assumed to follow both the forward and backward Fokker-Planck equations, just like the probability density. Using the statistical properties of the Wiener process, it is straightforward to show that the derivatives can be written as

$$\mathcal{D}f(x,t) = \partial_t f(x,t) + b(x,t)\partial_x f(x,t) + D_{\mathrm{Q}}\partial_x^2 f(x,t), \tag{2.13}$$

---

[3] In fluid mechanics, the material derivative along a line of flow is defined as $\mathcal{D}f(x,t) = \lim_{\Delta t\to 0}\Delta t^{-1}[f(x(t+\Delta t),t+\Delta t) - f(x(t),t)]_{x(t)=x}$, leading to $\mathcal{D}f(x,t) = \partial_t f(x,t) + v(t)\partial_x f(x,t)$, where $v(t)$ is the velocity of the fluid.

and

$$\mathcal{D}^* f(x,t) = \partial_t f(x,t) + b^*(x,t)\partial_x f(x,t) - D_\mathrm{Q}\partial_x^2 f(x,t). \tag{2.14}$$

These expressions are obtained by performing a Taylor expansion of the function f around $x(t)$ to the first order in Δt, which corresponds to the second order in Δx as $\langle \mathrm{d}W^2 \rangle \sim \Delta t$. We see that the difference between the forward and backward derivatives is the sign of the diffusion term. If the Wiener process were not present, the forward and backward derivatives would be identical, and we would recover the classical material derivative. If we apply this definition to the position x, we obtain the forward and backward velocity fields as

$$\mathcal{D}x = b(x,t) \qquad \text{and} \qquad \mathcal{D}^* x = b^*(x,t), \tag{2.15}$$

and since $b \neq b^*$, we see that the forward and backward derivatives are not the same, which is consistent with the non-differentiability of the trajectory.

2.2.3 Relation between the forward and backward processes

In Appendix B, we provide an explicit demonstration of the relationship between the forward and backward drifts by deriving the backward derivative in terms of forward process quantities. We find that the drifts are related by the equation

$$b^*(x,t) = b(x,t) - 2D_\mathrm{Q}\partial_x \ln P(x,t), \tag{2.16}$$

which is a direct consequence of the requirement that both forward and backward processes share the same probability density. The Fokker-Planck equation associated with the forward process is given by

$$\partial_t P = -\partial_x(bP) + D_\mathrm{Q}\partial_x^2 P, \tag{2.17}$$

and the one associated with the backward process is

$$\partial_t P = -\partial_x(b^* P) - D_\mathrm{Q}\partial_x^2 P. \tag{2.18}$$

It is straightforward to see that the relation between b and b^* allows us to derive one equation from the other. The sum of the two Fokker-Planck equations cancels out the diffusion terms and gives the equation

$$\partial_t P + \partial_x(vP) = 0, \tag{2.19}$$

where we define the velocity field as

$$v(x,t) = \frac{b(x,t) + b^*(x,t)}{2} = b(x,t) - D_\mathrm{Q}\partial_x \ln P(x,t), \tag{2.20}$$

as the mean of the forward and backward drifts. This equation is the continuity equation for the probability density P, and it closely resembles the one obtained from the Schrödinger equation. In the case of thermal Brownian motion, the velocity field v would correspond to an externally applied field, as b would be directly proportional to the force applied to the particle. If we subtract the two Fokker-Planck equations, the time derivative of the probability density cancels out, and we obtain the equation

$$\partial_x(uP) = D_\mathrm{Q}\partial_x P, \tag{2.21}$$

where we define the drift difference as

$$u(x,t) = \frac{b(x,t) - b^*(x,t)}{2} = D_\mathrm{Q}\partial_x \ln P(x,t), \tag{2.22}$$

which we call the osmotic velocity field, in reference to Einstein's theory of Brownian motion, where the velocity acquired by a Brownian particle (BP) in equilibrium with an applied force has the same form[4]. Morevoer, Eq. (2.22) is very similar to the Fick's law. Eq. (2.21) is equivalent to Eq. (2.16) and shows that the connection between b and b^* is mediated by the probability density P. We see that the two new velocity fields, v and u, both depend on the density. We can combine v and u to recover the drifts b and b^* as $b = v + u$ and $b^* = v - u$.

2.3 DEFINITION OF AN ACCELERATION LAW

The considerations in the previous section were based on the kinematics of stochastic motion. We discussed the necessity of ensuring time reversibility in a stochastic description of motion. To complete this kinematic description with a dynamic one, we need to introduce the concept of acceleration for the particle. The configuration space description of the motion, like the overdamped Langevin equation, is a non-inertial description. However, quantum mechanics involves inertial aspects, as indicated by the presence of mass in the Schrödinger equation. Therefore, it is essential to introduce an acceleration law.

2.3.1 Acceleration law in phase-space

Let us revisit the Ornstein-Uhlenbeck process discussed in the previous chapter to motivate the introduction of an acceleration law. The equation of motion for the particle is given by

$$m\mathrm{d}v(t) = [F(x(t),t) - m\gamma v(t)]\mathrm{d}t + \mathrm{d}W(t), \tag{2.23}$$

where v is the velocity of the particle, F is the force applied to the particle, γ is the friction coefficient, and $\mathrm{d}W$ is a Wiener process. If we use the definitions of the forward and backward derivatives introduced in the previous section and apply them to the velocity, we obtain

$$m\mathcal{D}v = F - m\gamma v, \tag{2.24}$$

and

$$m\mathcal{D}^*v = F + m\gamma v. \tag{2.25}$$

If we sum the two equations, we obtain

$$a = \frac{\mathcal{D}v + \mathcal{D}^*v}{2} = \frac{F}{m}, \tag{2.26}$$

which is Newton's second law for conservative forces in the case of the Ornstein-Uhlenbeck process. The quantity a can be viewed as the mean acceleration of the particle.

2.3.2 Acceleration law of Nelson

Inspired by this result, we can define the acceleration of the particle in configuration space. Since the mean forward and backward velocities of the particle are given by $\mathcal{D}x$ and $\mathcal{D}^*x$, it is possible to use these to define the mean acceleration. We must ensure

---

[4] The osmotic velocity ensures the time reversibility of Nelson's dynamics by effectively *compensating* for the fluctuations experienced by the particle.

that it is time-reversible, *i.e.*, that the forward and backward mean accelerations are the same. Several choices are possible; one possibility is to use

$$a = \frac{1}{2}(\mathcal{D}\mathcal{D}^* + \mathcal{D}^*\mathcal{D})x = \frac{1}{2}(\mathcal{D}b^* + \mathcal{D}^*b), \tag{2.27}$$

which is consistent with the mean acceleration of the Ornstein-Uhlenbeck process while remaining within the configuration space approach. We will not explore other possibilities, such as $a = \frac{1}{2}(\mathcal{D}\mathcal{D} + \mathcal{D}^*\mathcal{D}^*)x$, because the choice in Eq. (2.27) allows us to recover standard quantum mechanics, as we will demonstrate later. However, Ref. [37] compares the consequences of different choices. Replacing the forward and backward derivatives and drifts with their expressions in terms of v and u leads to the acceleration law

$$a = \partial_t v + v\partial_x v - u\partial_x u - D\partial_x^2 u. \tag{2.28}$$

2.4 NELSON DESCRIPTION OF QUANTUM SYSTEMS

In the previous section, we discussed the implications of imposing time reversibility on a system whose dynamics are governed by a stochastic equation in configuration space. Now, we will apply these concepts to the description of a quantum system. We will see that Nelson's theory of quantum mechanics allows us to derive the Schrödinger equation as a consequence of these considerations [38, 39]. Note that a similar approach was developed by Fényes in 1952 in an independent work [40].

2.4.1 Physical background

Nelson, like de Broglie, assumed that it is possible to define trajectories for quantum particles. These trajectories are hidden from the observer, and the wavefunction alone is insufficient to fully describe the quantum system. The quantum particle undergoes a random motion whose origin will not be debated in this work, as this stochastic approach will only be used as a mathematical tool for controlling quantum systems. To describe the dynamics of the quantum particle, Nelson rejected the phase-space description[5] of motion in favor of a configuration space approach. He then postulated that the equation of motion is given by Eq. (2.9), which we recall here for clarity:

$$\mathrm{d}x(t) = b(x(t), t)\mathrm{d}t + \mathrm{d}W(t), \tag{2.29}$$

where the process is assumed to be Markovian. We will refer to this as Nelson's equation. To determine the amplitude of the Wiener process W, we need to specify the value of the diffusion coefficient D_{Q}. We know that quantum effects become less significant as the mass increases. Thus, we can assume that the diffusion coefficient is inversely proportional to the mass m of the quantum particle, leading to[6]

$$D_{\mathrm{Q}} = \frac{\hbar}{2m}, \tag{2.30}$$

---

[5] He argued that if we were to use a phase-space description, it would require the inclusion of a friction force. A particle in rectilinear uniform motion would experience this dissipative force, leading to a gradual decrease in its velocity. Conversely, a particle at rest would not be subject to this friction, contradicting the principle of relativity, which states that the laws of physics are the same in all inertial frames. Therefore, motion at rest cannot be distinguished from uniform motion.

[6] This choice is not unique, and other choices are possible as shown in Ref. [41].

where $\hbar$, identified as the reduced Planck constant, sets the scale at which quantum effects become significant. The statistical properties of W are then

$$\langle \mathrm{d}W(t)\rangle = 0 \qquad \text{and} \qquad \langle \mathrm{d}W(t)\mathrm{d}W(t+\mathrm{d}t)\rangle = 2D_{\mathrm{Q}}\mathrm{d}t. \tag{2.31}$$

The key distinction between classical stochastic mechanics and Nelson's equation is that the deterministic term, denoted as b, is not externally prescribed as in the case of an external force applied to a classical system. Instead, it is regarded as an intrinsic quantity of the model, similar to the de Broglie-Bohm approach, where the gradient of the phase drives the trajectories, as shown in Eq. (2.8). In Sec. 2.3.2, we explained that the external force allows the definition of the mean acceleration of the particle. However, it does not accelerate the particle, as its influence is observed at the level of the velocity. This is because Nelson's equation takes the form of an overdamped Langevin equation, representing a large friction limit[7] within the context of classical stochastic mechanics.

2.4.2 Derivation of the Schrödinger equation

In Sec. 2.2, we discussed the mathematical requirements to obtain a process whose probability density P satisfies both the forward and backward equations. We introduced two mean velocity fields, $v(x,t)$ and $u(x,t)$, given by Eq. (2.20) and Eq. (2.22) respectively, such that P satisfies the continuity equation Eq. (2.19) and Newton's second law Eq. (2.28) holds for externally prescribed forces. From these equations, it is possible to derive the Schrödinger equation, as we will show below. To do so, let us express the external force $F(x,t)$ as the gradient of a potential $V(x,t)$:

$$F(x,t) = -\partial_x V(x,t), \tag{2.32}$$

and assume that $v(x,t)$ can be written as the gradient of a velocity potential $S(x,t)$:

$$v(x,t) = \frac{\hbar}{m}\partial_x S(x,t). \tag{2.33}$$

Substituting Eq. (2.32) and Eq. (2.33) into the acceleration law Eq. (2.28), and integrating with respect to x, we obtain the quantum Hamilton-Jacobi equation (HJE):

$$\hbar\partial_t S(x,t) + \frac{\hbar^2}{2m}(\partial_x S(x,t))^2 + V(x,t) + V_{\mathrm{Q}}(x,t) = 0. \tag{2.34}$$

Classically, the HJE is an equation of analytical mechanics, derived after a transformation of the system's Hamiltonian in phase-space. It simplifies the resolution of the equations of motion and provides an alternative description of particle motion[8], which can be regarded as wave-like, thus connecting more closely with quantum mechanics [43, 44]. This equation is a first-order, non-linear partial differential equation. In quantum mechanics, it has the same form as in classical mechanics, but with an additional potential term called the quantum potential V_{Q}, defined as

$$V_{\mathrm{Q}}(x,t) = -\frac{\hbar^2}{2m}\frac{\partial_x^2\sqrt{P(x,t)}}{\sqrt{P(x,t)}}. \tag{2.35}$$

---

[7] This might seem paradoxical, given that quantum mechanics is a frictionless theoretical framework.

[8] It is also used in other fields, such as mathematics in dynamic programming, where it is a special case of the Hamilton-Jacobi-Bellman equation [42].

This potential was initially introduced in the de Broglie-Bohm formulation [32, 33], but it can also be derived from the standard formulation by writing the Madelung's equations[9]. This extra potential depends on the curvature of the amplitude of the probability density [49], but it is independent of the magnitude itself. It is a non-local potential [50] responsible for quantum effects, such as quantum interferences [51]. For example, it can explain the Aharanov-Bohm effect [52]. In the limit $\hbar \to 0$, this term vanishes, and the quantum Hamilton-Jacobi equation reduces to the classical Hamilton-Jacobi equation, whose solution S can be called the Hamilton's principal function, or the action [53]. The concept of the quantum potential highlights the departure of quantum mechanics from classical mechanics, emphasizing the wave-like nature of particles and the role of the wavefunction's structure in determining the dynamics of quantum systems.
From the continuity equation Eq. (2.19) and the quantum HJE Eq. (2.34), we can derive the Schrödinger equation. Indeed, by combining the function S and the probability density P as a complex function

$$\psi(x,t) = \sqrt{P(x,t)}\mathrm{e}^{iS(x,t)}, \tag{2.36}$$

it is possible to show that the Schrödinger equation

$$i\hbar\partial_t\psi(x,t) = -\frac{\hbar^2}{2m}\partial_x^2\psi(x,t) + V(x,t)\psi(x,t) \tag{2.37}$$

is satisfied by this function. The solution of Eq. (2.37) will be referred to as the wavefunction, as in standard quantum mechanics. Using the form Eq. (2.36), it is straightforward to rewrite the forward drift in Nelson's theory as

$$b(x,t) = \frac{\hbar}{m}\partial_x S(x,t) + D_{\mathrm{Q}}\partial_x \ln P(x,t) = \frac{\hbar}{m}\partial_x(\mathrm{Re}+\mathrm{Im})\ln\psi(x,t). \tag{2.38}$$

It is important to note that in Nelson's theory, the Schrödinger equation is a consequence of the theory, not an assumption as in the de Broglie-Bohm approach. One interesting subtlety to discuss is the quantization condition. If the Hamilton-Jacobi equation is derived from the Schrödinger equation, S is defined as the phase of the wavefunction, with values lying within an interval of 2π. However, in Nelson's approach, S is introduced as a velocity potential, with no such restriction on its values. The wavefunction is constructed from S and the probability density, and the quantization condition is not imposed on S, it is a continuous function. Then, although both equations take the same form, the solutions of Eq. (2.37) are not exactly the same as those of the standard Schrödinger equation, as the conditions on the multivaluedness of the wavefunction are not imposed in the same manner. See Ref. [54] for a deeper discussion on this point.
This distinction is important when considering the numerical resolution of Nelson's equation, as we will see in the next section. Finally, Nelson's equation is a stochastic equation that describes the trajectory of a single particle. Various interpretations can be given to this trajectory, and whether it has a true physical significance is not the focus of this work. It is interesting to note that the wavefunction of a quantum system describes the probability of finding the particle at a given position, while Nelson's equation provides a possible trajectory for this particle. However, a single trajectory by itself provides

---

[9] This is a reformulation of the Schrödinger equation in terms of the probability density and the velocity field (gradient of the phase) of the wavefunction. It consists of two coupled equations: one is the continuity equation, and the other is the Euler equation or the quantum Hamilton-Jacobi equation [45]. This reformulation allows quantum mechanics to be expressed in terms of hydrodynamic variables, similar to the Navier-Stokes equation in fluid mechanics [46, 47]. See Ref. [32, 48] for more details.

limited information about the quantum system; it is the ensemble of trajectories that is pertinent. Therefore, to describe a quantum system using Nelson's approach, we need to solve Nelson's equation multiple times, with different initial conditions, to obtain a statistical description of the quantum system. We expect that the ensemble of trajectories will yield results consistent with the wavefunction.

2.5 NUMERICAL RESOLUTION OF THE NELSON EQUATION

In this section, we will describe a numerical method for solving the Nelson equation. For simplicity, we will assume that the wavefunction of the quantum system is known analytically. If the wavefunction is not known, we must first solve the Schrödinger equation and address the numerical challenges associated with computing the gradient of its phase. The procedure for this is detailed in Appendix D. If the wavefunction is known, we can derive an analytical expression for the forward drift b that appears in the Nelson equation Eq. (2.29), enabling us to compute the trajectories of the quantum particles. To achieve this, we will use the Helfand-Greenside method [55], also known as Heun's method, a numerical scheme specifically adapted for stochastic differential equations. While other approaches, such as the Euler-Maruyama method or the Wright algorithm, are possible, we will not discuss them here. Due to the stochastic nature of the problem, standard numerical methods, like the Runge-Kutta methods, are not suitable, as we will explain below.

2.5.1 Discretization of the variables

Throughout the remainder of this chapter, we will use a system of units where $\hbar = 1$ and $m = 1$. In this system, the Nelson diffusion coefficient given by Eq. (2.30) simplifies to $D_{\mathrm{Q}} = 1/2$. As mentioned at the end of the previous section, we will solve the Nelson equation for different initial conditions to obtain a statistical description of the quantum system. This approach is equivalent to considering an ensemble of N independent particles, each following the Nelson equation. These particles will be indexed by n. To proceed, we need to discretize both time and space. There are two grids for space: a fixed grid and a moving grid. The fixed grid is evenly spaced with N_x increments of Δx, and the positions are denoted by x_j. The moving grid consists of the positions of each particle at a given time. The wavefunction, which is a solution of the Schrödinger equation, is defined on the fixed grid. When solving the Nelson equation, we evaluate the wavefunction and the drift b at the positions of the particles, which are on the moving grid. Time is divided into N_t values, t_i, with $0 \leq i \leq N_t - 1$, uniformly spaced with increments Δt. The position of a particle at time t_i is denoted as $x(t_i) = x_i$, and the function b, with arguments $x(t_i)$ and t_i, is written as $b_i = b(x_i, t_i)$. An increment of position $\mathrm{d}x(t_i) = \mathrm{d}x_i$ corresponds to the difference $x_{i+1} - x_i$.

2.5.2 Second-order Helfand-Greenside method

Deterministic differential equation To solve differential equations, it is common to use numerical schemes such as finite differences or Runge-Kutta methods [56, 57]. For a deterministic equation of the form

$$\mathrm{d}x(t) = b(x(t))\mathrm{d}t, \tag{2.39}$$

the solution can be expressed as

$$x(t+\Delta t) = x(t) + \int_t^{t+\Delta t} \mathrm{d}t_1 \; b\Big(x(t) + \int_t^{t_1} \mathrm{d}t_2 \; b(x(t) + \cdots)\Big), \tag{2.40}$$

and it is possible to truncate the integral at the desired order in Δt, leading to

$$x(t+\Delta t) = x(t) + \Delta t b(x(t)) + \frac{1}{2}\Delta t^2 b(x(t))b'(x(t)) \tag{2.41}$$

for the second order. The aim of the Runge-Kutta method is to express $x(t+\Delta t)$ as a linear combination of the values of b at specific points, thereby eliminating derivative terms. The solution can be written as

$$x(t+\Delta t) = x(t) + (A_1 g_1 + A_2 g_2)\Delta t, \tag{2.42}$$

where g_1 and g_2 are linear combinations of b, defined as

$$g_1 = b(x(t)), \tag{2.43}$$

$$g_2 = b(x(t) + \beta g_1 \Delta t), \tag{2.44}$$

with $A_1 + A_2 = 1$ and $A_2\beta = 1/2$. A Taylor expansion of Eq. (2.43) and Eq. (2.44) in Eq. (2.42) shows that it recovers Eq. (2.41).

Stochastic differential equation If we now add a Wiener process to the differential equation, we obtain a stochastic differential equation of the form

$$\mathrm{d}x(t) = b(x(t))\mathrm{d}t + \mathrm{d}W(t), \tag{2.45}$$

with $\langle W(t)\rangle = 0$ and $\langle W(t)W(t')\rangle = 2D_\mathrm{Q}(t-t')$. The variable x becomes a stochastic process, and its values do not exactly describe the system's dynamics; rather, its probability density does. This means that numerical schemes used to solve Eq. (2.45) must recover the statistical properties of x rather than its exact values at specific mesh points. However, the Wiener process introduces subtleties when adopting the same procedure as in the Runge-Kutta approach: the stochastic term cannot be written as an integer power of Δt in a Taylor expansion, as the variance of the Wiener process is proportional to the time increment. To address this issue, the Helfand-Greenside method [58, 59] was developed. This method is a stochastic extension of Runge-Kutta, where the coefficient g contains randomly generated terms labeled as Z_i, with statistical properties $\langle Z_i\rangle = 0$ and $\langle Z_i Z_j\rangle = \delta_{ij}$. A formal solution of Eq. (2.45) can be written as

$$\begin{aligned} x(t+\Delta t) =& x(t) + \int_t^{t+\Delta t} \mathrm{d}t_1 \; b\Big(x(t) + \int_t^{t_1} \mathrm{d}t_2 \; b(x(t) + \cdots) + w_0(t_1)\Big) \\ &+ w_0(\Delta t), \end{aligned} \tag{2.46}$$

where w_0 is a Wiener process. Expanding the right-hand side leads to

$$\begin{aligned} x(t+\Delta t) =& x(t) + \Delta t b(x(t)) + \frac{1}{2}\Delta t^2 b(x(t))b'(x(t)) \\ &+ w_0(\Delta t) + b'(x(t)) \int_t^{t+\Delta t} \mathrm{d}t_1 \; w_0(t_1) + \cdots . \end{aligned} \tag{2.47}$$

The difference with Eq. (2.41) lies in the second line of the right-hand side, which contains the Wiener process, involving terms of order $\Delta t^{1/2}$ or higher when averaged. Without delving into the detailed procedure, truncating the expansion at the second order yields a scheme that recovers the statistical properties of Eq. (2.47) and does not involve the derivatives of the drift:

$$x(t+\Delta t) = x(t) + \Delta t(A_1 g_1 + A_2 g_2) + \lambda_0 \sqrt{2D_{\mathrm{Q}}\Delta t}\ Z_0, \tag{2.48}$$

where g_1 and g_2 are defined as

$$g_1 = b(x(t) + \lambda_1 \sqrt{2D_{\mathrm{Q}}\Delta t}\ Z_1), \tag{2.49}$$

$$g_2 = b(x(t) + \beta g_1 \Delta t + \lambda_2 \sqrt{2D_{\mathrm{Q}}\Delta t}\ Z_2), \tag{2.50}$$

and the coefficients involved in the expansion must satisfy

$$A_1 + A_2 = 1, \tag{2.51}$$

$$\beta A_2 = \frac{1}{2}, \tag{2.52}$$

$$\lambda_0^2 = 1, \tag{2.53}$$

$$\lambda_0(A_1\lambda_1 + A_2\lambda_2) = \frac{1}{2}, \tag{2.54}$$

$$A_1\lambda_1^2 + A_2\lambda_2^2 = \frac{1}{2}, \tag{2.55}$$

with Z_0, Z_1, and Z_2 being three random variables following a normal distribution. In the following, we will use

$$A_1 = A_2 = \frac{1}{2}, \tag{2.56}$$

$$\beta = 1, \tag{2.57}$$

$$\lambda_0 = \lambda_2 = 1, \tag{2.58}$$

$$\lambda_1 = 0. \tag{2.59}$$

2.5.3 Methodology

Before providing numerical examples of the Nelson dynamics, let us summarize the entire procedure to solve a quantum problem using the Nelson formalism.

- Choose an initial guiding wavefunction $\psi(x,0)$ and the fixed spatial grid.
- Solve the Schrödinger equation. We assume an analytical solution for simplicity. If this is not the case, solve it numerically using the Crank-Nicolson scheme [60] (see Appendix C).
- Compute the real and imaginary parts of the wavefunction $\psi(x,t)$ and compute $b(x,t)$ using Eq. (2.38).
- Generate N independent particles, each with an initial position $x_n(0)$ randomly chosen according to the probability density $P(x,0) = |\psi(x,0)|^2$. If the shape of the initial wavefunction is not simple, it is possible to use the inverse transform sampling method [61] to generate the initial positions.
- Compute the trajectories of the particles using the second-order Helfand-Greenside method. Since it is necessary to evaluate the drift $b(x,t)$ on the moving grid, spline interpolation [62] can be used to interpolate the drift from the fixed grid.

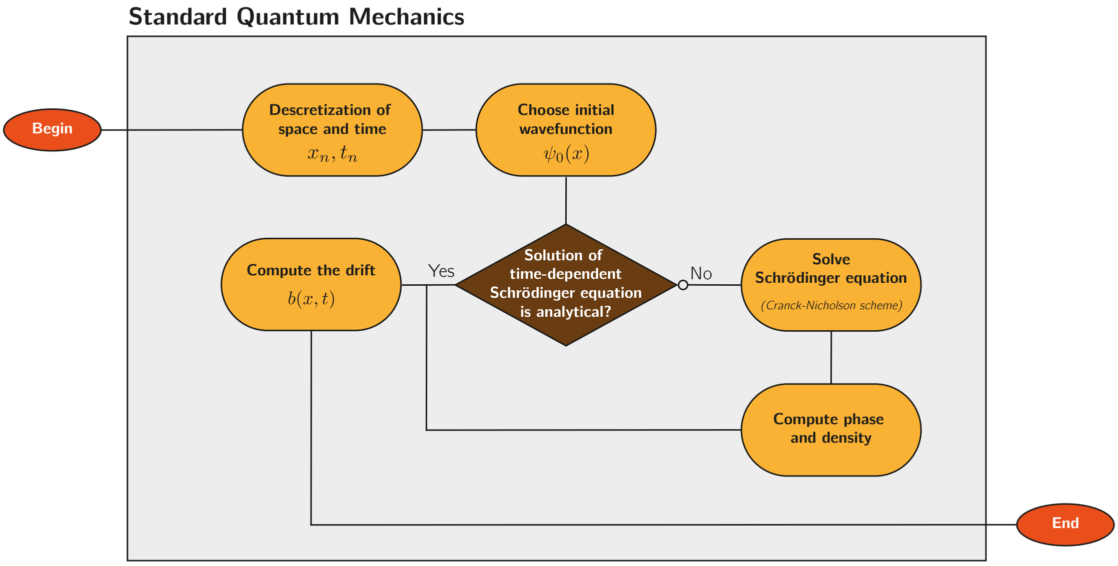

FIGURE 2.1: Diagram of the methodology to compute the drift of the Nelson equation.

- Verify that the probability density $P(x,t)$ obtained from the positions of the particles matches the squared modulus of the wavefunction by creating a histogram of the particle positions and interpolating the probability density from it using spline interpolation.

- Use the trajectories to compute the statistical properties of the quantum system, such as the mean position or the variance.

To provide a more visual understanding of the methodology, Fig. 2.1 and Fig. 2.2 illustrate the flowcharts for solving the Schrödinger equation and the Nelson equation, respectively. These diagrams summarize the steps required to tackle a quantum problem using the Nelson formalism. In the next section, we will apply this methodology to numerically study the quantum dynamics of a different system, for which we have an analytical expression for the wavefunction.

2.6 NUMERICAL EXAMPLES

In this section, we will apply the methodology described in the previous section to two different quantum systems. The first system is a free Gaussian wavepacket, for which we have an analytical solution of the wavefunction. The second system is a potential barrier, for which we can have an approximated analytical solution of the wavefunction.

2.6.1 Free Gaussian wavepacket

We consider the free Schrödinger equation in one dimension, given by

$$i\hbar\partial_t\psi(x,t) = -\frac{\hbar^2}{2m}\partial_x^2\psi(x,t), \tag{2.60}$$

with a Gaussian wavepacket as the initial condition

$$\psi(x,0) = \left(\frac{1}{2\pi\sigma_0^2}\right)^{1/4} \exp\left(-\frac{(x-\mu)^2}{4\sigma_0^2}\right), \tag{2.61}$$

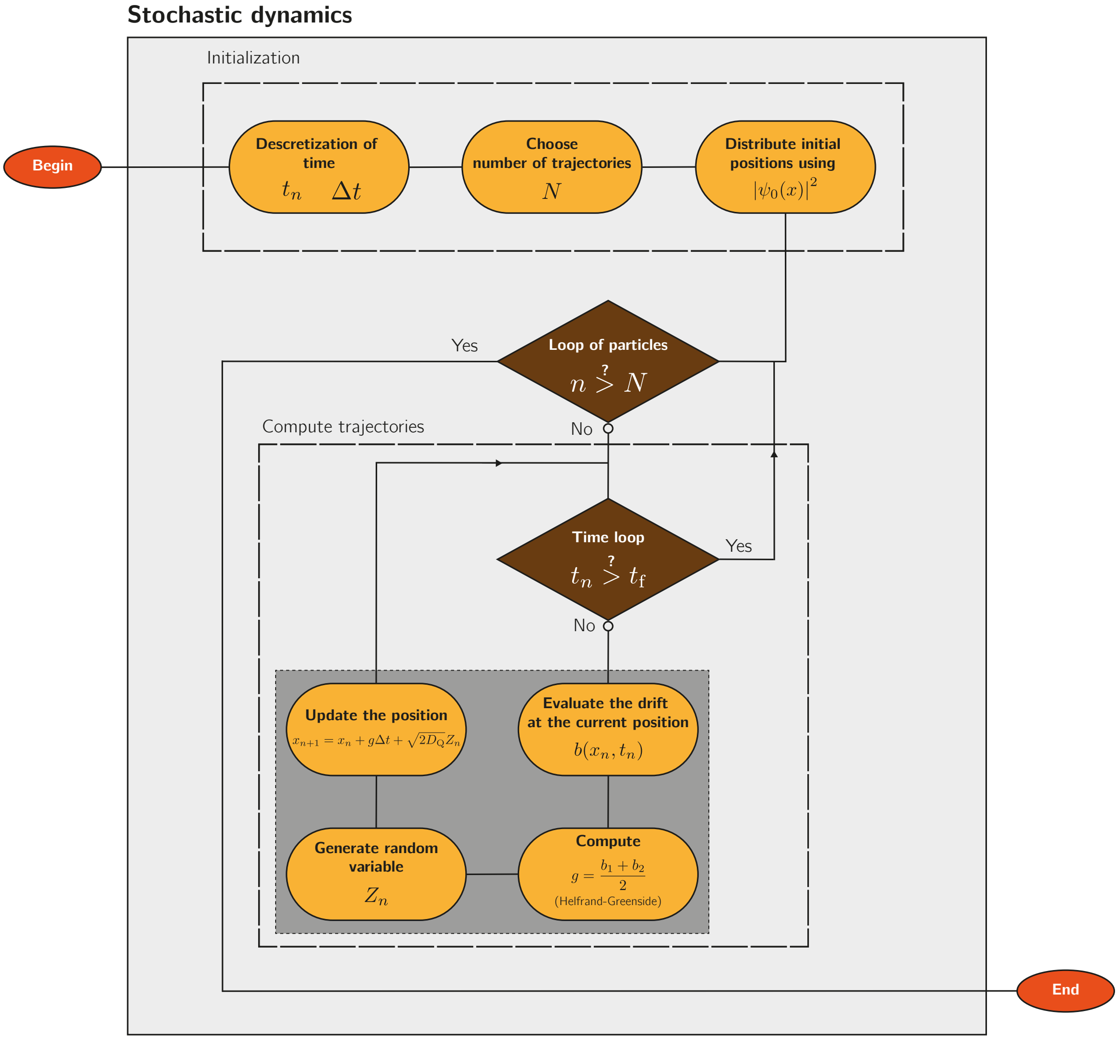

Figure 2.2: Flowchart of the algorithm to solve the stochastic Nelson equation.

where μ is the mean position of the wavepacket and σ_0 is the standard deviation. We consider that the wavevector of the wavepacket is zero, which is the same as being in the reference frame of the particle. In the following, we will show the shape of the Nelson's trajectories and use them to recover known results of the standard quantum mechanics. In particular, we will use the trajectories to show that the Heisenberg uncertainty principle is verified while we deal with particles possesing an exact position. To do so, we will use a theorem demonstrated by Shucker [63], saying that the limit

$$p = \lim_{t \to \infty} \frac{x(t) - x(0)}{t} \tag{2.62}$$

exists for almost every sample path of the Nelson process guided by a free Gaussian wavefunction. Moreover, it says that the values of p are distributed according to the Fourier transform $\tilde{\psi}_0$ of the initial wavefunction, *i.e.*

$$P(p) = \left| \tilde{\psi}_0(p, 0) \right|^2. \tag{2.63}$$

This encourages to interpret p as the own constant momentum of the trajectory, and to use it as the momentum involved in the position-momentum uncertainty relation. We will work with units such that $\hbar = 1$ and $m = 1$. Moreover, we choose $\sigma_0 = 1/\sqrt{2}$ and $\mu = 0$. The initial wavefunction is then given by

$$\psi(x,0) = \left(\frac{1}{\pi}\right)^{1/4} \exp\left(-\frac{x^2}{2}\right). \tag{2.64}$$

It is straightforward to show that the wavefunction at time t is given by

$$\psi(x,t) = \left(\frac{1}{\pi}\right)^{1/4} \frac{1}{\sqrt{1+it}} \exp\left(-\frac{(1-it)}{2(1+t^2)}x^2\right) \tag{2.65}$$

and using Eq. (2.38) we can compute the drift $b(x,t)$ as

$$b(x,t) = \frac{(t-1)x}{1+t^2}. \tag{2.66}$$

The Nelson equation is then given by

$$\mathrm{d}x(t) = \frac{(t-1)}{1+t^2}x(t)\mathrm{d}t + \mathrm{d}W(t). \tag{2.67}$$

We solve this equation for $N = 10^4$ independent trajectories with the following numerical parameters: the time step is $\Delta t = 10^{-2}$ for $N_t = 10^3$ time iterations, so that the final time is $t_\mathrm{f} = 10$. We plot the results in Fig. 2.3. The trajectories are depicted on the central panel, in black lines, the horizontal axis being the time t. Initially, the positions are distributed according to $|\psi(x,0)|^2$ as shown on the left panel: where the histogram of the position, in orange, fits the squared modulus of the initial wavefunction, in dashed red line. We see that all along the time evolution, this is still the case. Indeed, on the right panel we show the histogram of the positons also matches the squared modulus of the final wavefunction. For each trajectory we can compute the values of the momentum p. As, numerically, we are forced to use finite time, the values of p are approximated. In the limit of large time, the initial position becomes negligeable in Eq. (2.62) and we can approximate the momentum of the n^{th} trajectory $x^{(n)}$ as $p^{(n)} \approx x^{(n)}(t_\mathrm{f})/t_\mathrm{f}$. In Fig. 2.4 we compare the distributions of the values of p for the $N = 10^4$ trajectories for two final times $t_\mathrm{f} = 5$ (left panel) and $t_\mathrm{f} = 10$ (right panel). In dashed green lines we show the squared modulus of the Fourier transform of the initial wavefunction. We see that the distribution of the momentum is closer to the theoretical prediction for $t_\mathrm{f} = 10$ than for $t_\mathrm{f} = 5$. It ensures that $t_\mathrm{f} = 10$ is large enough to obtain the correct distribution of the momentum and to be a good approximation to the limit of Eq. (2.62), while $t_\mathrm{f} = 5$ is not. We can use the trajectories to compute the statistical properties of the quantum system. We will compute the variance on position and momentum and verify the uncertainty relation for $t_\mathrm{f} = 100$. To compute statistical quantities, we use the ensemble average over of this quantity the trajectories. For example, the average of the momentum is given by

$$\langle p \rangle = \left\langle \frac{x(t_\mathrm{f})}{t_\mathrm{f}} \right\rangle = \frac{1}{N}\sum_{n=1}^{N} \frac{x^{(n)}(t_\mathrm{f})}{t_\mathrm{f}}. \tag{2.68}$$

To verify the uncertainty relation, we compute the variance $\Delta(x(t_\mathrm{f}))$ and $\Delta(p)$ of the position and the momentum at the final time. Note that even if the p-distribution is the Fourier transform of the initial wavefunction, $\Delta(p)$ corresponds to the final p

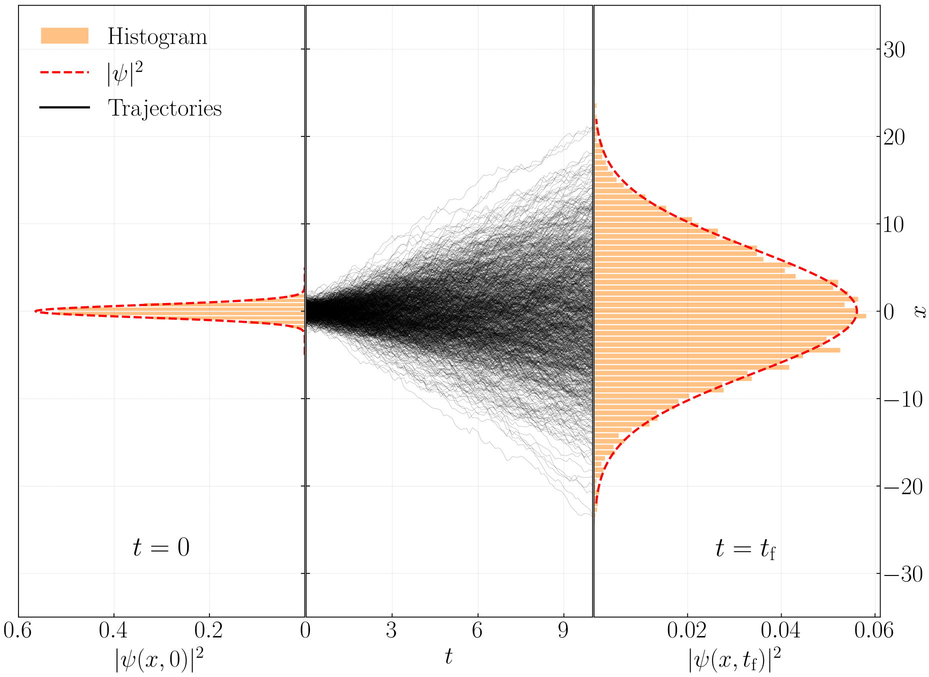

FIGURE 2.3: Evolution of particle trajectories under the Nelson equation. The central panel displays the trajectories of the first $N = 10^3$ particles as a function of time t, where the initial positions are sampled according to the distribution $|\psi(x,0)|^2$. The left panel shows the initial position distribution at $t = 0$, where the orange histogram represents the numerical results, and the red dashed line corresponds to the theoretical distribution $|\psi(x,0)|^2$. The right panel illustrates the final position distribution at $t_f = 10$, with the orange histogram and red dashed line representing the numerical and theoretical distributions $|\psi(x,t_f)|^2$, respectively. The close agreement between the histograms and the theoretical distributions indicates that the numerical solution accurately follows the expected quantum mechanical behavior.

dispersion as the moment variance is independent of the time in the case of a free Gaussian wavepacket[10]. They are given by

$$\Delta(x(t_\mathrm{f})) = \sqrt{\frac{1}{N-1}\sum_{i=1}^{N}\left(x^{(n)}(t_\mathrm{f}) - \langle x(t_\mathrm{f})\rangle\right)^2} \tag{2.69}$$

and

$$\Delta(p) = \Delta\left(\frac{x(t_\mathrm{f})}{t_\mathrm{f}}\right) = \sqrt{\frac{1}{N-1}\sum_{i=1}^{N}\left(\frac{x^{(n)}(t_\mathrm{f})}{t_\mathrm{f}} - \langle p\rangle\right)^2}. \tag{2.70}$$

We find $\Delta(x(t_\mathrm{f})) = 70.456$ and $\Delta(p) = 0.706$, so that their product is indeed larger to $\hbar/2 = 0.5$ and the uncertainty relation is verified. But we can go further, as a stronger form of the uncertainty inequality has been demonstrated by Golin in Ref. [64]. It says that

$$\Delta(x(t_\mathrm{f}))\Delta(p) \geq \sqrt{\mathrm{Cov}^2(x,p) + \frac{\hbar^2}{4}} \tag{2.71}$$

---

[10] This is straightforward to show it by computing $\sigma_p^2 = -\hbar^2 \langle\psi|\partial_x^2|\psi\rangle$. and using the Gaussian form of the wavefunction given by Eq. (2.65)

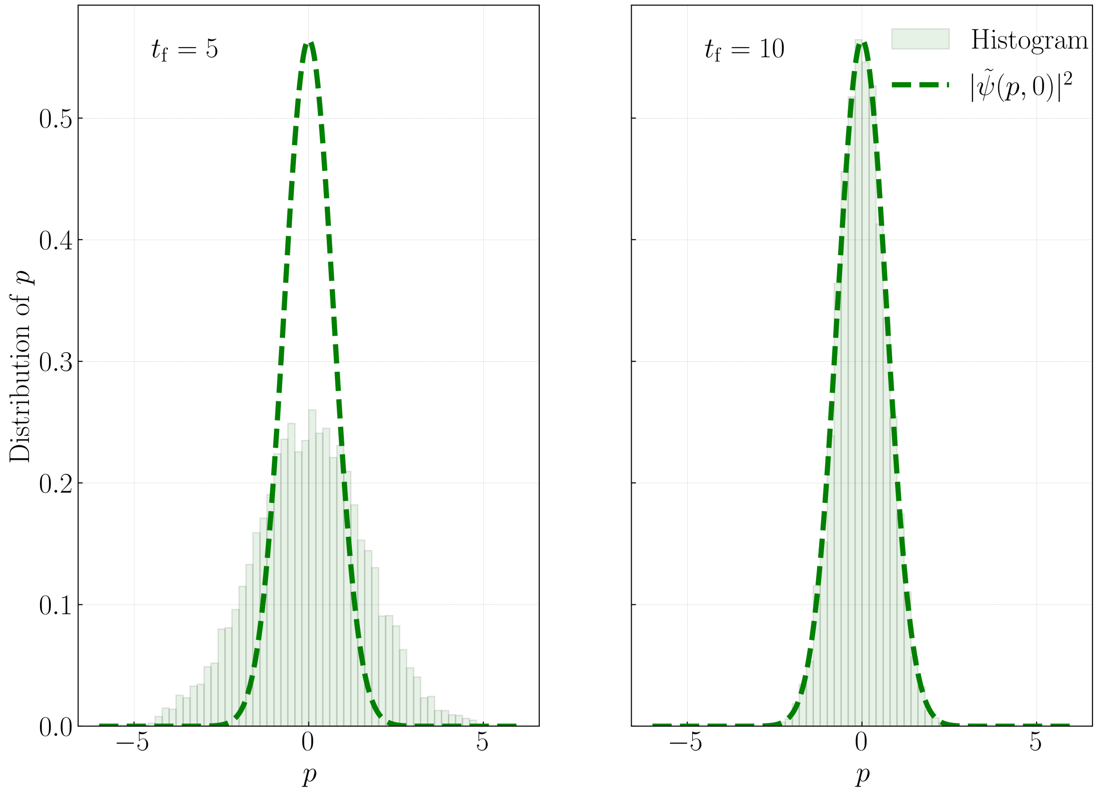

FIGURE 2.4: Comparison of momentum distributions for $N = 10^4$ trajectories at different final times. The left panel shows the momentum distribution at $t_f = 5$, while the right panel shows it at $t_f = 10$. The green histograms represent the numerically obtained momentum distributions, and the dashed green lines correspond to the theoretical prediction given by the squared modulus of the Fourier transform of the initial wavefunction. The closer agreement between the histogram and the theoretical curve at $t_f = 10$ indicates that the distribution of momentum better approximates the theoretical prediction for larger final times. This comparison ensures that the final time $t_f = 10$, used in the main simulation, is sufficiently large to approximate the correct momentum distribution.

where $\mathrm{Cov}(x,p)$ is the covariance of the position and the momentum and is defined as

$$\mathrm{Cov}(x,p) = \frac{1}{N-1}\sum_{i=1}^{N}\Big(x^{(n)}(t_{\mathrm{f}}) - \langle x(t_{\mathrm{f}})\rangle\Big)\left(\frac{x^{(n)}(t_{\mathrm{f}})}{t_{\mathrm{f}}} - \langle p\rangle\right). \tag{2.72}$$

We finally obtain $\mathrm{Cov}(x,p) = 49.736$, so that $\Delta(x(t_{\mathrm{f}}))\Delta(p) = 49.740 > 49.738 = (\mathrm{Cov}^2(x,p) + \hbar^2/4)^{1/2}$ and the stronger form of the uncertainty relation is also verified. We see that it is possible to find the statistical properties of the quantum system using the Nelson trajectories, instead of computing it from averages with the wavefunction.

2.6.2 Potential barrier

In quantum mechanics, the potential barrier system that allows us to study the quantum tunneling effect and the wavefunction reflection. In one dimension x, it is common to assume that a free particle arrives from the left side of the barrier ($x < 0$). If the system were classical, the particle would be reflected by the barrier and would not be able to pass through it, if its energy is lower than the potential energy of the barrier. However, in quantum mechanics, the wavefunction can tunnel through the barrier, and the particle can be found on the right side of the barrier ($x > 0$) with a non-zero probability. This is an interesting problem as theoretical physicists noted the relevance of the tunneling effect, more precisely they questioned a definition for the tunneling time [65, 66], which is the time associated to the passage of a particle through the barrier. While experiments tried to measure the time by a particle spent traversing the barrier while tunneling [67], no clear consensus exists about this definition, as there is no time operator in quantum mechanics. Then, a lot of different proposal for the time spent by a particle in the classical forbiden region of the potential barrier have been proposed [68–70]. Nelson's approach can be used to study this problem, as it gives a trajectory for the particle, and hence also a natural definition of the tunneling time. This kind of approach has been proposed in Ref. [71] where they use the collective motion of electrons flow in SGM (Scanning Gate Microscopy) to propose a ray-tracing approach and obtain effective quantum trajectories to describe the physics of the electrons in graphene junctions. Note that in this case, the potential barrier is given by the Lorentzian shape of the SGM tip. In the following, we will investigate the simple case of a rectangular potential barrier of height V_0 and width d. The Schrödinger equation is given by

$$i\hbar\partial_t\psi(x,t) = -\frac{\hbar^2}{2m}\partial_x^2\psi(x,t) + V(x,t)\psi(x,t), \tag{2.73}$$

where the potential barrier is given by

$$V(x) = V_0[\Theta(x) - \Theta(x-d)] = \begin{cases} 0 & \text{if} \quad x < 0 \\ V_0 & \text{if} \quad 0 \leq x \leq d \\ 0 & \text{if} \quad x > d \end{cases} \tag{2.74}$$

with V_0 the height of the barrier, d the width and Θ the Heaviside step function. The barrier is centered at $x = d/2$. We want to consider a Gaussian wavepacket arriving on the barrier. However Eq. (2.73) does not have an analytical solution. To adress this issue, as proposed in Ref [72], we can decompose the wavefunction on the eigenstates φ_k of the Hamiltonian such as

$$\psi(x,t) = \int_{-\infty}^{+\infty} \mathrm{d}k \; A(k)\mathrm{e}^{-ikx_0}\varphi_k(x)\mathrm{e}^{iE_kt/\hbar} \tag{2.75}$$

where $A(k)$ is the weight of the eigenstate φ_k in the wavefunction, x_0 is the initial mean position of the wavepacket and E_k the eingenenergy of the k^{th} eigenfunction, defined as the energy of free wave propagating with a wavevector k, such as

$$E_k = \frac{\hbar^2k^2}{2m}. \tag{2.76}$$

. To obtain an initial Gaussian wavefunction, $A(k)$ is also chosen to be a Gaussian as

$$A(k) = N\mathrm{e}^{-(k-k_0)^2/4\sigma^2} \tag{2.77}$$

where N is a constant that ensures the normalisation of the wavefunction, k_0 the mean wavevector of the wavefunction, *i.e.* the mode that contributes most. Then σ is the width of the distribution of the modes and gives the modes around k_0 that contributes to ψ. The width of $\psi(x,0)$ is inversely proporitional to σ. The mean energy of the wavepacket is given by $E = \frac{\hbar^2}{2m}\left(k_0^2 + \sigma^2\right) = E_{k_0} + E_\sigma$ where E_{k_0} is the energy of the mode k_0 and $E_\sigma = \frac{\hbar^2\sigma^2}{2m}$ is the energy contribution of the width of the distribution of the modes. If we suppose that $E < V_0$, we are in the tunneling situation. The eigenstates of the Hamiltonian are defined by part in three different regions: the region I where $x < 0$, the region II where $0 \leq x \leq d$ and the region III where $x > d$. In total[11], it is given as

$$\varphi_k(x) = \begin{cases} \mathrm{e}^{ikx} + r_k \mathrm{e}^{-ikx} & \text{if} \quad x < 0 \\ c_k \mathrm{e}^{\kappa_k x} + d_k \mathrm{e}^{-\kappa_k x} & \text{if} \quad 0 \leq x \leq d \\ t_k \mathrm{e}^{ikx} & \text{if} \quad x > d \end{cases} \tag{2.78}$$

where r_k and t_k are the reflection and transmission amplitude coefficients, c_k and d_k are the amplitude of the wavefunction in the barrier and $\kappa_k = \sqrt{2m(V_0 - E_k)}/\hbar$. This amplitude coefficient can be computed by imposing the continuity of the wavefunction and its derivative at $x = 0$ and $x = d$. They are given by

$$\begin{pmatrix} r_k \\ t_k \\ c_k \\ d_k \end{pmatrix} = \beta_k \begin{pmatrix} -i(k^2 + \kappa_k^2)\sinh(\kappa_k d) \\ 2k\kappa_k \mathrm{e}^{ikd} \\ k(\kappa_k + ik)\mathrm{e}^{-\kappa_k d} \\ k(\kappa_k - ik)\mathrm{e}^{\kappa_k d} \end{pmatrix} \tag{2.79}$$

where

$$\beta_k = \frac{1}{2k\kappa_k \cosh(\kappa_k d) + i(\kappa_k^2 - k^2)\sinh(\kappa_k d)}. \tag{2.80}$$

Fig. 2.5 shows the shape of the potential barrier and a schematic view of the eigenfunction in the three regions, for a given k. To illustrate how Nelson's theory can be employed to estimate key quantities in quantum scattering problems through particle trajectories, we start by computing these trajectories by solving the Nelson equation, using the wavefunction given by Eq. (2.75) as a guiding function whose shape is represented on Fig. 2.6 for different times. In this study, we consider a system with $N = 10^4$ particles, using the same system of units as in previous sections, with $\hbar = 1$ and $m = 1$. The parameters under consideration are the ratio between the potential height and the mean energy of the wavefunction, V_0/E, and the potential width d, which is expressed in units of $1/k_0$. Fig. 2.7 presents the trajectories of the first thousand particles, under the conditions $V_0 = 3E$, $d = 1/k_0$ with $k_0 = 5$, $\sigma = 0.5$, and $x_0 = -5$. The left panel of the figure depicts the initial spatial distribution of the particles, shown in orange, which aligns with the squared modulus of the initial wavefunction, represented by the dashed red line. The right panel illustrates the final spatial distribution of the particles, also in orange, fitting the squared modulus of the final wavefunction, again indicated by the dashed red line. The inset in central panal provides a closer look at the particle trajectories in two scenarios: one where the particle is reflected by the potential barrier and another where it tunnels through the barrier. For short times, both paths look like free particle motion. Then they are distorted close to the barrier. Note that the trajectories are reflected before they actually reach the barrier at $x = 0$ because they are guided by the (non-local) wavefunction, which generates the Bohm potential. As a result, the particles feel the influence of the barrier before they encounter it. The transmitted trajectory looks like a free particle motion again. We see in the central panel that the interferences present in the wavefunction are also manifested in the particle trajectories, as the particles' paths are influenced by the wavefunction. This phenomenon is particularly evident

---

[11] As we consider a continuity of modes, it is possible that modes k whose energy E_k is higher than V_0 are involved. In this case, we use $\kappa_k = i\sqrt{2m(E_k - V_0)}/\hbar$, $\cosh(ix) = \cos(x)$ and $\sinh(ix) = i\sin(x)$ to compute the eigenfunctions.

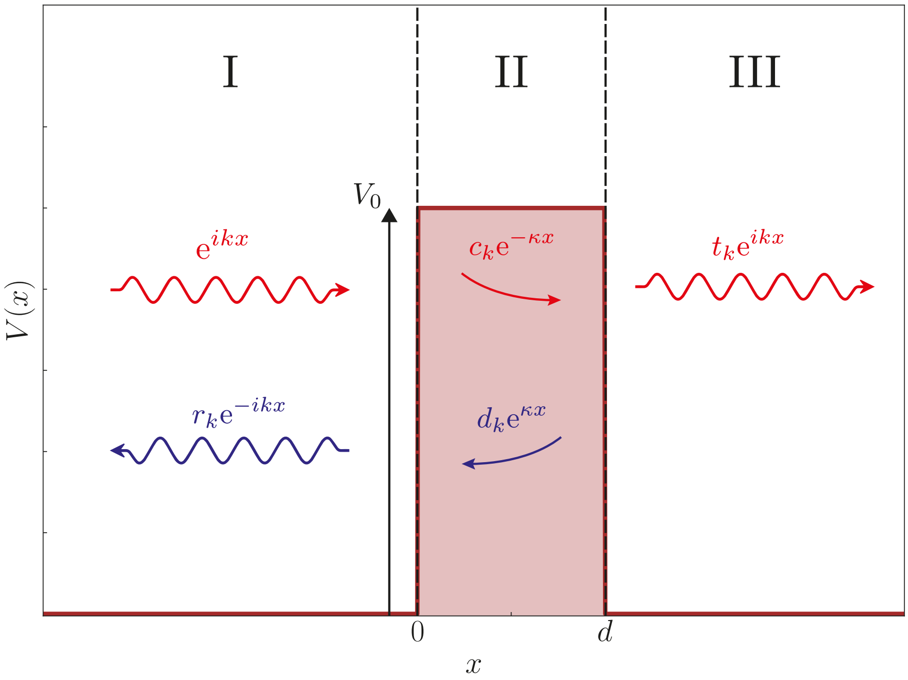

Figure 2.5: Schematic representation of the potential barrier and the corresponding eigenfunction in the three regions: region I where $x < 0$, region II where $0 \leq x \leq d$, and region III where $x > d$. The potential barrier is depicted as a step potential, and the eigenfunction $\varphi_k(x)$ is illustrated in each region for a given wavevector k. In region I, the eigenfunction consists of an incident wave and a reflected wave, in region II it is a combination of exponentially decaying and growing solutions, and in region III, it consists of a transmitted wave. The coefficients r_k, t_k, c_k, and d_k correspond to the reflection, transmission, and amplitude of the wavefunction in the barrier, respectively. These coefficients are determined by ensuring the continuity of the wavefunction and its derivative at the boundaries $x = 0$ and $x = d$.

in the regions around $t = 1.00$, where alternating regions of intense black and white are observed, corresponding to areas of constructive and destructive interference. From the trajectories, we can see that it is straightforward to obtain two interesting quantities: the ratio between the number of trajectories that crosses the barrier and the total number trajectories, and the time needed for a trajectory to cross the barrier.

Transmission Coefficient The transmission coefficient for a given mode k is defined as the squared modulus of the transmission amplitude, as given by the second expression in Eq. (2.79), *i.e.*,

$$T_k = |t_k|^2 = \frac{1}{1 + \frac{V_0^2 \sinh^2\left(\sqrt{\kappa_k d}\right)}{4E_k(V_0 - E_k)}}. \tag{2.81}$$

In the scenario where the contribution of the width of the wavefpacket, $E_\sigma = \hbar^2\sigma^2/2m$, is negligible compared to the compribution of a mean mode, $E_{k_0} = \hbar^2 k_0^2/2m$, the total transmission coefficient can be approximated by the transmission coefficient corresponding to the mode k_0. However, if this condition does not hold, the total transmission coefficient is determined by the ratio of the integral of the squared modulus of the trans-

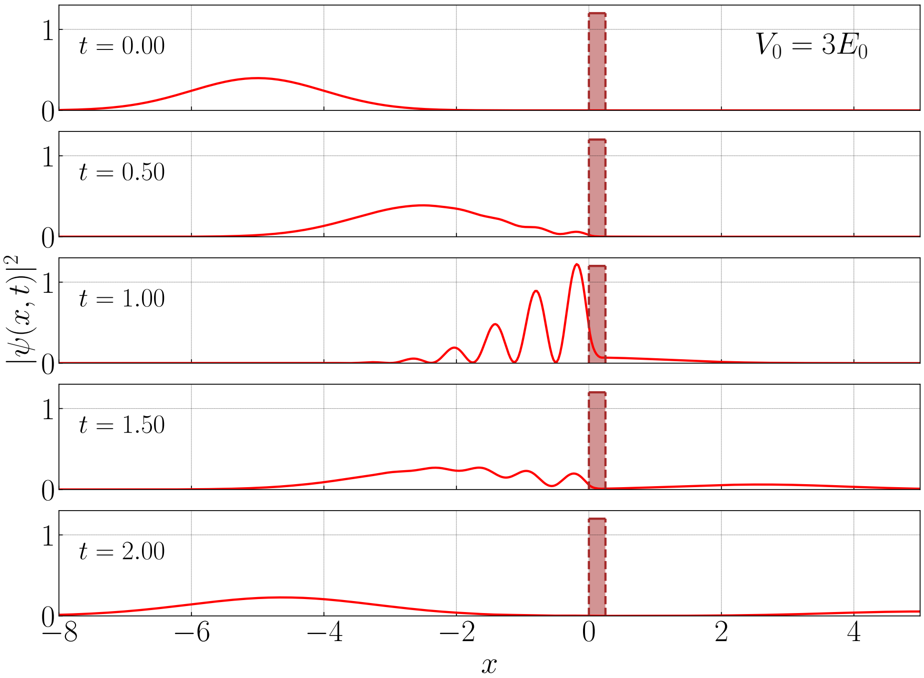

Figure 2.6: Time evolution of the squared modulus of the wavefunction $|\psi(x,t)|^2$, for $V_0 = 3E$, $\sigma = 0.5$ and $d = 1/k_0$ with $k_0 = 5$, used as a guiding function in solving the Nelson equation for estimating key quantities in quantum scattering problems. The figure displays the shape of $|\psi(x,t)|^2$ at different times, showing how the wavefunction evolves from an initial state at $t = 0$ to later times $t = 0.50$, $t = 1.00$, $t = 1.50$, and $t = 2.00$. This wavefunction serves as the guiding function in the computation of particle trajectories, providing insight into the dynamics of the scattering process. Initially, the wavefunction is a Gaussian wavepacket centered at $x = -5$, and as time progresses, it encounters the potential barrier at $x = 0$ (in dark red). At $t = 1.00$ there is the apparition of interference fringes, resulting of the superposition of the incident and reflected waves. The wavefunction is then split into two parts: one that is reflected by the barrier and another that tunnels through it.

mitted amplitude at long times to the integral of the squared modulus of the initial incoming wave packet. Given that the weight function $A(k)$ is normalized to unity, the total transmission coefficient is expressed as

$$T = \lim_{t\to\infty} \frac{\int_{-\infty}^{+\infty} \mathrm{d}x\ \left|\psi^{\mathrm{t}}(x,t)\right|^2}{\int_{-\infty}^{+\infty} \mathrm{d}x\ \left|\psi^{\mathrm{i}}(x,0)\right|^2} = \frac{\int_{-\infty}^{+\infty} \mathrm{d}k\ |t_k|^2 |A(k)|^2}{\int_{-\infty}^{+\infty} \mathrm{d}k\ |A(k)|^2} = \int_{-\infty}^{+\infty} \mathrm{d}k\ T_k \mathrm{e}^{-(k-k_0)^2/2\sigma^2}. \quad (2.82)$$

This quantity can also be obtained using particle trajectories by counting the number of particles that traverse the barrier, N_{t}, and comparing it to the total number of particles, N. We can then compare the transmission coefficient obtained from these trajectories with the theoretical prediction. In Fig. 2.8, this ratio is shown for various values of V_0/E. Two scenarios are considered: one where E_σ is negligible compared to E_{k_0} (left panel), and another where it is not (right panel). The parameters selected are $k_0 = 5$ and $\sigma = 0.5$ (so that $E_\sigma/E_{k_0} = 10^{-2}$), and $k_0 = 1$ and $\sigma = 1$ (so that $E_\sigma = E_{k_0}$), respectively. Additionally, two barrier widths are considered: $d = 1/k_0$ and $d = 5/k_0$. In all cases, N_{t}/N, represented by the blue circled and red squared points, converges toward

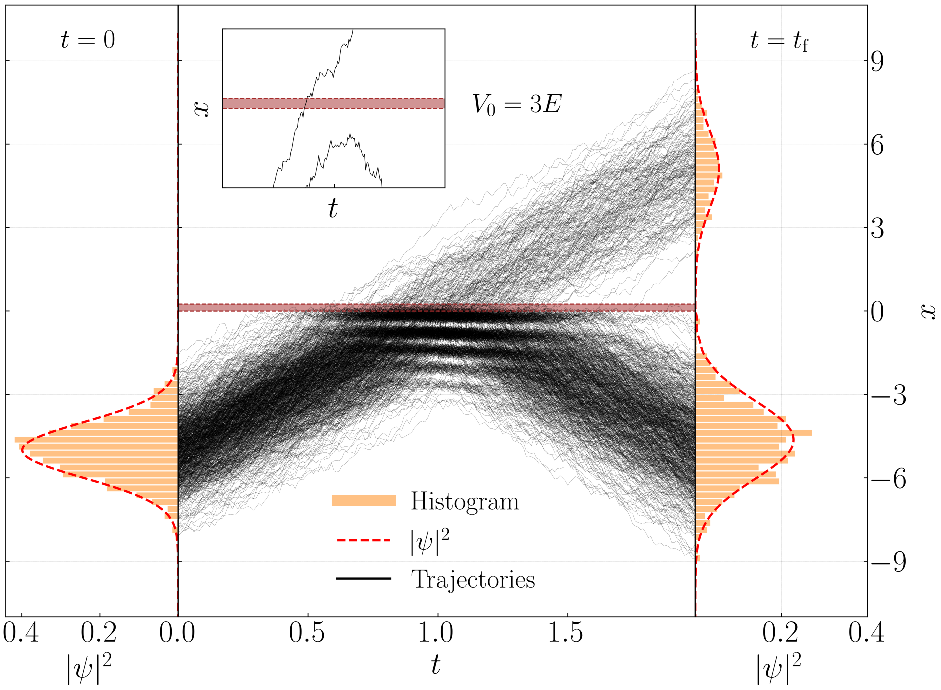

Figure 2.7: Trajectories of the first thousand particles in a system with $N = 10^4$ particles, under the conditions $V_0 = 3E$, $d = 1/k_0$ with $k_0 = 5$, $\sigma = 0.5$, and $x_0 = -5$. The left panel shows the initial spatial distribution of particles (orange histogram), which matches the squared modulus of the initial wavefunction (dashed red line). The right panel illustrates the final spatial distribution of the particles, again represented by an orange histogram, which aligns with the squared modulus of the final wavefunction (dashed red line). The central panel displays the particle trajectories over time, where the interference patterns of the wavefunction are visible in the trajectories as alternating regions of constructive and destructive interference. The potential barrier is represented in dark red at $x = 0$. The inset provides a detailed view of particle trajectories in two scenarios: one where the particle is reflected by the potential barrier and another where it tunnels through the barrier.

the theoretical prediction, represented by small dotted lines and given by Eq. (2.81) for the transmission coefficient associated to the single mode k_0 and Eq. (2.82) for the total transmission coefficient, obtained by the summation over all the modes involved in the wavepacket. In the left panel, these points closely follow the curves given by T_{k_0}. In the right panel, they align well with the curves representing the total transmission coefficient but deviate significantly from the dotted line, which represents the transmission coefficient associated with the mode k_0. This figure demonstrates that particles tend to tunnel more effectively through a barrier of large width when E_σ is not negligible, as more high-energy modes contribute to the tunneling process. This scenario will be explored further in next paragraph.

Tunneling Time The tunneling time refers to the duration a particle spends within the classically forbidden region of a potential barrier. It provides important insights into the time taken by a particle to cross the barrier. Using the classical definition of the time spent by a particle in a certain region, as discussed in Ref. [73, 74], we can define the

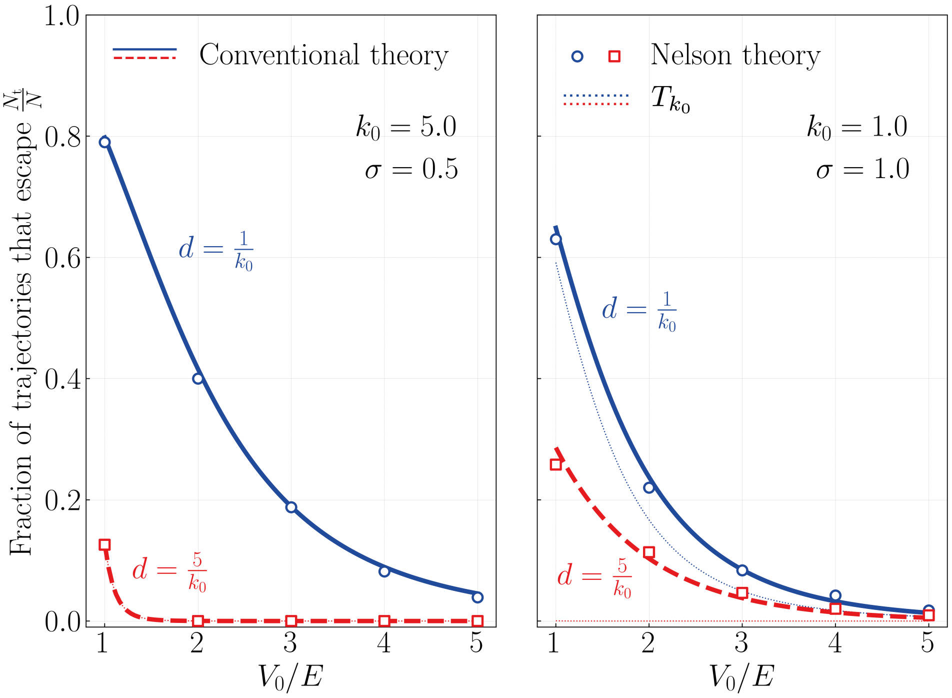

Figure 2.8: Comparison of the transmission coefficient from particle trajectories with the theoretical prediction for different values of V_0/E. The left panel shows a case where E_σ is small compared to E_{k_0}, with parameters $k_0 = 5$ and $\sigma = 0.5$. The right panel shows a case where $E_\sigma = E_{k_0}$, with $k_0 = 1$ and $\sigma = 1$. Two barrier widths are considered: $d = 1/k_0$ (blue curves and circles) and $d = 5/k_0$ (red curves and squares). The blue circles and red squares represent the ratio N_t/N from the particle trajectories, which converge to the transmission coefficient predicted by conventional theory, from equation 2.82, shown as solid and dashed lines. The dotted lines represent the single-mode transmission, T_{k_0}. In the left panel, they overlap with the solid and dashed lines because k_0 is the dominant mode, while in the right panel, they deviate significantly due to the involvement of more modes in the wavepacket. The figure shows that particles tunnel more effectively through a wide barrier when E_σ is not negligible, as higher-energy modes contribute to the tunneling process.

tunneling time τ_n for each trajectory n that successfully crosses the barrier at the final time as

$$\tau_n = \int_{t_\mathrm{i}}^{t_\mathrm{f}} \mathrm{d}t \; \Theta(x_n(t))\Theta(d - x_n(t)), \tag{2.83}$$

where the mean tunneling time is then obtained as the sample average of these individual tunneling times, *i.e.*,

$$\langle\tau\rangle = \frac{1}{N_\mathrm{t}} \sum_{n=1}^{N_\mathrm{t}} \tau_n. \tag{2.84}$$

Here, we assume that the trajectories labeled from $n = 1$ to $n = N_\mathrm{t}$ correspond to those that have successfully tunneled through the barrier. By collecting these transmitted trajectories, a statistical distribution of the tunneling times can be constructed, allowing for the computation of its mean value. We calculate the tunneling time first for a fixed barrier width $d = 6/k_0$, varying the ratio V_0/E from 1 to 12 (see Fig. 2.9), and then for a fixed value of $V_0/E = 3$ while varying d from $2/k_0$ to $14/k_0$ (see Fig. 2.10), both

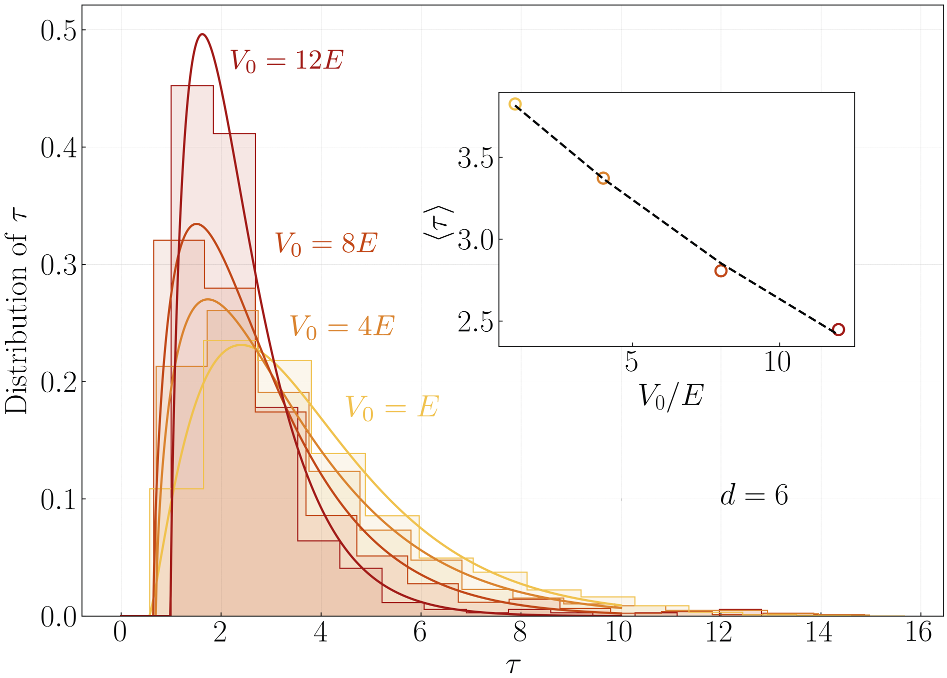

Figure 2.9: Distribution of tunneling times τ for different potential heights $V_0 = E$, $4E$, $8E$, and $12E$, with a fixed barrier width $d = 6/k_0$. The histogram bin number is chosen accord to Sturges's formula. The distribution of tunneling times fits well with a gamma distribution represented by solid lines. The inset shows the mean tunneling time $\langle\tau\rangle$ as a function of the ratio V_0/E, fitted by a decreasing exponential function. As V_0/E increases, the mean tunneling time decreases, and the distribution of tunneling times becomes narrower, consistent with theoretical expectations. The parameters used are $k_0 = 1$, $\sigma = 1$, and $x_0 = -10$.

cases with $k_0 = 1$ and $\sigma = 1$. In both figures, the tunneling time of the N_t transmitted trajectories is computed, and the corresponding histograms are plotted. We observe that the distribution of the tunneling time, denoted $P(\tau)$, follows a gamma distribution

$$P(\tau) = \frac{1}{\beta^\alpha \Gamma(\alpha)} \tau^{\alpha-1} \mathrm{e}^{-\tau/\beta}, \tag{2.85}$$

where α and β represent the shape and scale parameters of the distribution, respectively, and Γ is the Euler gamma function. The mean tunneling time is given by $\langle\tau\rangle = \alpha\beta$, with the variance expressed as $\Delta\tau = \alpha\beta^2$. In Fig. 2.9, the mean tunneling time, fitted with a decreasing exponential function, decreases as the ratio V_0/E increases, consistent with the expectations outlined in Ref. [72]. Additionally, the distribution of the tunneling time becomes narrower for larger values of V_0/E. In Fig. 2.10, the mean tunneling time increases with the barrier width d, as particles must traverse a greater distance to cross the barrier, while the distribution of tunneling times broadens. The inset of the figure shows that for large d, the mean tunneling time is proportional to d (see the balck dashed line that fits the bullets), following a WKB-like approximation as discussed in Ref. [75]. This approximation assumes that within the region $0 \leq x \leq d$, the wavefunction can be approximated by

$$\psi(x,t) \approx \psi^{\mathrm{WKB}}(x) \sim \exp(-\kappa x). \tag{2.86}$$

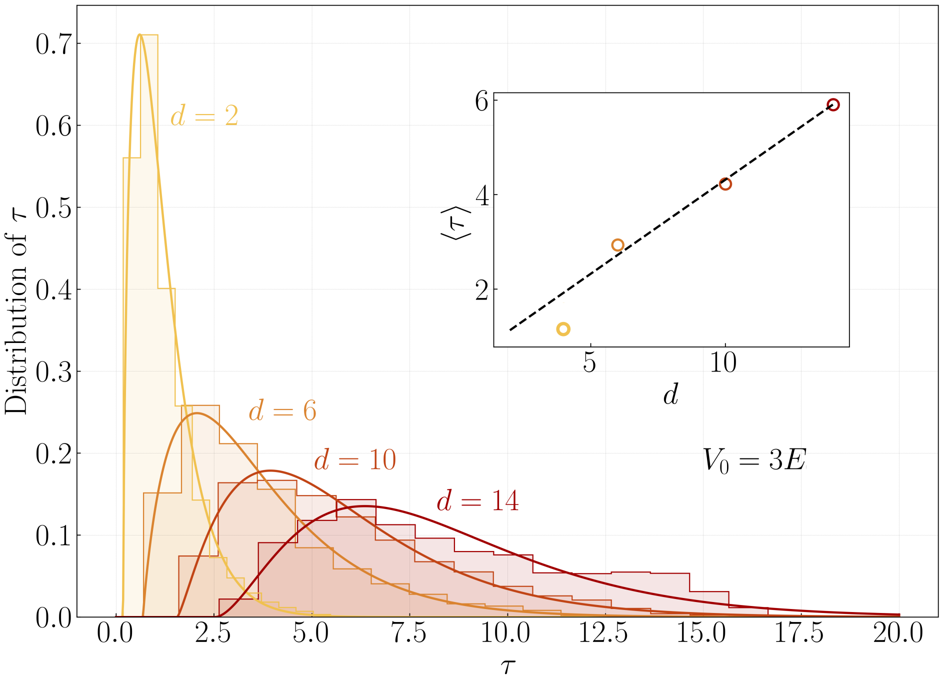

Figure 2.10: Distribution of tunneling times τ for different barrier widths $d = 2/k_0$, $6/k_0$, $10/k_0$, and $14/k_0$, with $V_0 = 3E$. The tunneling time distributions fit well with a gamma distribution. The inset shows the mean tunneling time $\langle \tau \rangle$ as a function of the barrier width d, which follows a linear trend for larger d, consistent with the WKB-like approximation. The parameters used are $k_0 = 1$, $\sigma = 1$, and $x_0 = -10$.

This form of the wavefunction leads to a drift coefficient b in the Nelson equation given by $b = -\hbar\kappa/m$, which in turn yields a Fokker-Planck equation of the form

$$\partial_t P = \left(\frac{\hbar\kappa}{m} \partial_x + \frac{\hbar}{2m} \partial_x^2 \right) P, \tag{2.87}$$

with a solution

$$P(x,t) \sim \exp\left(- \frac{\left(\frac{x}{d} - 1 + \frac{t}{\tau_{\mathrm{c}}} \right)^2}{\frac{t}{\tau_{\mathrm{D}}}} \right), \tag{2.88}$$

where $\tau_{\mathrm{c}} = d/\hbar\kappa$ is the time required for the particle to cross the barrier, and $\tau_{\mathrm{D}} = md^2/\hbar$ is the characteristic time associated with the diffusion of the density. The mean tunneling time is thus given by $\langle \tau \rangle = \tau_{\mathrm{c}}$. This approximation holds for large values of κd, where $\tau_{\mathrm{c}} \ll \tau_{\mathrm{D}}$, rendering the diffusion effects negligible. However, we observe that for $d = 4/k_0$, the mean tunneling time deviates from the WKB approximation. Finally, as highlighted in Ref. [76], it is noteworthy that the distribution of tunneling times exhibits properties that *reveal the wave-particle duality in the tunneling phenomenon*. Specifically, if the parameter α is kept constant, we find that $\Delta\tau \propto \langle \tau \rangle$, which mirrors the statistical properties of the photon number in a Glauber coherent state of light [77]. Conversely, if β remains constant, we have $\Delta\tau \propto \sqrt{\langle \tau \rangle}$, aligning with the statistical properties of the position of a Brownian particle, as discussed in Chap. 1.

It is important to note that the tunneling time is not an observable in the strict quantum mechanical sense, as it does not correspond to the eigenvalue of an operator. However, it may be associated with characteristic times of observables that are intrinsically linked to the tunneling process.

2.7 CONCLUSION

In this chapter, we explored the Nelson formalism of quantum mechanics, which provides a framework for describing quantum particles with well-defined trajectories, similar to the de Broglie-Bohm theory. However, the two theories differ in several key aspects. In both approaches, the wavefunction of the system satisfies the Schrödinger equation, but in Nelson's theory, this equation is derived from an acceleration law, whereas in the de Broglie-Bohm theory, it is assumed as a postulate (even if for Nelson's approach, the conditions on the multivaluedness of the wavefunction are not imposed in the same manner).

Moreover, while de Broglie-Bohm's dynamics is purely deterministic, with randomness arising from the unknown initial conditions of particle trajectories, Nelson's approach introduces intrinsic stochasticity. In Nelson's formalism, the motion of the particle includes a Wiener process term, which provides an additional interpretation to the probabilistic nature of quantum systems. This stochastic component is absent in the de Broglie-Bohm theory.

Nelson's formalism can also be more suitable for solving certain types of problems. For instance, it is particularly useful for calculating tunneling times (as discussed earlier) or tackling Kramers-like problems, such as the mean first passage time in a bi-stable potential. Nelson's theory is well-suited for these cases, as it can leverage techniques already developed in classical stochastic mechanics (*e.g.*, for overdamped Langevin dynamics, Kramers' problem is well-known, see Ref. [21, 78] for details). In the same spirit, as we will see in Chap. 4, stochastic trajectories allow the creation of classical analogues of quantum systems and the application of optimization techniques originally developed for classical systems to quantum systems. For a detailled discussion of the differences between the two theories, see Ref. [79].

Importantly, neither Nelson's nor de Broglie-Bohm's theory conflicts with Bell's theorem [80], as both theories remain non-local. The wavefunction, which is defined over the entire space, guides the particle's motion, maintaining the non-local character of quantum mechanics. We showed how Nelson's approach introduces randomness into the motion of particles, which is responsible for the probabilistic nature of quantum theory. The Nelson equation, discussed in detail, combines both predictable (deterministic) and random (stochastic) elements to describe particle motion in a quantum system. We have demonstrated that Nelson's formalism is equivalent to standard quantum mechanics, as the wavefunction solution to the Schrödinger equation can be constructed by ensuring that the probability density satisfies both the forward and backward Fokker-Planck equations.

To illustrate how the formalism works in practice, we applied Nelson's theory to two examples: a free Gaussian wave packet and a particle encountering a potential barrier. These examples helped us understand quantum phenomena, such as tunneling, in terms of trajectories. In particular, we explored how a particle can pass through a barrier that, according to classical mechanics, should not be passed as the particle does not have enough energy. These cases demonstrated how Nelson's approach can be used to calculate not only particle trajectories but also important statistical properties, such as the momentum distribution and the tunneling time, which agree with the predictions of quantum theory.

Overall, the Nelson formalism offers an alternative perspective on quantum mechanics, focusing on an ensemble of effective particle trajectories while remaining consistent with the broader framework of quantum theory.

While our study was restricted to spinless particles, it is possible to extend Nelson's theory to particles with spin [81, 82]. Additionally, stochastic mechanics can be seen as a reformulation of Feynman's path integral theory [83], and the Nelson equation can be derived from a variational approach [36].

KEY TAKEAWAYS

This chapter has been devoted to developing the Nelson formalism of quantum mechanics. We have demonstrated that this approach introduces the concept of trajectories for quantum particles, in a manner similar to the de Broglie-Bohm theory. The trajectories are determined by solving the Nelson equation

$$\mathrm{d}x(t) = b(x(t), t)\mathrm{d}t + \mathrm{d}W(t),$$

where the term b represents the mean velocity, defined as

$$b = \frac{\hbar}{m}\partial_x S + D_{\mathrm{Q}}\partial_x \ln\rho,$$

with S being the phase of the wavefunction and ρ the probability density, such that

$$\psi(x,t) = \sqrt{\rho(x,t)}\exp(iS(x,t)).$$

The stochastic term $W(t)$ is a Wiener process that introduces the probabilistic nature of the theory, with its statistical properties given by

$$\begin{cases} \langle W(t)\rangle = 0, \\ \langle W(t)W(t+\mathrm{d}\tau)\rangle = 2D_{\mathrm{Q}}\mathrm{d}\tau, \end{cases}$$

where $D_{\mathrm{Q}} = \hbar/2m$ is the diffusion coefficient of the stochastic process. The wavefunction still satisfies the Schrödinger equation

$$i\hbar\partial_t\psi = -\frac{\hbar^2}{2m}\partial_x^2\psi + V\psi,$$

but it can be useful to express it as the Madelung equations by separating the real and imaginary parts of the equation, resulting in a continuity equation and a quantum Hamilton-Jacobi equation

$$\begin{cases} \partial_t\rho + \dfrac{\hbar}{m}\partial_x(\rho\partial_x S) = 0, \\ \partial_t S + \dfrac{1}{2m}(\partial_x S)^2 + V + V_{\mathrm{Q}} = 0. \end{cases}$$

with

$$V_{\mathrm{Q}} = -\frac{\hbar^2}{2m}\frac{\partial_x^2\sqrt{\rho}}{\sqrt{\rho}}$$

the non-local quantum potential, responsible of the quatum interferences. The continuity equation can further be rewritten as a diffusion equation

$$\partial_t\rho + \partial_x(b\rho) = D_{\mathrm{Q}}\partial_x^2\rho,$$

which corresponds to the Fokker-Planck equation associated with Nelson's equation.

REFERENCES

[21] Kramers, H. A. *Physica* **1940**, *7*, 284–304.

[30] Schrödinger, E *Sitzungsber. Preuss. Akad. Phys. Math. Klasse* **1931**, 144.

[31] Nelson, E. *Physical Review* **1966**, *150*, 1079–1085.

[32] Bohm, D. *Physical Review* **1952**, *85*, 166–179.

[33] Bohm, D. *Physical Review* **1952**, *85*, 180.

[34] Holland, P. R., *The Quantum Theory of Motion: An Account of the de Broglie-Bohm Causal Interpretation of Quantum Mechanics*; Cambridge University Press: Cambridge, 1993.

[35] Bacciagaluppi, G.; Valentini, A., *Quantum Theory at the Crossroads: Reconsidering the 1927 Solvay Conference*; Cambridge University Press: Cambridge, 2009.

[36] Guerra, F. *Physics Reports* **1981**, *77*, 263–312.

[37] Kyprianidis, A. *Foundations of Physics* **1992**, *22*, 1449–1483.

[38] Nelson, E., *Dynamical Theories of Brownian Motion*; Princeton University Press.: 1967.

[39] De la Peña, L.; Cetto, A. M. *Foundations of Physics* **1982**, *12*, 1017–1037.

[40] Fényes, I. *Zeitschrift für Physik* **1952**, *132*, 81–106.

[41] Davidson, M. *Letters in Mathematical Physics* **1979**, *3*, 271–277.

[42] Kalman, R. E., *The Theory of Optimal Control and the Calculus of Variations*; Research Institute for Advanced Studies: 1960; 31 pp.

[43] Goldstein, H., *Classical Mechanics*; Addison-Wesley Publishing Company: 1980; 696 pp.

[44] Sakurai, J. J.; Napolitano, J., *Modern Quantum Mechanics*; Cambridge University Press: 2017; 569 pp.

[45] Hiley, B. J.; Callaghan, R. E. *Foundations of Physics* **2012**, *42*, 192–208.

[46] Navier, *Mémoire sur les lois du mouvement des fluides*, 1827; Vol. 6; 440 pp.

[47] Stokes, G. G., *On the Theories of the Internal Friction of Fluids in Motion and of the Equilibrium and Motion of Elastic Solids*, 1845; Vol. 8; 305 pp.

[48] Bohm, D.; Hiley, B. J., *The Undivided Universe: An Ontological Interpretation of Quantum Theory*; Routledge: 1995; 347 pp.

[49] Wyatt, R. E.; Bittner, E. R. *The Journal of Chemical Physics* **2000**, *113*, 8898–8907.

[50] Bohm, D. J.; Hiley, B. J. *Foundations of Physics* **1975**, *5*, 93–109.

[51] Philippidis, C.; Dewdney, C., et al. *Il Nuovo Cimento B (1971-1996)* **1979**, *52*, 15–28.

[52] Philippidis, C.; Bohm, D., et al. *Il Nuovo Cimento B (1971-1996)* **1982**, *71*, 75–88.

[53] Hand, L. N.; Finch, J. D., *Analytical Mechanics*; Cambridge University Press: 1998; 598 pp.

[54] Wallstrom, T. C. *Physical Review A* **1994**, *49*, 1613–1617.

[55] McClendon, M.; Rabitz, H. *Physical Review A* **1988**, *37*, 3479–3492.

[56] Kutta; Wilhelm, *Beitrag Zur Naherungsweisen Integration Totaler Differentialgleichungen*; Teubner: 1901.

[57] Runge; König, *Vorlesungen Über Numerisches Rechnen*; Springer: 1924.

[58] Helfand, E. *Bell System Technical Journal* **1979**, *58*, 2289–2299.

[59] Greenside, H. S.; Helfand, E. *The Bell System Technical Journal* **1981**, *60*, 1927–1940.

[60] Crank, J.; Nicolson, P. *Mathematical Proceedings of the Cambridge Philosophical Society* **1947**, *43*, 50–67.

[61] Monahan, J. F. *Mathematics of Computation* **1985**, *45*, 559–568.

[62] Schoenberg, I. J. In *Spline Functions and Approximation Theory: Proceedings of the Symposium Held at the University of Alberta, Edmonton May 29 to June 1, 1972*, Meir, A., Sharma, A., Eds.; Birkhäuser: Basel, 1973, pp 277–327.

[63] Shucker, D. S. *Journal of Functional Analysis* **1980**, *38*, 146–155.

[64] Golin, S. *Journal of Mathematical Physics* **1985**, *26*, 2781–2783.

[65] Büttiker, M.; Landauer, R. *Physical Review Letters* **1982**, *49*, 1739–1742.

[66] Lee, H.-W.; Scully, M. O. *Foundations of Physics* **1983**, *13*, 61–72.

[67] Martinis, J. M.; Devoret, M. H., et al. *Physica B: Condensed Matter* **1988**, *152*, 159–161.

[68] Wigner, E. P. *Physical Review* **1955**, *98*, 145–147.

[69] Büttiker, M. *Physical Review B* **1983**, *27*, 6178–6188.

[70] Sokolovski, D.; Baskin, L. M. *Physical Review A* **1987**, *36*, 4604–4611.

[71] Guerra, M. Electron Optics in Ballistic Graphene Studied by Scanning Gate Microscopy, Ph.D. Thesis, Université Grenoble Alpes, 2021.

[72] Imafuku, K.; Ohba, I., et al. *Physics Letters A* **1995**, *204*, 329–335.

[73] Muga, J. G.; Leavens, C. R. *Physics Reports* **2000**, *338*, 353–438.

[74] Kudo, T.; Nitta, H. *Physics Letters A* **2013**, *377*, 357–361.

[75] Imafuku, K.; Ohba, I., et al. *Physical Review A* **1997**, *56*, 1142–1153.

[76] Hara, K.; Ohba, I. *Physical Review A* **2003**, *67*, 052105.

[77] Glauber, R. J. *Physical Review* **1963**, *131*, 2766–2788.

[78] Pollak, E.; Grabert, H., et al. *The Journal of Chemical Physics* **1989**, *91*, 4073–4087.

[79] Bacciagaluppi, G. In World Scientific, Singapore: 2005, p 367.

[80] Bell, J. S. *Physics Physique Fizika* **1964**, *1*, 195–200.

[81] Dankel, T. G. *Archive for Rational Mechanics and Analysis* **1970**, *37*, 192–221.

[82] Nelson, E. *Journal of Physics: Conference Series* **2012**, *361*, 012011.

[83] Feynman, R. P. *Reviews of Modern Physics* **1948**, *20*, 367–387.

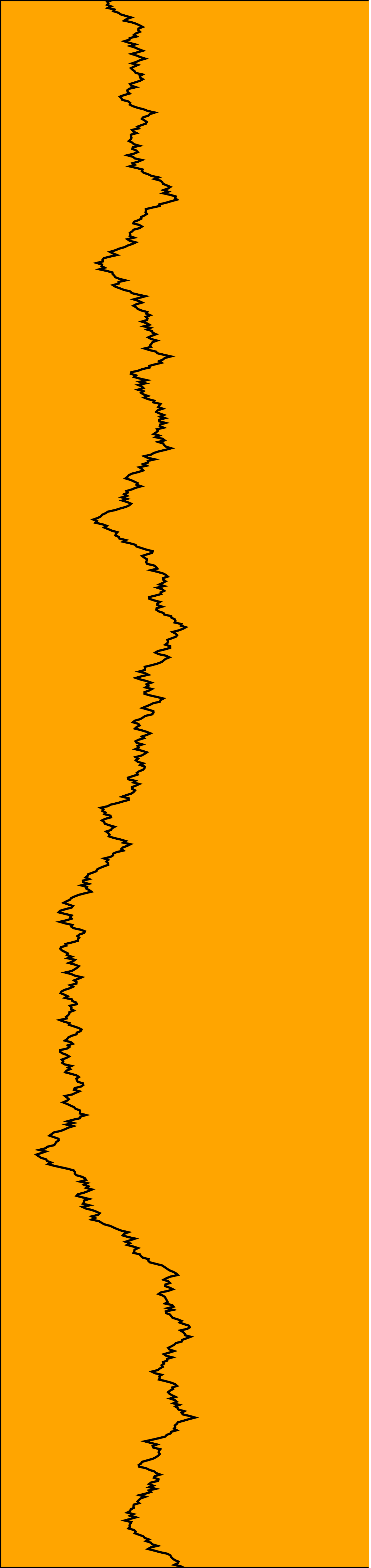

PART II

Applications of Nelson's mechanics

PREFACE OF PART II

> *A human being is a part of the whole called by us universe, a part limited in time and space. He experiences himself, his thoughts and feeling as something separated from the rest, a kind of optical delusion of his consciousness. This delusion is a kind of prison for us, restricting us to our personal desires and to affection for a few persons nearest to us. Our task must be to free ourselves from this prison by widening our circle of compassion to embrace all living creatures and the whole of nature in its beauty.*
>
> — A. Einstein

In the first part of this thesis, we introduced two important theoretical frameworks: the Langevin theory and the Nelson theory. These represent classical and quantum perspectives that, at first glance, may seem quite different. This part focuses on the Nelson formulation of Quantum Mechanics and its applications. The aim is to demonstrate how this theory can address fundamental questions in Quantum Mechanics, while also providing a practical tool for optimizing the dynamics of quantum systems.

To begin, in Chap. 3, we will explore the foundations of the Born rule in Quantum Mechanics, particularly within the framework of the Nelson approach. The Born rule is a fundamental principle in Quantum Mechanics, and we will investigate how Nelson's theory can provide insight into the emergence and understanding of this rule. Understanding the Born rule is crucial, as it dictates how probabilities are assigned to different outcomes in quantum experiments.

Following this, the second half of this part, covered in the last two chapters, shifts toward the practical applications of Nelson's theory for optimizing the behavior of quantum systems. In Chap. 4, we will focus on the dynamics of a quantum harmonic oscillator, deriving a quantum-classical analogy from Nelson's stochastic interpretation of quantum mechanics. This analogy will help us explore how to optimize the motion and behavior of the oscillator, potentially leading to more efficient control over quantum systems, based on optimization techniques that have already been developed for classical systems.

Finally, in Chap. 5, we will attempt to extend this framework to open quantum systems, where the system interacts with its environment. We will study various effective approaches to model this situation and examine how classical analogies can be extended to open systems. This would allow the use of optimization techniques from classical stochastic thermodynamics to develop quantum heat engines by optimizing the system parameters' cycles (such as temperature or stiffness).

CHAPTER 3

RELAXATION TO QUANTUM EQUILIBRIUM

The belief that there is only one truth and that
oneself is in possession of it seems to me the root of
all the evil that is in the world.
— M. Born

In this chapter, we investigate the relaxation to quantum equilibrium within Nelson's stochastic quantization framework, focusing on the emergence of the Born rule in quantum mechanics. By numerically simulating the dynamics of quantum systems initialized in non-equilibrium states that violate the Born rule, we study the convergence towards quantum equilibrium for three canonical systems: the double-slit experiment, the harmonic oscillator, and quantum particles in a gravitational field. Our results show that, in the cases of the double-slit experiment and the harmonic oscillator, the relaxation to quantum equilibrium occurs faster than the appearance of quantum interference patterns, suggesting that observable quantum phenomena are equilibrium phenomena. However, for quantum particles in a gravitational field, we find that quantum interference can emerge before the system reaches quantum equilibrium, opening the possibility of observing deviations from the Born rule in such systems. The chapter is organized as follows. In Sec. 3.1, we introduce the foundational questions surrounding the Born rule and its role in quantum mechanics. Sec. 3.2 provides a brief recall of Nelson's stochastic quantization. In Sec. 3.3, we discuss how to quantify the distance to quantum equilibrium and the relaxation towards it. Sec. 3.4 presents numerical simulations for the double-slit experiment, the harmonic oscillator, and quantum particles in a gravitational field. Finally, conclusions are drawn in Sec. 3.5.

Contents

3.1 Introduction

Quantum mechanics (QM) has raised innumerable foundational questions since its formalization in the early twentieth century. Most of those questions arise from two "weird" properties of QM, which single it out from earlier physical theories: (i) QM is an intrinsically probabilistic theory, meaning that its outcomes can only be predicted on average, and (ii) quantum probabilities do not follow the same rules as classical ones, inasmuch as in QM probability amplitudes are additive, and not the probabilities themselves[1]. This fact is encapsulated into Born's rule [85], which defines quantum probabilities as the squared modulus of complex amplitudes.

The first of these properties was the source of much controversy at the dawn of QM, because earlier fundamental theories were all deterministic. Being capable of predicting with virtually perfect accuracy a physical event (*e.g.*, an eclipse or the passage of a comet) was seen as the hallmark of a rigorous physical theory, the kind of achievement that gave Newton's and Maxwell's theories all their prestige. Besides, just a few years earlier, Boltzmann had shown how to bridge the gap between reversible macroscopic motion at the molecular level and irreversible heat and matter diffusion at the macroscopic scale. It was natural, then, to assume that also the randomness of QM could one day be explained in a similar fashion.

However, it is the second property that poses the hardest foundational questions – and is also at the heart of the spooky action at a distance first highlighted in the celebrated Einstein-Podolsky-Rosen (EPR) paper [86], and later confirmed in many experiments, mainly based on John Bell's extension to spin states of the original EPR argument [87]. Born's rule is at the heart of these "weird" features of QM and, for this reason, deserves some special attention. Indeed, Born's rule stands alone in the mathematical machinery of QM, and is employed only when one needs to translate the abstract wavefunction into an actual prediction about probabilities of outcomes. We also note that, while the Schrödinger equation is linear in the wavefunction, Born's rule, which is quadratic, reinstates some nonlinearity into the theory.

It is well-known that in some nonlocal hidden-variable theories [88], such as the Bohm-de Broglie version of QM (also known as Bohmian mechanics), the Born rule needs not necessarily be satisfied[2]. In the Bohm-de Broglie mechanics [32], if an ensemble of trajectories satisfies Born's rule at a certain initial time $t = 0$, *i.e.* if $P(x, t = 0) = |\psi(x, t = 0)|^2$ (where P is the probability density of the position variable x and ψ is the wavefunction), then this property will always be satisfied for any subsequent time $t > 0$. But the equations of the Bohm-de Broglie mechanics remain perfectly valid also when one takes $P(x, t = 0) \neq |\psi(x, t = 0)|^2$, *i.e.*, if Born's rule is violated. In that case, the two quantities $P(x, t)$ and $|\psi(x, t)|^2$ will remain distinct for all later times.

In the context of the Bohm-de Broglie mechanics, Valentini [89] suggested that the Born rule is the analogue of thermal equilibrium in classical statistical mechanics. In the latter, non-equilibrium states are possible during transient evolutions, but the system eventually relaxes to its thermal equilibrium, given for instance by a Maxwellian probability distribution. In the same fashion, Valentini postulated that the Bohm-de Broglie distribution of positions may in general differ from that given by Born's rule, and only relaxes

---

[1] It is possible to formulate QM in terms of ordinary probabilities, provided that these are allowed to take negative values (see, for instance, Ref. [84] and references therein). This is another manifestation of the weirdness of quantum theory.

[2] Strictly speaking, actual ensembles in experiments only have a finite number of particles N, so that these theories always violate the Born rule. Here, we mean that the latter may be violated even in the limit $N \to \infty$.

to it in a finite (albeit fast) timescale. Hence, the standard distribution that satisfies Born's rule corresponds to a sort of *quantum equilibrium* defined by $P = |\psi|^2$, although quantum non-equilibrium states with $P \neq |\psi|^2$ may also exist during short transients (this is referred to as "subquantum dynamic" by Valentini). The possibility of finding signatures of subquantum dynamics in the primordial universe was also suggested [90, 91].

Just like in standard statistical mechanics, quantum-equilibrium distributions are much more probable than non-equilibrium ones (they are *typical*, in a technical sense[3]) and therefore should be observed most of the time, which is of course the case in all known experiments. From a dynamical point of view, non-equilibrium distributions will typically converge to quantum equilibrium. Earlier numerical simulations [96] showed that relaxation to equilibrium is indeed observed, provided some coarse graining procedure is applied.

An alternative, and perhaps more appropriate, avenue to study such convergence to quantum equilibrium is to resort to Nelson's stochastic quantization [31, 97, 98]. As detailed in the next section, Nelson's dynamics is similar to the Bohm-de Broglie mechanics, with the important difference that the equations of motion are not deterministic, but rather stochastic with a diffusion coefficient equal to $\hbar/2m$, where $\hbar$ is the reduced Planck constant and m the mass. Nelson's theory reproduces standard QM when the Born rule is satisfied at the initial time. When this is not the case, the distribution P will converge to the Born rule value $|\psi|^2$, without any need for an artificial coarse graining procedure, thanks to the stochastic nature of the dynamics. Hence, Nelson's approach appears to be particularly adapted to investigate subquantum physics and the relaxation to quantum equilibrium.

Of course, one would also need to postulate a mechanism through which a quantum particle could find itself at quantum non-equilibrium. Although we do not have a theory for such a mechanism, we may conjecture that fundamental processes – such as beta decay or particle-antiparticle pair production – generate quantum particles that are, at least at the very early stages, out of quantum equilibrium. Indeed, during such processes the quantum particles are created *ex nihilo* and may not have had enough time to relax to the Born rule. We will not try to justify or explore any further this speculative conjecture. Our purpose here is merely to investigate what happens *if*, for whatever reason, Born's rule is at some point violated.

Within this framework, an important question is whether quantum thermalization occurs faster than any typical quantum effect, such as interference. If this is the case, it would mean that all typically quantum phenomena are "equilibrium" phenomena and hence indistinguishable from standard QM. In the opposite case (*i.e.*, quantum interference occurring before relaxation), one could hope to observe some anomaly in the interference pattern due to subquantum corrections. If true, this would be an appealing prediction for future experiments.

In this chapter, we investigate this topic by means of numerical simulations of Nelson's stochastic dynamics, for three relevant cases: (i) a standard double-slit interference setup, (ii) a harmonic oscillator, and (iii) quantum particles in a gravity field, such as ultracold neutrons in the gravitational field of the Earth [99]. The next section is devoted to a brief description of Nelson's approach to QM. In Sec. 3.3, we illustrate how to quantify the distance to quantum equilibrium and the relaxation towards it. Sec. 3.4 includes the numerical results for the three physical systems mentioned above. Finally, conclusions

---

[3] For a definition of typicality in statistical mechanics, see [92, 93], and in the Bohm-de Broglie theory, see [94, 95].

are drawn in Sec. 3.5.

3.2 Reminder of Nelson's stochastic quantization

In the Bohm-de Broglie theory [32], particles have a well-defined position $x(t)$, and their trajectories evolve according to a deterministic law of the type:

$$\frac{\mathrm{d}x(t)}{\mathrm{d}t} = u(x,t), \tag{3.1}$$

where the velocity $u(x,t)$ is related to the phase of the wavefunction, which satisfies the standard time-dependent Schrödinger equation. In particular, writing the wavefunction in polar coordinates

$$\psi(x,t) = R(x,t)\,\mathrm{e}^{iS(x,t)},$$

where $R(x,t)$ is the amplitude and $S(x,t)$ is the phase, one has that $u = \hbar\partial_x S/m$. Note that, in the present work, we will always consider one-dimensional problems.

In contrast, in Nelson's dynamics [31, 97] the particles obey a Langevin equation

$$\mathrm{d}x(t) = b(x(t),t)\mathrm{d}t + \mathrm{d}W(t), \tag{3.2}$$

where $b(x(t),t)$ is the deterministic velocity and $W(t)$ is a stochastic Wiener process. The latter is characterized by a zero mean $\langle \mathrm{d}W\rangle = 0$ and a finite variance

$$\langle \mathrm{d}W^2\rangle = D_Q \equiv \frac{\hbar}{2m}, \tag{3.3}$$

with D_Q the quantum diffusion coefficient. The origin of such Brownian motion with diffusion coefficient D_Q was not specified by Nelson, and here we just assume the presence of some universal force agitating all quantum particles. We also note that similar stochastic theories have been discussed by Bohm and Hiley [100], Peruzzi and Rimini [101], as well as Bohm and Vigier [102].

In Nelson's theory, the total velocity $b(x,t)$ is written as the sum of two terms:

$$b(x,t) = \frac{\hbar}{m}\frac{\partial}{\partial x}S(x,t) + 2D_Q\frac{\partial}{\partial x}\ln R(x,t), \tag{3.4}$$

where the first term (drift velocity) is proportional to the gradient of the phase and is identical to the velocity of the Bohm-de Broglie model, while the second term (osmotic velocity) depends on the amplitude R.

The wavefunction follows the standard Schrödinger equation $i\hbar\partial_t\psi(x,t) = \hat{H}\psi(x,t)$, with Hamiltonian $\hat{H} = \hat{p}^2/2m + \hat{V}(x,t)$. Hence, the phase S obeys the following quantum Hamilton-Jacobi equation:

$$\hbar\frac{\partial S}{\partial t} + \frac{\hbar^2}{2m}\left(\frac{\partial S}{\partial x}\right)^2 - \frac{\hbar^2}{2mR}\frac{\partial^2 R}{\partial x^2} + V = 0. \tag{3.5}$$

Finally, the stochastic Langevin Eq. (3.2) can also be expressed as an equivalent Fokker-Planck equation for the probability density $P(x,t)$:

$$\frac{\partial P}{\partial t} + \frac{\partial}{\partial x}\left[b(x,t)P\right] = D_Q\frac{\partial^2 P}{\partial x^2}. \tag{3.6}$$

In summary, Nelson's theory is captured in the Eq. (3.2) (stochastic process), Eq. (3.4) (definition of the velocity), and Eq. (3.5) (quantum Hamilton-Jacobi).

When the initial particle distribution $P(x,0)$ is identical to the squared amplitude of the wavefunction $|\psi(x,0)|^2 = R^2(x,0)$, Nelson's dynamics is equivalent to the standard quantum theory and reproduces the same results as the time-dependent Schrödinger equation. Like the Bohm-de Broglie theory, it can be seen as a nonlocal hidden variable theory, where the hidden variable is the position of the particles, but it differs from the Bohm-de Broglie mechanics inasmuch as it is non-deterministic. However, it is important to stress that, despite Eq. (3.2) being a stochastic process, the whole Nelsonian dynamics is reversible in time [31], as it should be to guarantee the equivalence with the Schrödinger equation. This can easily be seen from the Fokker-Planck Eq. (3.6), by noting that the osmotic velocity exactly cancels the diffusion term.

3.3 QUANTUM EQUILIBRIUM

In the standard formulation of QM, the Born rule is a crucial postulate: the probability density of finding a particle at a position x at time t is given by the squared modulus of the wavefunction $|\psi(x,t)|^2$. However, this postulate is not needed in the Nelson and Bohm-de Broglie formalisms, where the wavefunction is viewed as a field that guides the dynamics of the particles and is not necessarily linked to the probability of finding a particle in a certain region of space. Hence, it is perfectly consistent within these approaches to consider cases where $P(x,t) \neq |\psi(x,t)|^2$, in which case the predictions of standard QM would differ from those of the Nelson [4] and Bohm-de Broglie theories.

As suggested by Valentini [103], the Born rule may correspond to a situation of *quantum equilibrium*, analogue to the thermal equilibrium of classical mechanics. According to this view, non-equilibrium states with $P(x,t) \neq |\psi(x,t)|^2$ can exist, but they relax to quantum equilibrium on a very short timescale, so that they are difficult to observe in practice. Valentini developed these ideas in the context of the Bohm-de Broglie mechanics which, being deterministic, requires some form of coarse graining to observe such relaxation [96]. But in Nelson's theory the approach to equilibrium should occur more naturally, thanks to the stochastic nature of the motion. This fact was first analyzed in detail by Petroni and Guerra [104], building on earlier work by Bohm and Vigier [102], although the convergence to quantum equilibrium may not be proven in general for any initial condition and potential. More recently, Hatifi et al. [105] have studied analytically and numerically the relaxation to quantum equilibrium, in relation with the experiments of Couder et al. on bouncing oil droplets as an analogue of quantum motion [106, 107].

The aim of the present work is to investigate, by means of numerical simulations, whether quantum thermalization occurs faster than any typical quantum effect, such as interference. In order to do so, one first needs to reconstruct the probability density $P(x,t)$ of he particles at each time. This is done by partitioning the space $x \in \mathbb{R}$ into bins of size Δx, such that each bin contains a sufficiently large number of particles, and constructing

---

[4] In Chap. 2, we built Nelson's theory by introducing the wavefunction as the square root of the probability density multiplied by a complex phase. We then showed that this wavefunction is a solution of the Schrödinger equation. This established the equivalence between Nelson's theory and standard quantum mechanics. A necessary result was that the squared modulus of the wavefunction represents the probability density, which means that Born's rule holds. However, once Nelson's theory is set up, we can relax this condition. We can assume that the wavefunction is an intrinsic quantity that follows the Schrödinger equation and guides the particles, but is independent of the probability density. This allows us to initially distribute the particle positions according to a probability density that does not have to be $|\psi|^2$. Assuming this breaks the equivalence with standard quantum mechanics. However, we will show that the probability density converges to $|\psi|^2$ after some time, ensuring that Born's rule holds after this period. At that point, the equivalence between the two approaches is restored.

the corresponding histogram. The stochastic Nelson Eq. (3.2) is solved using a second-order Helfand-Greenside's method [55, 108, 109]. In order to reduce the statistical noise, the simulations are repeated independently many times and the results are averaged to reconstruct the probability density. In order to compute the velocity $b(x, t)$, we need to solve the Schrödinger equation to obtain the phase S and amplitude R of the wavefunction. In the three examples considered in this work, the solution could be obtained analytically or semi-analytically, as detailed in the next section.

The probability density $P(x, t)$ must then be compared to the squared modulus of the wavefunction $|\psi(x, t)|^2 = R^2$. For this, we need to define a distance between these two quantities. Out of the many possibilities, one can use the L_p distance between two functions f and g, defined as

$$L_p[f, g]\,(t) = \sqrt[p]{\int_{-\infty}^{+\infty} \mathrm{d}x \; |f(x, t) - g(x, t)|^p}. \tag{3.7}$$

In particular, the L_1 distance was advocated by Petroni and Guerra [104] as the appropriate tool to quantify the relaxation to quantum equilibrium. The infinite distance L_∞ can be seen as its limit when $p \to \infty$ and is given by

$$L_\infty[f, g](t) = \max_x |f(x, t) - g(x, t)|. \tag{3.8}$$

Other criteria can also be defined, such as the entropy-like function used by Valentini [110]:

$$H \equiv L_H[f, g]\,(t) = \int_{-\infty}^{+\infty} \mathrm{d}x \; f(x, t) \ln\left(\frac{f(x, t)}{g(x, t)}\right), \tag{3.9}$$

which is related to the Kullback-Leibler divergence, also called relative entropy [111]. Taking $f = P$ and $g = |\psi(x, t)|^2$, all these distances vanish when the Born rule is satisfied, *i.e.* at quantum equilibrium. Of course, in order to estimate the relaxation time, it will be necessary to define a somewhat arbitrary threshold below which the distance is assumed to be practically zero. Finally, using the entropy-like quantity Eq. (3.9), Hatifi et al. [105] were able to prove a H-theorem which ensures that a generic probability distribution $P(x, t)$ converges to $|\psi(x, t)|^2$ as $t \to \infty$ (with some caveats, as will be seen in the next section).

3.4 SIMULATION RESULTS

The main question we try to answer in this work is whether quantum thermalization occurs faster than any other typical quantum effects, such as the appearance of interferences. If that were the case, it would mean that all quantum phenomena are “equilibrium" phenomena and hence indistinguishable from standard QM. In the opposite case, one could hope to observe some anomaly in the interference pattern due to subquantum corrections, which would be an appealing prediction for future experiments.

In this section, we will use the distance functionals defined in Sec. 3.3 to estimate the time of relaxation to quantum equilibrium, and compare it with the time of appearance of quantum effects. This problem will be investigated for three emblematic physical systems: the double-slit experiment, the harmonic oscillator, and the evolution of a wavepacket in a linear potential representing the gravity field of the Earth.

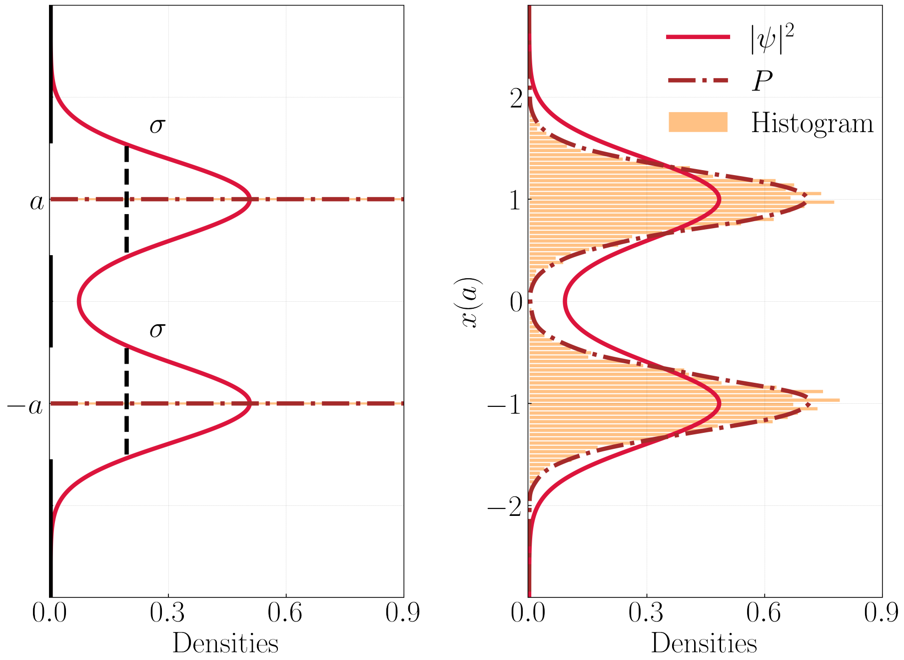

FIGURE 3.1: Left panel: Initial densities for the wavefunction $|\psi(x,t)|^2$ (red continuous line) and the particles $P(x,0)$ (brown dashed line). Here, P is the sum of two Dirac delta functions centered at $\pm a$, while $|\psi(x,t)|^2$ is the sum of two Gaussians of width $\sigma = 0.3\,a$. Right panel: Same quantities at time $t = 0.09\,\tau$, when quantum equilibrium is not yet attained.

3.4.1 Double-slit experiment

We consider a standard double-slit experiment, where the two slits have an aperture of width σ and are separated by a distance $2a$, see Fig. 3.1. We shall use units in which $\hbar = m = a = 1$, so that the only free parameter is the width σ and actually represents the ratio σ/a. This choice also defines a timescale $\tau = ma^2/\hbar$ (= 1, in these units).
In order to model the configuration of a double-slit experiment, we take an initial wavefunction that is the sum of two Gaussians of width σ and centered at $x = \pm a$:

$$\psi(x,0) = \frac{1}{\left[2\sqrt{\pi}\sigma\left(1 + \mathrm{e}^{-a^2/\sigma^2}\right)\right]^{1/2}} \left(\mathrm{e}^{-(x+a)^2/2\sigma^2} + \mathrm{e}^{-(x-a)^2/2\sigma^2}\right). \tag{3.10}$$

As we want to investigate the relaxation to quantum equilibrium, the initial particle distribution should not satisfy the Born rule, *i.e.* $P(x,0) \neq |\psi(x,0)|^2$. Hence, we assume that all particles are concentrated at the same position, at the centre of each slit:

$$P(x,0) = \frac{\delta(x-a) + \delta(x+a)}{2}, \tag{3.11}$$

where δ denotes the Dirac delta function. This initial configuration is plotted in Fig. 3.1 (left panel), while the right panel of the same figure shows both $|\psi(x,t)|^2$ and $P(x,t)$ at a later time when the system has evolved but has not yet reached the quantum equilibrium. The free evolution of this initial wavefunction can be computed analytically [55], yielding the following square modulus at time t:

$$
\begin{aligned}
|\psi(x,t)|^2 = \frac{\sigma}{2\sqrt{\pi\left(\sigma^4+\frac{\hbar^2t^2}{m^2}\right)\left(1+\mathrm{e}^{-a^2/\sigma^2}\right)}} &\left[\exp\left\{-\frac{\sigma^2(x+a)^2}{\sigma^4+\frac{\hbar^2t^2}{m^2}}\right\}\right. \\
\left. + \exp\left\{-\frac{\sigma^2(x-a)^2}{\sigma^4+\frac{\hbar^2t^2}{m^2}}\right\} + 2\exp\left\{-\frac{\sigma^2(x^2+a^2)}{\sigma^4+\frac{\hbar^2t^2}{m^2}}\right\}\cos\left(\frac{\frac{2\hbar t a x}{m}}{\sigma^4+\frac{\hbar^2t^2}{m^2}}\right)\right]&.
\end{aligned}
\tag{3.12}
$$

The particle density P is obtained numerically by solving the stochastic Nelson Eq. (3.2) for a large number N of trajectories. In order to do so, one needs the expression of the velocity term b that appears in the Nelson equation, which is obtained by injectingEq. (3.12) into Eq. Eq. (3.4). We obtain [55]:

$$
\begin{aligned}
b(x,t) = (\mathrm{Re}+\mathrm{Im})\left(\frac{\hbar}{m}\frac{-\left(\sigma^2-i\frac{\hbar t}{m}\right)}{\sigma^4+\frac{\hbar^2t^2}{m^2}}\right.&\left[(x+a)\exp\left\{-\frac{\left(\sigma^2-i\frac{\hbar t}{m}\right)(x+a)^2}{2\left(\sigma^4+\frac{\hbar^2t^2}{m^2}\right)}\right\}\right. \\
&\left.+(x-a)\exp\left\{-\frac{\left(\sigma^2-i\frac{\hbar t}{m}\right)(x-a)^2}{2\left(\sigma^4+\frac{\hbar^2t^2}{m^2}\right)}\right\}\right] \\
\times\left[\exp\left\{-\frac{\left(\sigma^2-i\frac{\hbar t}{m}\right)(x+a)^2}{2\left(\sigma^4+\frac{\hbar^2t^2}{m^2}\right)}\right\}\right.&\left.\left.+\exp\left\{-\frac{\left(\sigma^2-i\frac{\hbar t}{m}\right)(x-a)^2}{2\left(\sigma^4+\frac{\hbar^2t^2}{m^2}\right)}\right\}\right]\right),
\end{aligned}
\tag{3.13}
$$

where $(\mathrm{Re}+\mathrm{Im})$ denotes the sum of the real and imaginary parts of the expression between parenthesis. Then, at each instant t, we construct a histogram of the particle positions, and finally interpolate the histogram to obtain the density $P(x,t)$. This procedure is illustrated in Fig. 3.2.

Given the analytical expression of $|\psi|^2$ and the numerically-computed density P, it is possible to compare these two objects using the distances L_{X} defined in Sec. 3.3. These quantities are represented as a function of time in Fig. 3.3, for the case $\sigma = 0.3a$. For all cases, the distance between P and $|\psi|^2$ decreases to zero for long times, signalling the convergence to the quantum equilibrium and the emergence of the Born rule. Due to numerical errors occurring during the computation of P, the minimal distance is never zero, but approximately $10^{-2} - 10^{-3}$, depending on the adopted measure. It is also interesting to note that the qualitative behavior is similar for all distances, so that they can be fitted with the same type of function in order to extract the relaxation time τ_{q}. Numerically, one can show that a good candidate for the fitting function is

$$
L_{\mathrm{X}}(t) = \alpha_1 \exp\left(-\alpha_2 \mathrm{e}^{\alpha_3 t}\right), \tag{3.14}
$$

where α_1, α_2, and α_3 are free fitting parameters, to be determined for each distance and each value of σ. From this expression, we define the quantum relaxation time τ_{q} as the time at which the tangent of the curve $L_{\mathrm{X}}(t)$ at $t = 0$ intersects the abscissa axis, which gives: $\tau_{\mathrm{q}} = 1/(\alpha_2\alpha_3)$.[5]

Next, we need a suitable definition of a “typical" quantum time τ_{int}, defined as the time of appearance of quantum interferences, in order to compare it with the relaxation time τ_{q}. Interferences occur because the two initial Gaussian wavepackets spread in space, and after a certain time they overlap in the region between the two slits. As illustrated in Fig. 3.4, we define τ_{int} as the time when the first maximum appears in between the two

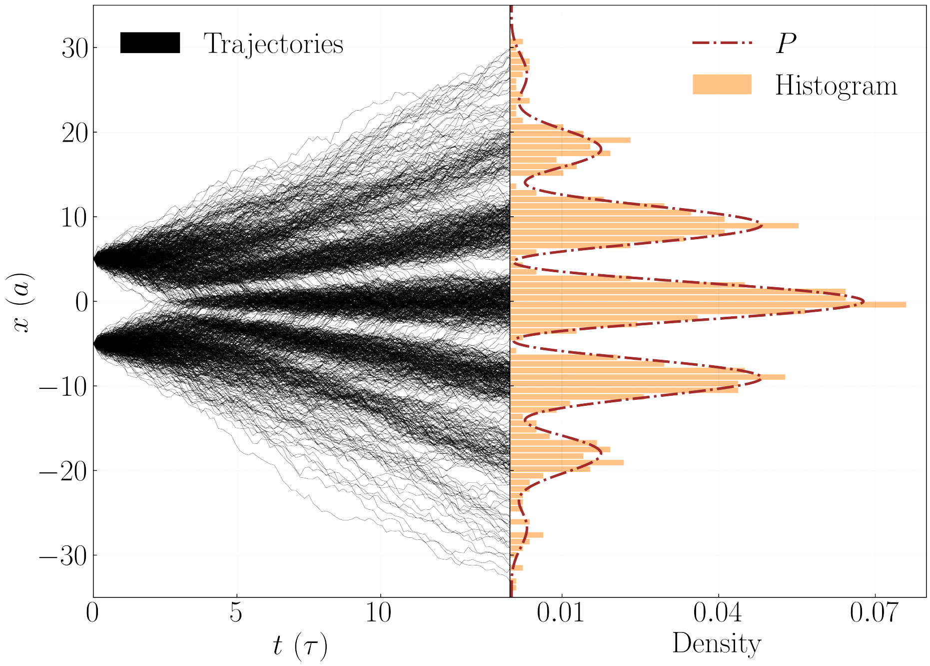

Figure 3.2: Trajectories of $N = 1000$ particles (left side, black curves) initially distributed at the center of each slit. The histogram of the distribution of the positions (right side, orange segments) at the end of the evolution is interpolated to obtain the corresponding density $P(x, t)$ (right side, dashed brown line).

original wavepackets. Further maxima appear at later times, until the full interference pattern is formed.

We now have all the elements to compare τ_q and τ_{int} for different values of σ. The ratio σ/a has to be smaller than unity to ensure that there is no significant overlap between the two Gaussian wavepackets at the initial time, but not too small because we want to ensure that P and $|\psi|^2$ are significantly different. Hence, we will consider values of σ/a in the interval $[0.2, 0.7]$. The computed values of τ_{int} and τ_q, for different distances L_X, are shown in Fig. 3.5 as a function of the initial width σ.

The important result of Fig. 3.5 is that, whatever the value of σ, it is not possible to find a situation where the interference occurs before the system has converged to the quantum equilibrium. In other words, for the double slit experiment, all typically quantum physical phenomena occur after the Born rule has been established. Or, to put it differently, the subquantum dynamics displays no quantum effects such as interferences.

A possible extension of the study presented in this section would be to consider three or more slits and check if it possibly increases the relaxation time beyond the quantum interference time. Experimental investigations in this direction have been performed recently [112, 113]. However, in the present work, we will rather focus on two other configurations: the harmonic oscillator and a linear potential truncated by a perfectly reflecting wall.

---

[5] Indeed, a Taylor expansion of Eq. (3.14) near $t = 0$ yields: $L_X(t) \simeq L_X(0)\,(1 - \alpha_2\alpha_3 t)$.

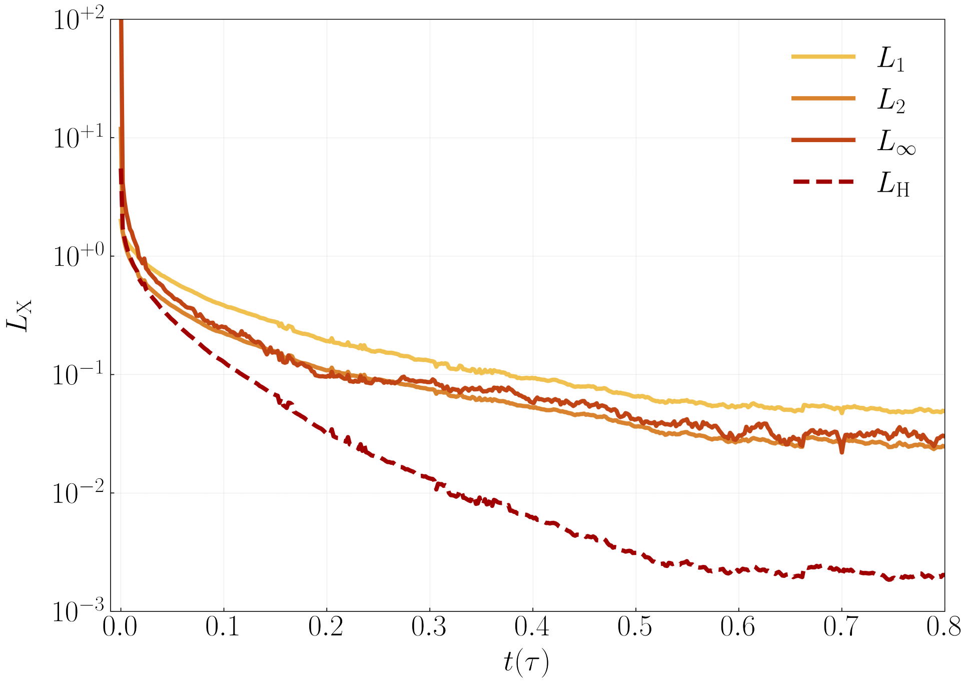

Figure 3.3: Semi-logarithmic plots of the various functionals (see Sec. 3.3) used to quantify the distance between the probability density P and the squared modulus of the wavefunction $|\psi|^2$, as a function of the time t (in units of τ), for $\sigma = 0.3a$.

3.4.2 Harmonic oscillator

The harmonic oscillator is perhaps the most important and studied system in quantum mechanics and is crucial to the development of quantum field theory. It is both interesting in itself and a common approximation to many physical systems. Here, we will further investigate the interplay between the establishment of the Born rule (quantum relaxation) and the appearance of typical quantum effects.

We consider the Schrödinger equation

$$i\hbar\frac{\partial}{\partial t}\psi(x,t) = \left(-\frac{\hbar^2}{2m}\frac{\partial^2}{\partial x^2} + \frac{1}{2}m\omega^2 x^2\right)\psi(x,t), \tag{3.15}$$

where m is the mass of the particle and ω the frequency of the oscillator. Normalizing space to $x_0 \equiv \sqrt{\hbar/(m\omega)}$ and time to $t_0 \equiv 2/\omega$, the Schrödinger equation becomes

$$i\frac{\partial}{\partial t}\psi(x,t) = \left(-\frac{\partial^2}{\partial x^2} + x^2\right)\psi(x,t). \tag{3.16}$$

This system of units amounts to taking $\omega = 2$, $\hbar = 1$ and $m = 1/2$, so that the quantum diffusion coefficient is $D_Q = \hbar/2m = 1$ and the ground state energy $E_0 = m\omega^2/2 = 1$.

We want to study the convergence to the quantum equilibrium when the initial particle probability density P is given by a Dirac distribution centred at the bottom of the harmonic potential ($x = 0$). The initial wavefunction is also a Gaussian of given width, but not necessarily the ground state of the system, hence it will display breathing oscillations

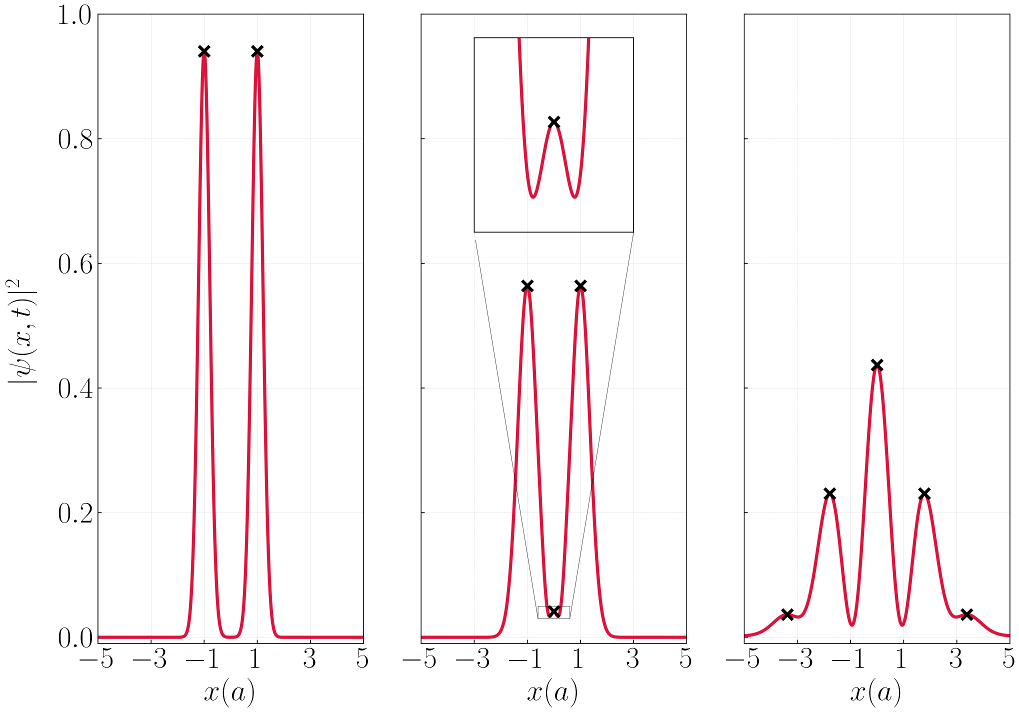

Figure 3.4: Squared modulus of the wavefunction for $\sigma = 0.09a$, at times $t = 0$ (left panel), $t = 0.12\tau$ (middle panel), and $t = 0.6\tau$ (right panel). Initially, only two peaks exist, one for each Gaussian wavepacket. At $t = 0.12\tau$, a third peak has appeared between the two initial ones: this event defines the interference time τ_{int}. At later times, several new peaks appear and form the full interference pattern.

while remaining Gaussian for all times. A similar study, but only considering a ground state wavefunction for the Schrödinger equation, was performed by Hatifi et al. [105].

In practice, our initial condition is as follows:

$$\psi(x,0) = \left(\frac{1}{2\pi\sigma_0^2}\right)^{\frac{1}{4}} \exp\left\{-\frac{x^2}{4\sigma_0^2} + i\big[\alpha_0 x^2 + \beta_0\big]\right\} \quad \text{and} \quad P(x,0) = \delta(x), \tag{3.17}$$

where σ_0, α_0 and β_0 are appropriate constants that define the wavefunction's width and phase. At any time $t > 0$, the wavefunction will keep the same functional form, so that it can be written as:

$$\psi(x,t) = \left(\frac{1}{2\pi\sigma^2(t)}\right)^{\frac{1}{4}} \exp\left\{-\frac{x^2}{4\sigma^2(t)} + i\big[\alpha(t)x^2 + \beta(t)\big]\right\}, \tag{3.18}$$

with initial conditions $\alpha(0) = \alpha_0$, $\beta(0) = \beta_0$ and $\sigma(0) = \sigma_0$. Note that the ground state corresponds to $\alpha_0 = \beta_0 = 0$ and $\sigma_0 = 1/\sqrt{2}$.

Injecting this *ansatz* into the Schrödinger Eq. (3.16), we obtain a system of first-order

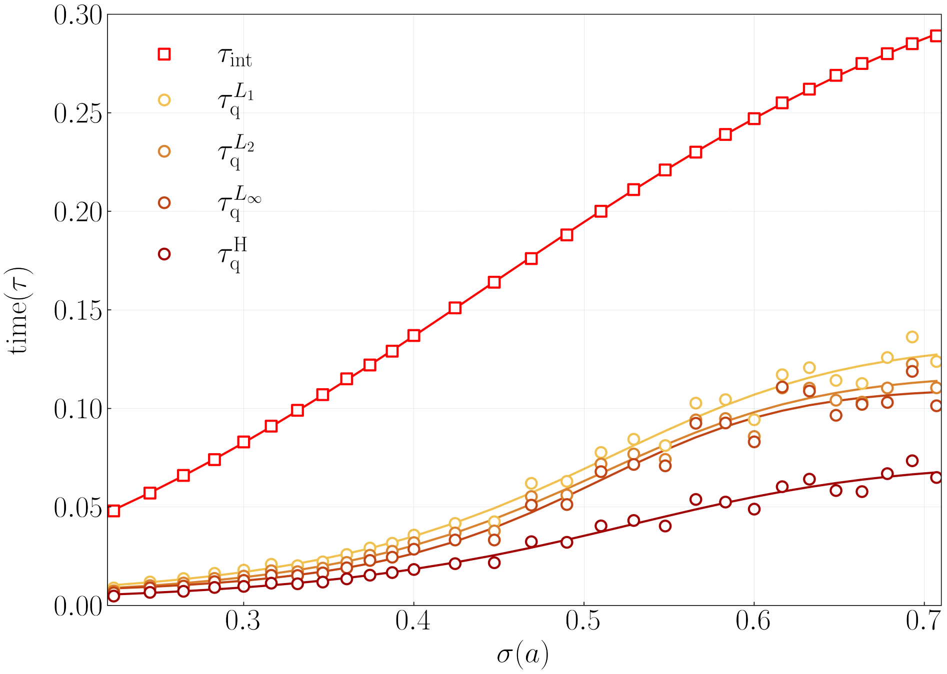

Figure 3.5: Time of appearance of the interferences τ_{int} (red dots) and times of convergence to quantum equilibrium τ_{q}^{X} (shades of blue dots) associated with the different distances defined in Sec. 3.3, as a function of the initial width σ/a. All of the different times can be nicely fitted with a hyperbolic tangent function (dashed lines) of the type: $\tau_{\text{q}}(\sigma) = \beta_1 \tanh\bigl(\beta_2\sigma^2 + \beta_3\bigr) + \beta_4$, where the β_i are fitting parameters. For every value of σ and for every distance L_{X}, quantum equilibrium (Born's rule) is reached before the appearance of quantum interferences.

differential equations, where the dot denotes differentiation with respect to time:

$$\begin{cases} \dot{\alpha}(t) = \dfrac{1}{4\sigma^2(t)} - 4\alpha^2(t) - 1, \\ \dot{\beta}(t) = -\dfrac{1}{2\sigma^2(t)}, \\ \dot{\sigma}(t) = 4\alpha(t)\sigma(t). \end{cases} \tag{3.19}$$

The solution to the above equations completely determines the wavefunction $\psi(x,t)$, and hence the term $b(x,t)$ in Nelson's equation Eq. (3.4): $b(x,t) = [\alpha(t) - 1/\sigma^2(t)]x$, so that the Nelson equation can be written as

$$\mathrm{d}x(t) = \left[4\alpha(t) - \frac{1}{\sigma^2(t)}\right] x\mathrm{d}t + \mathrm{d}W(t). \tag{3.20}$$

The corresponding Fokker-Planck equation can be obtained using the Kramers-Moyal expansion [21, 22] and reads as:

$$\frac{\partial}{\partial t}P(x,t) = \frac{\partial}{\partial x}\left\{-\left[4\alpha(t) - \frac{1}{\sigma^2(t)}\right] x\, P(x,t)\right\} + \frac{\partial^2}{\partial x^2}P(x,t). \tag{3.21}$$

Supposing that the probability density is also Gaussian (which is an exact *ansatz*):

$$P(x,t) = \frac{1}{\sqrt{2\pi\sigma_P^2(t)}} \exp\left(\frac{x^2}{2\sigma_P^2(t)}\right), \tag{3.22}$$

and injecting the above density into Eq. (3.21), one obtains that $\sigma_P(t)$ should obey the following equation

$$\dot{\sigma}_P(t) = \sigma_P(t)\left[4\alpha(t) - \frac{1}{\sigma^2(t)}\right] + \frac{1}{\sigma_P(t)}. \tag{3.23}$$

The convergence to the quantum equilibrium can be studied by investigating the convergence of $\sigma_P(t)$ to $\sigma(t)$. To do so, we introduce the new variable $\gamma(t) = [\sigma(t)/\sigma_P(t)]^2$, which, from Eq. (3.19) and Eq. (3.23), must be a solution of the Riccati equation

$$\dot{\gamma}(t) = \frac{2\gamma(t)}{\sigma^2(t)}[1-\gamma(t)]. \tag{3.24}$$

Hence, one needs to first solve the system of Eq. (3.19) to obtain $\sigma(t)$ and then inject it into Eq. (3.24) in order to obtain $\gamma(t)$. Introducing $B(t) = 1/\sigma^2(t)$, the solution to Eq. (3.24) can be obtained pseudo-analytically and reads as [114]:

$$\gamma(t) = 1 + \frac{\phi(t)}{2\int_0^t \mathrm{d}\tau\ B(\tau)\phi(\tau)}, \quad \text{with} \quad \phi(t) = \mathrm{e}^{-2\int_0^t \mathrm{d}\tau B(\tau)} \tag{3.25}$$

with the initial conditions $B_0 = 1/\sigma_0^2$ and $\gamma(0) = \infty$, which corresponds to the situation where P is initially a Dirac delta function. Moreover, the system of Eq. (3.19) possesses the analytical solution [115]:

$$B(t) = \frac{1}{\sigma^2(t)} = \frac{8B_0}{B_0^2 + 4 - (B_0^4 - 4)\cos(4t)}. \tag{3.26}$$

In Fig. 3.6, we present the solution of Eq. (3.19) and Eq. (3.24) for the initial conditions $\alpha(0) = 0, \beta(0) = 0, B(0) = \sqrt{2}$ and $\gamma(0) = \infty$, meaning, respectively, no initial phase, a wavefunction that is not the ground state of the harmonic oscillator, and a δ-distributed probability $P(x,0)$. The phase function A and the width B of the wavefunction are both periodic in time, with period $T = (\pi/2)t_0 = \pi/\omega$, equal to half the natural period of the harmonic oscillator $2\pi/\omega$ (this is because they are quadratic quantities in x). In contrast, the ratio $\gamma = [\sigma/\sigma_P]^2$ relaxes to $\gamma = 1$ over a timescale τ_q. When this has occurred, then both P and $|\psi|^2$ are Gaussian functions of the same width and the Born rule is satisfied. The purpose here is to compute τ_q for different values of σ_0, *i.e.* different initial widths of the wavefunction, and to check whether or not it is possible to find a situation where the period of quantum oscillations T is shorter than the relaxation time τ_q. In the following, we will consider different initial widths $\sigma_0 = \sqrt{2/B_0}$ of the wavefunction from 0.25 to 4, in units of x_0. Note that, for the ground state, one has: $\sigma_0 = 1$.

This can be done using several methods, like arbitrarily defining a cutoff value, so that the relaxation time is defined as the time when γ reaches such value. Here, we shall use a similar, but subtler, technique. We first compute the root mean-square deviation of γ over a sliding window in time [116]. We construct a window, centred at the data point i, which contains $n+1$ other data points between $i - n/2$ and $i + n/2$, and compute the mean square deviation Θ_i of γ inside this window using the expression

$$\Theta_i^2 = \frac{1}{n+1} \sum_{j=i-n/2}^{i+n/2} (\gamma_j - \bar{\gamma}_i)^2, \tag{3.27}$$

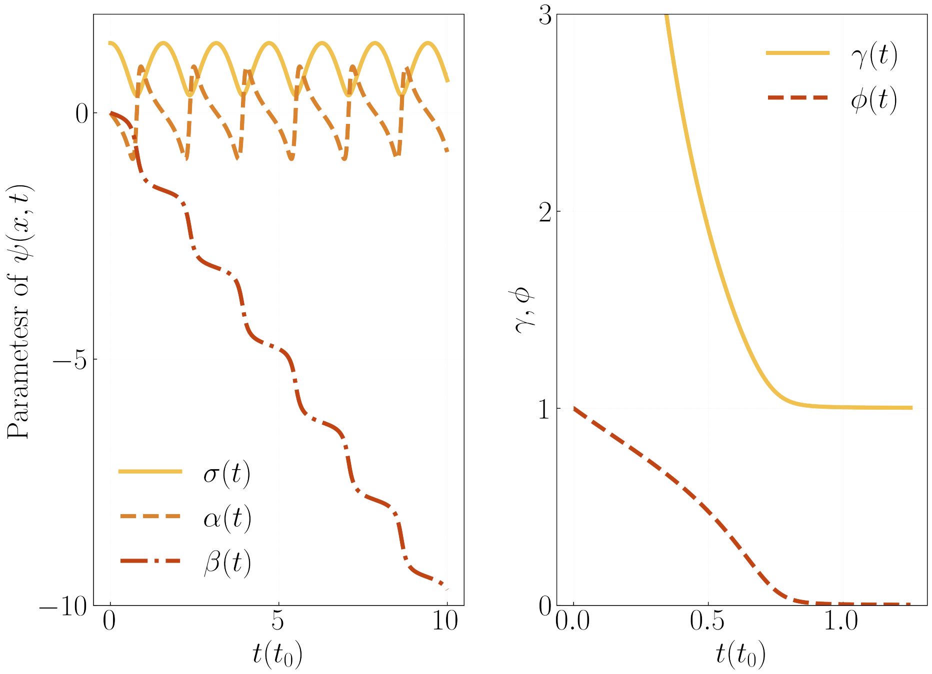

FIGURE 3.6: Left panel: Time evolution of the phase functions $\alpha(t)$ and $\beta(t)$, and the width $\sigma(t)$ of the wavefunction ψ. $\alpha(t)$ and $\sigma(t)$ are periodic with period $T = (\pi/2)t_0$, while $\beta(t)$ is monotonously decreasing, in accordance with the second Eq. (3.19). Right panel: Time evolutions of the ratio $\gamma(t) = [\sigma(t)/\sigma_P(t)]^2$ and of the function $\phi(t)$ appearing in Eq. (3.25); γ and ϕ converge respectively to unity and zero over a relaxation timescale denoted τ_{q}.

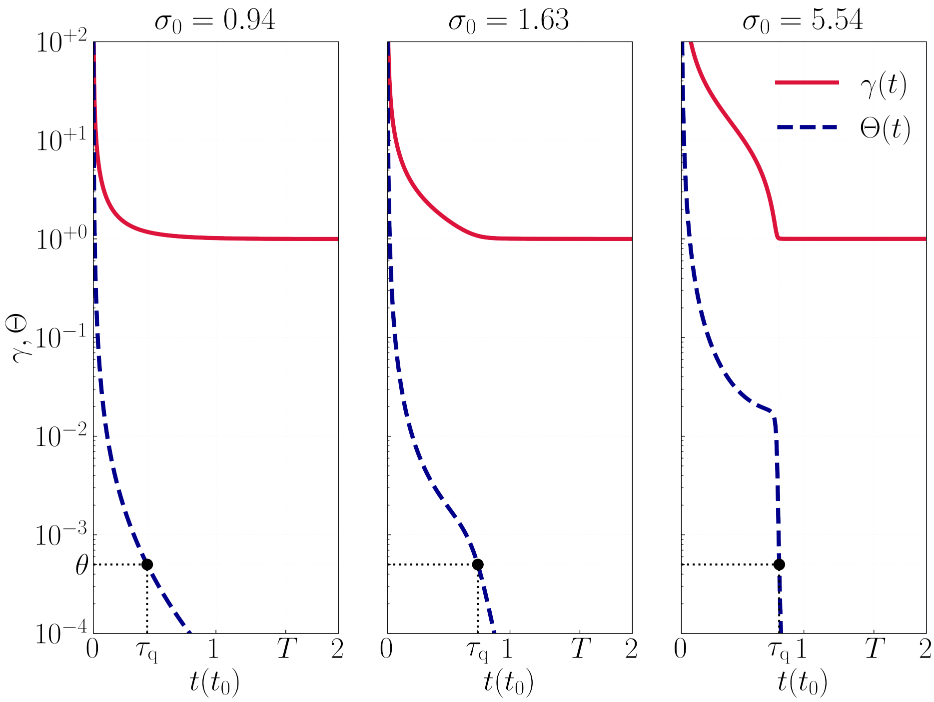

Figure 3.7: Evolution of $\gamma(t)$ (blue dashed curve) and its mean-square deviation $\Theta(t)$ (red solid curve) as a function of time (in units of t_0), for three different values of the initial wave-function width σ_0. The cutoff value $\theta = 5 \times 10^{-4}$ is represented as a horizontal line which cuts the curve $\Theta(t)$ at $t = \tau_\mathrm{q}$, defining the relaxation time. We note that τ_q is always smaller than the period $T = (\pi/2)t_0$ of the harmonic oscillator (also represented on the abscissa axis), but increases when σ_0 increases.

where $\gamma_i = \gamma(t_i)$ and $\bar{\gamma}_i = \sum_{i-n/2}^{i+n/2} \gamma_j$ is the mean value of γ inside the window. Typically, we take $n = 10$. Hence, as $\gamma(t)$ approaches a constant value (here, $\gamma = 1$), the function Θ will tend to zero. By choosing a threshold θ, one can define the relaxation time τ_q as the time for which $\Theta < \theta$.

To visualize this procedure, the evolutions of γ and Θ (dashed blue) are represented in Fig. 3.7, for three values of the initial width $\sigma_0 = 0.94$, 1.63, and 5.54. The convergence time is represented on the horizontal axis as the abscissa of the black dot, which is the point corresponding to $\Theta = \theta$, where in the present case $\theta = 5 \times 10^{-4}$. For the different values of σ_0, the behavior of $\gamma(t)$ differs slightly, but the curve is always strictly decreasing, and no ambiguity arises for the determination of τ_q.

One may wonder about the dependence of the relaxation time on the threshold value θ, but, as it appears in Fig. 3.7, Θ decays fast close to the convergence time, so one can expect this effect to be minor. To check this point, τ_q was computed using different values of threshold, ranging from $\theta = 10^{-2}$ to $\theta = 5 \times 10^{-4}$ and its dependence on the initial width σ_0 is plotted in Fig. 3.8. For every threshold and for every value of σ_0, the relaxation time τ_q is smaller than the period of quantum oscillations T. In particular, we note the two limiting cases: (i) For $\sigma_0 \to 0$, then $\tau_\mathrm{q} \to 0$: this is rather natural, as it corresponds to the case where P and $|\psi|^2$ already have the same vanishing width at $t = 0$; (ii) For large σ_0, $\tau_\mathrm{q} \to \pi/4 = T/2$, in other words relaxation is completed in half an oscillation period.

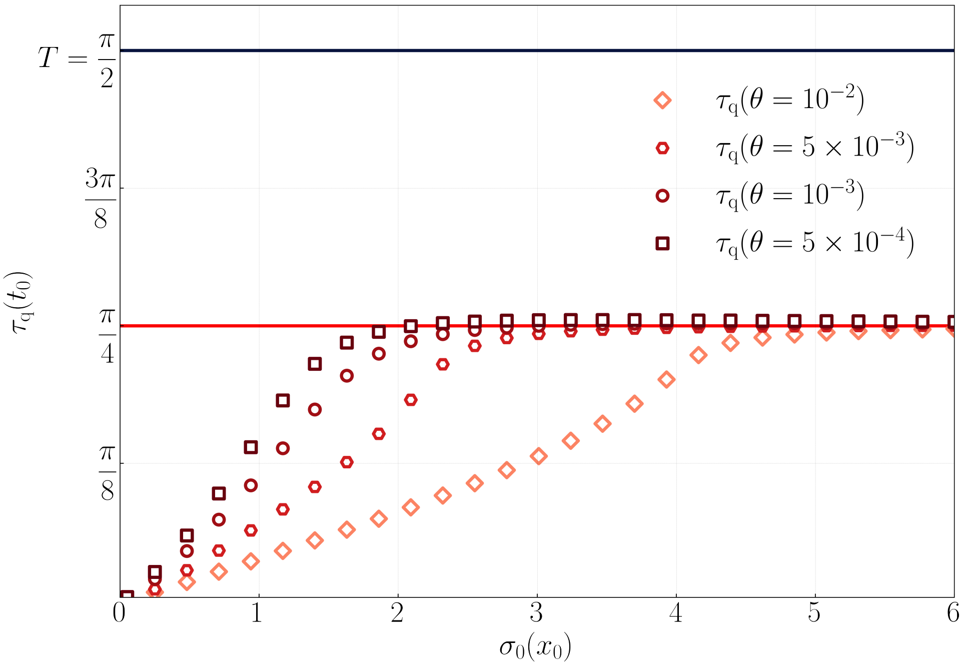

Figure 3.8: Evolution of the quantum relaxation time τ_q with respect to the initial width σ_0 of the wavefunction, for different thresholds θ, ranging from 1.0×10^{-2} to 5.0×10^{-4} (shades of red dots). For each threshold, the value of τ_q increases with σ_0 and saturates at $\tau_q = \pi/4$ (dotted red line). Hence, the convergence time is always at least twice as small as the quantum oscillator period $T = \pi/2$ (blue dashed line).

The limit $\tau_q \to \pi/4$, obtained for large initial dispersions, can be recovered analytically as follows. For large σ_0, corresponding to small B_0, the function $B(t) = 1/\sigma^2(t)$ becomes [see Eq. (3.26)]:

$$B(t) \simeq \frac{2B_0}{1 + \cos(4t)} = \frac{B_0}{\cos^2(2t)}, \tag{3.28}$$

so that, from Eq. (3.25): $\phi(t) \simeq \exp[-B_0 \tan(2t)] = \exp\left[-\tan(2t)/\sigma_0^2\right]$ which goes to zero when $t \to \pi/4$.

All in all, these results show that relaxation to quantum equilibrium (Born's rule) occurs much faster than an oscillation period of the quantum oscillator, and is completed at the latest over half such a period. As in the double-slit case, the system will always reach the quantum equilibrium before quantum phenomena become observable, preventing the possibility of observing a situation where the Born rule does not hold.

So far, we considered wavefunctions that are Gaussians, albeit not necessarily the ground state of the harmonic oscillator. To end this section, we now turn to the case where ψ represents an excited state. In this case, the wavefunction possesses nodes (zeroes), leading to singularities (asymptotes) in the velocity field $b(x,t)$, which becomes infinite at the location of the nodes. These singularities constitute infinite barriers that the trajectories cannot cross. For instance, for the first excited state of the oscillator, there is one singularity at $x = 0$, where $\lim_{x \to 0^\pm} b(x) = \pm\infty$. Hence, a particle approaching zero from the right ($x > 0$) will develop an ever increasing velocity directed in the positive x direction, and will never manage to cross the origin. Similarly, for a particle

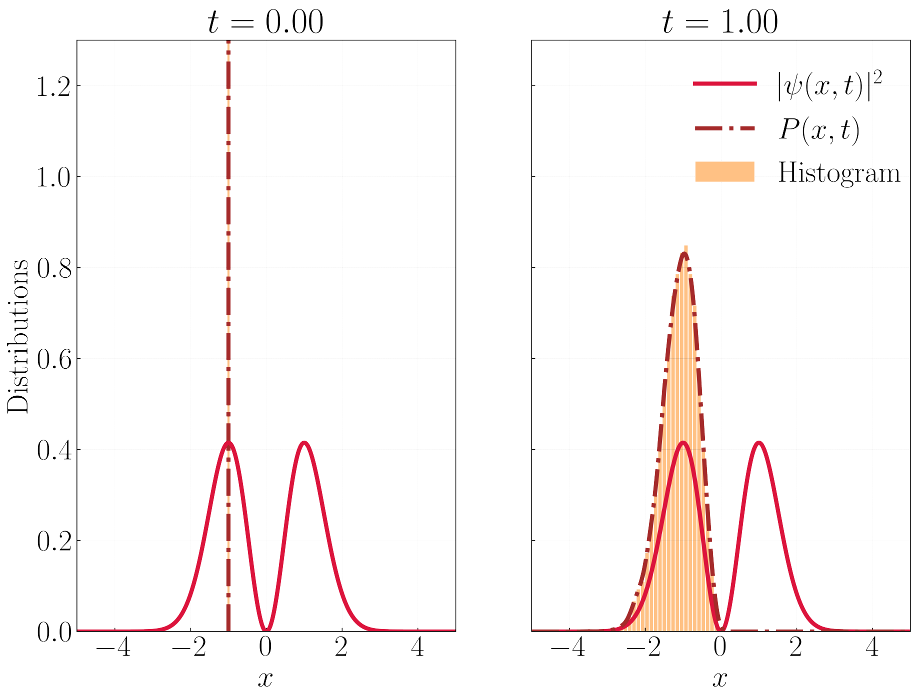

FIGURE 3.9: Particle probability density $P(x,t)$ (dashed blue line) and squared wavefunction $|\psi|^2$ (red solid line) at times $t = 0$ (left panel) and $t = 1$ (right panel). Time is expressed in units of t_0 and space in units of x_0. The wavefunction corresponds to the first excited state of the harmonic oscillator. The initial particle distribution is a Dirac delta function centred at $x = -1$ and cannot cross the barrier located at the origin. The time step is $\mathrm{d}t = 10^{-4}$.

approaching zero from the left ($x < 0$).

This is illustrated in Fig. 3.9, where the initial distribution P is a Dirac delta function located at $x = -1$, in the centre of the left lobe of the wavefunction density. At $t = 1$ (right panel), the initial particle distribution has considerably spread, but it has not crossed the barrier at $x = 0$. We note that this result is in disagreement with a similar simulation of Hatifi et al. [105], who found numerically that the barrier is eventually crossed and full relaxation is observed. Nevertheless, some important differences exist: firstly, Hatifi et al. [105] simulate a single trajectory and appeal to the ergodic theorem to reconstruct the particle density P; secondly, their final simulation time $t_{\text{final}} = 1000$ is much longer than ours (this is because they have to average on time slices to compensate for the presence of a single trajectory). But the main difference is in the time step, which is $\mathrm{d}t = 0.01$ in their simulation and $\mathrm{d}t = 10^{-4}$ in ours. Indeed, if the time step is large enough, the particle can sometimes cross the barrier, because it cannot "see" it during times shorter than $\mathrm{d}t$. This is confirmed by three long-time simulations using different values of $\mathrm{d}t$ (see Fig. 3.10), which show that, as the time step decreases, fewer and fewer particles cross the barrier. Hence, in the limit $\mathrm{d}t \to 0$, no crossings should be observed.

The result of Fig. 3.9 may seem in contradiction with what was claimed earlier, namely that the relaxation time τ_q is smaller than any typical quantum timescale. In Fig. 3.9, relaxation never occurs, so effectively $\tau_q \to \infty$. To better understand this issue, we have performed one further simulation (see Fig. 3.11) for an initial wavefunction that is equal to the first excited state $\psi_1(x)$, plus a small perturbation proportional to the ground state

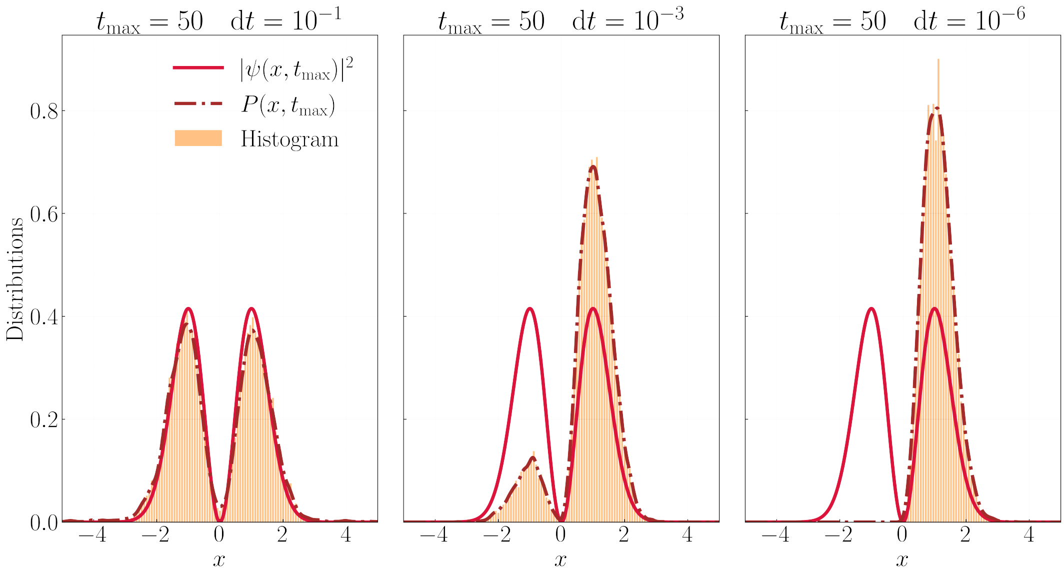

Figure 3.10: Particle probability density $P(x,t)$ (blue histograms) and squared wavefunction $|\psi|^2$ (red solid line) at times $t = 50$, for three values of the time step: $\mathrm{d}t = 0.1$ (left panel), $\mathrm{d}t = 10^{-3}$ (middle panel), and $\mathrm{d}t = 10^{-6}$ (right panel). Time is expressed in units of t_0 and space in units of x_0. The wavefunction corresponds to the first excited state of the harmonic oscillator and the particles are initially all located at $x = 1$. For the smallest time step virtually no particles have crossed the barrier situated at $x = 0$.

$\psi_0(x)$: $\psi(x,0) = \cos(0.1^\circ)\psi_1(x) + \sin(0.1^\circ)\psi_0(x)$ (note that $\sin(0.1^\circ) \approx 0.0017 \ll 1$). In this case, relaxation takes place again and occurs on a timescale $\tau_{\mathrm{q}} \approx 2.8t_0$, shorter than the oscillator period $2\pi/\omega = \pi t_0$ (remember that $\omega = 2/t_0$ in our units). In summary, the relaxation time τ_{q} is indeed always smaller than the typical oscillator timescale, except in the special case of an initial wavefunction that is an eigenstate of the system and possesses one or more nodes.

3.4.3 Uniform gravity field

3.4.3.1 Ultracold neutron experiments

Let us now consider the case of a particle in a constant field, like the one generated by the gravitational attraction of the Earth. This type of problems are motivated by ongoing experiments on the gravitational response of antimatter, in which anti-hydrogen atoms fall in the gravity field of the Earth and are annihilated at the lower surface of the device [117, 118]. By measuring the duration of the fall, it will be possible to estimate the gravitational acceleration of antimatter $\bar{g}$, and check whether it is identical to that of standard matter g.

When the quantum nature of the anti-hydrogen atoms is taken into account, more subtle phenomena can arise, leading to the quantum reflection of the atoms at the surface through the Casimir-Polder potential [119] and the subsequent formation of an interference pattern. Exploiting this effect can considerably improve the estimation of $\bar{g}$, because of the great precision with which frequency differences can be measured [120–122].

Similar experiments were performed over two decades ago using free-falling ultracold neutrons confined between a lower reflecting mirror and an upper absorbing surface [99], and led to the observation of the quantized gravitational energy levels of the neu-

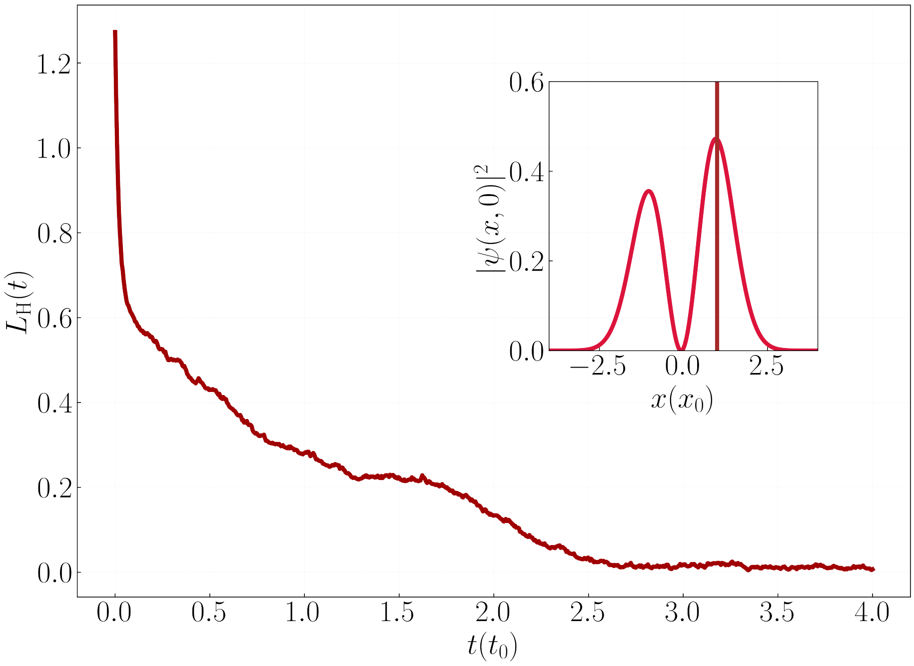

Figure 3.11: Time evolution of the distance $L_{\mathrm{H}}(t)$ for an initial state that is a superposition of the ground state $\psi_0(x)$ and the first excited state $\psi_1(x)$: $\psi(x,0) = \sin(0.1^\circ)\psi_0(x) + \cos(0.1^\circ)\psi_1(x)$ (the corresponding density is shown in the inset). Initially, the particles are localized at $x = 1$ (blue vertical line in the inset). Time is expressed in units of t_0 and space in units of x_0. Relaxation is completed for $t = \tau_{\mathrm{q}} \approx 2.8t_0$, shorter than the oscillator period $2\pi/\omega = \pi t_0$.

trons. These techniques were further used to realize high-precision gravity-resonance spectroscopy studies on ultracold neutrons [123], which were recently exploited to search for anomalous gravitational interactions [124]. Gravitational experiments that use cold hydrogen atoms are also envisaged [125]

Here, we will focus on the relaxation to quantum equilibrium of a quantum particle (typically, a neutron) falling in the gravitational field of the Earth from a height h. The initial wavefunction is a Gaussian of width ζ centered at $x = h$, where x is the coordinate representing the altitude with respect to the lower reflecting mirror, whereas the particles are initialized as a Dirac delta function at the same height h. After bouncing on the mirror, the wavefunction develops quantum interferences. Our purpose will be again to investigate whether quantum relaxation and the establishment of the Born rule occurs before or after the formation of the quantum interference pattern.

3.4.3.2 Gravitational quantum states

Assuming a constant gravitational force at the surface of the Earth, the corresponding gravitational potential is mgx, where m is the mass of the neutron, g the free-fall acceleration, and x the altitude with respect to the reflecting mirror, located at $x = 0$. The corresponding wavefunction is a solution of the time-dependent Schrödinger equation

$$i\hbar\frac{\partial}{\partial t}\psi(x,t) = \left(-\frac{\hbar^2}{2m}\frac{\partial^2}{\partial x^2} + mgx\right)\psi(x,t), \tag{3.29}$$

with boundary conditions $\psi(x=0,t)=\psi(x\to\infty,t)=0$, for all times. The system is then bound and admits a discrete set of eigenstates. The initial wavefunction is given by

$$\psi(x,0)=\Theta(x)\frac{1}{(2\pi\zeta^2)^{\frac{1}{4}}}\exp\left[-\frac{(x-h)^2}{4\zeta^2}\right], \tag{3.30}$$

with $\Theta(x)$ the Heaviside function, ensuring that the wavefunction is strictly zero for $x\leq 0$. We choose $\zeta\ll h$, so that the wavefunction is correctly normalized.
The eigenstates χ_n of the problem are obtained by solving the stationary Schrödinger equation

$$\left(-\frac{\hbar^2}{2m}\frac{\partial^2}{\partial x^2}+mgx\right)\chi_n(x)=E_n\chi_n(x). \tag{3.31}$$

We further define dimensionless units of length, energy and time as follows:

$$x_0=\left(\frac{\hbar^2}{2m^2g}\right)^{\frac{1}{3}},\quad \epsilon_0=mgx_0=\left(\frac{\hbar^2mg^2}{2}\right)^{\frac{1}{3}},\quad t_0=\frac{\hbar}{\epsilon_0}=\left(\frac{2\hbar}{mg^2}\right)^{\frac{1}{3}}. \tag{3.32}$$

Using these units, the eigenfunctions read as:

$$\chi_n(x)=\Theta(x)\,\frac{\mathrm{Ai}(x-E_n)}{\mathrm{Ai}'(-E_n)}, \tag{3.33}$$

where $\mathrm{Ai}(x)$ denotes the first Airy function and $\mathrm{Ai}'(x)$ its derivative. Because the eigenenergies are obtained by imposing $\chi_n(0)=0$, they correspond to the zeros of the Airy function Ai, which are well-known and have been tabulated [126]. It is also possible to convert each E_n to a corresponding “eigenaltitude" h_n above the mirror surface, by setting E_n equal to the potential energy mgh_n, leading to: $h_n=E_n/mg$. The presence of an upper absorbing plate ensures that only a finite number $n_{\max}$ of eigenstates can be present simultaneously in the device. The first ten eigenfunctions are represented in Fig. 3.12, together with the eigenenergies/eigenaltitudes and the gravitational potential mgx.
Using the eigenbasis Eq. (3.33), the solution to the Schrödinger equation Eq. (3.29) can be written as

$$\psi(x,t)=\sum_{n=0}^{n_{\max}}c_n\chi_n(x)\mathrm{e}^{-iE_nt}, \tag{3.34}$$

where the c_n are the coefficients of the expansion [127]. Their expression can be obtained semi-analytically under the assumption that the width ζ of the wavepacket is small compared to its altitude h [128]:

$$c_n=\frac{(8\pi\zeta^2)^{\frac{1}{4}}}{\mathrm{Ai}'(-E_n)}\mathrm{Ai}\big(h-E_n+\zeta^4\big)\exp\left\{\zeta^2\left(h-E_n+\frac{2}{3}\zeta^4\right)\right\}. \tag{3.35}$$

Some details of the derivation are given in the Appendix E.

3.4.3.3 Relaxation to quantum equilibrium

In order to investigate the relaxation to quantum equilibrium, we take an initial probability distribution P that does not follow the Born rule, but is rather given by a Dirac delta function: $P(x,0)=\delta(x-h)$, so that all particles are at the same altitude h from the mirror. In the forthcoming simulations the altitude varies from $h=1.50$ – which is lower than the ground-state eigenaltitude ($h_0=2.34$) – to $h=5$. The width of the initial

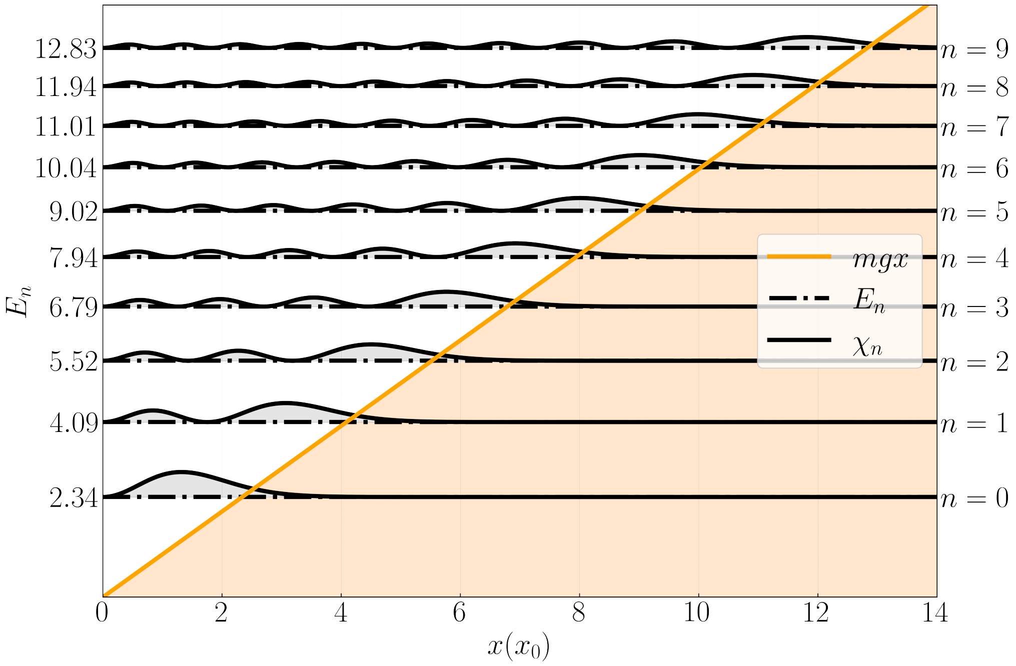

Figure 3.12: Representation of the first ten gravitational quantum states χ_n (red solid lines), which are given by the same Airy function Ai(x) shifted of an amount equal to E_n, where E_n is the n-th energy eigenvalue; see Eq. (3.33) for the full formula. The horizontal axis represents the altitude x, in units of x_0. The blue line represents the gravitational potential mgx.

wavefunction is fixed and equal to $\zeta = 0.09$. A schematic representation of the initial system, along with a typical random trajectory obtained by solving Nelson's stochastic equation, is shown in Fig. 3.13.

The trajectories of $N = 1000$ particles initially distributed at a height $h = 2.00$ from the mirror are shown in Fig. 3.14. The histogram of the distribution of the positions at the end of the evolution is interpolated to obtain the corresponding density $P(x, t)$.

The L_{H} distance as a function of time is shown in Fig. 3.15 (upper panel) and displays a peculiar behaviour. First, it decreases rather abruptly until a time τ_1, then it increases up to time τ_2, and finally decreases again for $t > \tau_2$. In order to understand this behaviour, the squared modulus of the wavefunction $|\psi|^2$ and the probability density P are also shown in Fig. 3.15 (lower panels) for three different times $t = 0.005$, $t = 0.07$ and $t = 0.5$, corresponding to three different phases of the evolution: (i) $t < \tau_1$, (ii) $\tau_1 < t < \tau_2$, and (iii) $t > \tau_2$. During the first phase, both $|\psi|^2$ and P remain approximately Gaussian and their distance is progressively reduced, as it was found for the harmonic oscillator in Sec. 3.4.2. However, after τ_1, interferencexs start building up in $|\psi|^2$, but not in P, so that the distance between such two functions increases again. For $t > \tau_2$, the interference pattern is fully formed and the particle distribution again converges towards $|\psi|^2$.

Finally, for even longer times, of the order of the relaxation time $\tau_{\text{q}} \approx 0.5$, the L_{H} distance goes to zero and the Born rule is eventually satisfied (Fig. 3.15, upper panel). Hence, it appears that some quantum interference phenomena do occur before the quantum relaxation is fully completed, in particular during the intermediate phase where $\tau_1 < t < \tau_2$, where the distributions $|\psi|^2$ and P start diverging again. During that phase, the interference pattern forms too quickly for the particle distribution to catch up with the wavefunction. This type of effect was not observed in the two other situations (double slit and harmonic oscillator) that were analysed earlier in the present work.

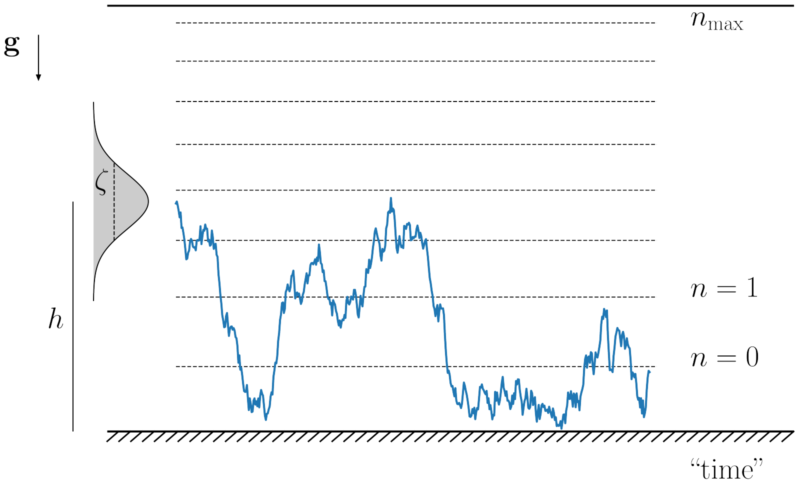

Figure 3.13: Schematic view of the physical system under study. The initial wavefunction (grey curve on the left) is a Gaussian of width ζ, centered at an altitude h from the mirror (hatched horizontal line at the bottom). The different eigenaltitudes (dashed horizontal lines) are represented for $n = 0, 1, \cdots n_{\max}$, where $n_{\max}$ is the highest-energy state allowed by the upper absorbing plate. The trajectory of a typical particle (blue line), initially located at $x = h$, shows the presence of bounces, not only at the level of the mirror, but also in correspondence of the various eigenaltitudes.

In order to show that the time τ_1 (when the distance between $|\psi|^2$ and P starts increasing again) actually coincides with the time of appearance of the early interference pattern τ_{int}, we need a recipe to estimate the latter. The procedure runs as follows. First, we normalize the squared modulus of the wavefunction so that its maximum is equal to unity, and search for extrema in the region $0 < |\psi|^2/\max|\psi|^2 < 0.6$, thus focussing on the tail of the wavefunction (shaded green area in Fig. 3.16). Then, we define the prominence of a peak as the height between two neighbouring extrema (a maximum and a minimum). We consider that interference occurs when at least two peaks have appeared with prominence larger than a threshold value p. This defines the appearance time of the interference pattern, τ_{int}. This procedure is illustrated in Fig. 3.16, where the wavefunction at the interference time is plotted for three values of p.

Now, we can compare the interference time τ_{int} with the time τ_1 at which the L_{H} distance starts increasing. The result is plotted in Fig. 3.17, including error bars accounting for different choices of the prominence p. As expected, these two times are very similar, confirming that the increasing distance between $|\psi|^2$ and P between τ_1 and τ_2 is due to the formation of an early interference pattern in the former, but not in the latter.

In summary, simulations of a quantum particle falling in a uniform gravitational field have shown that quantum interference phenomena could indeed be observed before the Born rule is satisfied, in contrast to what was found for the double slit and harmonic cases. This opens the way to possible experimental verifications of the Born rule using gravitational quantum states of ultracold neutrons [99] or hydrogen atoms [125], which, in the case of neutrons, have reached extremely high accuracy levels [124]. We recall that we expressed our results in units of $x_0 = 5.87\mu$m for distances and $t_0 = 1.09\,$ms for times, see Eq. (3.32). Hence, for the case of Fig. 3.15, a significant discrepancy from

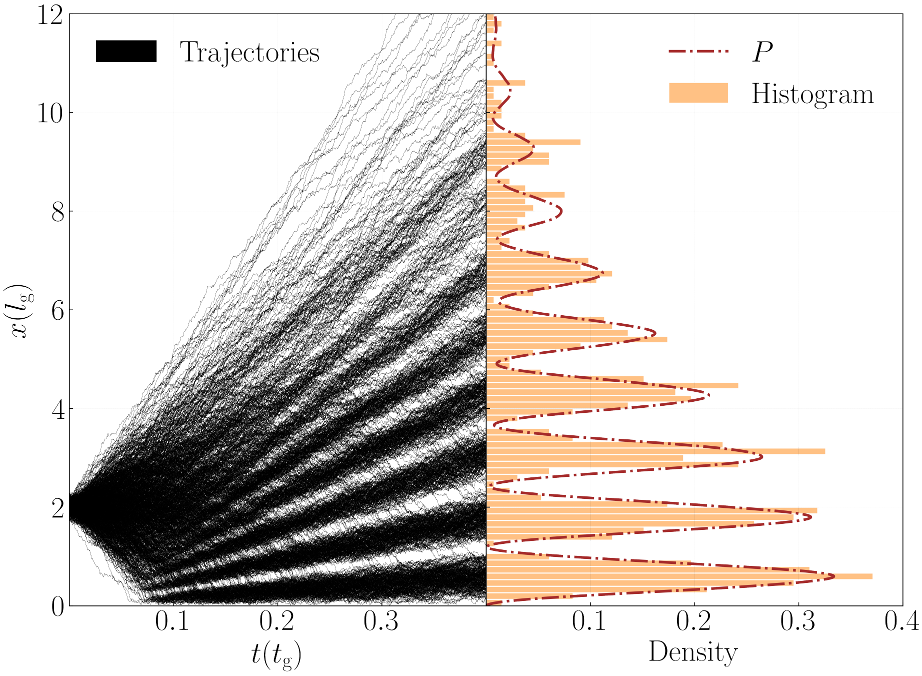

FIGURE 3.14: Trajectories of $N = 1000$ particles (left side, black curves) initially distributed at a height $h = 2.00$ from the mirror. The histogram of the distribution of the positions (right side, orange segments) at the end of the evolution is interpolated to obtain the corresponding density $P(x,t)$ (right side, dashed brown line).

the Born rule should still be observable around $t \approx 0.2t_0 \approx 0.2$ms, if all neutrons were initially perfectly localized at an altitude $h = 1.5x_0 \approx 8.8\mu$m. This level of accuracy in the time resolution should be attainable with current experimental setups.

3.5 CONCLUSION

The Born rule was introduced by Born in 1926 in order to provide an interpretation of the wavefunction that appears in the Schrödinger equation. Interestingly, in the original paper by Born [85], the rule appears in a note added in proofs, and is expressed in words rather than mathematically.[6] Such simple rule stands alone with respect to the mathematical machinery of quantum mechanics, but is of course extremely important, as it bridges the gap between the abstract mathematical theory and the interpretation of actual experiments.

A question that has been raised by several researchers is whether the Born rule should be considered as fundamental, or rather an approximation. In particular, Valentini [89, 96] suggested that the Born rule plays the same role as thermal equilibrium in classical statistical mechanics. Just like an out-of-equilibrium classical system quickly relaxes towards a Maxwell-Boltzmann equilibrium, a quantum system may exist in a “subquantum" state where the Born rule is not satisfied. We always observe the validity of the

---

[6] The footnote reads as [85]: *Anmerkung bei der Korrektur: Genauere Uberlegung zeigt, daß die Wahrscheinlichkeit dem Quadrat der ψ proportional ist.* (Note added in proofs: More careful consideration shows that the probability is proportional to the square of ψ).

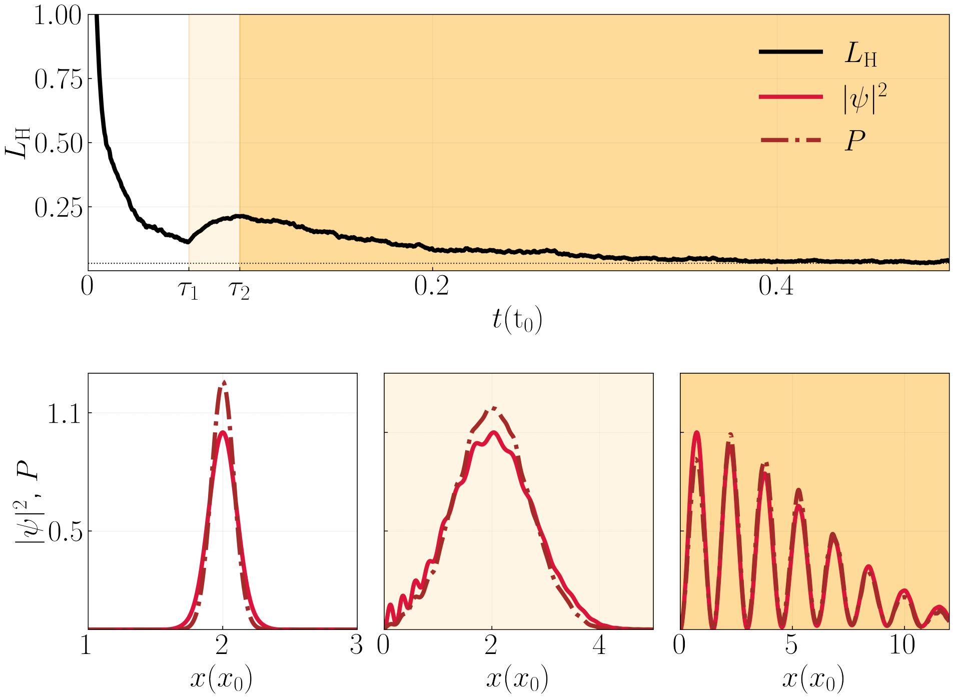

FIGURE 3.15: Upper panel: Time evolution of the distance $L_H(t)$ for an initial state with $h = 1.5$ and $\zeta = 0.09$. The shaded colours represent the three different phases of the evolution described in the main text. The two vertical dashed lines show the times τ_1 and τ_2 between which the L_H distance increases. The dashed horizontal line corresponds to the level below which L_H cannot go, for reasons due to the numerical integration (errors due to the finite number of particles and the interpolation method). Full convergence – hence establishment of the Born rule – is achieved for a relaxation time $\tau_q \approx 0.5$, significantly larger than τ_2. Lower panels: Squared modulus of the wavefunction $|\psi|^2$ (red solid curve) and particle distribution P (blue dashed curve) at three different times, $t = 0.005$ (left), $t = 0.07$ (middle), and $t = 0.5$ (right) (in units of t_0), corresponding to the three regions visible in the upper panel.

Born rule only because this relaxation to quantum equilibrium is extremely fast.

Nelson's stochastic version of quantum mechanics provides an ideal arena to test such subquantum dynamics, as it allows to initialize the system in an out-of-equilibrium state that does not respect the Born rule. Due to the random nature of Nelson's dynamics, the Born rule is quickly attained over a timescale that depends on the system under study. (The same is true for the Bohm-de Broglie theory, but the latter being deterministic, it requires some sort of coarse graining in order to recover Born's rule).

In the present work, we have investigated numerically this relaxation to quantum equilibrium for three relevant cases: a standard double-slit interference setup, a harmonic oscillator, and a quantum particle in a uniform gravity field, such as ultracold neutrons in the gravitational field of the Earth. For all cases, the Nelson stochastic trajectories are initially localized at a definite position, thereby violating the Born rule.

For the double slit and harmonic oscillator, we found that typical quantum phenomena, such as interferences, always occur well after the establishment of the Born rule. In contrast, for the case of quantum particles free-falling in the gravity field of the Earth, an interference pattern is observed *before* the completion of the quantum relaxation. The different behavior in the latter case is likely to arise from the nonlinearity induced by the

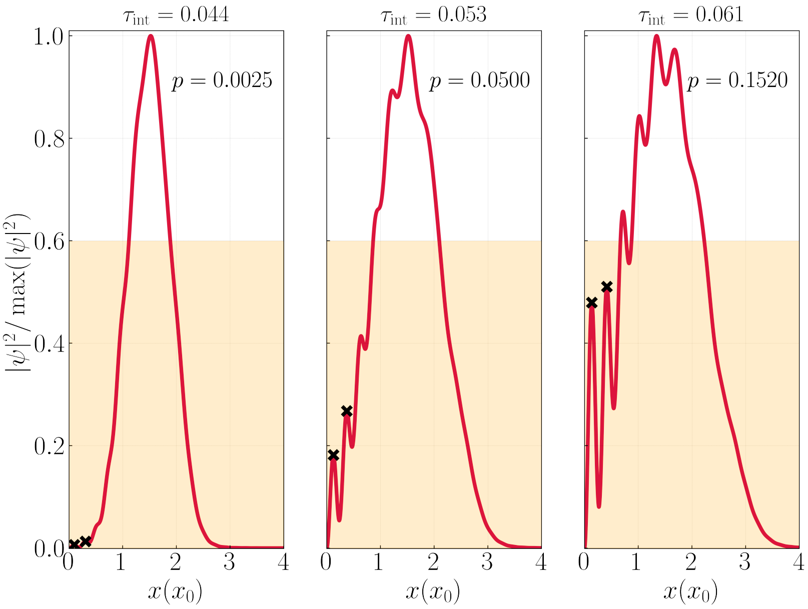

FIGURE 3.16: Normalized squared modulus of the wavefunction as a function of the distance x from the lower mirror, for an initial height $h = 1.50$ (in units of x_0) and three values of the prominence: $p = 0.0025$ (left panel), $p = 0.05$ (middle panel), and $p = 0.152$ (right panel). Interference is said to occur when at least two peaks are present in the green shaded region and have a prominence higher than p. The peaks are highlighted by a red cross on the curves. The corresponding interference time $\tau_{\rm int}$ depends on the chosen value of p and is also indicated on the figure.

reflecting mirror. If that is the case, a similar behaviour should be observed for generic non-quadratic Hamiltonians.

These findings may pave the way to experiments that are capable of discriminating standard quantum mechanics, where the Born rule is always verified, from Nelson's theory, for which an early subquantum dynamics may be present before full quantum relaxation has occurred.

One may argue that particles in our labs had a long and violent astrophysical history since the Big Bang, with ample time to relax to quantum equilibrium, so that it would be extremely difficult to observe any deviations from the Born rule at the present epoch. This is the line of argument followed by Valentini [103] in the context of the Bohm-de Broglie theory.

However, one might speculate on different scenarios. For instance, we could think of a decay-type experiment (beta or alpha decay, neutron or proton emission, etc.) in which a quantum particle (electron, positron, helium nucleus, neutron, proton...) is created from a fundamental process arising – for instance, but not exclusively – from the weak interaction. In this case, the particle might be born in a non-equilibrium situation where Born's rule has not had enough time to be established. Another example is the creation of a particle-antiparticle pair (*e.g.*, electron-positron) from a photon. This occurs in nuclear physics when a high-energy photon interacts with the nucleus, enabling the production of an electron-positron pair without violating the conservation of momentum. Just after the pair creation, the electron or positron should be in a non-equilibrium state. Of course, these are somewhat speculative proposals, but the findings put forward in this work at least suggest a viable way to test the existence of a subquantum dynamics in laboratory experiments.

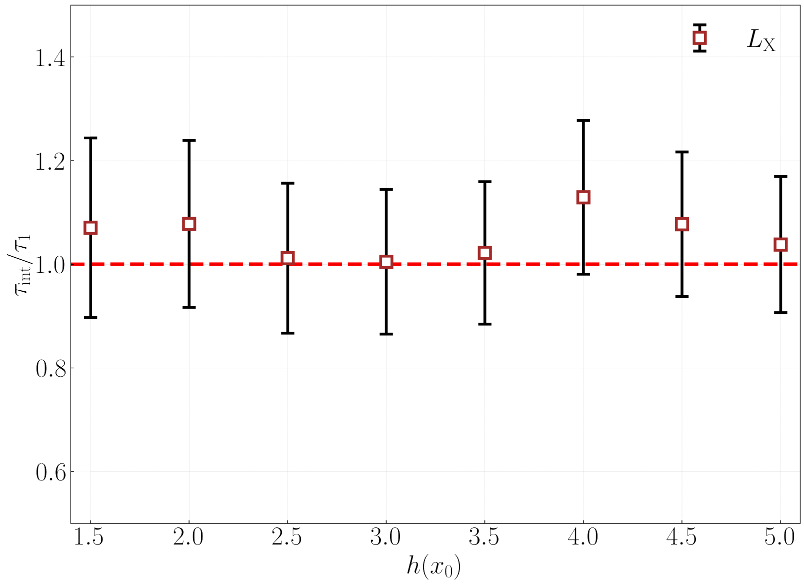

Figure 3.17: Ratio of the interference time τ_{int} and the time of increase of the L_H distance τ_1 (black squares) for different altitudes h and an intermediate value of the prominence, $p = 0.05$, see Fig. 3.16. The "error bars" are obtained using the upper and lower values $p = 0.0152$ and $p = 0.0025$. All ratios are close to unity, indicating that the two times relate to the same physical phenomenon.

KEY TAKEAWAYS

This chapter explored the relaxation to quantum equilibrium within Nelson's stochastic quantization framework, focusing on the emergence and implications of the Born rule in quantum mechanics.

- **Quantum Equilibrium**: $P(x,t) = |\psi(x,t)|^2$ (Born rule)
- **Nelsons's Stochastic Quantization**: Initially distribute particles according to $P(x,0) \neq |\psi(x,0)|^2$. Trajectories evolve according to

$$\mathrm{d}x(t) = b(x(t),t)\,\mathrm{d}t + \mathrm{d}W(t).$$

- **Measuring Convergence to Quantum Equilibrium**: To quantify the distance between $P(x,t)$ and $|\psi(x,t)|^2$ and study the relaxation process, several measures were used:
  - p norm:

$$L_p = \left(\int_{-\infty}^{+\infty} \left| P(x,t) - |\psi(x,t)|^2 \right|^p \mathrm{d}x \right)^{1/p}.$$

  - Inifinite norm (L_∞):

$$L_\infty = \max_x \left| P(x,t) - |\psi(x,t)|^2 \right|.$$

  - Relative Entropy (L_H):

$$L_H = \int_{-\infty}^{+\infty} P(x,t) \ln \left(\frac{P(x,t)}{|\psi(x,t)|^2} \right) \mathrm{d}x.$$

  Allows to determine the relaxation time τ_q to quantum equilibrium.

- **Systems studied**:
  - ✗ **Double-Slit Experiment**
    Characteristic time: apparition of the intereference pattern τ_int.
    Result: $\tau_\mathrm{q} < \tau_\mathrm{int}$
  - ✗ **Harmonic Oscillator**:
    Characteristic time: oscillation period T
    Result: $\tau_\mathrm{q} < T$
  - ✓ **Quantum Particles in a Gravitational Field**:
    Characteristic time: apparition of the intereference pattern τ_int
    Result: $\tau_\mathrm{q} > \tau_\mathrm{int}$

In conclusion, while relaxation to quantum equilibrium is generally rapid, the interplay between relaxation dynamics and the emergence of quantum phenomena varies across systems. It seems possible to observ deviations from the Born rule in certain setups, such as particles in a gravitational field.

References

[21] Kramers, H. A. *Physica* **1940**, *7*, 284–304.

[22] Moyal, J. E. *Journal of the Royal Statistical Society: Series B (Methodological)* **1949**, *11*, 150–210.

[31] Nelson, E. *Physical Review* **1966**, *150*, 1079–1085.

[32] Bohm, D. *Physical Review* **1952**, *85*, 166–179.

[55] McClendon, M.; Rabitz, H. *Physical Review A* **1988**, *37*, 3479–3492.

[84] Manfredi, Giovanni *4open* **2022**, *5*, 8.

[85] Born, M. *Zeitschrift für Physik* **1926**, *37*, 863–867.

[86] Einstein, A.; Podolsky, B., et al. *Physical Review* **1935**, *47*, 777–780.

[87] Bell, J. S., *Speakable and Unspeakable in Quantum Mechanics: Collected Papers on Quantum Philosophy*, 2nd ed.; Cambridge University Press: Cambridge, 2004.

[88] Styer, D. F.; Balkin, M. S., et al. *American Journal of Physics* **2002**, *70*, 288–297.

[89] Valentini, A. *Physics Letters A* **1991**, *156*, 5–11.

[90] Valentini, A. *Physical Review D: Particles and Fields* **2010**, *82*, 063513.

[91] Underwood, N. G.; Valentini, A. *Physical Review D: Particles and Fields* **2015**, *92*, 063531.

[92] Lebowitz, J. L. *Physics Today* **1993**, *46*, 32–38.

[93] Lebowitz, J. L. *Physica A: Statistical Mechanics and its Applications* **1999**, *263*, 516–527.

[94] Dürr, D.; Goldstein, S., et al. *Journal of Statistical Physics* **1992**, *67*, 843–907.

[95] Dürr, D.; Struyve, W. In *Do Wave Functions Jump? Perspectives of the Work of GianCarlo Ghirardi*, Allori, V., Bassi, A., et al., Eds.; Springer International Publishing: Cham, 2021, pp 35–43.

[96] Valentini, A.; Westman, H. *Proceedings of the Royal Society A: Mathematical, Physical and Engineering Sciences* **2005**, *461*, 253–272.

[97] Bacciagaluppi, G. *Foundations of Physics Letters* **1999**, *12*, 1–16.

[98] Beyer, M.; Paul, W. *Universe* **2021**, *7*, 166.

[99] Nesvizhevsky, V. V.; al, e. *Nature* **2002**, *415*, 297–299.

[100] Bohm, D.; Hiley, B. J. *Physics Reports* **1989**, *172*, 93–122.

[101] Peruzzi, G.; Rimini, A. *Foundations of Physics Letters* **1996**, *9*, 505–519.

[102] Bohm, D.; Vigier, J. P. *Physical Review* **1954**, *96*, 208–216.

[103] Valentini, A. In *Bohmian Mechanics and Quantum Theory: An Appraisal*, Cushing, J. T., Fine, A., et al., Eds.; Springer Netherlands: Dordrecht, 1996, pp 45–66.

[104] Petroni, N. C.; Guerra, F. *Foundations of Physics* **1995**, *25*, 297–315.

[105] Hatifi, M.; Willox, R., et al. *Entropy. An International and Interdisciplinary Journal of Entropy and Information Studies* **2018**, *20*, 1–32.

[106] Couder, Y.; Protière, S., et al. *Nature* **2005**, *437*, 208–208.

[107] Couder, Y.; Fort, E. *Physical Review Letters* **2006**, *97*, 154101.

[108] Greenside, H. S.; Helfand, E. *Bell System Technical Journal* **1981**, *60*, 1927–1940.

[109] Bayram, M.; Partal, T., et al. *Advances in Difference Equations* **2018**, *2018*, 17.

[110] Valentini, A. *Physics Letters A* **1991**, *158*, 1–8.

[111] Joyce, J. M. In *International Encyclopedia of Statistical Science*, Lovric, M., Ed.; Springer Berlin Heidelberg: Berlin, Heidelberg, 2011, pp 720–722.

[112] Pleinert, M.; von Zanthier, J., et al. *Physical Review Research* **2020**, *2*, 012051.

[113] Cotter, J. P.; Brand, C., et al. *Science Advances* **2017**, *3*, e1602478.

[114] Polyanin, A.; Zaitsev, V., *Handbook of Exact Solutions for Ordinary Differential Equations*; CRC press: New York, 2002.

[115] Tsuru, H. *Journal of the Physical Society of Japan* **1991**, *60*, 3657–3663.

[116] Zhang, L.; Guan, Y. In *Proceedings of the Twenty-Sixth ACM SIGMOD-SIGACT-SIGART Symposium on Principles of Database Systems*; Pods '07; Association for Computing Machinery: Beijing, China, 2007, pp 225–232.

[117] The ALPHA collaboration; Charman, A. E. *Nature Comm.* **2013**, *4*, 1785.

[118] Perez, P.; Sacquin, Y. *Class. Quantum Grav.* **2012**, *29*, 184008.

[119] Dufour, G.; Gérardin, A., et al. *Physical Review A: Atomic, Molecular, and Optical Physics* **2013**, *87*, 012901.

[120] Dufour, G. Quantum Reflection from the Casimir-Polder Potential, Theses, Université Pierre et Marie Curie - Paris VI, 2015.

[121] Crépin, P.-P. Quantum Reflection of a Cold Antihydrogen Wave Packet, Ph.D. Thesis, Sorbonne Université, 2019.

[122] Rousselle, O. Statistical Analysis of Classical and Quantum Measurements of Free Fall Acceleration of Antihydrogen for the GBAR Experiment, Theses, Sorbonne Université, 2022.

[123] Jenke, T.; Geltenbort, P., et al. *Nature Phys.* **2011**, *7*, 468–472.

[124] Jenke, T.; Cronenberg, G., et al. *Physical Review Letters* **2014**, *112*, 151105.

[125] Killian, C.; Burkley, Z., et al. *The European Physical Journal D* **2023**, *77*, 50.

[126] Suda, M.; Faber, M., et al. *Zeitschrift für Naturforschung A* **2022**, *77*, 875–898.

[127] Vallé, O.; Soares, M. In Imperial College Press: London, 2004.

[128] Crépin, P.-P.; Christen, C., et al. *Physical Review A: Atomic, Molecular, and Optical Physics* **2019**, *99*, 042119.

CHAPTER 4

QUANTUM-CLASSICAL ANALOGUES FOR OPTIMISATION

Le vrai point d'honneur n'est pas d'être toujours dans le vrai. Il est d'oser, de proposer des idées neuves, et ensuite de les vérifier.
— P-G. de Gennes

In this chapter, we develop a method to optimize the dynamics of a quantum harmonic oscillator by leveraging a quantum-classical analogy based on Nelson's stochastic formulation of quantum mechanics. Our goal is to transition the system from an initial stationary state to a final stationary state in the shortest possible time while minimizing a specified cost function. By establishing an analogy between the quantum harmonic oscillator and the classical overdamped dynamics of a Brownian particle in a harmonic potential, we apply a variational principle to derive optimal protocols for the control parameter, which is the stiffness of the potential. We consider two cost functions: the cumulative energy over time and the dynamical phase of the wavefunction. The latter allows us to construct protocols that are adiabatically optimal, minimizing the deviation from an adiabatic process for a given duration. Our numerical results demonstrate that the proposed optimal protocols can outperform existing methods, providing efficient shortcuts to adiabaticity in closed quantum systems. We begin in Sec. 4.1 by introducing the importance of optimization in quantum systems and outlining the objectives of this work. Sec. 4.2 presents the fundamentals of the quantum-classical analogy based on Nelson's stochastic mechanics, illustrating it with a simple numerical example. In Sec. 4.3, we describe the variational method used to derive optimal quantum protocols and explain how it is applied to minimize general cost functionals. Sec. 4.4 then provides numerical results for optimal protocols obtained using two different cost functions: the cumulative energy over time and the dynamical phase of the wavefunction. Finally, Sec. 4.5 summarizes our findings and discusses potential directions for future research.

Contents

4.1 INTRODUCTION

Optimization problems play an important role in both classical and quantum physics, providing an elegant framework for describing natural phenomena. Concepts such as Fermat's principle and the stationary-action principle, which serve as foundational pillars of physics, are deeply rooted in optimization principles. Optimization techniques are also crucial for efficient resource utilization, improving theoretical models, and controlling and manipulating the state of a physical system.

The central question in optimization research revolves around bringing a system from an initial state to a desired final state while minimizing a certain quantity, known as the cost function. A very diverse array of systems can be explored through the lens of optimization, ranging from Kramers-like problems with double well potentials [129] to trapped ions [130], cavity quantum electrodynamics [131], superconducting circuits [132], spin-orbit coupling [133], nitrogen-vacancy centers [134], many-body and spin-chain models [135], and even metrology applications [136]. Various methods can be employed depending on the specific circumstances. Optimization techniques based on variational principles are often utilized, such as in the quantum brachistochrone problem [137, 138] or in the context of Bose-Einstein condensates trapped in harmonic potentials [139, 140]. Additionally, optimization methods based on optimal control theory have gained prominence in recent years [141–145].

In this chapter, we focus on the case of the time-dependent quantum harmonic oscillator, a system of paramount importance across multiple fields of physics. Specifically, we will examine protocols for manipulating the stiffness of the potential in order to efficiently transition the system from one steady-state to another in a time shorter than that required by an adiabatic (*i.e.*, quasi-static) process. This concept is known as *shortcut to adiabaticity* (STA) (for recent reviews, see [146, 147]). While many of the basic ideas were put forward about two decades ago, with various approaches such as counterdiabatic driving [148–150], inverse engineering [151, 152], scaling laws [153], and others [154–161] being introduced, the development of STA methods has gained much momentum in recent years [162–165].

Here, we will employ an approach recently proposed for the classical overdamped dynamics of a Brownian particle confined in a harmonic trap and in contact with a heat bath at given temperature [166]. This method, based on a variational principle, allowed us to optimize the transfer from one thermal equilibrium to another, by minimizing both the duration of the transfer and the expended work. The trade-off between duration and work could be modulated at will by tuning a single Lagrange multiplier.

The main purpose of the present chapter is to develop a quantum-classical analogy that allows us to exploit the aforementioned method in order to control and optimize the dynamics of a *quantum* harmonic oscillator. Indeed, analogies may serve as powerful tools in physics. For instance, the experiments conducted by Couder in 2005 [106] established a hydrodynamic analogy to the behavior of quantum particles, as described by the pilot wave theory introduced by de Broglie [167] and later developed by Bohm [32]. With this approach, it was possible to demonstrate the existence of quantum-like diffraction using a fully classical experimental setup [168].

The analogy to be presented here is based on an alternative formulation of quantum mechanics originally due to Nelson [31, 97, 98]. In Nelson's representation, the quantum evolution is governed by a first-order stochastic equation, supplemented by Schrödinger's equation for the wave guiding the trajectory in a manner similar to the Bohm-de Broglie theory. Nelson's stochastic equation bears a close resemblance to the Langevin equation that governs the overdamped motion of a classical Brownian particle, thus suggesting the potential for a fruitful quantum-classical analogy. Such an analogy has already been considered in recent years for an open quantum system [169]. In the present chapter, we will demonstrate that this approach is particularly well-suited for solving optimization problems for closed quantum systems.

The objective of this chapter is to devise a protocol that transitions the system from a given stationary state to another in the shortest possible time, while minimizing a specified cost function throughout the temporal evolution. In classical stochastic thermodynamics, it is common to minimize the work done on the system, which also corresponds to minimizing the dissipated heat [151, 166, 170, 171]. However, for closed Hamiltonian systems, such work is simply equal to the difference between the final and the initial energies, and therefore it is not a pertinent quantity to minimize [162].

In the ensuing sections, we will outline a method – based on Nelson's dynamics and the quantum-classical analogy mentioned above – which allows us to minimize a generic cost function, usually written as the sum of the duration of the protocol plus a functional F of the control parameters. As relevant examples, we will choose for F either the cumulative energy of the system over time or the dynamical phase of the wavefunction. The latter case allows us to construct protocols that are "adiabatically optimal", *i.e.* protocols that, for a given duration, minimize their distance (in a precise mathematical sense) from an adiabatic process.

In Section 4.2, we will detail the basic features of the classical analog of the time-dependent quantum harmonic oscillator using Nelson's stochastic formulation, illustrating the analogy with a simple numerical example. In Section 4.3, we will show how this analogy can be applied to the quantum harmonic oscillator. We will also describe a general method to obtain a protocol that is optimal in regards of both its duration and another cost functional to be specified at will. In Sec 4.4 we will present numerical results for optimal protocols obtained using two different cost functions as illustrative examples. Conclusions and perspectives for future work will be detailed in Sec. 4.5.

4.2 QUANTUM-CLASSICAL ANALOGY

4.2.1 Fundamentals of the analogy

A one-dimensional particle of mass m trapped in a time-dependent harmonic potential obeys the Schrödinger equation

$$i\hbar\frac{\partial}{\partial t}\psi(x,t) = \hat{H}(t)\psi \equiv \left(-\frac{\hbar^2}{2m}\frac{\partial^2}{\partial x^2} + \frac{1}{2}\kappa(t)x^2\right)\psi(x,t), \tag{4.1}$$

where $\hbar$ is Planck's constant, $\kappa(t)$ is the time-dependent stiffness of the potential, and $\psi(x,t)$ is the wavefunction of the system at time t and position x. The optimization procedure developed in this work consists in designing a protocol $\kappa(t)$ which brings the system from an initial stationary state $\psi_{\mathrm{i}}(x)$ at time t_{i} to a final (also stationary) state $\psi_{\mathrm{f}}(x)$ at time t_{f}, in the shortest possible time $\Delta t = t_{\mathrm{f}} - t_{\mathrm{i}}$, while minimizing a given cost function [162, 172, 173].

The derivation of these optimal protocols will be based on Nelson's formulation of quantum mechanics. In this approach, similarly to the Bohm-de Broglie formalism, quantum particles are supposed to have a well-defined position $x(t)$ evolving in time. Unlike the deterministic trajectories followed by quantum objects in the Bohm-de Broglie theory, Nelson's theory postulates that each trajectory obeys the stochastic differential equation

$$\mathrm{d}x(t) = b(x(t),t)\mathrm{d}t + \sqrt{2D}\,\mathrm{d}W(t), \tag{4.2}$$

where $b(x,t)$ is the deterministic drift velocity, $D = \hbar/2m$ is the diffusion coefficient, and $\mathrm{d}W(t)$ is the Wiener increment for a Markov process: $\langle \mathrm{d}W(t)\rangle = 0$, $\langle \mathrm{d}W(t)\,\mathrm{d}W(t')\rangle = t - t'$. The origin of the stochastic nature of the dynamic of quantum particles is postulated but not explained by Nelson's theory. The key point in Nelson's approach is to define the drift coefficient as

$$b(x,t) = \frac{\hbar}{m}\frac{\partial S(x,t)}{\partial x} + \frac{\hbar}{2m}\frac{\partial \ln \rho(x,t)}{\partial x}, \tag{4.3}$$

where $S(x,t)$ and $\rho(x,t)$ are respectively the phase and squared modulus of the wavefunction $\psi(x,t)$, expressed in polar form as $\psi = \sqrt{\rho}\exp(iS)$. This definition of $b(x,t)$ ensures that the probability distribution of a large ensemble of trajectories $x(t)$ obeying Nelson's equation (4.2) converges to the square-modulus of the wavefunction, following Born's rule [174]. If the initial probabilistic distribution of the trajectories follows Born's rule at $t = 0$, it will do so for all successive times $t > 0$. Hence, Nelson's theory reproduces the same results as the standard quantum mechanics based on the Schrödinger equation.

For the ground state of the harmonic oscillator, the Gaussian form of the wavefunction yields a simple form for the drift term of Eq. (4.3), as we now show. Due to the quadratic nature of the Hamiltonian in Eq. (4.1), if the initial wavefunction $\psi_\mathrm{i}(x, t = 0)$ is Gaussian, then it remains Gaussian for all times $t > 0$, and can be written as

$$\psi(x,t) = \frac{1}{\sqrt[4]{2\pi s(t)}}\exp\left[-\frac{x^2}{4s(t)} + i\alpha(t)x^2 + i\beta(t)\right], \tag{4.4}$$

where $s(t) = \langle x(t)^2\rangle$ is the time-dependent variance of the density, while $\alpha(t)$ and $\beta(t)$ are the dynamical and geometrical phases of the wavefunction, respectively. For the wavefunction to be a solution of Eq. (4.1), the time-dependent coefficients $\alpha(t)$ and $\beta(t)$ must satisfy the following relations:

$$\alpha(t) = \frac{m}{4\hbar}\frac{\dot{s}(t)}{s(t)}, \quad \dot{\beta}(t) = -\frac{\hbar}{4ms(t)}, \tag{4.5}$$

where the dot denotes differentiation with respect to the time t. The variance $s(t)$ is related to the standard deviation $\sigma = \sqrt{2s}$, which must obey the following Ermakov equation [175]:

$$\ddot{\sigma}(t) + \frac{\kappa(t)}{m}\sigma(t) = \frac{4D^2}{\sigma^3(t)}. \tag{4.6}$$

The coupled equations (4.5)-(4.6) provide a full, exact solution of the Schrödinger equation in the Gaussian form (4.4).

From Eqs. (4.3) and (4.4), one obtains immediately Nelson's drift velocity:

$$b(x,t) = \frac{\hbar}{m}\left(2\alpha(t) - \frac{1}{2s(t)}\right)x, \tag{4.7}$$

which, importantly, is linear in x. Therefore, we can rewrite Nelson's stochastic equation (4.2) as

$$\mathrm{d}x(t) = \frac{\hbar}{m}\left(2\alpha(t) - \frac{1}{2s(t)}\right)x(t)\,\mathrm{d}t + \sqrt{2D}\,\mathrm{d}W(t). \tag{4.8}$$

The above Nelson equation (4.8) bears a striking resemblance with the Langevin equation for a classical overdamped Brownian particle in a harmonic potential of stiffness $\bar{\kappa}(t)$ and same diffusion coefficient D, which we write here as:

$$\mathrm{d}x(t) = -\frac{\bar{\kappa}(t)}{\gamma} x(t)\mathrm{d}t + \sqrt{2D}\,\mathrm{d}W(t), \tag{4.9}$$

where γ is the usual Stokes drag coefficient, which we keep for dimensional reasons in the classical equation, but will disappear in the quantum results. The equations (4.8) and (4.9) are identical if we define the classical stiffness as:

$$\bar{\kappa}(t) = \gamma \frac{\hbar}{m}\left(2\alpha(t) - \frac{1}{2s(t)}\right). \tag{4.10}$$

Hence, our physical analogy is based on the mathematical equivalence between Nelson's equation (4.8) for a quantum particle in a harmonic oscillator and the Langevin equation (4.9) for a classical Brownian particle. In addition, for the classical Langevin equation, the variance $s(t)$ obeys the following closed evolution equation [176, 177]

$$\frac{\mathrm{d}s(t)}{\mathrm{d}t} = \frac{2}{\gamma}[D\gamma - \bar{\kappa}(t)s(t)]. \tag{4.11}$$

To complete the analogy, we need to specify the relationship between the stiffness $\kappa(t)$ of the quantum oscillator and the the stiffness $\bar{\kappa}(t)$ appearing in the classical stochastic process. Taking the time derivative of Eq. (4.10) and using Eqs. (4.5) and (4.11), we arrive, after some algebra, at the following expression for the quantum stiffness

$$\kappa(t) = \frac{\hbar^2}{2ms^2(t)} + \frac{m}{\gamma}\dot{\bar{\kappa}}(t) - \frac{m}{\gamma^2}\bar{\kappa}^2(t), \tag{4.12}$$

written in terms of the classical stiffness $\bar{\kappa}(t)$ and its time derivative. Equation (4.12) serves as a crucial link in establishing the quantum-classical analogy, acting as a bridge between the quantum system and its classical analog.
Finally, from Eq. (4.11) it results that, at equilibrium: $\bar{\kappa}_{\mathrm{eq}} = D\gamma/s_{\mathrm{eq}}$ for the classical case. For the quantum case, from Eq. (4.12) we obtain

$$\kappa_{\mathrm{eq}} = \frac{m}{\gamma^2}\bar{\kappa}_{\mathrm{eq}}^2 = \frac{D^2 m}{s_{\mathrm{eq}}^2}, \tag{4.13}$$

which does not depend on the classical parameter γ, as expected.
Our strategy will be to suggest a classical protocol $\bar{\kappa}(t)$ and use Eq. (4.12) to obtain the corresponding quantum protocol. By construction, the evolution of the variance $s(t)$ will be identical for both cases and given by Eq. (4.11). Therefore, if we can devise a classical protocol that brings the variance from an initial equilibrium state with $s(t_{\mathrm{i}}) = s_{\mathrm{i}}$ to a final equilibrium state with $s(t_{\mathrm{f}}) = s_{\mathrm{f}}$, then the corresponding quantum protocol will do the same.

4.2.2 Example: STEP protocol

To illustrate the quantum-classical analogy, we examine a sudden protocol (frequently referred to as STEP) which consists in an abrupt change of the classical stiffness from $\bar{\kappa}_{\mathrm{i}}$ to $\bar{\kappa}_{\mathrm{f}}$. However, because of the presence of a first derivative in Eq. (4.12), it is necessary to smooth out such STEP protocol. The smoothed STEP is then defined as follows [178]

$$\bar{\kappa}(t) = \frac{\bar{\kappa}_{\mathrm{f}} + \bar{\kappa}_{\mathrm{i}}}{2} + \frac{\bar{\kappa}_{\mathrm{f}} - \bar{\kappa}_{\mathrm{i}}}{2}\tanh\left(\frac{t-\tau}{\epsilon}\right). \tag{4.14}$$

The classical stiffness is centered at $t = \tau$ and becomes steeper and steeper as $\epsilon \to 0$. For simplicity, we have used units for which: $\kappa_\mathrm{i} = 2$, $\hbar = \gamma = 1$, $m = 1/2$, so that the quantum diffusion coefficient is $D = \hbar/2m = 1$. In these units, time is measured in units of $2/\omega_\mathrm{i}$ and the variance in units of $\hbar/m\omega_i$, where $\omega_\mathrm{i} = \sqrt{\kappa_\mathrm{i}/m}$ is the initial angular frequency of the harmonic potential. In the examples below, we have used $\bar{\kappa}_\mathrm{i} = 2$ and $\bar{\kappa}_\mathrm{f} = 4$, which in virtue of Eq. (4.13) yields: $\kappa_\mathrm{i} = 2$ and $\kappa_\mathrm{f} = 8$, and variances $s_\mathrm{i} = 0.5$ and $s_\mathrm{f} = 0.25$.

In Fig. 4.1 (bottom panel), we show the classical and quantum protocols for two values of the width $\epsilon = 0.1$ and $\epsilon = 1$. For the smoother classical protocol ($\epsilon = 1$, dashed black curve), the quantum protocol (shown in the inset) has a similar shape as its classical counterpart, although its initial and final values are different, in accordance with Eq. (4.13). In contrast, the steeper classical protocol ($\epsilon = 0.1$, solid orange curve) yields an oscillating quantum protocol (inset). These oscillations become stronger as $\epsilon \to 0$. The time evolution of the variance $s(t)$ (top panel of Fig. 4.1) – which, as stated above, is by construction the same for the classical and quantum cases – shows that the variance of the system is smoothly brought from its initial value to its final value, even for the case ($\epsilon = 0.1$) where the quantum protocol is strongly oscillating.

It is clear from Fig. 4.1 that the steeper protocol achieves the transition more quickly, but let us try to quantify this speed-up more accurately. Classically, the relaxation time for a STEP protocol is given by the final stiffness $\bar{\kappa}_\mathrm{f}$, and reads as: $\tau_\mathrm{rel} = \gamma/\bar{\kappa}_\mathrm{f}$. Rewriting this in terms of the quantum quantities, we get: $\tau_\mathrm{rel} = \sqrt{m/\kappa_\mathrm{f}} = \omega_\mathrm{f}^{-1}$, where γ, being a purely classical parameter, has naturally disappeared. Hence, the relaxation time is the inverse of the final oscillator frequency. In the present case, we have, in our units, $\tau_\mathrm{rel} = \omega_\mathrm{f}^{-1} = 0.25\,(2\omega_\mathrm{i}^{-1})$.

Now, it is important to understand that, for the quantum oscillator (which is conservative), this is not really a relaxation time. If we apply a STEP protocol directly on the quantum stiffness κ, the quantum system will oscillate indefinitely, with no damping. The standard way to implement the transition without oscillations would be to proceed adiabatically, which takes an infinite time. Hence, any quantum protocols, like those of Fig. 4.1, that take a finite time to complete, already do much better than the adiabatic one. In the figure, the slower protocol takes about $\approx 6\,(2\omega_\mathrm{i}^{-1})$ to achieve the transition, while the faster protocol takes $\approx 0.75\,(2\omega_\mathrm{i}^{-1})$. This speeding up is achieved through the special temporal profile of the quantum protocol $\kappa(t)$, which was obtained thanks to the quantum-classical analogy.

But the classical STEP protocol will never be able to go faster than the relaxation time $\tau_\mathrm{rel} = \omega_\mathrm{f}^{-1}$, which therefore constitutes a fundamental limit also for the quantum protocol, as the evolution of the variance is by construction the same for both. In the next section, we will develop a method to construct optimal protocols that break this limit, and allow relaxation on a timescale shorter than ω_f^{-1}. Therefore, these optimal protocols not only outperform the adiabatic process ($\tau_\mathrm{rel} = \infty$), but also do better than “naive" protocols such as STEP, for which $\tau_\mathrm{rel} = \omega_\mathrm{f}^{-1}$. In addition, they also minimize some other quantity of physical interest, such as the cumulative energy over time.

4.3 OPTIMAL QUANTUM PROTOCOLS

As mentioned in the preceding sections, our objective is to transition a quantum system from an initial state, ψ_i, to a final state, ψ_f, in the shortest possible time, Δt, while minimizing a certain cost function. For the time being, we keep this cost function as general as possible. The initial and final states are supposed to be the ground states in

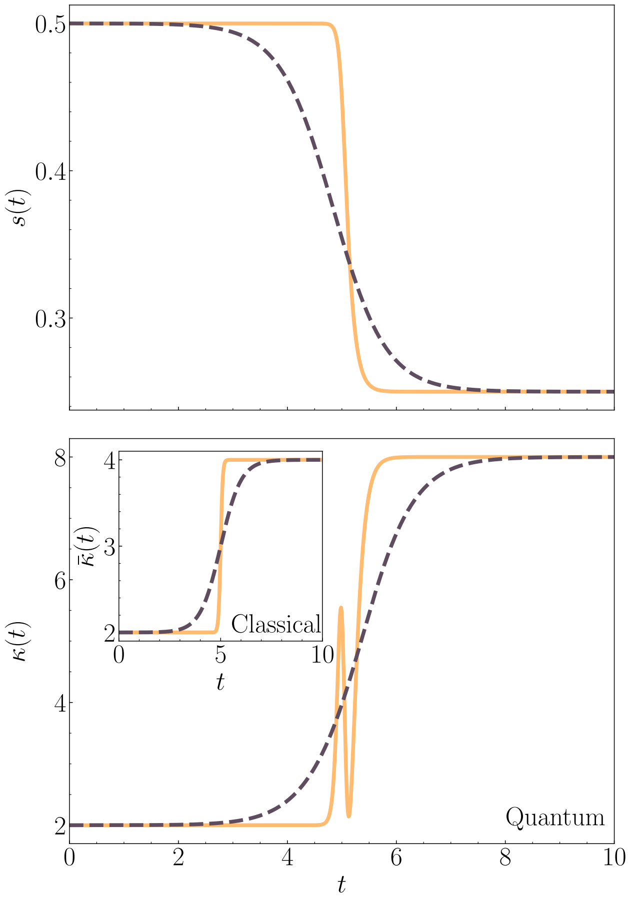

Figure 4.1: Top Panel: Evolution of the variance $s(t)$ as a function of time (measured in units of $2\omega_{\mathrm{i}}^{-1}$), for $\epsilon = 1$ (black dashed lines) and $\epsilon = 0.1$ (orange solid lines). The variance decreases from $s_{\mathrm{i}} = 0.5$ to $s_{\mathrm{f}} = 0.25$, in units of $\hbar/m\omega_i$ as detailed in the main text. The larger value of ϵ correspond to the smoother protocol. Bottom panel: Time evolution of the quantum stiffness $\kappa(t)$ (main plot) associated to the classical STEP protocol $\bar{\kappa}(t)$ (inset), for the same values of ϵ. When the classical STEP is smooth ($\epsilon = 1$, black dashed lines), the quantum protocol is also smooth and follows the same behavior as the classical one. In contrast, when the classical STEP protocol varies abruptly ($\epsilon = 0.1$, orange solid lines), an oscillation appears at mid-time in the quantum protocol.

the respective harmonic potentials at t_i and t_f. For a classical Brownian particle in a thermal bath, several methods already exist for finding the optimal protocol, especially when the cost function is the work done on the system [151, 166, 170].

In the following subsection, we will present the work of Ref. [166] which consitutes the basis of our work, based on a variational principle. Then, in the next subsection we will show how this method can be applied to the quantum case thanks to the classical analogy developed in Sec. 4.2, and how it can be used to find optimal protocols for the quantum harmonic oscillator. Along this subsection, we will explore various cost functions and, for each of them, find the optimal protocol.

4.3.1 Optimisation method for classical systems

We assume a classical Brownian particle whose dynamics is described by the overdamped Langevin equation, as Eq. (4.9). The particle is trapped in an harmonic potential whose stiffness $\bar{\kappa}(t)$ is modulated over time. As the probability distribution of the particle's position is Gaussian, with the variance $s(t)$ evolving according to Eq. (4.11). Then, the system is fully described by the path $(s(t), \bar{\kappa}(t))$ followed by the variance and the stiffness.

We seek a manner to change the stiffness from an initial value $\bar{\kappa}_\mathrm{i}$ to a final value $\bar{\kappa}_\mathrm{f}$ such as the state of the system evolves from an initial thermal equilibrium to a final thermal equilibrium. The equilibrium conditions are given by the stationary solution of Eq. (4.11), leading to $s_\mathrm{eq}\bar{\kappa}_\mathrm{eq} = D\gamma$, D being the diffusion coefficient and γ the friction, involved in Eq. (4.9). A possible manner to vary the stiffness is to do so adiabatically, which means that the system is always in an equilibrium state. However, the time duration of this protocol is very large, and we want to find a way to reduce it.

In Sec. 4.2.2, we discussed the STEP protocol case, which consists on an abrupt change of stiffness. This protocol is a shortcut to adiabaticity, as it allows to reach the final equilibrium state in a finite time. However, the time duration of the STEP protocol (given by the relaxation time $\gamma/\bar{\kappa}_\mathrm{f}$ of the variance) is not the shortest time possible for the transition, and this protocol does not ensure the minimisation of any desired cost function.

Then, we desire to find an optimisation method to minimise the time duration of the transition, while keeping a cost function (which is a functional of the stiffness), noted $F[\bar{\kappa}]$, as low as possible. Ref. [166] provides such method, based on a variational principle, by defining a functional

$$J[\bar{\kappa}] = \Delta t[\bar{\kappa}] + \lambda F[\bar{\kappa}]. \tag{4.15}$$

The Lagrange multiplier λ is the trade-off between the time duration and the cost function. Minimising this functional leads to the optimal protocol $\bar{\kappa}(t)$, which is the solution of the Euler-Lagrange equation $\delta J/\delta\bar{\kappa} = 0$. Taking the limit $\lambda \to \infty$ leads to the optimal protocol that minimises the cost function allowing the time duration to be as long as necessary (adiabatic limit), while taking $\lambda \to 0$ leads to the optimal protocol that minimises the time without taking into account the cost function.

In the next subsection, we will apply this method to the quantum harmonic oscillator, using the quantum-classical analogy developed in Sec. 4.2, and keep the cost function F as general as possible. Here, for the sake of illustration, we will consider tht the cost function is the average expended work $W(t)$ over time. It is a common cost function in classical stochastic thermodynamics. According to Ref. [179], the average work done on the system over time is given by

$$\Delta W = \int_{t_\mathrm{i}}^{t_\mathrm{f}} \mathrm{d}t \; \frac{1}{2} s(t)\dot{\bar{\kappa}}(t) \tag{4.16}$$

See Appendix I for the detailed derivation of this expression.

To use the Euler-Lagrange equation, we need to express the Lagrangian associated to the functional J. To do so, we assume that the variance is a monotonic function of the time, and we can use it as the independent variable, instead of the time. The stiffness then writes $\bar{\kappa}(s)$, such as $\bar{\kappa}(t) = \bar{\kappa}(s(t))$ (note that, for simplicity of notation, we use the same variable name for a function of t and the corresponding function of s). It allows to express the time duration and the work as functionals of $\bar{\kappa}$:

$$\Delta t[\bar{\kappa}] = \frac{1}{2} \int_{s_\mathrm{i}}^{s_\mathrm{f}} \mathrm{d}s \; \frac{\gamma}{[D\gamma - s\bar{\kappa}(s)]} \tag{4.17}$$

and

$$\Delta W = \frac{1}{2} \int_{s_\mathrm{i}}^{s_\mathrm{f}} \mathrm{d}s \; \bar{\kappa}(s). \tag{4.18}$$

The Lagrangian, defined as the integrand of the J-integral, is then given by

$$L[\bar{\kappa}] = \frac{\gamma}{[D\gamma - s\bar{\kappa}(s)]} + \lambda\bar{\kappa}(s) \tag{4.19}$$

where we remove the common 1/2 prefactor, and the Euler-Lagrange equation reads

$$\frac{\gamma}{[D\gamma - s\bar{\kappa}(s)]} = \lambda. \tag{4.20}$$

This is an algebraic equation, so no control on the boundary conditions is possible. The solution is analytical and is given by

$$\bar{\kappa}(s) = \frac{D\gamma}{s} + \sqrt{\frac{\gamma}{\lambda s}}. \tag{4.21}$$

We indeed recover the adiabatic limit for $\lambda \to \infty$. Inserting this solution Eq. (4.11) gives the evolution of the variance $s(t)$, such as

$$s(t) = \left(\sqrt{s_\mathrm{i}} - \frac{t}{\sqrt{\gamma\lambda}}\right)^2. \tag{4.22}$$

It allows to go back to the time evolution of the stiffness $\bar{\kappa}(t)$, leading to the optimal protocol

$$\bar{\kappa}(t) = \frac{D\gamma + \sqrt{\frac{\gamma s_\mathrm{i}}{\lambda} - \frac{t}{\lambda}}}{\left(\sqrt{s_\mathrm{i}} - \frac{t}{\sqrt{\lambda\gamma}}\right)^2}. \tag{4.23}$$

From this expression, as well as Eq. (4.21), we see that the optimal protocol does not satisfy the equilibrium condition at the initial and final times. Discontinuities are needed to ensure them, leading to extra-work contributions, associated to abrupt changes of stiffness.

If we desire to get rid of these discontinuities, we have to smooth the optimal protocol. For that purpose, we have to control the derivative of the stiffness, and we can add a term to the Lagrangian, such as L now depends on both the stiffness and its (variance) derivative, noted $\bar{\kappa}'$, as

$$L[\bar{\kappa}, \bar{\kappa}'] = \frac{\gamma}{D\gamma - s\bar{\kappa}(s)} + \mu\bar{\kappa}'^2(t) \tag{4.24}$$

with μ another Lagrange mutliplier, that monitors the smoothness of the protocol, notably at the edges of the time interval. In the limit $\mu \to 0$, we recover the previous Lagrangian. The Euler-Lagrange is modified as

$$2\mu\bar{\kappa}''(s) = \frac{\gamma s}{(D\gamma - s\bar{\kappa}(s))^2} - \lambda. \tag{4.25}$$

As it is a second-order ordinary differential equation, the two equilibrium conditions can be imposed for the optimal protocol, solution of previous equation. Analytical, numerical and experimental verifications of this optimisation method have been given in Ref [166]. We will not discuss them, as we just wanted to present the method developped for the classical harmonic oscillator. Brief explanations about the experimental parameters of the experiment and the realisation the optical harmonic trapping are given in Appendix J. The objective of the rest of the chapter is to apply the method to the quantum harmonic oscillator case.

4.3.2 Application of the method for quantum systems

In order to find the optimal quantum protocol, we can process as for the classical case. First, we need to define the functional to be minimized $J[\kappa, \dot{\kappa}]$, which is a function of the control parameter (stiffness of the oscillator) and its time derivative. This functional will be written as the sum of the total duration of the protocol, denoted $\Delta t[\kappa]$, plus another functional to be minimized, denoted $F[\kappa, \dot{\kappa}]$ (our cost function), the latter associated with a Lagrange multiplier λ. Then, the optimal protocol κ_{opt} is found as the solution of the Euler-Lagrange equation derived from the total functional J. In practice, it will be necessary to add a third functional $G[\dot{\kappa}]$, and its Lagrange multiplier μ, in order to ensure that the boundary conditions on $\kappa(t)$ are satisfied.

One has the choice to express the above functionals either in terms of the classical stiffness κ or the quantum stiffness $\bar{\kappa}$, and then derive the corresponding Euler-Lagrange equations accordingly. In practice, as we shall see, it will be easier to express all functionals as a function of $\bar{\kappa}$ (and its time derivative) using Eq. (4.12). For simplicity of notation, we will use the same symbols (J, F and G) for the functionals, irrespective of their arguments.

Let us first express the time duration as a functional. We adopt the method developed in Ref. [166], which consists in using the variance s as an independent variable, instead of the time t [1]. Each protocol can then be characterized by a trajectory in the stiffness-variance space (κ, s). This allows us to express the protocols as a function of s instead of t, so that we write: $\kappa(s) = \kappa(t(s))$ and $\bar{\kappa}(s) = \bar{\kappa}(t(s))$. Using Eq. (4.11) one obtains for the time duration functional

$$\Delta t[\bar{\kappa}] = \frac{1}{2}\int_{s_\text{i}}^{s_\text{f}} \mathrm{d}s\, \frac{\gamma}{D\gamma - s\bar{\kappa}(s)}. \tag{4.26}$$

Note that the above functional depends on the classical protocol $\bar{\kappa}(s)$, and not the quantum one $\kappa(s)$.

Since we are interested in the dynamics of the quantum system, the yet-unspecified cost functional F is usually expressed in terms of κ, the stiffness of the quantum harmonic

---

[1] This is possible only if $s(t)$ is a monotonic function of t.

oscillator. However it is easy to express it in terms of $\bar{\kappa}$, by using Eq. (4.12) rewritten in the s-domain:

$$\kappa(s) = \frac{\hbar^2}{2ms^2} + \frac{2m}{\gamma^2}[D\gamma - s\bar{\kappa}(s)]\bar{\kappa}'(s) - \frac{m}{\gamma^2}\bar{\kappa}^2(s), \tag{4.27}$$

where the prime denotes the derivative with respect to s. Then, we can write F in integral form as: $F[\bar{\kappa}, \bar{\kappa}'] = \int_{s_\mathrm{i}}^{s_\mathrm{f}} \mathrm{d}s \; f(s, \bar{\kappa}(s), \bar{\kappa}'(s))$, where f is a function obtained by transforming the quantum stiffness to the classical stiffness using Eq. (4.27).

The need for another functional $G[\kappa']$ results from the requirement to avoid strong gradients in $\kappa(s)$. As was noted in Ref. [166], without this term the resulting optimal protocol displays jumps, *i.e.* infinite gradients, at the initial and final times. Mathematically, this is because, in the absence of this term, the Euler-Lagrange equation is an algebraic one, so that one cannot fix the boundary conditions on the solution, and instead has to “stitch" them artificially as jumps. That was not an issue for the overdamped dynamics studied in Ref. [166], because a system with vanishing inertia remains at equilibrium when the stiffness is suddenly changed. But here the situation is different, as the underlying problem is the standard Schrödinger equation, which does include inertia. Hence, if the boundary conditions are not satisfied at $t = t_\mathrm{f}$, then the system will continue to evolve and deviate from the target stationary state. A way to ensure that boundary conditions are indeed satisfied is to render the Euler-Lagrange equation a second-order differential equation [180]. This can be achieved by adding the following functional

$$G[\bar{\kappa}'] = \int_{s_\mathrm{i}}^{s_\mathrm{f}} \mathrm{d}s \; \left|\bar{\kappa}'(s)\right|^2, \tag{4.28}$$

with the corresponding Lagrange multiplier μ. Note that we expressed $G[\bar{\kappa}']$ in terms of the classical stiffness, to be consistent with the other functionals Δt and F. But limiting the gradient of $\bar{\kappa}(s)$ also limits the gradient of $\kappa(s)$, in virtue of Eq. (4.27). We also recall that the boundary conditions are those for which the variance is stationary at the boundaries, *i.e.* $\dot{s}_\mathrm{i,f} = 0$. From Eq. (4.11), this is equivalent to imposing that $\bar{\kappa}_\mathrm{i,f}\, s_\mathrm{i,f} = D\gamma$.

In summary, the total functional to be minimized is $J = \Delta t + \lambda F + \mu G$, or explicitly:

$$J[\bar{\kappa}, \bar{\kappa}'] = \frac{1}{2}\int_{s_\mathrm{i}}^{s_\mathrm{f}} \mathrm{d}s \; \frac{\gamma}{D\gamma - s\bar{\kappa}(s)} + \lambda \int_{s_\mathrm{i}}^{s_\mathrm{f}} \mathrm{d}s \; f(s, \bar{\kappa}(s), \bar{\kappa}'(s)) + \mu \int_{s_\mathrm{i}}^{s_\mathrm{f}} \mathrm{d}s \; \left|\bar{\kappa}'(s)\right|^2. \tag{4.29}$$

It is important to understand that λ and μ play very different roles. While λ corresponds to the weight given to the cost functional we want to minimize on physical grounds, μ is present only to ensure that the equilibrium conditions are satisfied. Nevertheless, both Lagrange multipliers have an impact on the resulting optimal solution. The Lagrangian associated to Eq. (4.29) is

$$L[s, \bar{\kappa}, \bar{\kappa}'] = \frac{\gamma}{D\gamma - s\bar{\kappa}} + \lambda f + \mu \left|\bar{\kappa}'\right|^2, \tag{4.30}$$

where we removed the factor 1/2 from the first term, because it can be included in the Lagrange multipliers λ and μ. The optimal protocol is obtained by solving the Euler-Lagrange equation associated with L, which reads as

$$2\mu\bar{\kappa}'' = \frac{\gamma s}{[D\gamma - s\bar{\kappa}(s)]^2} + \lambda\frac{\partial f}{\partial \bar{\kappa}} - \lambda\frac{\mathrm{d}}{\mathrm{d}s}\frac{\partial f}{\partial \bar{\kappa}'}. \tag{4.31}$$

This equation is, as expected, a second-order differential equation for $\bar{\kappa}(s)$ and the two boundary conditions $\bar{\kappa}_\mathrm{i,f} = D\gamma/s_\mathrm{i,f}$ can thus be imposed.

4.4 OPTIMIZATION RESULTS

Some protocols have already been studied in the past for the case where the cost function is the work done on the system [170], *i.e.*: $F \equiv W = \int_{t_\mathrm{i}}^{t_\mathrm{f}} \langle\psi|\partial_t \hat{H}(t)|\psi\rangle \mathrm{d}t$. It was shown that the optimal protocol is highly degenerate [151], with the minimal work simply corresponding to the difference between the final and initial energies of the system [162]: $W_\mathrm{opt} = E_\mathrm{f} - E_\mathrm{i}$. In particular, for any protocol that satisfies the right boundary conditions – so that the initial and final states are both stationary – the work done on the system will be the optimal one, irrespective of the duration of the protocol [162]. This is not too surprising, as the quantum oscillator system is conservative, and therefore the energy expended to go from one stationary state to another should only depend on these states, and not on the path connecting them. For these reasons, the work W does not appear to be the pertinent cost functional to be minimized. The advantage of the method described in the preceding section is that it allows us to select any cost functional, and find the corresponding protocol that minimizes it for a given duration Δt. Here, we will consider two different functional forms of F and find the optimal protocol for each of them.

In all the forthcoming simulations, we employ units in which $\hbar = \gamma = 1$, $m = 0.5$, and then $D = 1$. The variance increases in time from $s_\mathrm{i} = 1$ to $s_\mathrm{f} = 2$, so that the classical equilibria correspond to $\bar{\kappa}_\mathrm{i} = D\gamma/s_\mathrm{i} = 1$ and $\bar{\kappa}_\mathrm{f} = D\gamma/s_\mathrm{f} = 0.5$. The quantum equilibrium conditions are such that: $\kappa_\mathrm{i} = mD^2/s_\mathrm{i}^2 = 0.5$ and $\kappa_\mathrm{f} = mD^2/s_\mathrm{f}^2 = 0.125$. The classical relaxation time is then: $\tau_\mathrm{rel} = \sqrt{m/\kappa_\mathrm{f}} = \omega_\mathrm{f}^{-1} = 2$. All optimal protocols considered in the next two subsections are such that $\Delta t < \tau_\mathrm{rel}$ (except for one case where $\Delta t = 2.1$), confirming that they can outperform the STEP protocols, as discussed in Sec. 4.2.2.

Finally, in the Appendix F, we will also treat the case of the classical optimal protocol developed in Ref. [166], and discuss how it can be translated into an analog quantum protocol.

4.4.1 Cumulative energy as cost function

First, we take the integral of the energy as the cost function, which, when divided by the total duration, corresponds to the time-averaged energy furnished to the system, a quantity of clear physical interest, both theoretically and for experimental applications. As the wavefunction is supposed to be Gaussian at all times, see Eq. (4.4), it is straightforward to write the energy as

$$E(t) = \langle\psi|\hat{H}(t)|\psi\rangle = \frac{m}{4s(t)}\left(\frac{1}{2}\dot{s}^2(t) + \frac{2s^2(t)\kappa(t)}{m} + 2D^2\right), \tag{4.32}$$

where $\hat{H}(t)$ is defined in Eq. (4.1). We define the functional $F \equiv F_E$ as the integral of the energy. After changing variable from t to s and writing $\kappa(s)$ in terms of $\bar{\kappa}(s)$ using Eq. (4.27), we obtain

$$F_E[\bar{\kappa}, \bar{\kappa}'] = \frac{m}{4\gamma}\int_{s_\mathrm{i}}^{s_\mathrm{f}} \mathrm{d}s \left[\frac{D\gamma - s\bar{\kappa}(s)}{s} + \frac{3D^2\gamma^2 - s^2\bar{\kappa}^2(s)}{s(D\gamma - s\bar{\kappa}(s))} + 2s\bar{\kappa}'(s)\right]. \tag{4.33}$$

The corresponding Lagrangian is then

$$L[s, \bar{\kappa}, \bar{\kappa}'] = \frac{\gamma}{D\gamma - s\bar{\kappa}} + \frac{\lambda}{\gamma}\left[\frac{D\gamma - s\bar{\kappa}}{s} + \frac{3D^2\gamma^2 - s^2\bar{\kappa}^2}{s(D\gamma - s\bar{\kappa})} + 2s\bar{\kappa}'\right] + \mu|\bar{\kappa}'|^2, \tag{4.34}$$

where the factor $m/4$ was absorbed in the Lagrange multiplier λ. The resulting Euler-Lagrange equation is a second-order nonlinear differential equation for $\bar{\kappa}(s)$, and the initial and final values of the classical protocol can be imposed according to Eq. (4.13). The Euler-Lagrange equation is

$$2\mu\gamma\,\bar{\kappa}'' = \frac{\gamma^2 s + 3D^2\gamma^2\lambda - s^2\bar{\kappa}^2\lambda}{(D\gamma - s\bar{\kappa})^2} - \frac{2s\bar{\kappa}\lambda}{D\gamma - s\bar{\kappa}} - 3\lambda, \tag{4.35}$$

and it can be solved numerically using an iterative method such as Thomas's algorithm [181]. Note that, had we not added the Lagrange multiplier μ, Eq. (4.35) would be an algebraic equation, and it would be possible to fix the correct boundary conditions.
The solutions of Eq. (4.35) are represented in Fig. 4.2, for two distinct situations: a case where μ is kept fixed (left panels) and a case where λ is kept fixed (right panels). For the first case ($\mu = 0.1$ fixed), three solutions, corresponding to $\lambda = 0.01$, 0.10, and 1.00 are represented, thus showing the impact of varying the Lagrange multiplier associated with the cost function F_E. The classical protocols are depicted in the upper panels of the figure, and the associated quantum protocols in the lower panels. The equilibrium conditions at the initial and final times are fulfilled, as expected, and all protocols are continuous functions of the variance s. Moreover, as μ is constant, the derivatives of each protocol at the boundaries of the s domain are the same. Each classical protocol exhibits a minimal value, which decreases as λ increases while its quantum associated protocol has both minimum and maximum values, whose amplitude increases as λ increases. Hence, both protocols can become negative, corresponding to a repulsive harmonic potential, when λ is large enough. This feature, while notable, is not necessarily problematic and has been previously reported in the literature [151, 162, 182].
The right panels of Fig. 4.2 show the solutions when $\lambda = 1$ is kept constant while μ varies, taking the values 0.1, 0.5 and 1.00. The shapes of the curves are similar to the preceding case, but it is notable that the larger μ, the smaller the gradient of the protocol around s_i and s_f, as expected because the functional G limits the derivative of $\bar{\kappa}(s)$. Moreover, the range of values taken by the protocols increases as μ decreases, and they can become negative for small values of μ. Caution should be taken for even smaller values of μ, which lead to large values of the quantum protocol, both positive and negative. The same remark can also be made for very large values of λ.
All the above results were given in the s-domain, *i.e.* as a function of the variance. In order to go back to the time representation, one needs to solve Eq. (4.11) for t:

$$t(s) = t_\mathrm{i} + \frac{\gamma}{2}\int_{s_\mathrm{i}}^{s} \frac{\mathrm{d}y}{D\gamma - s\bar{\kappa}(y)}, \tag{4.36}$$

which can also be used to obtain the total duration $\Delta t = t_\mathrm{f} - t_\mathrm{i}$. The time-dependent solutions $\bar{\kappa}(t) = \bar{\kappa}(s(t))$ and $\kappa(t) = \kappa(s(t))$ are depicted in Fig. 4.3, together with the time evolution of the energy of the system, whose integral is the cost functional F_E associated to λ. The curves corresponds to the same values of λ and μ as in Fig. 4.2, with total durations $\Delta t = 0.95$, 0.87 and 0.82 (left panels, μ fixed) and $\Delta t = 0.82$, 1.27 and 1.58 (right panels, λ fixed). We recall that here the classical relaxation time is equal to $\tau_\mathrm{rel} = \sqrt{m/\kappa_\mathrm{f}} = \omega_\mathrm{f}^{-1} = 2$, and therefore $\Delta t < \tau_\mathrm{rel}$ everywhere.
When the Lagrange multiplier λ, corresponding to the functional $F_E = \int_{t_\mathrm{i}}^{t_\mathrm{i}} \mathrm{d}t\, E(t)$, is increased, then the energy integral decreases, as seen in the inset of Fig. 4.3(e). This is natural, as the role of the λ-term is precisely to limit the value of the cumulative energy over time. However, we also observe that the time duration Δt decreases for increasing λ, while the opposite occurred for classical systems [166]. This may seem surprising, as increasing λ should reduce the value of the functional F_E while increasing Δt (energy-time trade-off). But, in contrast to the classical overdamped case, here there are two

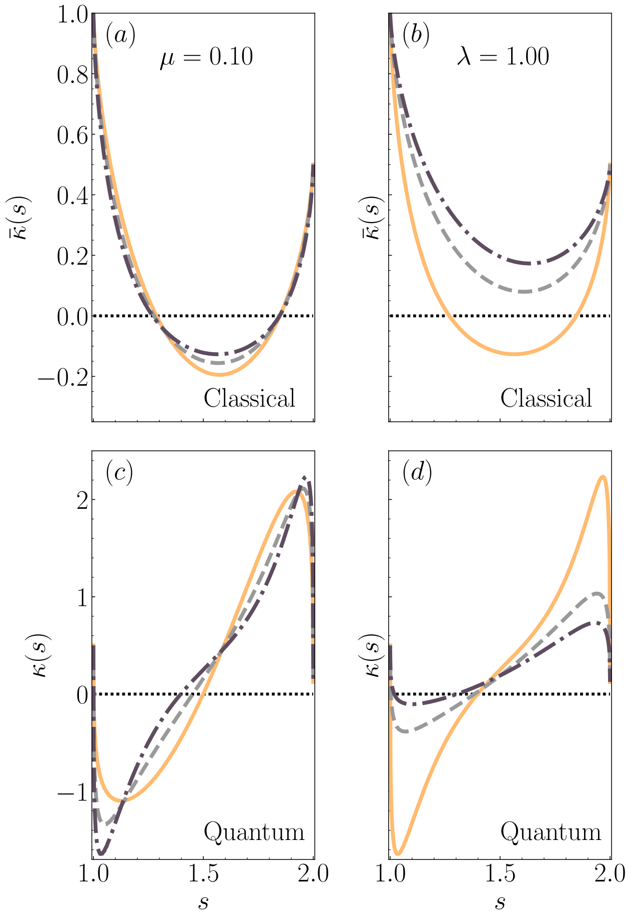

FIGURE 4.2: Energy-optimal protocols in the s-domain, where the variance increases from $s_\mathrm{i} = 1$ to $s_\mathrm{f} = 2$. Left panels: Classical protocols $\bar{\kappa}(s)$ (a) and quantum protocols $\kappa(s)$ (c), for a fixed value of $\mu = 0.10$, and $\lambda = 0.01$ (solid orange lines), 0.10 (dashed grey lines) and 1.00 (dot-dashed black lines). Right panels: Classical protocols $\bar{\kappa}(s)$ (b) and quantum protocols $\kappa(s)$ (d) for a fixed value of $\lambda = 1$, and $\mu = 0.1$ (solid orange lines), 0.50 (dashed grey lines) and 1.00 (dot-dashed black lines). Note that the quantum protocol can become negative for sufficiently large values of λ or sufficiently small values of μ.

Lagrange multipliers, so the trade-off is actually among *three* functionals, F_E, Δt, and G, which makes the whole situation more complex.
Conversely, the time duration increases as μ increases, which is more in line with a trade-off between G and Δt. At the same time, the cumulative energy over time increases with increasing μ, as seen in the inset of Fig. 4.3(f).
For all cases, the behavior of the variance appears very similar when plotted against time normalized to the duration Δt. As expected, $s(t)$ is strictly increasing in time and has vanishing derivatives close to the initial and final times. The energy $E(t)$ follows closely the evolution of $\kappa(t)$, which indicates that the potential energy is the preponderant contribution to the total energy of the system. It is important to note that, when μ becomes small enough, the energy might become negative, as seen in Fig. 4.3(f), although its time integral remains strictly positive, ensuring that the functional F_E is positive.
It is interesting to compare our results with other protocols, such as the ones that minimizes the work done on the system, proposed by Chen et al. [162]. This protocol is obtained from the Ermakov equation (4.6) rewritten in terms of the scale factor $q(t) = \sqrt{s(t)/s_\mathrm{i}}$, which reads as: $\ddot{q} + \frac{\kappa(t)}{m} q = \kappa_\mathrm{i}/q^3$. This equation can be inverted to obtain the stiffness as a function of the scale factor: $\kappa = \kappa_\mathrm{i}/q^4 - m\ddot{q}/q$. The protocol is then obtained by imposing a suitable temporal profile for $q(t)$. The authors of [162] chose a polynomial of fifth degree: $q(t) = (a-1)(6T^5 - 15T^4 + 10T^3 + 1)$, where $T = t/t_\mathrm{f}$ and $a = (\kappa_\mathrm{i}/\kappa_\mathrm{f})^{1/4}$, so that $q(t_\mathrm{i}) = 1$, $q(t_\mathrm{f}) = a$, and its first and second derivatives are zero at the initial and final times. We recall that imposing such boundary conditions is sufficient to minimize the external work, which becomes equal to the difference between the final and initial energies.
To compare Chen's polynomial protocol to our optimal protocol, we can fix a value of λ, for instance $\lambda = 10$, and vary the value of μ. For each protocol, we compute the energy integral $F_E = \int_{t_\mathrm{i}}^{t_\mathrm{f}} E(t)\mathrm{d}t$, as in Eq. (4.33), and the time duration Δt, Eq. (4.26). The results are shown in Fig. 4.4 for both our protocol (black squares) and Chen's (triangles). It appears that our protocol performs better, in terms of the integral of the energy, than the polynomial protocol for small values of Δt (gray area in Fig. 4.4). For larger Δt, the opposite is true, which can be explained by noticing that the long-duration regime corresponds to large values of μ. Indeed, the total functional $J = \Delta t + \lambda F + \mu G$, see Eq. (4.29), can be minimized by minimizing either F or G. If the Lagrange multiplier μ is large, then G dominates, and the variational procedure will end up minimizing J by essentially minimizing G instead of F. However, this is not a significant constraint for our purposes, since our aim is to minimize the energy integral for short durations, which correspond to small values of μ. In the inset of the same figure 4.4, we also plot the cumulative energy over time divided by Δt, which represents the *average* energy of the system. Again, our optimal protocol is the one that minimizes the averaged energy for short durations.

4.4.2 Dynamical phase as cost function

As a second example, we consider the following functional to be optimized: $F_\alpha = \int_{t_\mathrm{i}}^{t_\mathrm{f}} \mathrm{d}t\ \alpha^2(t)$, where $\alpha(t)$ is the dynamical phase given in Eq. (4.4). Before carrying out the optimization procedure, we provide some justification about the importance and meaning of such functional. According to Eq. (4.5), $\alpha(t)$ is proportional to the time derivative of the variance. During an adiabatic process, $\dot{s}(t) \approx 0$, because the process is infinitely slow, and therefore $\alpha(t) \approx 0$. Hence, the integral $F_\alpha = \int_{t_\mathrm{i}}^{t_\mathrm{f}} \mathrm{d}t\ \alpha^2(t)$ represents the departure from adiabaticity, and by minimizing such quantity we therefore minimize the “distance" of the optimal protocol from an adiabatic one.

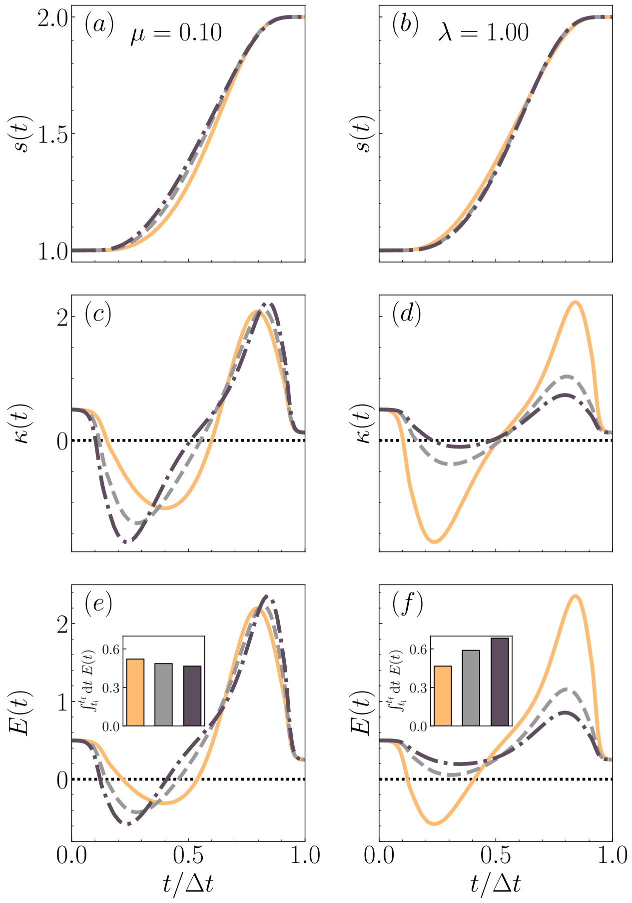

Figure 4.3: Energy-optimal protocols in the time domain, where the variance increases from $s_\mathrm{i} = 1$ to $s_\mathrm{f} = 2$. The time is normalized to the total duration of the protocol Δt, which is different for each pair of Lagrange multipliers (λ, μ). Left panels: variance $s(t)$ (a), quantum protocols $\kappa(t)$ (c), and instantaneous energy $E(t)$ (e), for a fixed value of $\mu = 0.10$, and $\lambda = 0.01$ (solid orange lines), 0.50 (dashed grey lines) and 1.00 (dot-dashed black lines). These values correspond to time durations: $\Delta t = 0.95$, 0.87 and 0.82. Right panels: variance $s(t)$ (b), quantum protocols $\kappa(t)$ (d), and instantaneous energy $E(t)$ (f), for a fixed value of $\lambda = 1$, and $\mu = 0.1$ (solid orange lines), 0.50 (dashed grey lines) and 1.00 (dot-dashed black lines). These values correspond to time durations: $\Delta t = 0.82$, 1.27 and 1.58. Note that, although the various protocols are quite different, the behavior of the variance is almost identical when time is scaled to the total duration Δt. The boundary values of the quantum protocols correspond to the conditions: $s_{\mathrm{i,f}}^2 \kappa_{\mathrm{i,f}} = mD^2$. The energy $E(t)$ is quite similar to the quantum stiffness $\kappa(t)$, indicating that the potential energy is the predominant contribution to the total energy of the system. The insets in (e) and (f) show the cumulative energy over time for the three protocols represented in the same panels.

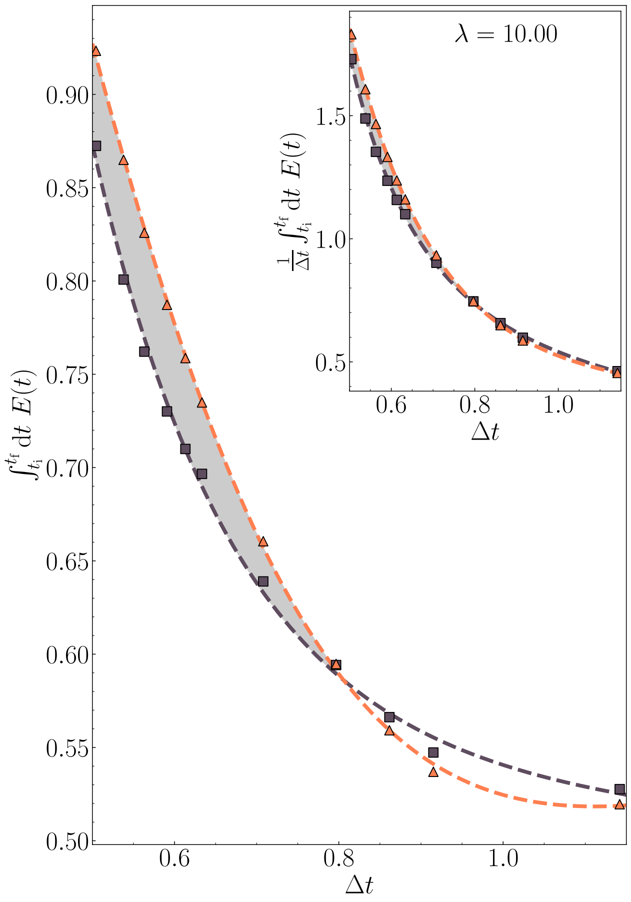

Figure 4.4: Cumulative energy of the system over time $\int_{t_i}^{t_f} \mathrm{d}t\, E(t)$ as a function of the total time duration Δt of the protocol. The black squares corresponds to the optimal protocol, solution of the Euler-Lagrange equation (4.35), while the orange triangles correspond to the polynomial protocol of Ref. [162]. In the gray shaded region, the optimal protocols display lower cumulative energy than the polynomial ones. The different times durations are obtained by varying the Lagrange multiplier μ, while keeping $\lambda = 10$ fixed. The dashed lines are empirical fits to the numerical data. The inset shows the same plots for the time-averaged energy, given by the integral of the energy divided by the time duration.

A visual way to represent the dynamical phase is to consider the Wigner function $W(x,p,t)$ [183] corresponding to the Gaussian wave packet of Eq. (4.4). The Wigner function is a quantum pseudo-probability density in the phase space (x,p). As the wavefunction is the exponential of a quadratic polynomial, its Wigner function is non-negative, and can be written as [184]

$$W(x,p,t) = A\exp\left(-\frac{x^2}{2s(t)} - \frac{2s(t)}{\hbar^2}\left[p - 2\alpha(t)\hbar x\right]^2\right), \tag{4.37}$$

where A is a normalization constant ensuring that $\int_{\mathbb{R}^2} W\,dx\,dp = 1$. Note that $W(x,p,t)$ peaks around the straight line in phase space $p_0(x,t) = 2\alpha(t)\hbar x = \hbar\partial_x S(x,t)$, where $S(x,t)$ is the total phase of the Gaussian wavefunction (4.4). When $\alpha = 0$, the Wigner function is symmetric with respect to both the position and momentum axes; when $\alpha \neq 0$, it is tilted of an angle θ such that $\tan\theta = 2\alpha\hbar/(m\omega_\mathrm{i})$ (obtained by expressing p and x in our normalized units). During an adiabatic protocol, $W(x,p,t)$ remains symmetric and only changes its aspect ratio. For instance, during an expansion ($s_\mathrm{f} > s_\mathrm{i}$), it becomes wider in x and narrower in p. Instead, during a faster-than-adiabatic process, W first gets tilted of an angle θ, then expands by increasing its spatial variance, and finally recovers a symmetric shape with $\alpha = 0$. This is illustrated in Fig. 4.5, where we show the phase space portraits for the optimal and adiabatic protocols at several instants in time. It is clear that the acceleration in the optimal protocol is achieved by tilting the Wigner function of a certain angle before coming back to a symmetric configuration at the end of the protocol.

Turning back to the minimization procedure, the F_α functional is given by, after changing variable from t to s and expressing the integrand in terms of $\bar{\kappa}(s)$,

$$F_\alpha[s,\bar{\kappa}] = \int_{t_\mathrm{i}}^{t_\mathrm{f}} \mathrm{d}t\ \alpha^2(t) = \frac{m^2}{8\gamma\hbar^2}\int_{s_\mathrm{i}}^{s_\mathrm{f}} \mathrm{d}s\ \frac{D\gamma - s\bar{\kappa}(s)}{s^2}, \tag{4.38}$$

where we have used Eq. (4.11). The total Lagrangian is

$$L[s,\bar{\kappa},\bar{\kappa}'] = \frac{\gamma}{D\gamma - s\bar{\kappa}(s)} + \lambda\frac{m^2}{8\gamma\hbar^2}\frac{D\gamma - s\bar{\kappa}(s)}{s^2} + \mu\bar{\kappa}'^2, \tag{4.39}$$

leading to the following Euler-Lagrange equation:

$$2\mu\,\bar{\kappa}'' = \frac{\gamma s}{(D\gamma - s\bar{\kappa})^2} - \frac{m^2\lambda}{8\gamma\hbar^2 s}. \tag{4.40}$$

Again, this is a second-order non-linear ordinary differential equation, whose initial and final conditions $\bar{\kappa}_\mathrm{i,f}$ can be imposed to ensure the equilibrium conditions.

We use the same parameters as in Sec. 4.4.1, notably $s_\mathrm{i} = 1$ and $s_\mathrm{f} = 2$. In Fig. 4.6 we represent the classical and quantum protocols for two cases: (i) a fixed value of $\mu = 0.10$ and λ varying in the range $\lambda \in [0.01, 0.10, 1.00]$ (left panels), and (ii) a fixed value of $\lambda = 1.00$ and μ varying in the range $\mu \in [0.10, 0.50, 1.00]$ (right panels). These correspond to the following time durations: $\Delta t = 0.95$, 0.97, and 1.00 (fixed μ, left) and $\Delta t = 1.00$, 1.67, and 2.10 (fixed λ, right). We recall that the classical relaxation time is equal to $\tau_\mathrm{rel} = \sqrt{m/\kappa_\mathrm{f}} = \omega_\mathrm{f}^{-1} = 2$. The general behaviors of the protocols look similar to those obtained in Sec. 4.4.1 for the energy cost function, probably because the solutions are somewhat dominated by the μ term. A notable difference is that the time duration is less sensitive to the values of the Lagrange multipliers. Also, the duration increases

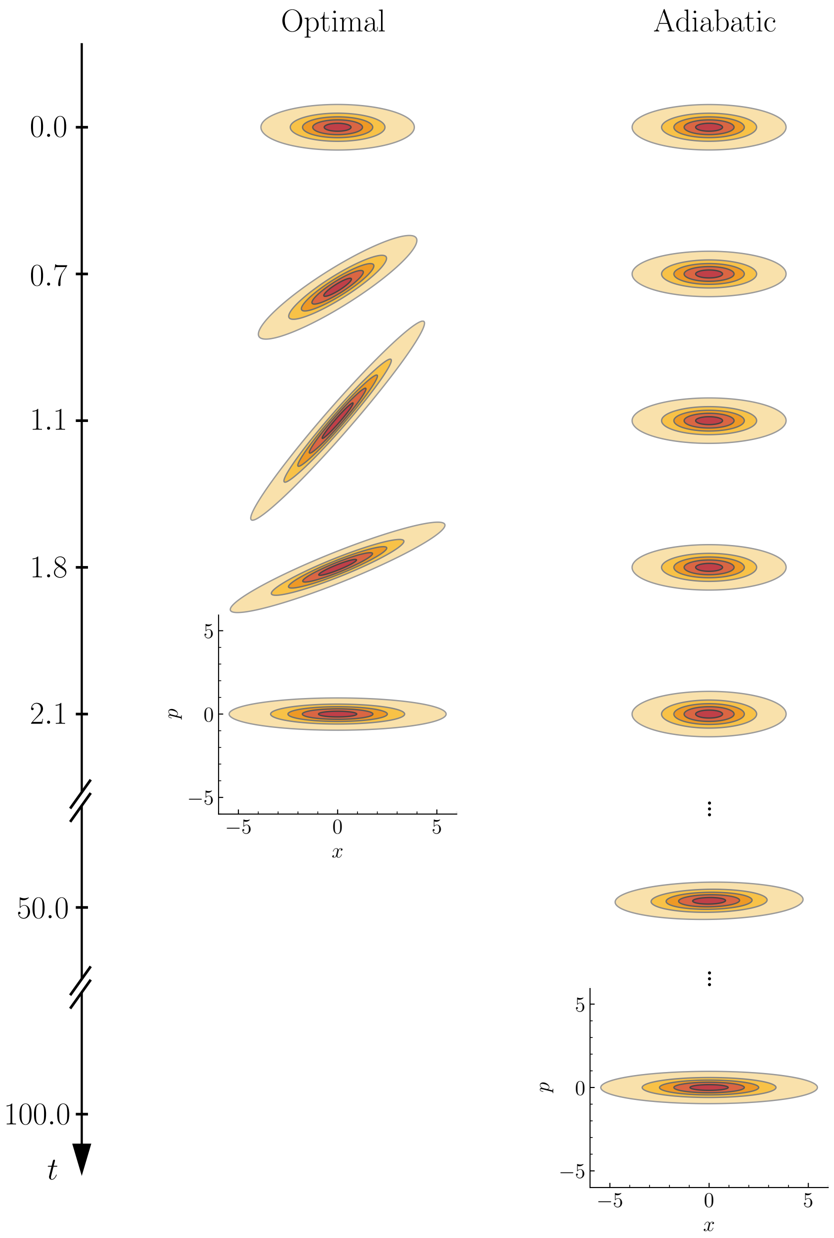

Figure 4.5: Wigner functions $W(x, p, t)$ at several instants indicated on the vertical time axis. The left panels refer to the phase-optimal protocol (with $\lambda = \mu = 1$), while the right panels correspond to an adiabatic protocol. The variance grows from $s_\mathrm{i} = 1$ to $s_\mathrm{f} = 2$. The Wigner function of the adiabatic protocol remains symmetric with respect to both the x and p axes, and slowly reduces its width in p while increasing its width in x. In contrast, the phase-optimal Wigner function first becomes elongated along the straight line $p = 2\alpha\hbar x$, before reaching the same final state in a time much shorter than the adiabatic protocol.

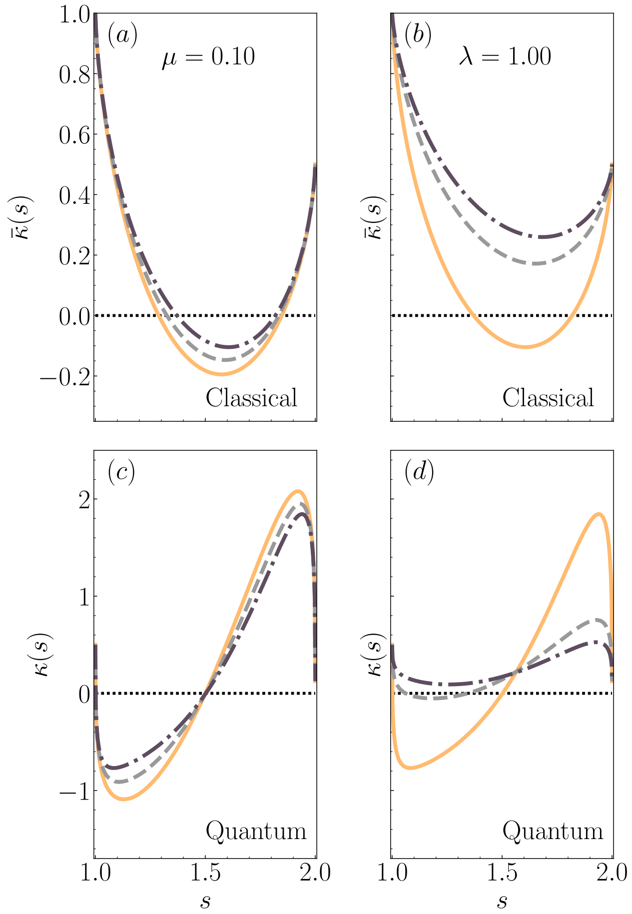

Figure 4.6: Phase-optimal protocols in the s-domain, where the variance increases from $s_{\mathrm{i}} = 1$ to $s_{\mathrm{f}} = 2$. Left panels: Classical protocols $\bar{\kappa}(s)$ (a) and quantum protocols $\kappa(s)$ (c), for a fixed value of $\mu = 0.10$ and $\lambda = 0.01$ (solid orange lines), 0.50 (dashed grey lines) and 1.00 (dot-dashed black lines). Right panels: Classical protocols $\bar{\kappa}(s)$ (b) and quantum protocols $\kappa(s)$ (d) for a fixed value of $\lambda = 1$ and for $\mu = 0.1$ (solid orange lines), 0.50 (dashed grey lines) and 1.00 (dot-dashed black lines). Note that the quantum protocol can become negative for sufficiently large values of λ or sufficiently small values of μ.

as λ increases, in contrast to what was observed for the energy-optimal protocols of Sec. 4.4.1.

The temporal evolution of the variance, the quantum stiffness, and the dynamical phase are depicted in Fig. 4.7, where the time has been normalized to the total duration of each protocol. In accordance with the above discussion on the Wigner functions, the dynamical phase vanishes at the initial and final times and is maximal around $\Delta t/2$. We also note that the maximum of $\alpha^2(t)$ and its time integral are smaller for the longer time durations of the protocols, *i.e.*, those protocols that are closer to adiabaticity, in agreement with our earlier interpretation of the functional F_α as quantifying the departure from adiabaticity.

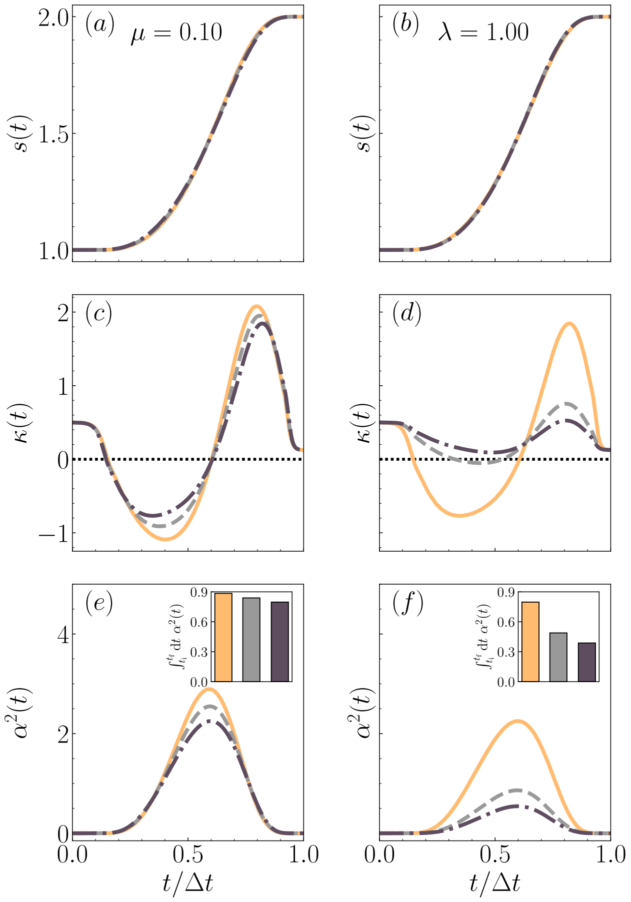

Figure 4.7: Phase-optimal protocols in the time domain, where the variance increases from $s_\mathrm{i} = 1$ to $s_\mathrm{f} = 2$. The time is normalized to the total duration of the protocol Δt, which is different for each pair of Lagrange multipliers $(\lambda, \mu$. Left panels: variance $s(t)$ (a), quantum protocols $\kappa(t)$ (c), and instantaneous energy $E(t)$ (e), for a fixed value of $\mu = 0.10$ and $\lambda = 0.01$ (solid orange lines), 0.50 (dashed grey lines) and 1.00 (dot-dashed black lines). These values correspond to time durations: $\Delta t = 0.95$, 0.97 and 1.00. Right panels: variance $s(t)$ (b), quantum protocols $\kappa(t)$ (d), and instantaneous energy $E(t)$ (f), for a fixed value of $\lambda = 1$ and $\mu = 0.1$ (solid orange lines), 0.50 (dashed grey lines) and 1.00 (dot-dashed black lines). These values correspond to time durations: $\Delta t = 1.00$, 1.67 and 2.10. The boundary values of the quantum protocols correspond to the conditions: $s_{\mathrm{i,f}}^2 \kappa_{\mathrm{i,f}} = mD^2$. The insets in (e) and (f) show the integral of $\alpha^2(t)$ over time for the three protocols represented in the same panels. Note that the shortest durations correspond to the largest values of the phase $\alpha(t)$.

In Fig. 4.8, we compare our results to the same polynomial protocol described in Sec. 4.4.1, by representing the values of the functional F_α for different time durations Δt

for both protocols. Here, we fix $\lambda = 10$ and vary μ from 0.001 to 2.50, in order to obtain different time durations for the optimal protocol. The optimal protocol displays significantly lower values of the cost function F_α for short durations, which is the regime of interest. For longer durations, the two protocols behave very similarly in this respect. The above result is important, inasmuch as it shows that, for the same time duration Δt, our optimal protocol is closer to adiabaticity than the polynomial protocol of Ref. [162]. Both protocols constitute shortcuts to adiabaticity, but the one we propose here is, in a precise sense, "adiabatically optimal".

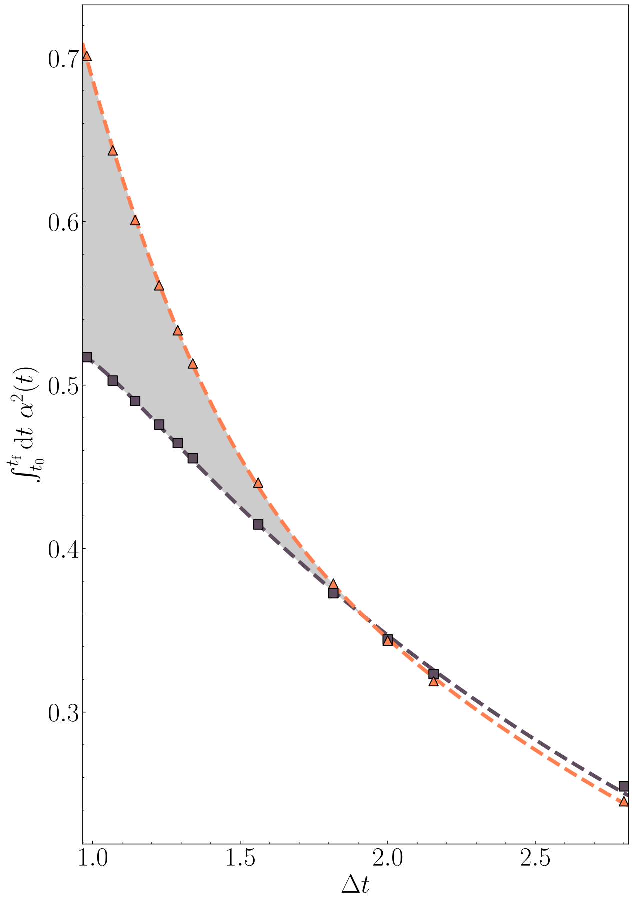

Figure 4.8: Integral of the square of the dynamical phase $\int_{t_i}^{t_f} \mathrm{d}t\, \alpha^2(t)$ as a function of the total time duration Δt of the protocol. The black squares corresponds to the optimal protocol, solution of the Euler-Lagrange equation (4.40), while the orange triangles correspond to the polynomial protocol of Ref. [162]. In the grey shaded region the optimal protocols perform better than the polynomial ones. The different times durations are obtained by varying the Lagrange multiplier μ (from 0.001 to 2.5), while keeping $\lambda = 10$ fixed. The dashed lines are empirical fits to the numerical data.

4.5 Conclusion

To bring a classical or quantum system from a stationary state to another, the simplest strategy is to vary an external parameter very slowly, *i.e.* adiabatically. By doing so, the system will be at steady state at each instant of the evolution, but the transition will take an infinite time. The growing field of research known as "shortcuts to adiabaticity" tries to accomplish the same transition within a finite duration.

In the present chapter, we proposed a new strategy to achieve faster-than-adiabatic transitions. The main idea is based on Nelson's representation of quantum mechanics as a classical stochastic process. In the case of a time-dependent harmonic oscillator this quantum-classical analogy is particularly simple and fruitful. Using Nelson's procedure, the Schrödinger equation is rewritten as an overdamped Langevin equation with a linear harmonic force of stiffness $\bar{\kappa}(t)$, which is related to the stiffness of the quantum oscillator $\kappa(t)$ through Eq. (4.12). Thanks to this mathematical analogy, it is possible to translate the classical protocols developed for an overdamped oscillator into quantum protocols for a system with finite inertia.

In particular, we utilized our experience on optimal classical protocols to devise quantum protocols that minimize both the time duration and some other arbitrary cost function. For instance, the cost function can be the cumulative energy over time. Even more interestingly, we showed that minimizing the dynamical phase of the wavefunction (again, together with the time duration) amounts to minimizing the distance of the protocol from an adiabatic one. Hence, we could devise a family of protocol that are "adiabatically optimal": for a given finite duration Δt, they are as close as possible to an adiabatic (*i.e.*, infinitely slow) process.

The proposed method is rather versatile, inasmuch as the cost functional to be minimized can be chosen at will. Nevertheless, some functionals may lead to complicated Euler-Lagrange equations, which are difficult to solve numerically. This occurs because the cost functional F that has a physical relevance is expressed in terms of the quantum stiffness κ and its time derivative, but must be rewritten in terms of the classical stiffness $\bar{\kappa}$ before performing the minimization procedure. This can transform relatively a simple functional $F[\kappa, \dot{\kappa}]$ into a rather complicated functional of $\bar{\kappa}$ and $\dot{\bar{\kappa}}$.

The original method proposed in this chapter, although limited here to the ground state of the harmonic potential, opens up many possible avenues for future research. For instance, as shown in [162], the same procedure also works for transitioning an excited state of the harmonic oscillator $\psi_n(x)$, which transforms according to the scale factor defined earlier as: $q(t) = \sqrt{s(t)/s_\mathrm{i}}$. In contrast, for anharmonic systems, the Gaussian wavefunction is no longer an exact solution. However, a Gaussian ansatz can be used as an approximate solution, leading to a modified Ermakov equation, similar to Eq. (4.6), which can be used as the basis for a generalization of the present theory. Similarly, one may consider many-body problems in the mean field approximation, either with contact interactions (Gross-Pitaevskii equation for Bose-Einstein condensates) [185] or Coulomb interactions (Schrödinger-Poisson equations for a quantum electron gas) [186]. These are nonlinear Schrödinger equations that are amenable to the Nelson representation utilized in the present chapter. For weak coupling, the exact solution can be approximated by a Gaussian wavefunction, leading again to a modified Ermakov equation. For the Gross-Pitaevskii case, an interesting goal would be to control the system by modulating the scattering length, which can be done experimentally by varying an external magnetic field. A further avenue for future research is to extend the present method to the case of an open quantum system in contact with a bath at finite temperature. To do this, it would be necessary to extend Nelson's formalism, for instance by adding a thermal noise to Eq. (4.2), for which several attempts have already been proposed [187, 188].

KEY TAKEAWAYS

In this chapter, we developed a method to optimize the dynamics of a quantum harmonic oscillator by leveraging a quantum-classical analogy.

- **Quantum-Classical Analogy**:
  - **Nelson** (Gaussian wavefunction of variance s):

$$\mathrm{d}x(t) = -\frac{\hbar}{m}\left[2\alpha(t) - \frac{1}{2s(t)}\right]x(t)\mathrm{d}t + \sqrt{2D}\mathrm{d}W(t)$$

  - **Classical overdamped Langevin** (harmonic oscillator):

$$\mathrm{d}x(t) = -\frac{1}{\gamma}\bar{\kappa}(t)x(t)\mathrm{d}t + \sqrt{2D}\mathrm{d}W(t)$$

  - **Relationship Between Quantum and Classical Stiffnesses**:

$$\overbrace{\kappa(t)}^{\text{quantum stiffness}} = \frac{\hbar^2}{2ms^2(t)} + \overbrace{\frac{m}{\gamma}\dot{\bar{\kappa}}(t) - \frac{m}{\gamma^2}\bar{\kappa}^2(t)}^{\text{classical stiffness}},$$

- **Variational Optimization Method**:
  - Evolve the quantum harmonic oscillator from an initial variance s_i to a final variance s_f (fundamental states).
  - Minimise the time duration Δt and given cost functionals $F[\kappa]$

  The total functional to be minimized is:

$$J[\bar{\kappa}, \bar{\kappa}'] = \overbrace{\Delta t[\bar{\kappa}]}^{\text{time duration}} + \overbrace{\lambda F[\bar{\kappa}, \bar{\kappa}']}^{\text{cost}} + \overbrace{\mu G[\bar{\kappa}']}^{\text{smoothing}},$$

  Go in s-domain using $\dot{s} = D\gamma - s\bar{\kappa}(s)$, solve **Euler-Lagrange equation**:

$$2\mu\,\bar{\kappa}''(s) = \frac{\gamma s}{[D\gamma - s\bar{\kappa}(s)]^2} + \lambda\frac{\partial f}{\partial \bar{\kappa}} - \lambda\frac{\mathrm{d}}{\mathrm{d}s}\left(\frac{\partial f}{\partial \bar{\kappa}'}\right),$$

  (f: integrand of the cost functional F)

  Gives optimal classical protocol:

  $\Longrightarrow$ bridge equation to get quantum protocol $\kappa(s)$ + go back to time domain

- **Cost Function Flexibility**:
  - versatile method, allowing for different cost functions to be minimized
  - considered the cumulative energy and the dynamical phase of the wavefunction as cost functions
  - compared the optimal protocol to a polynomial protocol from literature

REFERENCES

[31] Nelson, E. *Physical Review* **1966**, *150*, 1079–1085.

[32] Bohm, D. *Physical Review* **1952**, *85*, 166–179.

[97] Bacciagaluppi, G. *Foundations of Physics Letters* **1999**, *12*, 1–16.

[98] Beyer, M.; Paul, W. *Universe* **2021**, *7*, 166.

[106] Couder, Y.; Protière, S., et al. *Nature* **2005**, *437*, 208–208.

[129] Martínez-Garaot, S.; Torrontegui, E., et al. *Physical Review Letters* **2013**, *111*, 213001.

[130] Wineland, D. J.; Monroe, C., et al. In *Advances in Quantum Chemistry*, Löwdin, P.-O., Ed.; Academic Press: 1998; Vol. 30, pp 41–64.

[131] Marr, C.; Beige, A., et al. *Physical Review A* **2003**, *68*, 033817.

[132] Wendin, G. *Reports on Progress in Physics* **2017**, *80*, 106001.

[133] Khomitsky, D. V.; Gulyaev, L. V., et al. *Physical Review B* **2012**, *85*, 125312.

[134] Song, X.-K.; Zhang, H., et al. *New Journal of Physics* **2016**, *18*, 023001.

[135] Bachmann, S.; De Roeck, W., et al. *Physical Review Letters* **2017**, *119*, 060201.

[136] Pang, S.; Jordan, A. N. *Nature Communications* **2017**, *8*, 14695.

[137] Takahashi, K. *Journal of Physics A: Mathematical and Theoretical* **2013**, *46*, 315304.

[138] Takahashi, K. *Physical Review A* **2015**, *91*, 042115.

[139] Li, J.; Sun, K., et al. *Scientific Reports* **2016**, *6*, 38258.

[140] Li, J.; Fogarty, T., et al. *New Journal of Physics* **2018**, *20*, 015005.

[141] Pinch, E. R.; Pinch, E. R., *Optimal Control and the Calculus of Variations*; Oxford University Press: Oxford, New York, 1995; 242 pp.

[142] Kirk, D. E., *Optimal Control Theory: An Introduction*; Courier Corporation: 2012; 466 pp.

[143] Hegerfeldt, G. C. *Physical Review Letters* **2013**, *111*, 260501.

[144] Sun, C.; Saxena, A., et al. *Journal of Physics B: Atomic, Molecular and Optical Physics* **2017**, *50*, 175501.

[145] Zhou, B. B.; Baksic, A., et al. *Nature Physics* **2017**, *13*, 330–334.

[146] Guéry-Odelin, D.; Ruschhaupt, A., et al. *Reviews of Modern Physics* **2019**, *91*, 045001.

[147] Guéry-Odelin, D.; Jarzynski, C., et al. *Reports on Progress in Physics* **2023**, *86*, 035902.

[148] Berry, M. V. *Journal of Physics A: Mathematical and Theoretical* **2009**, *42*, 365303.

[149] Demirplak, M.; Rice, S. A. *The Journal of Physical Chemistry B* **2005**, *109*, 6838–6844.

[150] Demirplak, M.; Rice, S. A. *The Journal of Chemical Physics* **2008**, *129*, 154111.

[151] Schmiedl, T.; Dieterich, E., et al. *Journal of Statistical Mechanics: Theory and Experiment* **2009**, *2009*, P07013.

[152] Torrontegui, E.; Ibáñez, S., et al. *Physical Review A* **2011**, *83*, 013415.

[153] Muga, J. G.; Chen, X., et al. *Journal of Physics B: Atomic, Molecular and Optical Physics* **2009**, *42*, 241001.

[154] Unanyan, R. G.; Yatsenko, L. P., et al. *Optics Communications* **1997**, *139*, 48–54.

[155] Emmanouilidou, A.; Zhao, X.-G., et al. *Physical Review Letters* **2000**, *85*, 1626–1629.

[156] Couvert, A.; Kawalec, T., et al. *Europhysics Letters* **2008**, *83*, 13001.

[157] Motzoi, F.; Gambetta, J. M., et al. *Physical Review Letters* **2009**, *103*, 110501.

[158] Rezek, Y.; Salamon, P., et al. *Europhysics Letters* **2009**, *85*, 30008.

[159] Salamon, P.; Hoffmann, K. H., et al. *Physical Chemistry Chemical Physics* **2009**, *11*, 1027–1032.

[160] Masuda, S.; Nakamura, K. *Proceedings of the Royal Society A: Mathematical, Physical and Engineering Sciences* **2009**, *466*, 1135–1154.

[161] Demirplak, M.; Rice, S. A. *The Journal of Physical Chemistry A* **2003**, *107*, 9937–9945.

[162] Chen, X.; Ruschhaupt, A., et al. *Physical Review Letters* **2010**, *104*, 063002.

[163] Patra, A.; Jarzynski, C. *New Journal of Physics* **2017**, *19*, 125009.

[164] Plata, C. A.; Prados, A., et al. *Physical Review Letters* **2021**, *127*, 190605.

[165] Raynal, D.; de Guillebon, T., et al. *Physical Review Letters* **2023**, *131*, 087101.

[166] Rosales-Cabara, Y.; Manfredi, G., et al. *Physical Review Research* **2020**, *2*, 012012.

[167] De Broglie, L. *J. Phys. Radium* **1927**, *8*, 225.

[168] Pucci, G.; Harris, D. M., et al. *Journal of Fluid Mechanics* **2018**, *835*, 1136–1156.

[169] Goerlich, R.; Manfredi, G., et al. *Physical Review Research* **2021**, *3*, 033203.

[170] Schmiedl, T.; Seifert, U. *Physical Review Letters* **2007**, *98*, 108301.

[171] Gomez-Marin, A.; Schmiedl, T., et al. *The Journal of Chemical Physics* **2008**, *129*, 024114.

[172] Bulatov, A.; Vugmeister, B., et al. *Physical Review A* **1998**, *58*, 1346–1351.

[173] Feldmann, T.; Kosloff, R. *Physical Review E* **2000**, *61*, 4774–4790.

[174] Hardel, V.; Hervieux, P.-A., et al. *Foundations of Physics* **2023**, *53*, 89.

[175] Lewis, H. R. *Physical Review Letters* **1967**, *18*, 510–512.

[176] Manoliu, A.; Kittel, C. *American Journal of Physics* **1979**, *47*, 678–680.

[177] Gardiner, C., *Stochastic Methods: A Handbook for the Natural and Social Sciences*; Springer Series in Synergetics; Springer Berlin Heidelberg: 2009.

[178] Martínez-Tibaduiza, D.; Pires, L., et al. *Journal of Physics B: Atomic, Molecular and Optical Physics* **2021**, *54*, 205401.

[179] Sekimoto, K. *Progress of Theoretical Physics Supplement* **1998**, *130*, 17–27.

[180] Boltyanski, V. G.; Gamkrelidze, R. V., et al. *IFAC Proceedings Volumes* **1960**, *1*, 464–469.

[181] Lipitakis, A.-D. *Applied Mathematics* **2016**, *7*, 1225–1240.

[182] Albay, J. A. C.; Kwon, C., et al. *New Journal of Physics* **2020**, *22*, 123049.

[183] Wigner, E. *Physical Review* **1932**, *40*, 749–759.

[184] Hudson, R. *Reports on Mathematical Physics* **1974**, *6*, 249–252.

[185] Manfredi, G.; Hervieux, P.-A. *Physical Review Letters* **2008**, *100*, 050405.

[186] Haas, F.; Manfredi, G., et al. *Physical Review B* **2009**, *80*, 073301.

[187] Ruggiero, P.; Zannetti, M. *La Rivista del Nuovo Cimento* **1985**, *8*, 1–47.

[188] Kobayashi, K.; Yamanaka, Y. *Physics Letters A* **2011**, *375*, 3243–3249.

CHAPTER 5

EXTENSION TO OPEN QUANTUM SYSTEMS

What we observe is not nature itself, but nature
exposed to our method of questioning.
— W. K. Heisenberg

This chapter aims to extend classical analogies for protocols involving stiffness and temperature to open quantum systems, with a view toward optimizing cycles and possibly developing quantum heat engines. It explores three key approaches to modeling open quantum systems, paving the way for extending these analogies. In Sec. 5.1, we address the challenges of traditional methods and propose simplified strategies for system-environment interactions. Sec. 5.2 covers the Kostin approach, combining the Heisenberg and Langevin equations to derive the Schrödinger-Langevin equation, incorporating friction and random forces. The equation's solutions and noise properties are discussed. Sec. 5.3 introduces the Schuch approach, which modifies the Madelung equations to account for irreversibility, offering a framework for thermal diffusion and extending classical analogies. In Sec. 5.4, the Ruggiero approach blends Nelson's stochastic mechanics with the underdamped Langevin equation, analyzing thermodynamic aspects and the overdamped limit. Finally, Sec. 5.5 compares these methods, noting that while none fully succeeds in extending classical analogies, they explore promising paths, particularly Schuch's method, which offers a foundation for further research.

Contents

5.1 INTRODUCTION

In the previous chapters, we have focused on closed quantum systems, where the system is assumed to be isolated from the rest of the Universe, resulting in unitary and time-reversible dynamics. However, in many practical situations, the system of interest interacts with its surroundings, which we will refer to as the *environment*. In such cases, the system is no longer isolated, and we refer to it as an open quantum system. There are various approaches to describe the dynamics of open quantum systems. One of the most widely used frameworks is the Lindblad master equation, which is well-suited for Markovian interactions where memory effects of the environment can be neglected [189]. The Lindblad equation is fundamental in many fields of physics and provides a robust method to model the time evolution of the system's density matrix when connected to a bath of environmental degrees of freedom. The Gorini-Kossakowski-Sudarshan-Lindblad (GKSL) form [190, 191] is often used in these scenarios. For non-Markovian interactions, where memory effects are significant, alternative approaches such as the Redfield equation [192] or techniques developed by Shibata [193], Nakajima [194], and Zwanzig [195] can be more appropriate. These methods account for the influence of the environment over extended timescales and allow for a more detailed analysis of the system's dynamics. The quantum master equation is a fundamental tool in studying open quantum systems. It describes the evolution of the system, accounting for its coupling to the environment, and enables us to study the system's behavior in the presence of noise. This differential equation governs the time evolution of the system's density matrix and provides insights into both dissipative and decoherence processes. Another important approach is the Caldeira-Leggett model, where the system is coupled to a bath of harmonic oscillators, and the environmental degrees of freedom are averaged out to derive an effective dynamics for the system [15, 16, 196].

While considering environmental degrees of freedom leads to a more realistic representation of the system, it also requires significant computational resources. This is particularly challenging when accurate modeling of each individual interaction is necessary.

To address the computational challenges of these methods, alternative effective models offer a more practical solution. These approaches focus on capturing the overall influence of the environment on the system without modeling each individual interaction with every environmental degree of freedom [197]. By simplifying the complex interactions into effective descriptions, these methods significantly reduce the computational cost compared to detailed master equation approaches. This makes them particularly suitable for large-scale or complex systems where computational resources are limited. There exists a multitude of effective descriptions [198–200], but this thesis will focus on three approaches that align well with the Nelson formalism.

In Sec. 5.2 we will introduce the Kostin approach [201, 202], which combines the Heisenberg equation with the Langevin equation to describe open quantum systems. This method introduces friction and fluctuation terms into the Schrödinger equation, leading to a stochastic and non-linear version of the equation, called Schrödinger-Langevin equation[1]. In Sec. 5.3, we will present the Schuch approach [211], which modifies the Madelung equations to introduce irreversibility into the dynamics of the system. We will derive an extension of the classical analogues discussed in Chap. 4. We will finish with a purely Nelson-based method, the Ruggiero approach [187], which decomposes the

---

[1] The Refs. [198–201, 203–210] present several approaches leading non-linear Schrödinger equations, close to the Schrödinger-Langevin equation discussed in this chapter, that aim to describe open quantum systems.

quantum trajectories into a classical motion governed by the Langevin equation and a quantum motion following the Nelson equation.

5.2 KOSTIN'S APPROACH

In this section, we will discuss an approach to describe open quantum system that combines the Schrödinger equation with the Langevin equation. It has been introduced by Kostin [201], and then developped by Katz [202], leading to a stochastic version of the Schrödinger equation that involves two extra terms: a friction and a random. It aims at introducing irreversibility into the dynamics of the system and to describe the effect of the environment on the system. We will focus on the case of the harmonic oscillator, for which the solution of the stochastic Schrödinger equation is known.

5.2.1 Stochastic version of Schrödinger equation

5.2.1.1 Heisenberg-Langevin equation

Kostin's approach [201] aims to effectively incorporate the interaction between a system and its environment. This is similar to the classical Brownian motion discussed in Chap. 1, where Newton's equation is modified into the Langevin equation by adding a friction term and a random force to account for the environment's influence on the particle. Kostin's idea is to apply a similar modification, but at the quantum level, directly to the position $\hat{X}$ and momentum $\hat{P}$ operators.
In the Heisenberg picture, the quantum dynamics of a system is described by the Heisenberg equations for the position and momentum operators, which are given by

$$\partial_t \hat{X} = \frac{1}{m}\hat{P}, \tag{5.1}$$

$$\partial_t \hat{P} = -\partial_x \hat{V}. \tag{5.2}$$

Here, V represents the potential energy of the system. To include the effects of friction and diffusion in equation (5.2), one can introduce additional operators. According to Ref. [212], this modification arises naturally from the Caldeira-Leggett model, where the quantum system is coupled to a bath of harmonic oscillators. This coupling leads to the modified equations

$$\partial_t \hat{X} = \frac{1}{m}\hat{P}, \tag{5.3}$$

$$\partial_t \hat{P} = -\partial_x \hat{V} - \gamma \hat{P} + \hat{W}_{\mathrm{T}}, \tag{5.4}$$

where γ is the friction coefficient, and $\hat{W}_{\mathrm{T}}$ is a random force dependent only on time. This random force can be expressed as the gradient of a potential $\hat{V}_{\mathrm{T}} = \hat{X}\hat{W}_{\mathrm{T}}$. These equations together form the Heisenberg-Langevin equation, incorporating both the deterministic and stochastic influences of the environment on the quantum system.

5.2.1.2 Schrödinger-Langevin equation

We seek a Schrödinger equation associated with Eq. (5.3) and Eq. (5.4), giving the dynamics of a thermal wavefunction still noted ψ, of the form

$$i\hbar\partial_t\psi = -\frac{\hbar^2}{2m}\partial_x^2\psi + V\psi + V_\gamma\psi - xW_{\mathrm{T}}\psi, \tag{5.5}$$

where V_γ is an extra potential generated by the friction term in the Heisenberg-Langevin equations. Note that we drop the hat of the operator as we wrote the Schrödinger equation in the position representation. Before discussing the physics of the thermal wavefunction, notably its differences between the wavefunction of a thermal system and its link with the density matrix, we have to find the expression of V_γ, as V_T is already known if we assume W_T to be a noise. Noting $\langle\psi|\cdot|\psi\rangle$ the expectation value over the state ψ, one gets for Eq. (5.4)

$$\langle\psi|\partial_t\hat{P}|\psi\rangle = -\langle\psi|\partial_x\hat{V}|\psi\rangle - \gamma\langle\psi|\hat{P}|\psi\rangle + \langle\psi|\hat{V}_\mathrm{T}|\psi\rangle\,. \tag{5.6}$$

Note that two types of expectations will be involved: the expectation with respect to the state ψ and the expectation with respect to the values of the random force, simply noted $\langle\cdot\rangle_\mathrm{T}$. Differentiation of the expectation value of the momentum over the state ψ gives

$$\partial_t\langle\psi|\hat{P}|\psi\rangle = (\partial_t\langle\psi|)\hat{P}\,|\psi\rangle + \langle\psi|\,\hat{P}(\partial_t\,|\psi\rangle), \tag{5.7}$$

and using the Schrödinger equation, we obtain after some algebra

$$\partial_t\langle\psi|\hat{P}|\psi\rangle = -\langle\psi|\partial_x\hat{V}|\psi\rangle - \langle\psi|\partial_x\hat{V}_\gamma|\psi\rangle - \langle\psi|\partial_x\hat{V}_\mathrm{T}|\psi\rangle\,. \tag{5.8}$$

According to the Ehrenfest theorem, the expectation of the momentum is the momentum of the wavefunction, then equating Eq. (5.7) and Eq. (5.8) gives

$$\langle\psi|\partial_x\hat{V}_\gamma|\psi\rangle = \gamma\langle\psi|\hat{P}|\psi\rangle\,. \tag{5.9}$$

The expectation of $\hat{P}$ can be written as

$$\langle\psi|\hat{P}|\psi\rangle = -\frac{i\hbar}{2}\int \mathrm{d}x\;(\psi^*\partial_x\psi - \psi\partial_x\psi^*) = -\frac{i\hbar}{2}\int\mathrm{d}x\left(\frac{\partial_x\psi}{\psi} - \frac{\partial_x\psi^*}{\psi^*}\right)|\psi|^2 \tag{5.10}$$

so that the integrand is a real function. Moreover, the expectation of the potential energy is given by $\langle\psi|\partial_x\hat{V}_\gamma|\psi\rangle = \int\mathrm{d}x\;\partial_x V_\gamma|\psi|^2$ so that

$$-\frac{i\hbar}{2}\int\mathrm{d}x\left(\frac{\partial_x\psi}{\psi} - \frac{\partial_x\psi^*}{\psi^*}\right)|\psi|^2 = \gamma\int\mathrm{d}x\;\partial_x V_\gamma|\psi|^2 \tag{5.11}$$

for every ψ. This is possible only if the integrand is zero, so that we obtain the expression of V_γ, using the properties of the logarithm function and integrating with respect to x, as

$$V_\gamma = -\frac{i\gamma\hbar}{2}\ln\left(\frac{\psi}{\psi^*}\right) + C(t) \tag{5.12}$$

with $C(t)$ the constant of integration to be fixed. To do so, we have to impose that the mean energy (over the state ψ) is equal to the mean kinetic energy plus the mean potential energy and the mean random force, as V_γ is a friction-like term, that does not contribute explicitly to the energy[2]. This gives that the expectation of this term is zero, so that

$$V_\gamma = -\frac{i\gamma\hbar}{2}\left[\ln\frac{\psi}{\psi^*} - \left\langle\ln\frac{\psi}{\psi^*}\right\rangle_\psi\right]. \tag{5.13}$$

This leads to the Schrödinger-Langevin equation (SLE)

$$i\hbar\partial_t\psi = -\frac{\hbar^2}{2m}\partial_x^2\psi + V\psi - \frac{i\gamma\hbar}{2}\left[\ln\frac{\psi}{\psi^*} - \left\langle\ln\frac{\psi}{\psi^*}\right\rangle_\psi\right]\psi - xW_\mathrm{T}\psi. \tag{5.14}$$

---

[2] As in classical mechanics, the friction does not derive from a potential and it contributes to the total energy by its influence over the dynamics of the position and momentum.

The two extra terms arise as extra-potential terms: the friction yields an imaginary potential, non-local and non-linear in the wavefunction, and a random term that gives a stochastic dynamics to the wavefunction. The SLE is then a non-linear, non-local, and non-deterministic differential equation. Moreover, as the average is over the solution ψ of the SLE, the equation is self-consistent. Nevertheless, the friction is introduced in a way that it is linear in the velocity of the particle: the term $-i\ln(\psi/\psi^*)$ is the real phase of the wavefunction, so that its gradient is the velocity field of the particle. There exist manners to derive the SLE that involve a non-linear friction term (non-Markovian), see Ref. [210, 213]. The non-linearity of the equation invalidates the superposition principle. While the complexity of the SLE is increased, certain properties of the Schrödinger equation are preserved, such as the conservation of the norm of the wavefunction [214] and the uncertainty principle [215]. Moreover, only two parameters are added in this effective approach: the friction γ and the amplitude D_{T} of the thermal noise. Furthermore, there is no numerical difficulty in solving the SLE. While no direct connection between the SLE and the master equations of the Lindblad form is known, the difference in difficulty between both approaches is significant, encouraging the use of effective models such as the SLE to study open quantum systems [216, 217].

The random term W_{T}, being a noise, means that each realization of the SLE results in a different solution for the thermal wavefunction ψ. As mentioned, there are two types of averages: one over the state and one over the noise. Due to the statistical nature of interactions between the quantum system and its environment, the system must be described by a mixed state. This includes probabilistic information not only about the observable measurements but also about the state itself. The overall expectation value of an observable $\hat{A}$ is then given by

$$\left\langle \langle\psi|\hat{A}|\psi\rangle \right\rangle_{\mathrm{T}} = \lim_{N\to\infty} \frac{1}{N} \sum_{n=1}^{N} \left\langle \psi^{(n)} \middle| \hat{A} \middle| \psi^{(n)} \right\rangle , \tag{5.15}$$

where $\psi^{(n)}$ corresponds to the pure state solution of the n-th realization of the SLE. Solutions of the SLE in the free case, i.e., $V = 0$, and in the harmonic case have been studied in Refs. [218] and applied to atomic diffusion in solids in Ref. [219].

Note that we keep refer to ψ as the (thermal) wavefunction, but it is not the same object as in quantum mechanics for isolated systems. Here, it is more a mathematical object constructed in the same manner as the standard wavefunction and it is the solution of an equation close to the original Schrödinger equation.

5.2.1.3 Statistical properties of the noise for the harmonic oscillator

The noise operator $\hat{W}_{\mathrm{T}}$ arises from the coarse-graining of the bath's momentum and position operators. Due to the non-commutative nature of these quantum operators, the noise differs from the classical case. This effect is reflected in the expression for the amplitude of the noise, the diffusion coefficient D_{T}, which is modified compared to its classical counterpart [202, 218, 220, 221]. Here, we still assume that the noise is a Gaussian white noise with zero mean, such that

$$\left\langle \hat{W}_{\mathrm{T}}(t)\hat{W}_{\mathrm{T}}(t') \right\rangle_{\mathrm{T}} = 2D_{\mathrm{T}}\delta(t-t'), \tag{5.16}$$

where the diffusion coefficient D_{T} is related to the friction coefficient γ and the temperature T of the bath, according to Ref. [202, 218] by

$$D_{\mathrm{T}} = \frac{\hbar\omega}{2} m\gamma \left[\coth\left(\frac{\hbar\omega}{2k_{\mathrm{B}}T} \right) - 1 \right]. \tag{5.17}$$

This expression shows that in the high-temperature limit, one obtains $D_{\mathrm{T}} \approx m\gamma k_{\mathrm{B}}T$, which corresponds to the classical limit. Moreover, in the low-temperature limit, the diffusion coefficient tends to zero, and the stochasticity of the Schrödinger-Langevin Equation (SLE) disappears. It is possible to show that this choice of diffusion coefficient implies the Boltzmann weights when equilibrium is reached [202], as will be explained in the following subsection. Other possibilities are considered in the literature, see Ref. [222] for a white noise with a different amplitude, or Ref. [202, 220, 221, 223] for a colored noise.

According to equations (5.16) and (5.17), the noise operator is an operator that commutes with all other operators, meaning it is proportional to the identity operator. We will see that equation (5.17) allows for the recovery of the Boltzmann distribution for equilibrium thermal states.

5.2.2 Solving the SLE for the harmonic oscillator

We consider the harmonic oscillator with frequency ω. The Schrödinger-Langevin Equation (SLE) for the harmonic oscillator is given by

$$i\hbar\partial_t\psi = -\frac{\hbar^2}{2m}\partial_x^2\psi + \frac{1}{2}m\omega^2x^2\psi + \gamma\hbar\Big[S - \langle S\rangle_\psi\Big]\psi - xW_{\mathrm{T}}\psi, \tag{5.18}$$

where the logarithmic term is replaced by the phase S of the wavefunction (from the polar form of ψ). Using Madelung's transformation of the wavefunction, we obtain the following equations of motion for the probability density ρ and the velocity field S:

$$\partial_t\rho = -\frac{\hbar}{m}\partial_x(\rho\partial_x S), \tag{5.19}$$

$$\hbar\partial_t S = -\frac{\hbar^2}{2m}(\partial_x S)^2 - \frac{1}{2}m\omega^2x^2 - V_{\mathrm{Q}} - \gamma\hbar\Big[S - \langle S\rangle_\psi\Big] + xW_{\mathrm{T}} \tag{5.20}$$

where we used the notation $\langle S\rangle_\psi \equiv \langle\psi|S|\psi\rangle$. The Hamilton-Jacobi equation is modified by two additional terms: the friction term and the random noise, which makes the phase stochastic. However, the continuity equation remains unchanged compared to the zero-temperature case, but as S is stochastic, its solution will differ from the zero-temperature case.

We can then write the Nelson stochastic process associated with the SLE as

$$\mathrm{d}x = \frac{\hbar}{m}\left(\partial_x S(x(t),t) + \frac{1}{2}\partial_x \ln\rho(x(t),t)\right)\mathrm{d}t + \mathrm{d}W_{\mathrm{Q}}(t). \tag{5.21}$$

To go further, we need to find the expression of the wavefunction. We assume the *ansatz* of the Gaussian wavefunction as

$$\psi(x,t) = \frac{1}{[2\pi\sigma^2(t)]^{1/4}}\exp\left\{-\frac{[x-\mu(t)]^2}{4\sigma^2(t)} + i\Big(\alpha(t)[x-\mu(t)]^2 + k(t)[x-\mu(t)] + \theta(t)\Big\}\Big), \tag{5.22}$$

where $\mu \equiv \langle x\rangle_\psi$, $\sigma^2 \equiv \left\langle(x-\mu)^2\right\rangle_\psi$. It is necessary that $\mu \neq 0$ because, due to the noise, the wavefunction is not symmetric at every time with respect to the origin. We have five parameters: the mean position μ, the variance σ^2, the geometric phase θ, the dynamical phase α, and the mean momentum $p = \hbar k$. Inserting this *ansatz* into the SLE (or into Madelung's equations) gives the following equations of motion for the parameters:

$$\partial_t p = -m\omega^2\mu - \gamma p + W_\mathrm{T}, \tag{5.23}$$

$$\partial_t \mu = \frac{p}{m}, \tag{5.24}$$

which correspond to the classical Langevin equation if p is the momentum and μ is the position of the particle. The equations for the variance and the phases are

$$\partial_t \sigma = \frac{2\hbar\alpha\sigma}{m}, \tag{5.25}$$

$$\partial_t \alpha = \frac{\hbar}{8m\sigma^4} - \frac{2\hbar\alpha^2}{m} - \gamma\alpha - \frac{m\omega^2}{2\hbar}, \tag{5.26}$$

$$\partial_t \theta = \frac{\hbar}{2m}\left[\frac{p^2}{\hbar^2} + \frac{1}{2\sigma^2}\right] - \frac{m\omega^2\mu^2}{2\hbar} - \gamma\alpha\sigma^2 + \frac{\mu}{\hbar}W_\mathrm{T}. \tag{5.27}$$

By combining Eq. (5.25) and Eq. (5.26), we can show that the variance satisfies the damped Ermakov-Milne-Pinney equation:

$$\partial_t^2\sigma + \gamma\partial_t\sigma + \omega^2\sigma = \frac{D_\mathrm{Q}^2}{\sigma^3}. \tag{5.28}$$

From Eq. (5.22), we find that the drift of the Nelson process is given by

$$\mathrm{d}x(t) = \frac{\hbar}{m}\left(\left[\frac{1}{2\sigma^2(t)} + 2\alpha(t)\right](x(t) - \mu(t)) + \frac{p}{\hbar}\right)\mathrm{d}t + \mathrm{d}W_\mathrm{Q}(t). \tag{5.29}$$

The width is then damped over time and converges, when $\partial_t\sigma = 0$ and $\partial_t^2\sigma = 0$, to the width of the ground state $\sqrt{\hbar/2m\omega}$. We then see that the wave packet converges to a Gaussian wave packet with a width equal to that of the ground state of the zero-temperature harmonic oscillator. However, the center and momentum of the wave packet follow the classical Langevin equation, so the wavefunction is not equal to the ground state. It is a coherent state (we will discuss coherent states in more detail in section Sec. 5.4), which can be written as a superposition of all the eigenstates of the zero-temperature harmonic oscillator. According to the choice of the diffusion coefficient Eq. (5.17), the weight p_n associated with the n-th eigenstate is a Boltzmann weight, equal to $\exp(-E_n/k_\mathrm{B}T)$, where E_n is the energy of the n-th eigenstate and T is the temperature.

The difference between Eq. (5.29) and Eq. (4.9) is the presence of the term $p/\hbar$, which is not proportional to $x - \mu$. This means that the equation cannot be written as $\bar{\kappa}(x - \mu)\mathrm{d}t + \mathrm{d}W_\mathrm{Q}(t)$, where $\bar{\kappa}$ would have been analogous to a classical stiffness, so the Nelson equation is no longer mathematically equivalent to the overdamped Langevin equation describing a classical Brownian particle in a harmonic trap. This would only be the case if $p = 0$. However, if this were the case, according to Eq. (5.23) and Eq. (5.24), we would have $\mu = 0$ and $W_\mathrm{T} = 0$, which is not possible. There exist several formulations of the SLE that do not involve the stochastic noise W_T, see Refs. [224–227]. Further investigation would be needed to extend the classical analogy to this approach, either by exploring approaches to SLE with no stochastic term or by finding a way to include the $p/\hbar$ term in the classical analogy.

Conclusion

The Schrödinger-Langevin Equation (SLE) introduces friction and noise into the quantum dynamics of a harmonic oscillator, resulting in a stochastic phase and a modified wave packet that resembles a coherent state with a Boltzmann distribution. This approach offers a valuable perspective on quantum systems at finite temperatures, but further investigation is needed to address issues like the inclusion of the $p/\hbar$ term in the classical analogy.

To summarize

Modification of Heisenberg equation: Langevin equation for operators
Schrödinger-Langevin equation:

$$i\hbar\partial_t\psi = -\frac{\hbar^2}{2m}\partial_x^2\psi + V\psi + \gamma\hbar\left[\ln\frac{\psi}{\psi^*} - \left\langle \ln\frac{\psi}{\psi^*}\right\rangle_\psi\right]\psi - xW_\mathrm{T}\psi$$

- ✓ Provides natural definition for mixed states
- ✓ Well-known effective equation for open quantum systems
- • Stochastic phase
- ✗ Difficult to define a classical equivalent to quantum stiffness

In the next section, we will explore a different approach that is similar in some aspects but derived differently. Unlike the SLE, this method breaks reversibility at the continuity equation level, and the phase is not stochastic, with no noise directly affecting the wavefunction's dynamics into the stochastic dynamics of quantum systems at finite temperatures.

5.3 SCHUCH'S APPROACH

In section 5.2, we included the effects of the environment in the Heisenberg equations of motion for the position and momentum operators. This led us to the Schrödinger-Langevin Equation (SLE) and the Madelung equations for the density and phase.
Another way to approach this is to start by changing the Madelung equations directly and then derive a Schrödinger-Langevin-like equation. This is the method proposed by Schuch [211]. The goal is to introduce irreversibility in the continuity and Hamilton-Jacobi equations, given by Eq. (2.19) and Eq. (2.34), and then derive a modified Schrödinger equation and the associated Nelson equation.
We will investigate this approach in the case of the harmonic oscillator.

5.3.1 Modification of the Madelung equations

5.3.1.1 Non-modified equations

We recall the Madelung equations for the density ρ and the phase S of the wavefunction $\psi = \sqrt{\rho}e^{iS}$ in the case of the harmonic oscillator of frequency ω. The continuity equation reads

$$\partial_t\rho + \frac{\hbar}{m}\partial_x(\rho\partial_x S) = 0, \tag{5.30}$$

which can be written as a Fokker-Planck equation as

$$\partial_t \rho + \partial_x (b\rho) = D_{\mathrm{Q}} \partial_x^2 \rho \tag{5.31}$$

with $D_{\mathrm{Q}} = \hbar/2m$ and

$$b = \frac{\hbar}{m} \partial_x S + D_{\mathrm{Q}} \partial_x \ln \rho. \tag{5.32}$$

The Hamilton-Jacobi equation is given by

$$\hbar \partial_t S + \frac{\hbar^2}{2m} (\partial_x S)^2 + \frac{1}{2} m \omega^2 x^2 - \frac{\hbar^2}{2m} \frac{\partial_x^2 \sqrt{\rho}}{\sqrt{\rho}} = 0. \tag{5.33}$$

5.3.1.2 Modification of the Hamilton-Jacobi equations

It is possible to start by modifying the Hamilton-Jacobi equation. Taking the gradient of Eq. (5.33) gives

$$[\partial_t + v\partial_x] v = -\frac{1}{m} \partial_x [V + V_{\mathrm{Q}}], \tag{5.34}$$

where v is the velocity field of the particle, given by $v = \hbar \partial_x S/m$. This equation is the Euler equation describing the motion of a fluid in fluid dynamics theory. The operator $\partial_t + v\partial_x$ can be seen as the derivative in a frame of reference moving with the fluid, and the right-hand side $-\partial_x[V + V_{\mathrm{Q}}]$ represents the force felt by the fluid.
To introduce features of open systems into the dynamics, a simple option is to add a friction force $-\gamma v$ to the Euler equation, similar to what is done in classical mechanics. This leads to[3]

$$[\partial_t + v\partial_x] v = -\frac{1}{m} \partial_x [V + V_{\mathrm{Q}}] - \gamma v. \tag{5.35}$$

Integrating this equation gives the modified Hamilton-Jacobi equation:

$$\hbar \partial_t S + \frac{\hbar^2}{2m} (\partial_x S)^2 + V + V_{\mathrm{Q}} + \gamma \hbar S = 0. \tag{5.36}$$

At this stage, the dynamics is still deterministic because the continuity equation remains unchanged. However, this approach has been studied in the literature as a way to include environmental effects in the system's dynamics, see Ref. [206]. To fully introduce irreversibility, we need to go further and modify the continuity equation.

5.3.1.3 Modification of the continuity equation

We want to break the deterministic character of the dynamics. One way to do this is to introduce a new term in the continuity equation. The simplest way is to add a diffusion term, the Laplacian of the density, associated with a thermal diffusion coefficient D_{T}. The continuity equation then becomes a Fokker-Planck equation of the form

$$\partial_t \rho + \partial_x (b\rho) = D_{\mathrm{Q}} \partial_x^2 \rho + D_{\mathrm{T}} \partial_x^2 \rho, \tag{5.37}$$

---

[3] If we also introduce a stochastic force, we can show that this recovers the SLE equation from the previous section.

or[4]

$$\partial_t\rho + \frac{\hbar}{m}\partial_x(\rho\partial_x S) = D_\mathrm{T}\partial_x^2\rho. \tag{5.38}$$

This suggests introducing another Wiener process, associated with the thermal agitation, into the Nelson equation as

$$\mathrm{d}x(t) = b(x(t),t)\mathrm{d}t + \mathrm{d}W_\mathrm{Q}(t) + \mathrm{d}W_\mathrm{T}(t). \tag{5.39}$$

where b being the same as in the close systems case. Indeed, for an isolated system, we wanted to ensure the time reversibility of the dynamics, then we had to include the osmotic velocity $D_\mathrm{Q}\partial_x \ln\rho$ in b to counter-balance the diffusion. In the case of open systems, the thermal diffusion has to give a non-reversible dynamics, so no modification on the drift is needed. This stochastic differential equation is similar to the one discussed in Ref. [228] for the classical case of an overdamped Brownian particle affected by thermal noise and another noise from radiation pressure. From this observation, we can imagine to extend the classical analogues for open quantum systems in a similar way as was done in Chap. 4.

5.3.1.4 Derivation of the Schrödinger equation

For closed systems, the probability density ρ is equal to the product of the wavefunction ψ and its complex conjugate ψ^*. Usually, we derive the continuity equation by knowing the Schrödinger equation, either by taking its imaginary part or by combining the Schrödinger equation with its complex conjugate. Here, we want to do the reverse: finding the Schrödinger equation from the continuity equation. This method has been studied in Ref. [229], and is explained in Appendix H. It involves writing the density as $\rho = \psi\psi^*$ and assuming that the phase is $S \propto i\log(\psi/\psi^*)$, where ψ will be identified as the wavefunction. By inserting this expression into the continuity equation, it is possible to separate ψ and ψ^* and obtain the Schrödinger equation for each. This procedure works perfectly for the zero-temperature case, but it is subtler for the thermal case. The Laplacian of $\psi\psi^*$ is not separable into ψ and ψ^*, as it contains a cross-term. A solution is to assume that the density is a Gaussian function, which is an exact solution in the case of the harmonic oscillator. Doing so, we write the density as

$$\rho(x,t) = \frac{1}{\sqrt{2\pi\sigma^2(t)}}\exp\left\{-\frac{x^2}{2\sigma^2(t)}\right\}, \tag{5.40}$$

and the following relation holds:

$$-D\partial_x^2\rho = \gamma\Big(\ln\rho - \langle\ln\rho\rangle_\psi\Big)\rho, \tag{5.41}$$

where the brackets $\langle\cdot\rangle_\psi$ denote the average over the state ψ (whose squared modulus is ρ). Here, we have introduced the friction coefficient γ, which must be equal to

$$\gamma = \frac{2D_\mathrm{T}}{\sigma^2(t)} \tag{5.42}$$

---

[4] Eq. (5.38) motivates the introduction of an extra term in the velocity field v as

$$v(x,t) = \frac{\hbar}{m}\partial_x S(x,t) - D_\mathrm{T}\partial_x \ln\rho(x,t).$$

The velocity field is composed of a convection field $v_\mathrm{c} = \hbar\partial_x S/m$ and a diffusion field $v_\mathrm{d} = -D_\mathrm{T}\partial_x \ln\rho$. This is similar to the distinction between drift and osmotic velocity in the Nelson approach at zero temperature.

to ensure the validity of Eq. (5.41). This means that the friction or the thermal diffusion coefficient must be time-dependent. Under this separability condition, the Schrödinger equation reads[5]

$$i\hbar\partial_t\psi = -\frac{\hbar^2}{2m}\partial_x^2\psi + V\psi - i\gamma\hbar\Big[\ln\psi - \langle\ln\psi\rangle_\psi\Big]\psi. \tag{5.43}$$

We refer to this equation as the deterministic Schrödinger-Langevin equation (dSLE), even though no stochastic term is involved. As in the previous section, we have an extra-potential term that is non-local and non-linear in the wavefunction. The difference is that it is complex, so both the real and imaginary parts of the equation are modified. The associated Hamiltonian is consequently non-Hermitian, which could cause issues, especially concerning the real-valuedness of observables and the normalizability of the wavefunction. However, because of the substraction of the mean value of ψ in the Hamiltonian, the mean energy $E_\psi = \langle H\rangle_\psi$ remains real and is exactly the same as the one obtained from the Schrödinger equation of the closed system. The wavefunction also remains normalized due to the substraction of $\langle\rho\rangle$ in the continuity equation. Indeed, it is straightforward to compute $\frac{\mathrm{d}}{\mathrm{d}t}\rho$ and see that the new term contributes to this derivative as $-\gamma\int\mathrm{d}x\,(\log\rho - \langle\log\rho\rangle)\rho$, which is obviously zero since $\int\mathrm{d}x\;\rho\log\rho = \langle\log\rho\rangle$. Similar approaches to treat open quantum systems with a non-linear Schrödinger equation have been studied in the literature [230, 231], where imaginary terms in the Hamiltonian were also present, and the normalizability of ψ was ensured by substracting the mean value of the non-linear terms.

It is possible to find the modifications to the Hamilton-Jacobi equation by equating the real parts of both sides of the Schrödinger equation. Doing so, we obtain

$$\hbar\partial_t S + \frac{\hbar^2}{2m}(\partial_x S)^2 + V + V_{\mathrm{Q}} + \hbar\gamma\Big[S - \langle S\rangle_\psi\Big] = 0. \tag{5.44}$$

To better understand the meaning of the non-linearity, we can write the Euler equation by taking the gradient of the Hamilton-Jacobi equation. Still noting $v = \hbar\partial_x S/m$, we get

$$[\partial_t + v\partial_x]v = -\frac{1}{m}\partial_x[V + V_{\mathrm{Q}}] - \gamma v. \tag{5.45}$$

The new term corresponds to a friction force $-\gamma v$ in the Euler equation, exactly as in Eq. (5.35). We did not introduce it by assuming a *friction potential*; it is a consequence of modifying the continuity equation.

5.3.1.5 Gaussian solution for SLE

It is possible to solve the Schrödinger-Langevin equation (SLE) by assuming that the wavefunction is a Gaussian function, as in the previous section. We write it as

$$\psi(x,t) = \frac{1}{(2\pi\sigma^2(t))^{1/4}}\exp\left\{-\frac{x^2}{4\sigma^2(t)} + i\big[\alpha(t)x^2 + \theta(t)\big]\right\}. \tag{5.46}$$

Here, σ^2 is the variance of the wavefunction, α is the dynamical phase, and θ is the geometric phase. Unlike the previous section, since there is no random noise in the SLE, we can assume that the mean position is zero, so the Gaussian packet is centered at the minimum of the potential. This reduces the number of parameters to three.

---

[5] We assumed the Gaussian shape for the density to write the separability condition. In fact, any density satisfying Eq. (5.41) is sufficient.

Inserting this expression into Eq. (5.43) gives the following equations of motion for the parameters σ, α, and θ:

$$\partial_t \sigma = \left[\frac{2\hbar\alpha}{m} + \frac{\gamma}{2}\right]\sigma, \tag{5.47}$$

$$\partial_t \alpha = \frac{\hbar}{8m\sigma^4} - \frac{2\hbar\alpha^2}{m} - \frac{m\omega^2}{2\hbar} - \gamma\alpha, \tag{5.48}$$

$$\partial_t \theta = -\frac{\hbar}{4m\sigma^2} + \gamma\alpha\sigma^2. \tag{5.49}$$

In the limit $\gamma \to 0$, and therefore $D_{\mathrm{T}} \to 0$, we recover the Eq. (4.5) for the case without an environment. Combining the equations of motion for σ and α gives a modified Ermakov equation [232]:

$$\partial_t^2 \sigma + \Omega^2 \sigma = \frac{D_{\mathrm{Q}}^2}{\sigma^3}, \tag{5.50}$$

where we introduced the shifted squared frequency $\Omega^2 = \omega^2 - \frac{\gamma^2}{4}$ as an effect of the interaction with the environment, and used the quantum diffusion coefficient $D_{\mathrm{Q}} = \hbar/2m$. For $\partial_t^2 \sigma = 0$, the width converges to $\left[\frac{D_{\mathrm{Q}}^2}{\omega^2 - \gamma^2/4}\right]^{1/4}$.

This modeling of the effect of the environment does not give the same results as those obtained in the previous section, since the modified Ermakov equation followed by the width is different and has different stationary limits. However, in both cases, the limit $\gamma \to 0$ gives the same results, as described by Eq. (4.6), which corresponds to the situation without an environment.

These equations are the starting point for the study of the open quantum system. The next step is to extend the classical analogues to this model, as we did in Chap. 4.

5.3.2 Application to the classical analogues

5.3.2.1 Classical-quantum analogy for the harmonic oscillator

In the case of the harmonic oscillator, we derived the classical analogs for the zero-temperature case by writing the Nelson equation associated with the wavefunction of the system. To do this, we recall that the phase of Eq. (5.46) is given by

$$S(x,t) = \alpha(t)x^2 + \theta(t), \tag{5.51}$$

and its density by

$$\rho(x,t) = \frac{1}{\sqrt{2\pi\sigma^2(t)}} \exp\left\{-\frac{x^2}{2\sigma^2(t)}\right\}. \tag{5.52}$$

The Nelson trajectories $x(t)$ are given by the drift term of the Nelson equation, as recalled in Eq. (5.32). The Nelson equation is then

$$\mathrm{d}x(t) = \left[\frac{2\hbar}{m}\alpha(t) - \frac{D_{\mathrm{Q}}}{\sigma^2(t)}\right]x(t)\mathrm{d}t + \mathrm{d}W_{\mathrm{Q}}(t) + \mathrm{d}W_{\mathrm{T}}(t). \tag{5.53}$$

We rewrite the time-dependent coefficient as a function only of the variance $\sigma(t)$ to express $\alpha(t)$ in terms of it. From equation (5.47), we can write

$$\alpha(t) = \frac{m}{2\hbar}\left(\frac{\dot{\sigma}(t)}{\sigma(t)} - \frac{\gamma}{2}\right), \tag{5.54}$$

and the Nelson equation becomes

$$\mathrm{d}x(t) = \left[\frac{\dot{\sigma(t)}}{\sigma(t)} - \frac{\gamma}{2} - \frac{D_{\mathrm{Q}}}{\sigma^2(t)}\right] x(t)\mathrm{d}t + \mathrm{d}W_{\mathrm{Q}}(t) + \mathrm{d}W_{\mathrm{T}}(t). \tag{5.55}$$

Compared to the previous section, the drift is now proportional to the position $x(t)$, allowing the introduction of a stiffness $\bar{\kappa}$ analogous to the stiffness of a classical harmonic oscillator in the case of classical overdamped Brownian motion. We then write the Nelson equation as

$$\mathrm{d}x(t) = -\frac{\bar{\kappa}(t)}{\bar{\gamma}} x(t)\mathrm{d}t + \mathrm{d}W_{\mathrm{Q}}(t) + \mathrm{d}W_{\mathrm{T}}(t), \tag{5.56}$$

where $\bar{\gamma}$ is a classical friction-like coefficient, and $\mathrm{d}W_{\mathrm{T}}(t)$ is the Wiener process associated with a thermal diffusion coefficient D_{T}. By comparing both equations, we define the time-dependent classical stiffness $\bar{\kappa}(t)$ associated with the quantum stiffness $\kappa(t)$ as

$$\bar{\kappa}(t) = -\bar{\gamma}\left[\frac{\dot{\sigma}}{\sigma} - \frac{\gamma}{2} - \frac{D_{\mathrm{Q}}}{\sigma^2}\right]. \tag{5.57}$$

We recall that $\bar{\gamma}$ is an effective friction coefficient without any direct physical meaning. As in Chap. 4, we set $\bar{\gamma} = 1$. To use the classical-quantum analogy, it is important to express the quantum stiffness $\kappa(t) = m\omega^2(t)$ in terms of the classical one. To do this, we can use the Ermakov equation, given by (5.50), and invert (5.57) to obtain expressions for $\dot{\sigma}$ and $\ddot{\sigma}$ in terms of $\bar{\kappa}(t)$.
Introducing the variance $s(t) = \sigma^2(t)$, from Eq. (5.57), we show that its temporal evolution is given by

$$\dot{s} = 2(D_{\mathrm{Q}} - s\bar{\kappa}) + \gamma s, \tag{5.58}$$

which involves the classical stiffness instead of the quantum one. From the modified Ermakov equation Eq. (5.50), and after a few calculations, we obtain the modified bridge equation, expressing the quantum stiffness in terms of the classical one as

$$\kappa(t) = \frac{2mD_{\mathrm{Q}}^2}{s^2(t)} + m\dot{\bar{\kappa}}(t) - m\bar{\kappa}^2(t) + m\gamma\bar{\kappa}(t). \tag{5.59}$$

This equation is a generalization of Eq. (4.12) for this model to include the effect of the environment. The difference between the two equations is the presence of the term $m\gamma\bar{\kappa}(t)$, which is not present in the zero-temperature case. It involves the friction coefficient γ, so we recover the zero-temperature bridge equation in the limit $\gamma \to 0$.
Thus, the classical-quantum analogy is complete.

5.3.2.2 Extension of the optimisation method

We aim to use the same methods as in Chap. 4 to take the system from an initial state $(s_{\mathrm{i}}, \kappa_{\mathrm{i}})$ to a final state $(s_{\mathrm{f}}, \kappa_{\mathrm{f}})$.
We have not yet investigated this problem, but the method would be the same: we need to find the optimal protocol $\kappa(t)$ that minimizes the duration of the protocol and a given cost functional $F[\kappa, \dot{\kappa}]$. Using the change of variable $s = s(t) = \sigma^2(t)$ allows us to rewrite the bridge equation in the s-domain as

$$\hat{\kappa}(s) = \frac{2mD_{\mathrm{Q}}^2}{s^2} + 2m\big[D_{\mathrm{Q}} - s\hat{\bar{\kappa}}\big]\hat{\bar{\kappa}}'(s) - m\hat{\bar{\kappa}}^2(s) + m\gamma\big[\hat{\bar{\kappa}}(s) + s\hat{\bar{\kappa}}'(s)\big]. \tag{5.60}$$

The duration of the protocol, given by $\Delta t = \int_{t_\mathrm{i}}^{t_\mathrm{f}} \mathrm{d}t$, now writes as

$$\Delta t = \int_{s_\mathrm{i}}^{s_\mathrm{f}} \frac{\mathrm{d}s}{\dot{s}} = \int_{s_\mathrm{i}}^{s_\mathrm{f}} \frac{\mathrm{d}s}{2\big[D_\mathrm{Q} - s\hat{\bar{\kappa}}(s)\big] + \gamma s}. \tag{5.61}$$

The difference from the expression obtained in Chap. 4 is the presence of the term γs in the denominator. This term is equal to twice the thermal diffusion coefficient since $D_\mathrm{T} = \gamma s/2$, so we get

$$\Delta t = \int_{s_\mathrm{i}}^{s_\mathrm{f}} \frac{\mathrm{d}s}{2\big[D_\mathrm{Q} + D_\mathrm{T} - s\hat{\bar{\kappa}}(s)\big]}. \tag{5.62}$$

If we had an expression for D_T in terms of the temperature, we could use the same method as in Chap. 4 to find the optimal protocol, whether it is based on stiffness or temperature. This would allow us to design cycles to create a quantum heat engine, composed of optimal isochoric (constant stiffness) and isothermal (constant temperature) transformations.

The aim of the next section is to find an expression for the thermal diffusion coefficient in terms of the temperature.

5.3.2.3 Model of thermal diffusion coefficient

At this point, we have introduced D_T as a thermal diffusion coefficient, but we have not yet provided a model for it. We aim to link it to the temperature T of the environment. We introduce the inverse thermal energy $\beta = 1/k_\mathrm{B}T$. It is known [233] that the equilibrium distribution ρ_H for the quantum harmonic oscillator is given by the Hillery distribution:

$$\rho_\mathrm{H}(x) = \sqrt{\frac{\hat{\beta} m\omega^2}{2\pi}} \exp\left\{-\hat{\beta} V(x)\right\}, \tag{5.63}$$

with

$$\hat{\beta} = \frac{2}{\hbar\omega} \tanh\left(\frac{\beta\hbar\omega}{2}\right), \tag{5.64}$$

being an effective inverse temperature that depends on both the temperature of the environment and the frequency of the oscillator. The variance of this distribution is given by

$$\sigma_\mathrm{H}^2 = \frac{\hbar}{2m\omega} \coth\left(\frac{\beta\hbar\omega}{2}\right). \tag{5.65}$$

To relate the variance to the thermal diffusion coefficient, we use the relation previously established: $D_\mathrm{T} = \gamma\sigma^2/2$. We then obtain the thermal diffusion coefficient in terms of the friction, the frequency of the oscillator, and the temperature as

$$D_\mathrm{T} = \frac{D_\mathrm{Q}\gamma}{2\omega} \coth\left(\frac{\beta\hbar\omega}{2}\right). \tag{5.66}$$

However, we want an expression for D_T that is independent of the friction coefficient γ, since γ is defined as a function of D_T. To achieve this, we take the stationary limit of the Ermakov equation (5.50), where $\partial_t^2\sigma = 0$. This gives

$$\gamma = 2\omega\sqrt{1 - \tanh^2\left(\frac{\beta\hbar\omega}{2}\right)}, \tag{5.67}$$

and the thermal diffusion coefficient becomes

$$D_{\mathrm{T}} = D_{\mathrm{Q}} \sqrt{\coth^2\left(\frac{\beta\hbar\omega}{2}\right) - 1}, \tag{5.68}$$

which depends only on the temperature and the frequency of the oscillator. It follows that, at equilibrium, the variance $s = \sigma^2$ satisfies the relation

$$s^2\kappa = m\big(D_{\mathrm{Q}}^2 + D_{\mathrm{T}}^2\big) \qquad \text{or} \qquad \sigma^2 = \sqrt{\frac{D_{\mathrm{Q}}^2 + D_{\mathrm{T}}^2}{\omega^2}}, \tag{5.69}$$

where we have reintroduced the quantum stiffness $\kappa = m\omega^2$. This relation can be compared to the zero-temperature equilibrium relation given by Eq. (4.13) in Chap. 4.
Note that, compared to Eq. (5.17), the thermal diffusion coefficient has a different dimension. This is because, in Sec. 5.2, it represents diffusion in momentum space, while here it represents diffusion in position space, introduced at the level of the position distribution in the continuity equation. It is similar to the distinction between underdamped and overdamped diffusion coefficients. Both coefficients tend to zero at low temperatures and to the classical diffusion coefficient at high temperatures. Indeed, for $\beta \to 0$, the friction coefficient becomes $\gamma = 2\omega$, and the thermal diffusion coefficient tends to $2/(m\gamma\beta)$, which corresponds to the Einstein relation for the diffusion coefficient.

Conclusion

We have seen that this approach to treat the interaction of a quantum harmonic oscillator with an environment introduces irreversibility in the dynamics. The continuity equation is modified by introducing a thermal diffusion coefficient, which is related to the temperature of the environment. The Hamilton-Jacobi equation is also modified by adding a friction term. This leads to a modified Schrödinger equation with a complex, non-linear term.
With these changes, the classical-quantum analogy is complete, allowing us to use the same methods as in the previous chapter to transition the system from an initial state to a final state. We have also derived an expression for the thermal diffusion coefficient in terms of the temperature of the environment and the frequency of the oscillator. This section was based on the formalism developed in Ref. [197], and we used it to extend classical analogs to the case of an open quantum system. Additionally, we proposed a model for the thermal diffusion coefficient that is consistent with the equilibrium distribution of the harmonic oscillator.

To summarize

Modification of the continuity equation (add thermal diffusion term)
Deterministic Schrödinger-Langevin equation:

$$i\hbar\partial_t\psi = -\frac{\hbar^2}{2m}\partial_x^2\psi + V\psi - i\gamma\hbar\Big[\ln\psi - \langle\ln\psi\rangle_\psi\Big]\psi$$

- ✓ Directly incorporates irreversibility into continuity equation
- ✓ Easier to develop classical analogues than other approaches.
- Damped phase (HJE) and thermal diffusion term (FPE)
- ✗ Restricted to the harmonic oscillator and Gaussian wavefunctions

In the next section, we will introduce a further approach to treat open quantum systems, known as the Ruggiero approach, which combines Nelson's stochastic mechanics with the Langevin equation.

5.4 RUGGIERO'S APPROACH

The Ruggiero approach [187] is a method for describing open quantum systems by combining Nelson's stochastic mechanics with the Langevin equation, for th special case of the harmonic oscillator. The goal is to introduce thermal effects into the Nelson formalism. As in the previous sections we will use the harmonic oscillator as a model system. For simplicity, we will briefly recall the Nelson formalism for the harmonic oscillator before introducing temperature. Specifically, we will consider the zero-temperature case, focusing on the scenario where the guiding wavefunction is a pure coherent state. Next, we will see how this representation of position can be extended to a mixture of states. Using this new form of the process, we will then address the case of an oscillator coupled to a bath at a given temperature. Finally, we will solve the equations of motion numerically to verify the validity of the results.

5.4.1 Theoretical aspects

5.4.1.1 Coherent guiding for harmonic oscillator

A coherent state of the harmonic oscillator [234] is a quantum state that behaves similarly to a classical harmonic oscillator. It was the first example of quantum dynamics introduced by Erwin Schrödinger [235] in 1926 and played an important role [236] in Heisenberg's discovery of the uncertainty relation [237] in 1927.
For each solution $q(t)$ and $p(t)$ (representing the position and momentum, respectively) of the classical equations of motion for a harmonic oscillator with frequency ω,

$$\dot{q}(t) = \frac{p(t)}{m} \tag{5.70}$$

and

$$\dot{p}(t) = -m\omega^2 q(t), \tag{5.71}$$

with given initial conditions $q_0 = q(0)$ and $p_0 = p(0)$, there exists a corresponding coherent state denoted by a complex number α, whose wave function is $\psi_\alpha(x,t)$. The complex quantum number α is defined by the initial conditions as

$$\alpha = \frac{m\omega q_0 + ip_0}{\sqrt{2m\hbar\omega}}. \tag{5.72}$$

From this point on, we will denote $q_\alpha(t)$ and $p_\alpha(t)$ as the classical trajectory associated with the initial condition linked to α. The wave function $\psi_\alpha(x,t)$ is given by

$$\psi_\alpha(x,t) = \left(\frac{m\omega}{\pi\hbar}\right)^{1/4} \exp\left[-\frac{m\omega}{2\hbar}(x - q_\alpha(t))^2 + i\frac{p_\alpha(t)}{\hbar}(x - q_\alpha(t)) + i\theta(t)\right], \tag{5.73}$$

where

$$\theta(t) = \frac{1}{2\hbar}\int_0^t \left[\frac{p_\alpha^2(t)}{m} - m\omega^2 q_\alpha^2(t)\right] \mathrm{d}t - \frac{\omega t}{2} \tag{5.74}$$

is a phase that depends only on time. In the following, all quantities that depend on the chosen coherent state will be indexed by α. If we choose ψ_α as the guiding wave function in the Nelson equation, the stochastic process for the position x can be shown to be

$$\mathrm{d}x_\alpha(t) = \left[-\omega(x_\alpha(t) - q_\alpha(t)) + \frac{p_\alpha(t)}{m}\right]\mathrm{d}t + \mathrm{d}W_{\mathrm{Q}}(t), \tag{5.75}$$

where $W_{\mathrm{Q}}(t)$ is a Wiener process associated with quantum fluctuations. It is possible to rewrite Eq. (5.75) in a more intuitive way, which will be useful when we introduce temperature. Suppose that we set $q_\alpha(t) = 0$ and $p_\alpha(t) = 0$. The coherent wave function then becomes the ground state wave function of the harmonic oscillator:

$$\psi_0(x) = \left(\frac{m\omega}{\pi\hbar}\right)^{1/4} \exp\left[-\frac{m\omega}{2\hbar}x^2\right]. \tag{5.76}$$

The stochastic process corresponding to this guiding wave function is denoted by $x_0(t)$ and obeys the Nelson equation

$$\mathrm{d}x_0(t) = -\omega x_0(t)\mathrm{d}t + \mathrm{d}W_{\mathrm{Q}}(t). \tag{5.77}$$

Next, we introduce the three-dimensional process $(q_\alpha(t), p_\alpha(t), x_0(t))$, where $q_\alpha(t)$ and $p_\alpha(t)$ are solutions of Eq. (5.70) and Eq. (5.71). It is straightforward to see that from the set of equations Eq. (5.70), Eq. (5.71), and Eq. (5.77), the process defined by

$$x_\alpha(t) = q_\alpha(t) + x_0(t) \tag{5.78}$$

satisfies the process in Eq. (5.75). The Nelson stochastic process guided by a quantum harmonic oscillator coherent state α can then be rewritten as the sum of the classical motion $(q_\alpha(t), p_\alpha(t))$ and the quantum motion of the harmonic oscillator in its ground state, $x_0(t)$.

At this point, we have not yet included temperature in the system and have only considered the case of a pure state. The aim of the next section is to understand how to treat the case of a thermal mixture using this representation.

5.4.1.2 Thermal mixture of coherent statess

In quantum statistical mechanics, thermodynamic equilibrium states are represented by the density matrix

$$\rho_\beta = \frac{1}{Z}\exp\left(-\beta\hat{H}\right), \tag{5.79}$$

where Z is the partition function, β is the inverse thermal energy of the system, and $\hat{H}$ is the Hamiltonian of the quantum system. It is possible to decompose ρ_β in the basis of coherent states of the quantum harmonic oscillator [238]. This decomposition is known as the Glauber representation [77]. The weight of each coherent state α in the mixture is given by the Glauber distribution

$$P(\alpha) = c_0\hbar\omega_0 \exp\left(-c_0\hbar\omega_0|\alpha|^2\right), \tag{5.80}$$

where

$$c_0 = \frac{\exp\left(\beta\hbar\omega_0\right) - 1}{\hbar\omega_0}. \tag{5.81}$$

The term c_0 in Eq. (5.81) acts as an effective temperature for the coherent motion and tends to β in the high-temperature limit. It introduces quantum effects on the classical motion (q, p), as it involves $\hbar$. The density matrix is written as

$$\rho_\beta = \int \frac{\mathrm{d}^2\alpha}{\pi} \, P(\alpha) \, |\alpha\rangle\langle\alpha| \,, \tag{5.82}$$

where $|\alpha\rangle\langle\alpha|$ is the density matrix associated with the pure coherent state $|\alpha\rangle$, with wave function $\psi_\alpha(x) = \langle x|\alpha\rangle$. Note the double integration on α, as it is a complex number. Using (5.72), P can be rewritten as a function of the phase-space variables q and p:

$$P(q,p) = \frac{c_0\omega_0}{2\pi} \exp\left(-c_0\left[\frac{1}{2}m\omega_0^2 q^2 + \frac{p^2}{2m}\right]\right). \tag{5.83}$$

To describe the equilibrium state in the Nelson stochastic framework, we need to construct the stochastic analog of Eq. (5.82). This can be done using the representation given by Eq. (5.78). For a pure state α, since $x_0(t)$ and $q_\alpha(t)$ are statistically independent, the probability density $\rho_\alpha(x,t)$ associated with the stochastic variable $x_\alpha(t)$ can be written as a convolution product:

$$\rho_\alpha(x,t) = \int \mathrm{d}u \int \mathrm{d}v \; \rho_\alpha(u,v,t)\rho_0(x-u), \tag{5.84}$$

where $\rho_\alpha(u,v,t) = \delta(u - q(t))\delta(v - p(t))$ is the phase-space probability density of the classical and deterministic process, and $\rho_0(x_0)$ is the probability density of the Nelson process where the guiding wave function is the ground state of the harmonic oscillator.

Proof:
Let X and Y be two independent random variables, with probability densities ρ_X and ρ_Y, respectively. Since X and Y are independent, the joint probability density factorizes as $\rho_{XY}(x,y) = \rho_X(x)\rho_Y(y)$. We define Z as the sum of these random variables, $Z = X + Y$. Let ρ_Z be the associated density. Using the law of total probability, the density of Z can be rewritten as

$$\begin{aligned} \rho_Z(z) &= \rho_{X+Y}(z) \\ &= \int_{-\infty}^{+\infty} \mathrm{d}x \; \rho_{XY}(x, z-x) \\ &= \int_{-\infty}^{+\infty} \mathrm{d}x \; \rho_X(x)\rho_Y(z-x) \\ &= \rho_X \star \rho_Y(z). \end{aligned}$$

Thus, the probability density of Z is simply the convolution product of the probability densities of X and Y.

For the thermal mixture at equilibrium, which is a mixture of all the different coherent states weighted by Eq. (5.83), we replace the sharp density $\rho_\alpha(u,v,t)$ with the spread-out probability density of the coherent states. The probability density of the process x then becomes

$$\rho_\beta(x) = \int \mathrm{d}u \int \mathrm{d}v \; P(u,v)\rho_0(x-u). \tag{5.85}$$

In conclusion, Eq. (5.85) is the stochastic analog of the density matrix Eq. (5.82) in the position representation, which is what we were looking for.

Due to the mathematical analogy between Eq. (5.84) and Eq. (5.85), it is possible to obtain a representation of the thermal mixture process $x_\beta(t)$, where β indicates the temperature of the mixture, in the form

$$x_\beta(t) = q_\beta(t) + x_0(t), \tag{5.86}$$

where $q_\beta(t)$ is the configuration component of the phase-space process $(q_\beta(t), p_\beta(t))$ with the probability density $P(q,p)$.

In summary, we have found a representation of the process $x_\beta(t)$ corresponding to a mixture of states that is analogous in form to the representation given by Eq. (5.78). The associated equilibrium probability density (5.85) is simply the convolution of the coherent state weight Eq. (5.83) and the Nelson probability density.

However, the system described by $x_\beta(t)$ represents the time evolution of an isolated quantum oscillator initially prepared in a mixed state. What we want to consider is an open system, meaning a system in contact with a thermal reservoir.

5.4.1.3 Open system

We consider the case of a harmonic oscillator in contact with a reservoir. The total system consists of the oscillator and its environment, making it a more complex system than previously considered. Our objective is to describe the oscillator while eliminating the degrees of freedom of the reservoir, without losing the quantum features of the problem, using the stochastic representation of the coherent states.

For a classical Brownian oscillator, the thermal effects of the bath are introduced by adding friction and a random force to the equations of motion, resulting in the Langevin equation. As shown before, the stochastic process of a coherent state can be regarded as the classical deterministic trajectory surrounded by quantum noise. This allows us to include the effect of the bath in the classical part, resulting in the Langevin equation, while keeping the Nelson process unchanged:

$$\mathrm{d}q(t) = \frac{p(t)}{m}\mathrm{d}t, \tag{5.87}$$

$$\mathrm{d}p(t) = -\big[m\omega^2 q(t) + \gamma p(t)\big]\mathrm{d}t + \mathrm{d}W_{\mathrm{T}}(t), \tag{5.88}$$

$$\mathrm{d}x_0(t) = -\omega x_0(t)\mathrm{d}t + \mathrm{d}W_{\mathrm{Q}}(t), \tag{5.89}$$

where γ is the friction coefficient of the bath, and $W_{\mathrm{T}}(t)$ and $W_{\mathrm{Q}}(t)$ are two independent Wiener processes associated with the diffusion coefficients D_{T} and D_{Q}, respectively. Note that the coherent motion (q,p) is still decoupled from the Nelsonian motion x_0. The total process followed by the harmonic oscillator is given by

$$x(t) = q(t) + x_0(t). \tag{5.90}$$

Even though Eq. (5.87) and Eq. (5.88) form the Langevin equation, the distribution of coherent states Eq. (5.83) involves an effective temperature c_0. This means that the temperature felt by the coherent motion is not the actual temperature of the system, but the effective one. As a result, the diffusion coefficient of W_{T} changes from $m\gamma/\beta$ to $D_{\mathrm{T}} = m\gamma/c_0$.

We now have two independent processes: an underdamped Langevin process and a Nelson process. In Fig. 5.1, we give a simplified phase-space representation of the different processes.

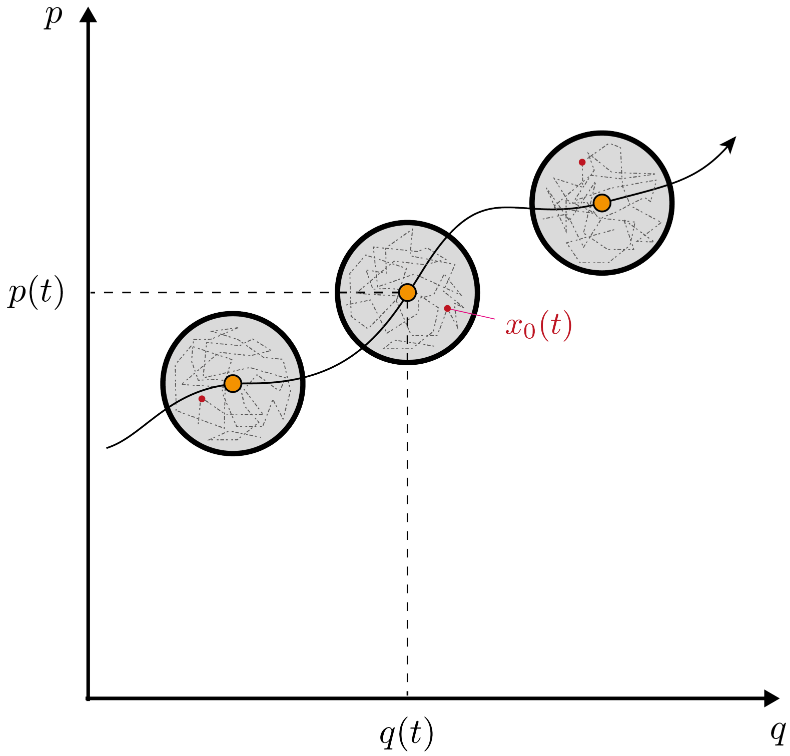

Figure 5.1: Simplified phase-space representation of the Langevin and Nelson processes, respectively (q, p) and x_0. The total process x can be viewed a trajectory in the phase space of the Langevin process (black curve), for which each point is associated with a Nelson process , existing in its own phase space (grey circle). This is a visual representation, if we wanted a more realistic representation, the Langevin process would be a non-smoothed ellipse spiral.

Due to the simplicity of the harmonic oscillator, it is possible to find the expression for the distribution of the position at equilibrium. Without going into detailed calculations, the equilibrium distribution of the particle is

$$P^{\mathrm{eq}}(x) = \left(\frac{\tilde{\beta} m \omega^2}{2\pi}\right)^{1/2} \exp\left(-\frac{\tilde{\beta} m \omega^2}{2} x^2\right), \tag{5.91}$$

where

$$\tilde{\beta} = \frac{2}{\hbar\omega} \tanh\left(\frac{\beta\hbar\omega}{2}\right). \tag{5.92}$$

As for c_0, it acts as an effective inverse temperature, but for the total motion x, while c_0 is the effective inverse temperature for the classical coherent motion (q, p). The distribution is Gaussian, with a width given by

$$\sigma = \frac{1}{\sqrt{\tilde{\beta} m \omega^2}}, \tag{5.93}$$

that corresponds to the Wigner equilibrium distribution for the harmonic oscillator [233] in the canonical ensemble. This approach to including temperature in the Nelson formalism is consistent with the known results.

5.4.2 Thermodynamical aspects and classical analogs

5.4.2.1 Thermodynamics from trajectories

Equations (5.87), (5.88), (5.89), and (5.90) form the foundation for describing open quantum systems using the Nelson formalism. This approach is particularly useful because it allows us to apply tools from stochastic thermodynamics, originally developed for classical systems, to the study of open quantum systems. Specifically, this method provides a direct way to define the system's entropy through the concept of path entropy. Path entropy, initially introduced in Ref. [239] for classical overdamped Langevin dynamics, is linked to the trajectory of a Brownian particle. It is associated with a single trajectory $x(t)$ and is defined as the logarithm of the probability of the particle's trajectory:

$$s(t) = -k_B \ln P(x(t), t). \tag{5.94}$$

By averaging over all possible trajectories, we recover the standard definition of non-equilibrium Gibbs mean entropy:

$$S(t) = -k_B \int \mathrm{d}x \; P(x,t) \ln P(x,t) = \langle s(t) \rangle \,, \tag{5.95}$$

where $\langle \cdot \rangle$ is the expectation value taken over the possible values of x. Path entropy depends on the initial position distribution and thus contains information about the entire space of possible trajectories. This definition of entropy and the Nelson framework are particularly valuable because they allow us to:

- Verify the laws of thermodynamics: we can compute the mean entropy, the mean energy, the free energy difference between two equilibrium states of the system, and the mean heat production.
- Investigate the generalization to quantum systems of out-of-equilibrium thermodynamics, such as the Jarzynski relation [240] and more generally, the fluctuation theorems [241, 242] that hold for classical systems.
- Design protocols to change the temperature of the system, change the stiffness of the oscillator, minimize the entropy production, minimize the heat production, etc., and explore thermodynamic cycles and heat engines in the quantum regime.

We have not yet investigated these possibilities within the Nelson framework, but exploring these aspects of open quantum systems is the aim of future work.
Nevertheless, the definition of path entropy given by Eq. (5.94) is particularly interesting. The equilibrium distribution of the system, Eq. (5.91), takes the form

$$P^{\mathrm{eq}}(x) = \frac{1}{Z} \mathrm{e}^{-\tilde{\beta} V(x)}, \tag{5.96}$$

where V is the potential energy of the harmonic oscillator. This corresponds to the Boltzmann distribution if $\tilde{\beta}$ were the real inverse temperature of the system. The entropy of the system at equilibrium is then given by

$$s(x) = -k_B \ln P^{\mathrm{eq}}(x) = k_B \Big(\tilde{\beta} V(x) + \ln Z \Big), \tag{5.97}$$

which suggests defining the free energy of the system as

$$F = \frac{1}{\tilde{\beta}} \ln Z, \tag{5.98}$$

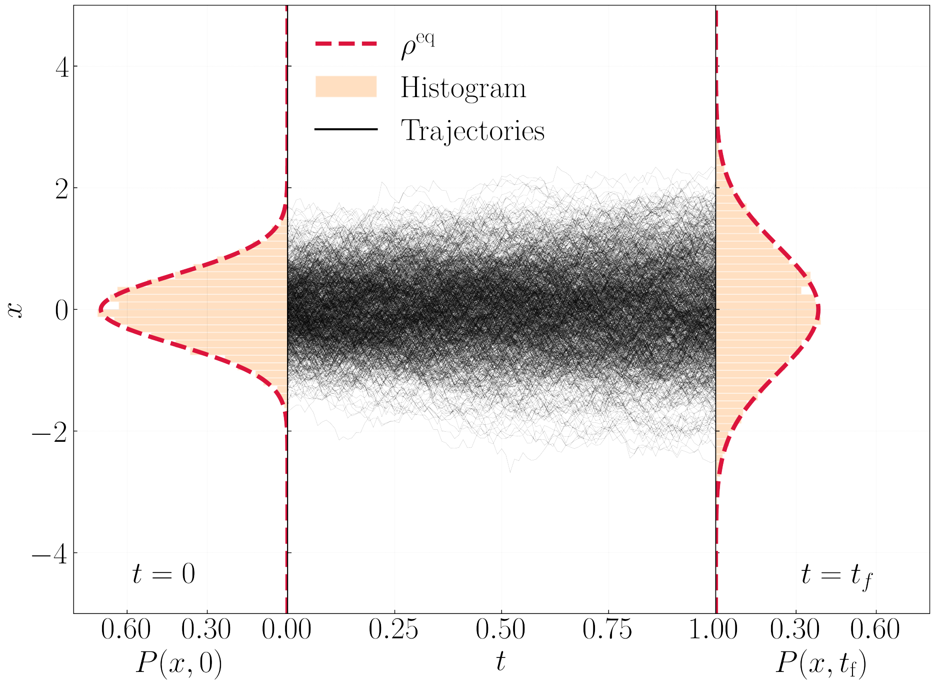

Figure 5.2: Stochastic trajectories of the system for the case where the stiffness of the harmonic oscillator is abruptly changed from ω_{i} to ω_{f}. The system is initially in the equilibrium state associated with ω_{i} and evolves to the equilibrium state associated with ω_{f}. Initially and finally, the histogram (orange) of the positions are fitted by the Hillery distribution (dashed red). The middle panel show the trajectories at intermediate times (black lines).

a form quite close to the classical one for the canonical ensemble, where Z is the partition function, such that

$$Z = \int \mathrm{d}x \; \mathrm{e}^{-\tilde{\beta} V(x)}, \tag{5.99}$$

and

$$F = \langle V \rangle - \tilde{T} S, \tag{5.100}$$

with $\tilde{T} = k_B / \tilde{\beta}$ and S the mean entropy, defined by *Eq.* (5.95), at equilibrium. We performed straightforward numerical calculations to gain a practical perspective on this approach. We considered the special case where the stiffness of the harmonic oscillator is abruptly changed from ω_{i} to ω_{f}, while the system is initially in the equilibrium state associated with ω_{i} (STEP protocol on the stiffness). This leads to a non-equilibrium evolution until reaching the equilibrium state associated with ω_{f}. We computed the entropy of the system over time and calculated the free energy difference between the two equilibrium states. We also computed the stochastic trajectories of the system, as shown in Fig. 5.2. We also computed the energy of the system, but its definition is still open to debate. Since the total process $x(t)$ is the sum of two independent processes, $q(t)$ and $x_0(t)$, the energy of the system could be defined as the sum of the energies of both processes. In this case, the mean energy of the system would be

$$E(t) = \frac{1}{2m} \left\langle p^2(t) \right\rangle_{q,p} + \frac{1}{2} m \omega^2 \left\langle q^2(t) \right\rangle_{q,p} + \frac{\hbar \omega}{2}, \tag{5.101}$$

where $\langle \cdot \rangle_{q,p}$ refers to the expectation value over all possible values of q and p. The last term is the zero-point energy of the harmonic oscillator.

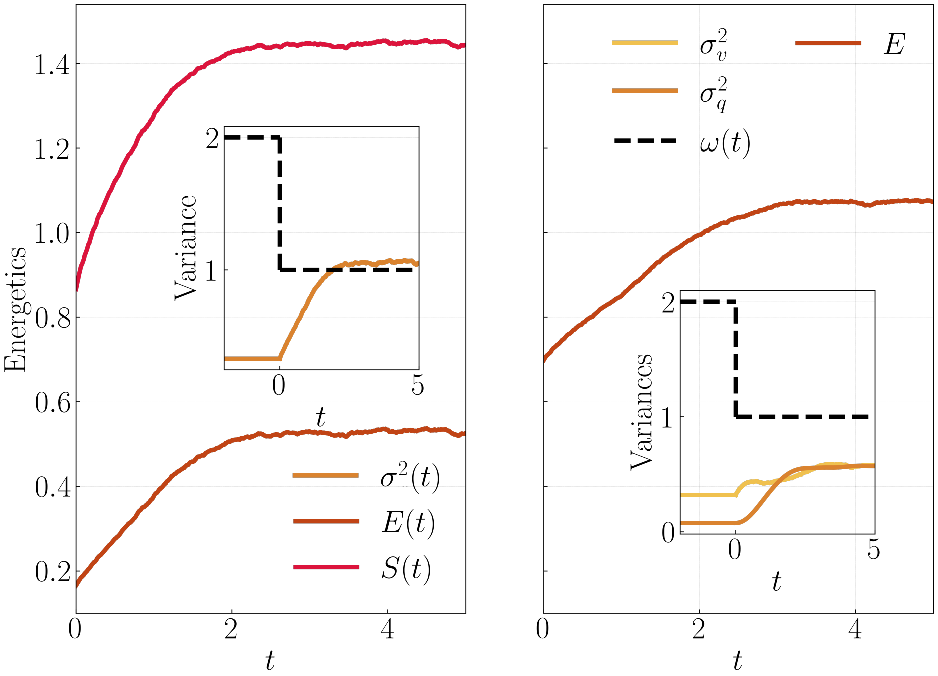

FIGURE 5.3: Time evolution of the system's energy and entropy. Time is expressed in units of $\sqrt{\hbar/(m\omega_\mathrm{f})}$ and lengths in units of $1/\omega_\mathrm{f}$. We take $\hbar = m = \omega_\mathrm{f} = 1$. The left panel shows the energy of the system based on the mean energy of x, along with the path mean entropy. The right panel displays the mean energy in terms of (p, q). The insets in both panels show the associated variances: σ for the left panel and σ_p and σ_q for the right panel. Although the mean energy values differ, the variances reach a plateau in both cases, indicating that the system has reached an equilibrium state. At intermediate times, the system is out of equilibrium. As the stiffness decreases, both the entropy and the energy of the system increase.

However, the definition of the free energy suggests defining the mean energy as the average of $V(x)$, with the expectation value taken over the values of x, leading to

$$E(t) = \frac{1}{2} m\omega^2 \left\langle x^2(t) \right\rangle . \tag{5.102}$$

In the simple case of an abrupt change in stiffness, the different densities of the system, associated with (q, p) and x, are all Gaussian with zero means. We will denote the variances by $\sigma_q^2 = \left\langle q^2 \right\rangle_{(p,q)}$, $\sigma_p^2 = \left\langle p^2 \right\rangle_{(p,q)}$, and $\sigma^2 = \left\langle x^2 \right\rangle$. The mean entropy of the system can be written in terms of the variance of x as

$$S(t) = \frac{k_\mathrm{B}}{2} \big(1 + \ln \left[2\pi\sigma^2(t) \right] \big). \tag{5.103}$$

Numerically, it is possible to compute the different variances by interpolating the q, p, and x histograms with Gaussians. This allows us to plot the time evolution of the entropy and the energy of the system, as shown in Fig. 5.3. In the left panel, the energy of the system is shown based on the mean energy of x. The path mean entropy is also depicted on the same graph. In the right panel, the mean energy in terms of (p, q) is displayed. The insets of both panels show the associated variances: σ for the left panel and σ_p and σ_q for the right panel. Although the values of the mean energy differ, we see that the variances reach a plateau in both situations, indicating that the system has reached an equilibrium state. At intermediate times, the system is out of equilibrium. As the stiffness decreases, both the entropy and the energy of the system increase.

Calculating the difference in free energy between the two equilibrium states, we find that

$$\Delta F = \frac{1}{2}m\left(\omega_{\mathrm{i}}^2 - \omega_{\mathrm{f}}^2\right) - \left(\frac{S(t_{\mathrm{f}})}{\tilde{\beta}_{\mathrm{f}}} - \frac{S(t_{\mathrm{i}})}{\tilde{\beta}_{\mathrm{i}}}\right) \tag{5.104}$$

$$= \frac{1}{\tilde{\beta}_{\mathrm{f}}}\ln\left(\frac{\tilde{\beta}_{\mathrm{f}} m\omega_{\mathrm{f}}^2}{2\pi}\right) - \frac{1}{\tilde{\beta}_{\mathrm{i}}}\ln\left(\frac{\tilde{\beta}_{\mathrm{i}} m\omega_{\mathrm{i}}^2}{2\pi}\right). \tag{5.105}$$

Note that while we assumed that T is constant over time, $\tilde{\beta}$ varies as ω changes, according to Eq. (5.92). Therefore, even during an isothermal transformation, the effective temperature of the system changes.

5.4.2.2 Overdamped limit in the thermal motion

If we investigate the overdamped limit of the Langevin equation, given by Eq. (5.87) and Eq. (5.88), we can obtain a full position description of the harmonic oscillator's motion. We know that the relaxation times for thermal motion are $\tau_p \sim 1/\gamma$ for the momentum and $\tau_q \sim \gamma/\omega^2$ for the position. Moreover, the relaxation time for purely quantum motion is $\tau_{x_0} \sim 1/\omega$. If we consider the case where $\omega/\gamma \ll 1$, we obtain $\tau_p \ll \tau_{x_0} \ll \tau_q$, meaning that the thermal motion is overdamped, but it is possible to choose a time scale between τ_{x_0} and τ_q where the quantum motion is still relevant. Then, we have

$$\mathrm{d}q(t) = -\frac{\omega^2}{\gamma}q(t)\mathrm{d}t + \mathrm{d}W'_{\mathrm{T}}(t), \tag{5.106}$$

where W'_{T} is a Wiener process whose diffusion coefficient becomes

$$D'_{\mathrm{T}} = \frac{1}{m\gamma c_0}. \tag{5.107}$$

The quantum part is still given by Eq. (5.89). The total process verifies the equation of motion

$$\mathrm{d}x(t) = -\left[\frac{\omega^2}{\gamma}q(t) + \omega x_0(t)\right]\mathrm{d}t + \mathrm{d}W'_{\mathrm{T}}(t) + \mathrm{d}W_{\mathrm{Q}}(t). \tag{5.108}$$

This shows that the two Wiener processes W_{T} and W_{Q} combine in the overdamped limit, with the amplitude of the thermal one being slightly modified. The sum $W'_{\mathrm{T}} + W_{\mathrm{Q}}$ is still a Wiener process. We expect to recover the classical overdamped Langevin equation in the limit of high temperature and the Nelson equation in the limit of low temperature. To verify this, we can compute the autocorrelation function of the system's position, which is given by

$$\begin{aligned}\langle x(t)x(0)\rangle &= \langle q(t)q(0)\rangle + \langle x_0(t)x_0(0)\rangle \\ &= \frac{1}{m\omega^2 c_0}\exp\left(-\frac{\omega^2 t}{\gamma}\right) + \frac{\hbar}{2m\omega}\exp(-\omega t).\end{aligned} \tag{5.109}$$

We see that if $\beta \to 0$, then $c_0 \to 0$ and $\langle x(t)x(0)\rangle \sim \langle q(t)q(0)\rangle$, while if $\beta \to \infty$, then $c_0 \to \infty$ so that $\langle x(t)x(0)\rangle \sim \langle x_0(t)x_0(0)\rangle$. Therefore, we can write the following limits:

$$\lim_{\beta \to 0} x(t) = q(t), \tag{5.110}$$

$$\lim_{\beta \to \infty} x(t) = x_0(t). \tag{5.111}$$

This shows that for these two temperature regimes, the process x becomes a Markovian Gaussian process, as q and x_0 are. However, in the general case, the sum of q and x_0 does not have to be Markovian, although it is still Gaussian. Indeed, q and x_0 cannot be expressed in terms of x only; they are coupled in Eq. (5.108).

If we want to extend the classical analogues shown in Chap. 4, we would prefer to express $\mathrm{d}x$ in terms of x only and make it Markovian. To do so, it is possible to interpolate $x(t)$ with a Markovian process, denoted x^{M}. According to Ref. [187], the process x^{M} is given by

$$\mathrm{d}x^{\mathrm{M}}(t) = -\frac{\omega^2}{\gamma^{\mathrm{M}}} x^{\mathrm{M}}(t)\mathrm{d}t + \mathrm{d}W^{\mathrm{M}}(t), \tag{5.112}$$

where

$$D^{\mathrm{M}} = D'_{\mathrm{T}} + D_{\mathrm{Q}} \tag{5.113}$$

is the diffusion coefficient of the Wiener process W^{M}, and γ^{M} is the friction associated with it by

$$D^{\mathrm{M}} = \frac{1}{m\gamma^{\mathrm{M}}\beta^{\mathrm{M}}}. \tag{5.114}$$

Here, β^{M} is the inverse thermal energy. Eq. (5.112) is the overdamped Langevin equation for a particle in a harmonic oscillator of frequency ω, in a bath with friction coefficient γ^{M} and at a temperature given by $1/\beta^{\mathrm{M}}$. The autocorrelation of this protocol is given by

$$\langle x^{\mathrm{M}}(t)x^{\mathrm{M}}(0)\rangle = \frac{1}{m\omega^2\beta^{\mathrm{M}}} \exp\bigl(-\beta^{\mathrm{M}}\sigma^{\mathrm{M}}m\omega^2 t\bigr). \tag{5.115}$$

To see the difference between the Markovian and non-Markovian processes, we plot the autocorrelation functions of both in Fig. 5.4. We see that in both the high and low temperature limits, the autocorrelation functions match perfectly. This is not the case for intermediate temperatures, where they are only close for small t (compared to $1/\omega$). The Markovian process is then a good candidate for studying the system's dynamics in the large friction regime and in the low and high temperature limits. For example, if we study a quantum system weakly coupled to a thermal bath, we can use the Markovian process x^{M} as a good approximation for the position.

This almost concludes this section devoted to Ruggiero's approach to describing open quantum systems.

5.4.2.3 Relation to the Schrödinger-Langevin equation

We will see that Ruggiero's approach allows to recover the Schrödinger-Langevin equation, given by Eq. (5.43). To do so, we follow the same method as Ref. [187] which is a similar strategy as when deriving the Schrödinger equation from the Nelson equation. We need to write the time-evolution equation for the probability density associated with the process $x(t) = q(t) + x_0(t)$. However, the sum of two Markovian processes is not necessarily Markovian itself. Therefore, the equation for the probability density of $x(t)$ is not a Fokker-Planck equation, and it is not possible to derive the desired equation directly from the quantities involved in the Nelson equation.

In Ref. [187], the authors showed that if one chooses a fixed path λ for the thermal motion (p_λ, q_λ), then q_λ is a continuous function of time and is no longer a random process. Thus, $x_\lambda(t) = q_\lambda(t) + x_0(t)$ is simply the sum of a deterministic process and a Markov process. The equation for the probability density of $x_\lambda(t)$ is then a Fokker-Planck equation of the form

$$\partial_t P_\lambda(x,t) = -\partial_x j_\lambda(x,t), \tag{5.116}$$

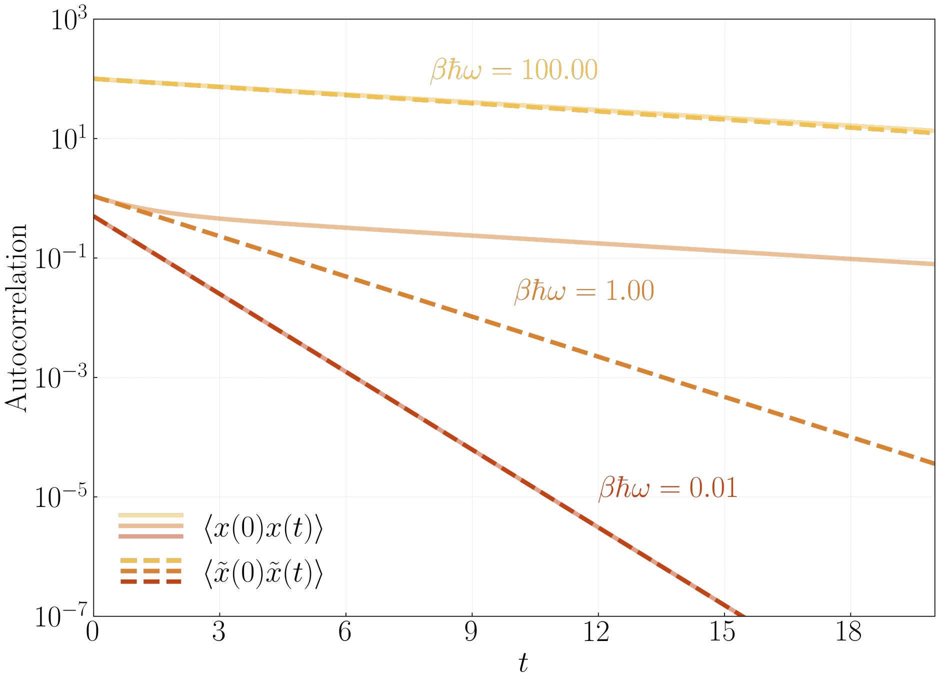

FIGURE 5.4: Time evolution of the system's energy and entropy. Time is expressed in units of $\sqrt{\hbar/(m\omega_\mathrm{f})}$ and lengths in units of $1/\omega_\mathrm{f}$. We take $\hbar = m = \omega_\mathrm{f} = 1$.Autocorrelation functions of the non-Markovian (solid lines) and Markovian processes (dashed lines) for three different temperature regimes, with respect to the energy of the harmonic oscillator: low (yellow), intermediate (orange) and high (brown). In both the high and low temperature limits, the autocorrelation functions match perfectly. For intermediate temperatures, they are only close for small t (compared to $1/\omega$).

where the diffusion term is included in the current density $j_\lambda(x,t) = v_\lambda(x,t)P_\lambda(x,t)$. Here, v_λ is the current velocity of the process $x_\lambda(t)$, given by

$$v_\lambda(x(t),t) = \frac{p_\lambda(t)}{m}. \tag{5.117}$$

Using the tools of stochastic calculus described in Chap. 2, we obtain an acceleration law of the form

$$ma_\lambda(t) = -m\omega^2 x - \gamma p_\lambda(t) + W_{\mathrm{T},\lambda}(t), \tag{5.118}$$

where $W_{\mathrm{T},\lambda}$ is the noise term that gives the path λ. If we assume that v_λ derives from a velocity potential such that

$$v_\lambda = -\frac{1}{m}\partial_x S_\lambda(x,t), \tag{5.119}$$

and introduce the λ-dependent wave function $\psi_\lambda(x,t)$ as

$$\psi_\lambda(x,t) = \sqrt{P_\lambda(x,t)}\exp\left(\frac{i}{\hbar}S_\lambda(x,t)\right), \tag{5.120}$$

then the Schrödinger-like equation for the open system is obtained following the same steps as in the Nelson case. The equation is

$$\begin{aligned} i\hbar\partial_t\psi_\lambda(x,t) = &-\frac{\hbar^2}{2m}\partial_x^2\psi_\lambda(x,t) + V(x)\psi_\lambda(x,t) \\ &+\frac{\gamma}{m}(S_\lambda(x,t) - \langle S_\lambda(x,t)\rangle)\psi_\lambda(x,t) - xW_{\mathrm{T},\lambda}(t)\psi_\lambda(x,t). \end{aligned} \tag{5.121}$$

If we now consider $W_{\mathrm{T},\lambda}$ as a Wiener process, we obtain the Schrödinger-Langevin equation for the open system and can drop the λ index, leading to

$$i\hbar\partial_t\psi = \left[-\frac{\hbar^2}{2m}\partial_x^2 + \frac{1}{2}m\omega^2x^2 + \frac{\gamma}{m}\Big(S - \langle S\rangle_\psi\Big) - xW_\mathrm{T}\right]\psi. \tag{5.122}$$

This equation is the Schrödinger-Langevin equation for the open system. It is interesting to note that the term $\gamma(S - \langle S\rangle)$ is a non-Hermitian term, which is responsible for the dissipation in the system. The term $-xW_\mathrm{T}$ is the noise term, which accounts for the fluctuations in the system. The Schrödinger-Langevin equation obtained is the same as the one obtained in Sec. 5.2, meaning that there might exists a deeper connexion between approaches, while one is obtained from an operator point-of-view and the other from the Nelson formulation.

Conclusion

This approach, while it allows us to compute the equilibrium distribution of the system and thermodynamic quantities of the systems, cannot create classical analogs as in the case of closed quantum systems. The reason is that the total motion is decomposed as the sum of two independent processes, a Langevin process and a Nelson process. Consequently, it is not possible, even in the case of the harmonic oscillator, to write the drift term in terms of one of the processes only; it always involves both. It might be possible to find a way to overcome this limitation, and it might be the aim of future works to find a way to do so.

Nevertheless, this approach to open quantum systems provides a new perspective on the dynamics of these systems and their thermodynamic properties. By considering the system as a combination of two independent processes, we can gain insights into the behavior of open quantum systems and their interactions with the environment. This approach could lead to new developments in the field of open quantum systems and their applications in various domains.

To summarize

Combines underdamped Langevin dynamics and Nelson's dynamics:
Position process formulation:

$$\overbrace{\mathrm{d}x(t)}^{\text{Thermal quantum motion}} = \overbrace{\mathrm{d}q(t)}^{\text{underdamped Langevin dynamics}} + \overbrace{\mathrm{d}x_0(t)}^{\text{Nelson dynamics}}$$

- ✓ Stochastic thermodynamic tools can be used
- ✓ Recovers Schrödinger-Langevin equation
- ✓ Provides natural definition for mixed states and density matrix
- ✗ Split in two processes makes it difficult to develop classical analogues

Future work could focus on finding methods to unify these processes or develop new frameworks that allow for the creation of classical analogs in open quantum systems. Additionally, further investigation into the Schrödinger-Langevin equation could provide deeper insights into the dynamics of open systems and their thermodynamic properties. Understanding these aspects could lead to significant advancements in the field of open quantum systems and their applications in various domains.

5.5 CONCLUSION

In this chapter, we looked at three different ways to describe open quantum systems: the first method from Kostin, the second from Schuch, and the third from Ruggiero. Both the first and third methods lead to the same Schrödinger-Langevin equation. This is useful because it helps us understand how the environment affects the system in a clear way. These methods give us important insights into how open quantum systems behave and interact with their surroundings.

Our original goal was to use these methods to create classical analogues of quantum systems. However, we ran into some problems that made this difficult. In the Ruggiero approach, breaking the motion into two independent processes—a Langevin process and a Nelson process—makes it hard to describe the drift term using just one process. In the Kostin approach, the mean momentum involved in the drift makes it difficult to define a classical equivalent of quantum stiffness. These challenges make it tough to create classical analogues for open quantum systems using these methods.

In contrast, the second method by Schuch is more suitable for creating classical analogues and is easier to work with. We explored this method in detail and found it to be effective in extending classical analogues to open quantum systems. This approach offers a new way of looking at the dynamics and thermodynamics of open quantum systems. Using Schuch's method, we could model how the system interacts with its environment more accurately and create useful classical analogues that match our theoretical expectations.

In summary, while the first and third methods provide a simple and insightful way to study the effects of the environment on quantum systems, Schuch's method is currently better for extending classical analogues. Future work could focus on overcoming the limitations of the first and third methods, like finding a unified process to express the drift term. We believe that the Kostin and Ruggiero approaches could have a great potential in the elaboration of new optmisations techniques for the open quantum systems. The overall goal would be to create optimal cycles for open quantum systems, leading to quantum engines, by optimizing different parts of these cycles (such as isothermal or isochoric protocols) based on methods from classical analogues.

KEY TAKEAWAYS

Want to extend classical analogues to open quantum systems:

Goal: **create optimal cycles for quantum engines**.

Effective models for open quantum systems:

- **Kostin Approach** (Heisenberg)

  Modification of the Heisenberg equation: Langevin equation for operators

  Schrödinger-Langevin equation:

  $$i\hbar\partial_t\psi = -\frac{\hbar^2}{2m}\partial_x^2\psi + V\psi + \gamma\hbar\left[\ln\frac{\psi}{\psi^*} - \left\langle \ln\frac{\psi}{\psi^*}\right\rangle_\psi\right]\psi - xW_\mathrm{T}\psi$$

  ✓ Provides natural definition for mixed states

  ✓ Well-known effective equation for open quantum systems

  − Stochastic phase

  ✗ Difficult to define a classical equivalent to quantum stiffness

- **Schuch Approach** (Continuity)

  Modification of the continuity equation (add thermal diffusion term)

  Modified Schrödinger equation:

  $$i\hbar\partial_t\psi = -\frac{\hbar^2}{2m}\partial_x^2\psi + V\psi - i\gamma\hbar\Big[\ln\psi - \langle\ln\psi\rangle_\psi\Big]\psi$$

  ✓ Directly incorporates irreversibility into continuity equation

  ✓ Easier to develop classical analogues than other approaches.

  − Damped phase (HJE) and thermal diffusion term (FPE)

  ✗ Restricted to the harmonic oscillator and Gaussian wavefunctions

- **Ruggiero Approach** (Nelson)

  Combines underdamped Langevin dynamics and Nelson's dynamics:

  Position process formulation:

  $$\overbrace{\mathrm{d}x(t)}^{\text{Thermal quantum motion}} = \overbrace{\mathrm{d}q(t)}^{\text{underdamped Langevin dynamics}} + \overbrace{\mathrm{d}x_0(t)}^{\text{Nelson dynamics}}$$

  ✓ Stochastic thermodynamic tools can be used

  ✓ Recovers Schrödinger-Langevin equation

  ✓ Provides natural definition for mixed states and density matrix

  ✗ Split in two processes makes it difficult to develop classical analogues

Further work needed to overcome limitations and develop new optimization techniques for open quantum systems.

References

[15] Caldeira, A. O.; Leggett, A. J. *Annals of Physics* **1983**, *149*, 374–456.

[16] Leggett, A. J.; Chakravarty, S., et al. *Reviews of Modern Physics* **1987**, *59*, 1–85.

[77] Glauber, R. J. *Physical Review* **1963**, *131*, 2766–2788.

[187] Ruggiero, P.; Zannetti, M. *La Rivista del Nuovo Cimento* **1985**, *8*, 1–47.

[189] Manzano, D. *AIP Advances* **2020**, *10*, 025106.

[190] Gorini, V.; Kossakowski, A., et al. *Journal of Mathematical Physics* **1976**, *17*, 821–825.

[191] Lindblad, G. *Communications in Mathematical Physics* **1976**, *48*, 119–130.

[192] Redfield, A. G. *IBM Journal of Research and Development* **1957**, *1*, 19–31.

[193] Shibata, F.; Takahashi, Y., et al. *Journal of Statistical Physics* **1977**, *17*, 171–187.

[194] Nakajima, S. *Progress of Theoretical Physics* **1958**, *20*, 948–959.

[195] Zwanzig, R. *The Journal of Chemical Physics* **1960**, *33*, 1338–1341.

[196] Weiss, U., *Quantum Dissipative Systems*; World scientific: 1993.

[197] Schuch, D.; Bonilla-Licea, M. *Entropy* **2023**, *25*, 312.

[198] Caldirola, P. *Il Nuovo Cimento (1924-1942)* **1941**, *18*, 393–400.

[199] Kanai, E. *Progress of Theoretical Physics* **1948**, *3*, 440–442.

[200] Albrecht, K. *Physics Letters B* **1975**, *56*, 127–129.

[201] Kostin, M. D. *The Journal of Chemical Physics* **1972**, *57*, 3589–3591.

[202] Katz, R.; Gossiaux, P. B. *Annals of Physics* **2016**, *368*, 267–295.

[203] Bialynicki-Birula, I.; Mycielski, J. *Annals of Physics* **1976**, *100*, 62–93.

[204] Bateman, H. *Physical Review* **1931**, *38*, 815–819.

[205] Diósi, L.; Halliwell, J. J. *Physical Review Letters* **1998**, *81*, 2846–2849.

[206] Hasse, R. W. *Journal of Mathematical Physics* **1975**, *16*, 2005–2011.

[207] Nassar, A. B. *Journal of Mathematical Physics* **1986**, *27*, 2949–2952.

[208] Nassar, A. B. *International Journal of Theoretical Physics* **2007**, *46*, 548–552.

[209] Chavanis, P.-H. *The European Physical Journal Plus* **2017**, *132*, 286.

[210] Bargueño, P.; Miret-Artés, S. *Annals of Physics* **2014**, *346*, 59–65.

[211] Schuch, D., *Quantum Theory from a Nonlinear Perspective*; Springer International Publishing: 2018.

[212] Ford, G. W.; Kac, M., et al. *Journal of Mathematical Physics* **1965**, *6*, 504–515.

[213] Vargas, A. F.; Morales-Durán, N., et al. *Annals of Physics* **2015**, *356*, 498–504.

[214] Garashchuk, S.; Dixit, V., et al. *The Journal of Chemical Physics* **2013**, *138*, 054107.

[215] Sanin, A. L.; Smirnovsky, A. A. *Materials physics and mechanics* **2014**, *34*, 98–105.

[216] Breuer, H.-P.; Petruccione, F., *The Theory of Open Quantum Systems*; Oxford University Press: 2007.

[217] Weiss, U., *Quantum Dissipative Systems*, 4th ed.; WORLD SCIENTIFIC: 2012.

[218] Messer, J. *Acta Physica Austriaca* **1978**, *50*, 75–91.

[219] Weiner, J. H.; Forman, R. E. *Physical Review B* **1974**, *10*, 325–337.

[220] Li, X. L.; Ford, G. W., et al. *Physical Review E* **1995**, *51*, 5169–5171.

[221] Ford, G. W.; Kac, M., et al. *Journal of Mathematical Physics* **1965**, *6*, 504–515.

[222] Senitzky, I. R. *Physical Review* **1961**, *124*, 642–648.

[223] Gardiner, C.; Zoller, P., *Quantum Noise: A Handbook of Markovian and Non-Markovian Quantum Stochastic Methods with Applications to Quantum Optics*; Springer Science & Business Media: 2004.

[224] Kan, K. .-.; Griffin, J. J. *Physics Letters B* **1974**, *50*, 241–243.

[225] Dekker, H. *Physics Reports* **1981**, *80*, 1–110.

[226] Immele, J. D.; Kan, K.-K., et al. *Nuclear Physics A* **1975**, *241*, 47–60.

[227] Zander, C.; Plastino, A. R., et al. *Annals of Physics* **2015**, *362*, 36–56.

[228] Goerlich, R.; Pires, L. B., et al. *Physical Review E* **2022**, *106*, 054617.

[229] Madelung, E., *Die Mathematischen Hilfsmittel des Physikers*; Springer-Verlag: 1950; 547 pp.

[230] Gisin, N. *Journal of Physics A: Mathematical and General* **1981**, *14*, 2259.

[231] Gisin, N. *Physica A: Statistical Mechanics and its Applications* **1982**, *111*, 364–370.

[232] Schuch, D.; Kaushal, R. S. *Journal of Physics: Conference Series* **2011**, *306*, 012032.

[233] Hillery, M.; Mlodinow, L. D. *Physical Review A* **1984**, *30*, 1860–1865.

[234] Klauder, J.; Skagerstam, B., *Coherent States*; WORLD SCIENTIFIC: 1985.

[235] Schrödinger, E. *Annalen der physik* **1926**, *385*, 437–490.

[236] Steiner, F. *Physica B+C* **1988**, *151*, 323–326.

[237] Heisenberg, W. *Zeitschrift für Physik* **1927**, *43*, 172–198.

[238] Glterra, F.; Loffeedo, M. I. *Lettere al Nuovo Cimento (1971-1985)* **1981**, *30*, 81–87.

[239] Crooks, G. E. *Physical Review E* **1999**, *60*, 2721–2726.

[240] Jarzynski, C. *Physical Review Letters* **1997**, *78*, 2690–2693.

[241] Seifert, U. *Physical Review Letters* **2005**, *95*, 040602.

[242] Seifert, U. *Reports on Progress in Physics* **2012**, *75*, 126001.

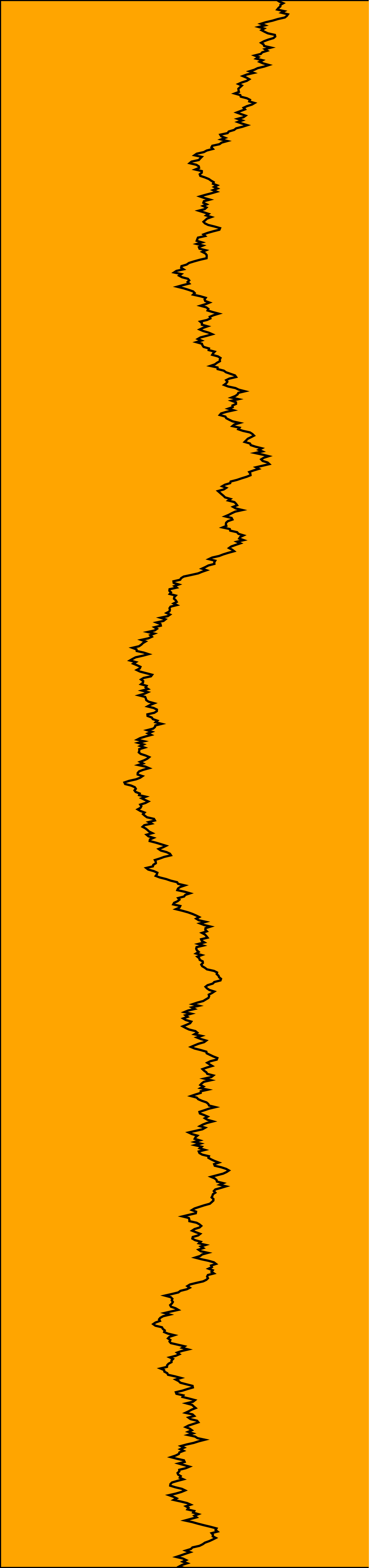

Conclusion

CONCLUSION AND PERSPECTIVES

I would rather have questions that can't be answered
than answers that can't be questioned.
— R. P. Feynman

SUMMARY OF THE THESIS

This thesis investigated the connections between classical and quantum systems, with a particular emphasis on how classical models and techniques can enhance our understanding and control of quantum behavior. The work was based on Nelson's stochastic mechanics, which describes quantum particles in terms of stochastic trajectories. This theory was used to explore various aspects of quantum mechanics, from fundamental concepts to practical applications.

In Chap. 1 and Chap. 2, we presented the theoretical tools necessary to understand the core of this thesis. We introduced the classical stochastic formalism, focusing on the Langevin and Fokker-Planck equations, and discussed the overdamped limits. This framework allowed us to introduce Nelson's theory, which describes quantum particles using a stochastic formalism similar to that of classical particles, while noting subtle differences, such as the reversibility of the process.
We discussed the advantages of Nelson's theory, emphasizing that it can simplify the solution of certain quantum problems that are challenging in standard quantum mechanics. This was illustrated by the example of tunneling time, a concept that is well-defined in Nelson's theory but more difficult to establish within the conventional quantum mechanical framework.

These discussions set the stage for the main part of the thesis, where we apply Nelson's theory to the description of quantum systems, spanning the final three chapters of the manuscript. We demonstrated that Nelson's theory can be applied to both fundamental aspects of quantum mechanics and practical applications.
Chap. 3 was dedicated to the fundamental aspects of Nelson's theory. We discussed the Born rule, *i.e.* the fact that the squared modulus of the wavefunction is the probablility density, and introduced the concept of quantum equilibrium, a concept absent in standard quantum mechanics. This was followed by a discussion on the relaxation time of a quantum system, demonstrating that, for certain systems, the relaxation time can be comparable to the timescales relevant for measurements. A notable example is the free fall of a quantum particle in the gravitational field of the Earth , an experimentally accessible system. This led to the conclusion that if a system is not in quantum equilibrium, it

may exhibit unusual behavior before reaching equilibrium, particularly in scenarios such as high-energy particle collisions where new particles are created.

While this theoretical discussion was of interest as it highlights how Nelson's theory can explore concepts beyond standard quantum mechanics, it was not the primary focus of the thesis. The main objective was to utilize Nelson's theory to address practical problems in quantum mechanics, which is the subject of the final two chapters.

In Chap. 4, we established a correspondence between classical and quantum systems, specifically for the harmonic oscillator. We derived a classical equivalent for the stiffness of a quantum harmonic oscillator. Subsequently, by employing well-established optimization techniques from classical systems, we derived optimal protocols for controlling quantum systems, enabling transitions from an initial to a target state in an optimal manner—that is, minimizing both the duration of the transition and a general cost associated with the process. This method was illustrated with two examples, demonstrating that the optimal protocols we derived outperform well-known protocols from the literature. We emphasized that this approach is versatile, capable of adapting to various cost functions, which is a powerful characteristic for the control of quantum systems.

In the final chapter of the thesis, Chap. 5, we addressed the problem of open quantum systems, which interact with their surroundings, such as an environment or heat bath. Our aim was to extend the classical analogies of quantum systems to include open systems. To this end, we studied three effective approaches to describe open quantum systems and attempted to derive their classical analogues by adapting Nelson's formalism to the open systems framework. Several challenges arose when trying to establish these classical analogues; however, we demonstrated that each model exhibits unique and intriguing properties that warrant further investigation.

One of the most promising models was the Ruggiero model, which is based on Nelson's theory and allows for the recovery of the Schrödinger-Langevin equation derived in the Kostin approach. This model facilitated the introduction of stochastic thermodynamics within the context of open quantum systems in the framework of Nelson's theory. Despite its potential, the derivation of classical analogues within this model is not straightforward. On the other hand, the Schuch approach also presents notable features, with its classical analogues being easier to derive. However, due to time constraints, we were unable to explore this model in greater depth.

FUTURE DIRECTIONS

The work presented in this thesis paves the way for several avenues of future research. Up to this point, we have primarily considered the case of the harmonic oscillator, a simple system that nonetheless provides a good approximation for more realistic systems. However, to further validate the usefulness of our methods, it would be beneficial to extend our results to more complex systems.

In fact, whenever the Nelson drift and the Langevin force share the same form (linear in position in the harmonic Gaussian case), it is possible to derive a classical analogue. This suggests that it may be feasible to find classical analogues for a broader range of quantum systems beyond the harmonic oscillator.

Beyond the harmonic oscillator

A natural next step would be to consider anharmonic oscillators, which are more challenging to solve can be approached using the same techniques as the harmonic case. Under the Hartree approximation, an effective harmonic potential can be constructed to describe the system's dynamics. This effective potential could then be used to derive the classical analogues for systems such as the quartic oscillator.

Bose-Einstein Condensates and Many-Body Systems

Another promising direction for future research is the consideration of many-body systems, which are inherently more complex than single-particle systems. These systems could be effectively described using the mean-field approximation, similar to the approach taken in the Gross-Pitaevskii equation (GPE) for Bose-Einstein condensates (BEC) or the Schrödinger-Poisson equations for a quantum electron gas. These equations are nonlinear Schrödinger equations and share similarities with the Schrödinger-Langevin equation used in the present work.

In the case of the BEC, the GPE is given by

$$i\hbar\frac{\partial\psi}{\partial t} = -\frac{\hbar^2}{2m}\nabla^2\psi + V\psi + g|\psi|^2\psi,$$

where V is the external potential, g is the interaction strength between particles, and ψ is the wavefunction of the BEC. For weak coupling, the exact solution can be approximated by a Gaussian wavefunction, leading to a modified Ermakov equation. This suggests that the methods developed in this thesis could be extended to many-body systems, potentially offering valuable insights into the behavior of interacting particles.

With this framework, one could explore the collective behavior of quantum particles and study the emergence of complex phenomena. For instance, the dynamics of the BEC in a harmonic trap could be analyzed, or the interaction strength g could be controlled in time to investigate its effect on the system's dynamics. Such an approach could lead to the development of optimal protocols for g that enhance the dynamics of the BEC, providing new perspectives on the behavior and control of quantum matter.

Quantum engines and and optimal cycles

We concluded the thesis by discussing the extension of Nelson's theory and the optimization methods to open quantum systems. The ultimate goal would be to apply these methods to control the thermodynamic properties of such systems, specifically focusing on quantities like entropy production during system evolution, which can be defined within the framework of the Ruggiero model.

In addition, through the study of Schuch's model, we derived classical analogues for the harmonic oscillator. If optimal protocols for the stiffness of the potential (which corresponds to controlling the volume of the system) are found, and these methods can be extended to derive protocols on the system's temperature—affecting the thermal diffusion coefficient—it would be possible to develop optimal cycles for quantum engines. Such cycles would involve both temperature and volume (related to the stiffness of the harmonic oscillator), resembling Stirling cycles in classical thermodynamics. Each branch of these cycles could be optimized using classical analogies (see Fig. A1 for a visual representation of this type of cycle). Investigating the optimization of quantum engines through classical techniques may yield new insights into the efficiency and performance of quantum machines.

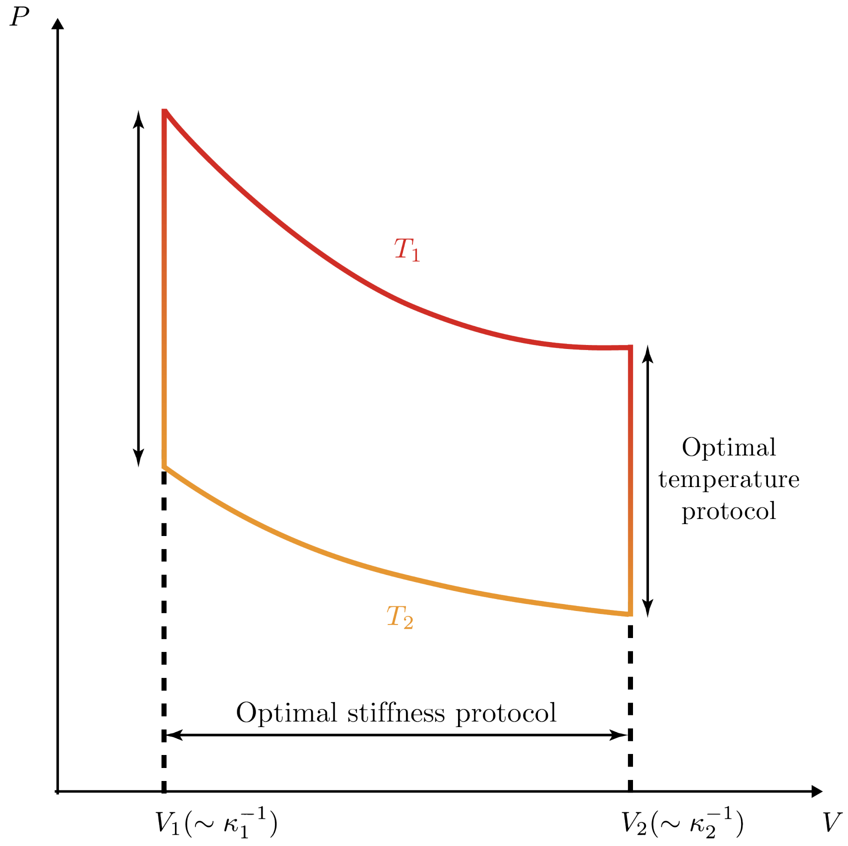

FIGURE A1: Representation of a Stirling-like cycle in the pressure (P) - volume (V) plane. The cycle consists of four branches: two isochoric processes (vertical lines, associated with an optimal variation of the temperature), where the volumes V_1 and V_2 correspond to the inverse stiffnesses κ_1^{-1} and κ_2^{-1} of a trapping potential, and two isothermal processes (during which the volume is optimally changed). The work done by the engine is represented by the area enclosed by the cycle. The efficiency of the engine is given by the ratio of the work performed by the engine to the heat absorbed.

Once achieved, this could lead to the realization of quantum engines whose efficiency is optimized using the methods developed in this thesis, enabling the conversion of heat into work with minimal energy loss.

Controlling the colour of the noise

Independent of the project on thermal engines, it is valuable to develop new classical methods for controlling the state of a system over time. Within the framework of stochastic physics, instead of focusing on protocols that modify the parameters of the system's potential, one could control the interaction with the environment—essentially, the noise. It is commonly assumed that Gaussian white noise sufficiently describes the interaction between a Brownian particle and its surroundings. However, this approach relies on certain approximations, notably neglecting memory effects in these interactions. To overcome these limitations, other types of noise, such as colored noise, must be considered. Moreover, the "color" of the noise can become a tunable parameter in the model, allowing for the development of protocols that control the system's state evolution over time. In this way, optimal protocols can be designed based on the noise color (as demonstrated in Ref. [228]).

Once this method is well-established, it could be applied to quantum systems by leveraging the analogies discussed earlier. Indeed, throughout the derivation of Nelson's theory, we assumed that the noise is a Wiener process, which is essentially white noise. There exist Nelson-like theories involving colored noise (see Ref. [249]), which could potentially extend the methods developed in this thesis to the case of colored noise and enable the derivation of optimal protocols for controlling the noise's color.

Conclusion

Overall, this thesis has demonstrated that non-standard formulation of quantum physics, such as Nelson's theory, offer valuable insights into quantum systems and can lead to novel methods for their control, without necessarily engaging with the ontological questions of the theory. This opens up numerous possibilities for further research, spanning multiple directions and a wide range of applications. Extensive future investigations are required to fully realize the potential of these methods and to develop new techniques for the control of quantum systems. The results presented in this thesis represent only the beginning of a long journey, and we hope that the methods developed here will inspire new research in the fields of quantum control and quantum thermodynamics.

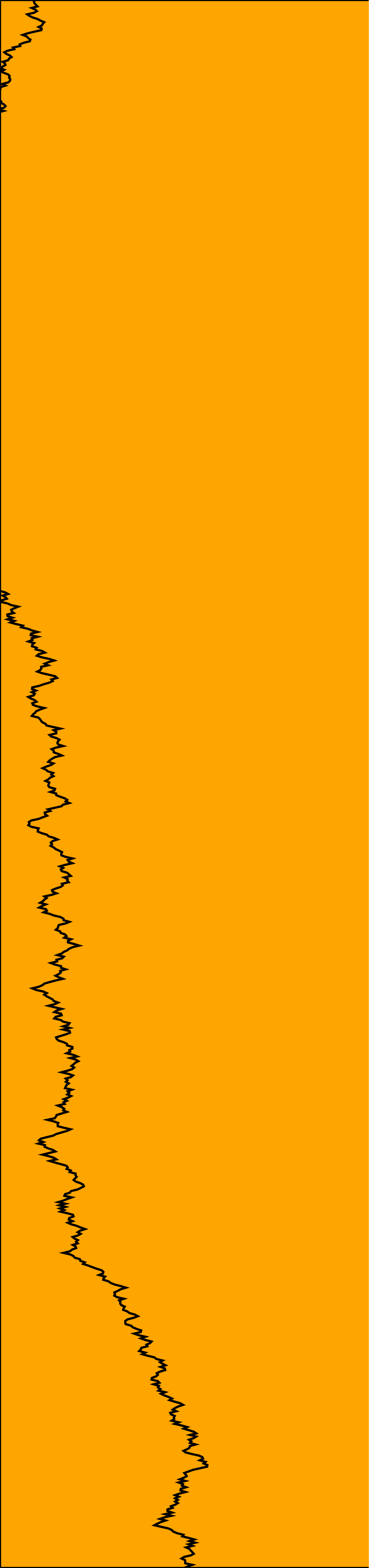

APPENDICES

APPENDIX A

LANGEVIN EQUATION FROM A CLASSICAL CALDEIRA-LEGGETT MODEL

> *Et j'ai pris la décision quasiment instantanément d'essayer de comprendre ce qu'il y avait dans ces ouvrages*
>
> — P. A. Hervieux

In this appendix, we will investigate the question of how a microscopical descritpion of the interactions between the solvant particles and the Brownian particle can lead to the Langevin equation [221]. In addition, we will directly show how the irreversibility of the motion of the Brownian particle arises from the reversible microscopic laws.

To begin, let us denote the mas of the Brownian particle by M, its position and momentum at time t by $x(t)$ and $p(t)$. We supposed that it is in a potential $U(x)$ that depends on the position of the BP. This last is imerged in a fluid modeled a thermostat composed of N harmonic oscillators, labelled by the index i and located at the positions r_i, with momentums p_i, angular frequencies ω_i, and of same masses m. The coupling between the BP and the harmonic oscillators are supposed to be bilinear in the positions and characterized by the coupling constants c_i. While this is not a real coupling to model the interactions of the particles of the fluid with the BP, it is sufficient to reproduce the correct phenomenology, notably to recover the Langevin equation for the dynamics of the BP. The total hamiltonian is given by the sum of the BP hamiltonian

$$H_{\mathrm{BP}} = \frac{p^2}{2M} + U(x). \tag{A.1}$$

and the thermostat hamiltonian is

$$H_{\mathrm{T}} = \sum_{i=1}^{N} \left(\frac{p_i^2}{2m} + \frac{1}{2} m\omega_i^2 r_i^2 \right). \tag{A.2}$$

The coupling between both systems is given by the term

$$H_{\mathrm{int}} = -\sum_{i=1}^{N} c_i r_i x. \tag{A.3}$$

The total hamiltonian is then the sum of the three terms, but it is interesting to rewrite it in a more suggestive form. Indeed, it is possible to put the coupling directly in the thermostat hamiltonian by renormalizing the potential of the BP. The total hamiltonian can then be written as

$$H_{\text{tot}} = \frac{p^2}{2M} + V(x) + \sum_{i=1}^{N}\left(\frac{p_i^2}{2m} + \frac{1}{2}m\omega_i^2\left[r_i - \frac{c_i}{m\omega_i^2}x\right]^2\right) \tag{A.4}$$

with $V(x) = U(x) + \sum_{i=1}^{N}\frac{c_i^2}{2m\omega_i^2}x^2$ being the renormalized potential of the BP. This form of the hamiltonian is interesting because it shows that the BP is coupled to the thermostat through a renormalized potential. This feature gives the system a mean-field character, as the interaction is of infinite range when $N \to \infty$. This is a consequence of the bilinear coupling between the BP and the harmonic oscillators. To find the equation of motion of the system, we need to write the Hamilton equations for the BP and the thermostat. From Eq. (A.4), we find

$$\dot{x} = \frac{p}{M}, \qquad \dot{p} = -\frac{\partial V(x)}{\partial x} + \sum_{i=1}^{N} c_i\left(r_i - \frac{c_i}{m\omega_i^2}x\right), \tag{A.5}$$

$$\dot{r}_i = \frac{p_i}{m}, \qquad \dot{p}_i = -m\omega_i^2 r_i + c_i x. \tag{A.6}$$

and combining both equations of Eq. (A.6), we find the equation of motion for the thermostat being

$$\ddot{r}_i(t) + \omega_i^2 r_i(t) = \frac{c_i}{m}x(t). \tag{A.7}$$

that corresponds to an harmonic oscillator linearly coupled to the BP. The solution of this equation can be obtained using the Green function method. The solution is given by

$$r_i(t) = r_i(0)\cos(\omega_i t) + \frac{p_i(0)}{m\omega_i}\sin(\omega_i t) + \frac{c_i}{m}\int_0^t \mathrm{d}s\ x(s)\frac{\sin(\omega_i(t-s))}{\omega_i}. \tag{A.8}$$

where $r_i(0)$ and $p_i(0)$ correspond to the initial values of r_i and p_i. The solution can be rewritten so that it is easier to interpret. After integration by part of last term of Eq. (A.8), we find

$$\begin{aligned} r_i(t) = \frac{c_i}{m\omega_i^2}x(t) + \left(r_i(0) - \frac{c_i}{m\omega_i^2}x(0)\right)\cos(\omega_i t) + \frac{p_i(0)}{m\omega_i}\sin(\omega_i t) \\ - \frac{c_i}{m\omega_i^2}\int_0^t \mathrm{d}s\ \dot{x}(s)\cos(\omega_i(t-s)) \end{aligned} \tag{A.9}$$

where we made appear the velocity of the BP in the integral term. If we now insert this solution into Eq. (A.5), we find

$$\begin{aligned} \dot{p} = &-\frac{\partial V}{\partial x} - \int_0^t \mathrm{d}x\ \dot{x}(s)\left(\sum_{i=1}^{N}\frac{c_i^2}{m\omega_i^2}\cos(\omega_i[t-s])\right) \\ &+ \sum_{i=1}^{N} c_i\left(\frac{c_i}{m\omega_i^2}x(t) + \left[r_i(0) - \frac{c_i}{m\omega_i^2}x(0)\right]\cos(\omega_i t) + \frac{p_i(0)}{m\omega_i}\sin(\omega_i t)\right). \end{aligned} \tag{A.10}$$

Introducing $\zeta(t) = \sum_{i=1}^{N}\frac{c_i}{m\omega_i^2}\cos(\omega_i t)$ and $F_{\text{B}}(t) = \sum_{i=1}^{N} c_i\left(r_i(0) - \frac{c_i}{m\omega_i^2}x(0)\right)\cos(\omega_i t) + c_i\frac{p_i(0)}{m\omega_i}\sin(\omega_i t)$, we can rewrite the equation of motion of the BP as

$$\dot{p}(t) = -\left.\frac{\partial V}{\partial x}\right|_{x=x(t)} - \frac{1}{M}\int_0^t \mathrm{d}s\quad \zeta(t-s)\dot{p}(s) + F_{\text{B}}(t). \tag{A.11}$$

At this point, this evolution equation for the velocity is exact and originates from the total Hamiltonian. The integral term can be interpreted as a memory kernel for the previous values of velocity. In other words, because of this term, the velocity of the BP depends on its own past value, and the dynamics is not Markovian. As it generates a force opposed to the motion, proportional to the velocity, it is straightforward to interpret it as a non local friction force. The last term $F_{\mathrm{B}}(t)$ is totally determinisitic, as it depends on the initial values of the bath degrees of freedom as well on the BP initial position. However, as there are a very large number N of harmonic oscillators, it is impossible to have a complete knowledge of the initial conditions of the bath, rather a statistical knowledge. It is then possible to describe them satistically and to suppose that they follow a probability density. If the bath is initially at the equilibrium, at the temperature T, then the probability density is given by the Boltzmann distribution, from the expression of the (renormalised) Hamiltonian of the bath, one gets

$$\rho(\{x_i\},\{p_i\},t=0) \propto \exp\left(-\frac{1}{k_{\mathrm{B}}T}\sum_{i=1}^{N}\left[\frac{p_i^2}{2m}+\frac{1}{2}m\omega_i^2(r_i-\frac{c_i}{m\omega_i^2}x(0))^2\right]\right). \tag{A.12}$$

Doing so, the term $F_{\mathrm{B}}(t)$ becomes a random variable and can be viewed as being a noise. Then, Eq. (A.11) becomes a stochastic equation. The averaged quantities can be computed considering this probability distribution. From Eq. (A.12), it is clear that

$$\langle p_i(0)\rangle = 0 \qquad \text{and} \qquad \langle r_i(0)\rangle = \frac{c_i}{\omega_i^2}x(0) \tag{A.13}$$

and using the expression of the noise, we find

$$\langle F_{\mathrm{B}}(t)\rangle = 0 \qquad \text{and} \qquad \left\langle F_{\mathrm{B}}(t)F_{\mathrm{B}}(t')\right\rangle = k_{\mathrm{B}}T\zeta(t-t'). \tag{A.14}$$

This last relation is an example of fluctuation-dissipation theorem, as it relates the noise to the friction. The name comes from the fact that the noise is due to the fluctuations of the bath, and the friction is due to the dissipation of the energy of the BP in the bath. At this point, the noise is not supposed to be a white noise, as Eq. (A.14) shows. If one wants to recover the standard Langevin equation from Eq. (A.11), one needs make the friction term local in time and obtain a δ-correlated noise. This necessitated a separation of the time scales between the BP and the bath degrees of freedom. Indeed, the friction term in the Langevin equation Eq. (A.11) proportional to $\int_0^t \mathrm{d}s\ \zeta(t-s)p(s)$. As the friction kernel ζ is a function of the bath degrees of freedom only, it is natural to suppose that the time interval for which the friction kernel takes significant values is rougthly $[-\tau_{\mathrm{s}},\tau_{\mathrm{s}}]$ with τ_{s} the time scale of the bath. On the other hand, the time scale at which the momentum of the BP changes is τ_{B}. As we assumed that $\tau_{\mathrm{B}} \gg \tau_{\mathrm{s}}$, we can make the approximation $\int_0^t \mathrm{d}s\ \zeta(t-s)p(s) \approx \int_0^t \mathrm{d}s\ \zeta(t-s)p(t) \approx \gamma p(t)$ with $\gamma = \int_0^\infty \mathrm{d}s\ \zeta(s)$, or reversly $\zeta(t) = \gamma\delta(t)$. This is the Markovian approximation, and it is equivalent to suppose that the time scale of the bath is much smaller than the time scale of the BP, so that all the memory effects cancel. The Langevin equation finally becomes

$$\dot{p}(t) = -\left.\frac{\partial V}{\partial x}\right|_{x=x(t)} - \frac{1}{M}\gamma p(t) + F_{\mathrm{B}}(t). \tag{A.15}$$

with

$$\langle F_{\mathrm{B}}(t)\rangle = 0 \qquad \text{and} \qquad \left\langle F_{\mathrm{B}}(t)F_{\mathrm{B}}(t')\right\rangle = 2\gamma k_{\mathrm{B}}T\delta(t-t'). \tag{A.16}$$

which is the Langevin equation with a Gaussian white noise.

REFERENCES FOR APPENDIX A

[221] Ford, G. W.; Kac, M., et al. *Journal of Mathematical Physics* **1965**, *6*, 504–515.

APPENDIX B

RELATION BETWEEN FORWARD AND BACKWARD PROCESSES

Faut pas prendre tout ce qu'il dit au sérieux ...
— G. Manfredi

In this appendix, we demonstrate the form of the backward derivative, introduced in Chap. 2. It will justify the relation between the forward and the backward drifts. Recall that the forward derivative of a function f of the position x and of the time t is defined by Eq. (2.13) as

$$\mathcal{D}f = \partial_t f + b\partial_x f + D_{\mathrm{Q}}\partial_x^2 f. \tag{B.1}$$

We want to demonstrate the form of the backward derivative $\mathcal{D}^* f$ given by Eq. (2.14). In order to do so, we first have to demonstrate a usefull relation.

DERIVATIVE OF THE AVERAGE OF A PRODUCT

Let $f(x,t)$ and $g(x,t)$ be two functions of the position x and of the time t. We want to demonstrate that the derivative of the average of the product of these two functions is expressed in terms of forward and backward derivatives [243] as

$$\frac{\mathrm{d}}{\mathrm{d}t}\left\langle f(x,t)g(x,t)\right\rangle = \left\langle \mathcal{D}f(x,t)g(x,t)\right\rangle + \left\langle f(x,t)\mathcal{D}^* g(x,t)\right\rangle \tag{B.2}$$

where the average $\langle\cdot\rangle$ is taken over the possible values of the Wiener process. As done in Ref. [187], we will use the notation $f(t) := f(x(t),t)$ and $g(t) := g(x(t),t)$ to simplificate the notation. We will make the assumptioin that both f and g are smooth functions that vanishes at the space-time boundaries. Proving Eq. (B.2) is equivalent to proving that

$$\left\langle f(t_{\mathrm{f}})g(t_{\mathrm{f}}) - f(t_0)g(t_0)\right\rangle = \int_{t_0}^{t_{\mathrm{f}}} \mathrm{d}t\ \left\langle \mathcal{D}f(t)g(t) + f(t)\mathcal{D}^* g(t)\right\rangle. \tag{B.3}$$

Let us divide the time in n steps of size $\Delta t = t_{\mathrm{f}}/n$, such that $t_i = i\Delta t$ for $0 \le i \le n$ and with t_0 the initial time and t_{f} is the final time.

Using the trick of the sum of the differences, we can write the left-hand side of Eq. (B.3) as

$$
\begin{aligned}
&\langle f(t_\mathrm{f})g(t_\mathrm{f}) - f(t_0)g(t_0)\rangle \\
&= \lim_{n\to\infty} \sum_{i=1}^{n} \langle f(t_{i+1})g(t_i) - f(t_i)g(t_{i-1})\rangle \\
&= \lim_{n\to\infty} \sum_{i=1}^{n} \left\langle [g(t_{i+1}) - g(t_i)]\frac{f(t_i)+f(t_{i-1})}{2} + \frac{g(t_{i+1})+g(t_i)}{2}[f(t_i) - f(t_{i-1})] \right\rangle
\end{aligned}
$$

and using the fact that $\langle\langle\cdot|x(t)=x\rangle\rangle = \langle\cdot\rangle$, we can write, under the assumption of smooth functions, that

$$
\lim_{n\to\infty} \left\langle [g(t_{i+1}) - g(t_i)]\frac{f(t_i)+f(t_{i-1})}{2} \right\rangle = \lim_{n\to\infty} \frac{t_\mathrm{f}-t_0}{n} \langle \mathcal{D}g(t_i)f(t_i)\rangle
$$

and

$$
\lim_{n\to\infty} \left\langle \frac{g(t_{i+1})+g(t_i)}{2}[f(t_i) - f(t_{i-1})] \right\rangle = \lim_{n\to\infty} \frac{t_\mathrm{f}-t_0}{n} \langle g(t_i)\mathcal{D}^* f(t_i)\rangle \,.
$$

yielding to

$$
\begin{aligned}
\langle f(t_\mathrm{f})g(t_\mathrm{f}) - f(t_0)g(t_0)\rangle &= \lim_{n\to\infty} \sum_{i=1}^{n} \frac{t_\mathrm{f}-t_0}{n} \langle \mathcal{D}g(t_i)f(t_i) + g(t_i)\mathcal{D}^* f(t_i)\rangle \\
&= \int_{t_0}^{t_\mathrm{f}} \mathrm{d}t \ \langle \mathcal{D}g(t)f(t) + g(t)\mathcal{D}^* f(t)\rangle \,.
\end{aligned}
$$

This relation relates the forward and backward derivatives of two functions in terms of the average of their product, on the boundaries of the time interval. We will now use this relation to demonstrate the form of the backward derivative.

Expression of the backward derivative

If we suppose that f and g vanish at the boundaries of the time interval, the left-hand side of Eq. (B.2) is simply zero. Then, we can write that

$$
\int_{t_0}^{t_\mathrm{f}} \mathrm{d}t \ \langle \mathcal{D}g(t)f(t)\rangle = -\int_{t_0}^{t_\mathrm{f}} \mathrm{d}t \ \langle g(t)\mathcal{D}^* f(t)\rangle \,. \tag{B.4}
$$

Calculation Writing explicitly the averages, we have

$$
\int_{t_0}^{t_\mathrm{f}} \mathrm{d}t \int_{-\infty}^{+\infty} \mathrm{d}x \ \mathcal{D}g(x,t)f(x,t)P(x,t) = -\int_{t_0}^{t_\mathrm{f}} \mathrm{d}t \int_{-\infty}^{+\infty} \mathrm{d}x \ g(x,t)\mathcal{D}^* f(x,t)P(x,t).
$$

Using the definition of the forward, we can write, omiting to write the arguments of the functions for the sake of readibility, that

$$\int_{t_0}^{t_\mathrm{f}} \mathrm{d}t \int_{-\infty}^{+\infty} \mathrm{d}x \, \left[\partial_t g + b\partial_x g + D_\mathrm{Q}\partial_x^2 g\right] fP$$

$$= \int_{t_0}^{t_\mathrm{f}} \mathrm{d}t \int_{-\infty}^{+\infty} \mathrm{d}x \, \left[-\partial_t(fP) - \partial_x(bfP) + D_\mathrm{Q}\partial_x^2(fP)\right] g.$$

where with did an integration by parts on the time for the first term, on the space for the second term and two integration by part on the last term, so that g is the prefactor of all the terms. Then, one gets

$$\int_{t_0}^{t_\mathrm{f}} \mathrm{d}t \int_{-\infty}^{+\infty} \mathrm{d}x \, \left[-\partial_t(fP) - \partial_x(bfP) + D_\mathrm{Q}\partial_x^2(fP)\right] g = -\int_{t_0}^{t_\mathrm{f}} \mathrm{d}t \int_{-\infty}^{+\infty} \mathrm{d}x \, \mathcal{D}^* fgP$$

which is valid for any function g. This implies that the integrands are equal, yielding to

$$\partial_t(fP) + \partial_x(bfP) - D_\mathrm{Q}\partial_x^2(fP) = -\mathcal{D}^* fP.$$

Diving by the probability density, we get the expression of the backward derivative

$$\mathcal{D}^* f = \partial_t f + (b - 2D_\mathrm{Q}\partial_x \log P)\partial_x f - D_\mathrm{Q}\partial_x^2 f.$$

This shows that the backward derivative given by

$$\mathcal{D}^* f(x,t) = \partial_t f(x,t) + b^*(x,t)\partial_x f(x,t) - D_\mathrm{Q}\partial_x^2 f(x,t) \tag{B.5}$$

where the backward drift b^* is given by

$$b^*(x,t) = b(x,t) - 2D_\mathrm{Q}\partial_x \log P(x,t). \tag{B.6}$$

We recover that if $f(x,t) = x$, then $\mathcal{D}^* x = b^*$.

References for Appendix B

[187] Ruggiero, P.; Zannetti, M. *La Rivista del Nuovo Cimento* **1985**, *8*, 1–47.

[243] Nelson, E, *Quantum Fluctuations*; Princeton University Press: Prinston, 1984.

APPENDIX C

CRANK-NICOLSON METHOD

C'est exhubilarant.
— D. Jankovic

This appendix is dedicated to the Crank-Nicolson numerical scheme [60], which is used to solve the time-dependent Schrödinger equation:

$$i\hbar \frac{\partial \psi(x,t)}{\partial t} = \hat{H}\psi(x,t), \tag{C.1}$$

where $\hat{H}$ is the Hamiltonian of the system. It is well-known in quantum mechanics that the time-dependent solution is given by the application of the propagator operator $\hat{U}$ on the initial wavefunction, assuming a time-independent Hamiltonian. Thus, we have:

$$\psi(x,t) = \hat{U}(t)\psi(x,0) = \mathrm{e}^{-i\hat{H}t}\psi(x,0), \tag{C.2}$$

where we are using atomic units, so $\hbar = 1$. Note that the propagator is a unitary operator, $\hat{U}\hat{U}^\dagger = \hat{U}^\dagger\hat{U} = \mathbb{1}$, ensuring a unitary evolution of the system, which means that the norm of the wavefunction is conserved over time, i.e., $|\psi(x,t)|^2 = |\psi(x,0)|^2$. We represent $\psi(x,t)$ by its values at a set of grid points. The spatial domain is divided into J points, and for $j \in [0, J]$, we write $x_j = x_0 + j\Delta x$, where x_0 represents the first point of the grid, and Δx is the step between two consecutive points: $\Delta x = x_{j+1} - x_j$. Similarly, the time domain is divided into N values, denoted as $t_n = n\Delta t$, with $n \in [0, N]$ and $\Delta t = t_{n+1} - t_n$. The wavefunction is now written as

$$\psi(x_j, t_n) = \psi_j^n. \tag{C.3}$$

After applying this discretization to the time evolution given by Eq. (C.2), we obtain

$$\psi_j^{n+1} = \hat{U}(\Delta t)\psi_j^n = \mathrm{e}^{-i\hat{H}\Delta t}\psi_j^n. \tag{C.4}$$

Because the evolution is unitary and preserves the norm, any approximation of $\hat{U}(\Delta t)$ must also be unitary. Simply expanding the propagator using a Taylor series does not maintain unitarity. To derive a unitary approximation, we start by splitting $\hat{U}(\Delta t)$ as

$$\psi_j^{n+1} = \mathrm{e}^{-\frac{i\hat{H}\Delta t}{2}}\mathrm{e}^{-\frac{i\hat{H}\Delta t}{2}}\psi_j^n, \tag{C.5}$$

and multiplying from the left by $\hat{U}^\dagger(\frac{\Delta t}{2})$ leads to

$$\mathrm{e}^{\frac{i\hat{H}\Delta t}{2}}\psi_j^{n+1} = \mathrm{e}^{-\frac{i\hat{H}\Delta t}{2}}\psi_j^n. \tag{C.6}$$

Now, we can expand both exponential functions into Taylor series and truncate after the second term:

$$\left(\mathbb{1} + \frac{i\hat{H}\Delta t}{2}\right)\psi_j^{n+1} = \left(\mathbb{1} - \frac{i\hat{H}\Delta t}{2}\right)\psi_j^n. \tag{C.7}$$

Thus, we obtain a unitary method to approximate $\hat{U}$, known as Cayley's form:

$$\hat{U}(\Delta t) \approx \frac{1 - \frac{i\hat{H}\Delta t}{2}}{1 + \frac{i\hat{H}\Delta t}{2}}. \tag{C.8}$$

We know that $\hat{H}$ can be written as

$$\hat{H} = -\frac{1}{2}\frac{\partial^2}{\partial x^2} + V(x), \tag{C.9}$$

so, noting $V(x_j) = V_j$ and using a finite difference method for the second derivative,

$$\frac{\partial^2 \psi_j^n}{\partial x^2} \approx \frac{\psi_{j+1}^n + \psi_{j-1}^n - 2\psi_j^n}{\Delta x^2}, \tag{C.10}$$

we obtain

$$\begin{aligned} \psi_j^{n+1} - \frac{i\Delta t}{2}\left[\frac{\psi_{j+1}^{n+1} + \psi_{j-1}^{n+1} - 2\psi_j^{n+1}}{\Delta x^2} - V_j\psi_j^{n+1}\right] \\ = \psi_j^n + \frac{i\Delta t}{2}\left[\frac{\psi_{j+1}^n + \psi_{j-1}^n - 2\psi_j^n}{\Delta x^2} - V_j\psi_j^n\right], \end{aligned} \tag{C.11}$$

which is known as the Crank-Nicolson method.

REFERENCES FOR APPENDIX C

[60] Crank, J.; Nicolson, P. *Mathematical Proceedings of the Cambridge Philosophical Society* **1947**, *43*, 50–67.

APPENDIX D

COMPUTATIONAL METHODS FOR GRADIENT ESTIMATION OF PHASE

> : (){: | : &};:
> — Benjamin Bakri, *a.k.a.* Obi-Wan Kenobi

In the Nelson's model, the phase of the wave function is a quantity that guides the particle possible trajectories. The phase is a complex quantity, and its gradient is required to calculate the drift given by Eq. (2.38). As the phase in standard quantum mechanics is not continuous, as it takes its values in the interval $(-\pi, \pi]$, its gradient might exhibit divergences at the discontinuity points. In this appendix, we present two numerical method to obtain a continuous phase from the wavefunction, a simple one that uses the arctangent function and a more sophisticated one that is based on building the phase on a spatial grid following a recursive law.

The wavefunction is a complex function, so can be written in polar form as

$$\psi(x,t) = \sqrt{P(x,t)}\exp\left\{\frac{i}{\hbar}S(x,t)\right\} \tag{D.1}$$

where $P(x,t)$ is the probability density and $S(x,t)$ is the phase. By definition, the phase of a complex number is defined as

$$S(x,t) = \arctan\left(\frac{\mathrm{Im}(\psi(x,t))}{\mathrm{Re}(\psi(x,t))}\right) \tag{D.2}$$

where Im and Re are the imaginary and real parts of the wavefunction, respectively. Then, using the chain rule, the gradient of the phase can be written as

$$\partial_x S(x,t) = \frac{\partial_x \mathrm{Im}(\psi(x,t))\,\mathrm{Re}(\psi(x,t)) - \mathrm{Im}(\psi(x,t))\partial_x \mathrm{Re}(\psi(x,t))}{\mathrm{Re}^2(\psi(x,t)) + \mathrm{Im}^2(\psi(x,t))}. \tag{D.3}$$

This approach is simple as it only necessitates the calculation of the real and imaginary parts of the wavefunction, and their derivatives. The discontinuities of the phase are then avoided.

However, if one desires to have a continuous expression of the phase, and not only its derivatives, a more sophisticated method is required to extract S. Two possibilities exist. We compute the phase using Eq. (D.2) and remove the discontinuities by adding $\pm 2k\pi$ for each discontinuity point. This can be done by the python code given in the Listing D.1.

LISTING D.1: Python code to remove discontinuities in the phase of a wavefunction

```python
import numpy as np

x       =  np.linspace(-3,3,1000)
psi     =  np.exp(1j*x**3)

# Python method to calculate the phase of a complex number
# between -pi and pi
phase   =  np.angle(psi)

# Loop over the phase array
for i in range(1,len(phase)):
    # Difference between two consecutive elements > than pi
    # -2pi from the rest of the array
    if phase[i]-phase[i-1]>np.pi:
        phase[i:] -=  2*np.pi
    # Difference between two consecutive elements < than -pi
    # +2pi to the rest of the array
    if phase[i]-phase[i-1]<-np.pi:
        phase[i:] +=2*np.pi
```

The other possibility is to follow the procedure given in Ref. [202] and to construct the phase on a grid by following a recursive law. The grid is divided into N_x points, spaced by a space increment Δx and the phase is calculated at each point x_j, $j \in [0, N_x - 1]$ by using the previous value of the phase. As the time does not play any role here, we drop it from the argument of the phase. The recursive law is given by

$$S(x + \Delta x) = S(x) + \Delta S(x) \tag{D.4}$$

where

$$\Delta S(x) = \arctan\left(\frac{\mathrm{Im}(\psi(x + \Delta x))}{\mathrm{Re}(\psi(x + \Delta x))}\right) - \arctan\left(\frac{\mathrm{Im}(\psi(x))}{\mathrm{Re}(\psi(x))}\right). \tag{D.5}$$

Starting from a reference point x_0, this leads to

$$S(x_j) = S(x_0) + \sum_{k=0}^{j-1} \Delta S(x_k). \tag{D.6}$$

If the phase is calculated on a grid, the gradient can be obtained by a simple finite difference scheme. Moreover the value of the phase on the reference point does not matter as the gradient cancels it. There is a subtlety in this method: at the nodes of the wavefunction, the phase is not defined. The method given by Eq. (D) yields to a pahse sift of π at the level of the nodes, so to a discontinuity of the phase. These discontinuities do not originate from the multi-valuedness of the phase, but from the fact that the phase is not defined at the nodes. These discontinuities have not to be removed.

In Fig. A1, we summarize these two methods for calculating the phase of the wavefunction. In the left panel, we show the phase of the wavefunction $\psi(x) = \exp(ix^3)$ calculated using the arctangent method (dark blue) and the recursive method (blue). The phases are shown in units of 2π. We observe that the arctangent method exhibits discontinuities at the nodes of the wavefunction, whereas the recursive method does not. In the right panel, we present a situation where the wavefunction has several nodes: specifically, the case of the fifth eigenstate of the harmonic oscillator. The phase calculated using the recursive method is shown in blue. Here, the phase exhibits discontinuities of $0.5 \times 2\pi$ at the nodes of the wavefunction.

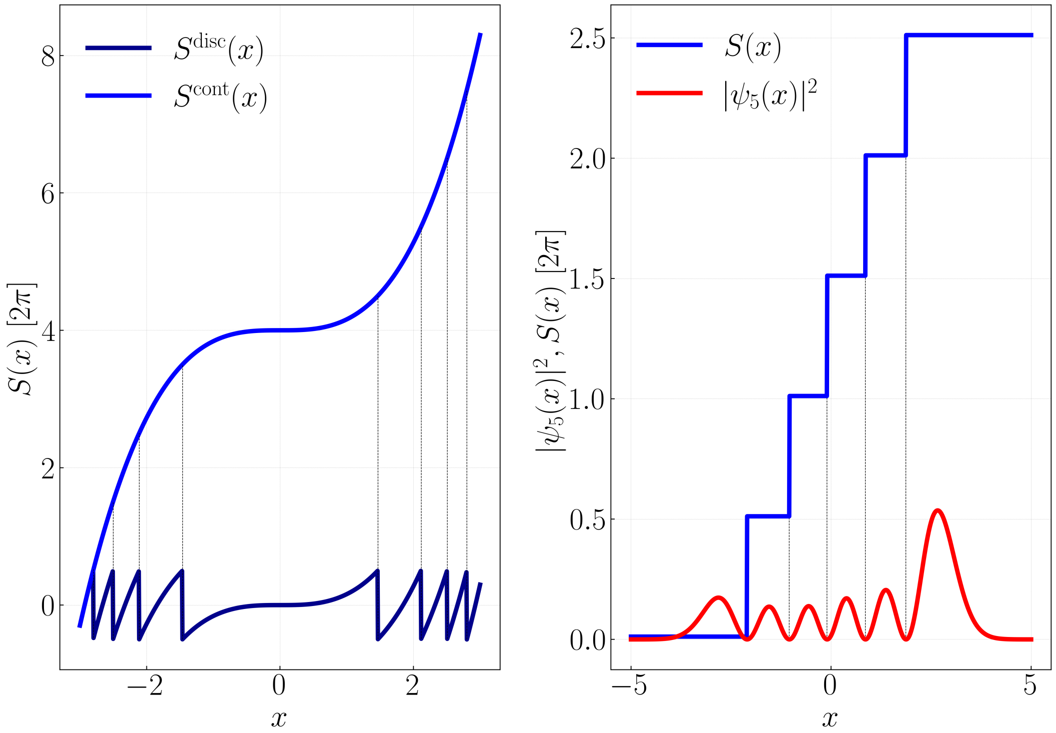

FIGURE A1: Illustration of the two methods for calculating the phase of the wavefunction. On the left, the phase of the wavefunction $\psi(x) = \exp(ix^3)$ is calculated using the arctangent method (dark blue) and the recursive method (blue). The phases are shown in units of 2π. It is observed that the arctangent method exhibits discontinuities at the nodes of the wavefunction, whereas the recursive method does not. On the right, a case where the wavefunction has several nodes is shown: the fifth eigenstate of the harmonic oscillator. The phase calculated using the recursive method is shown in blue. The phase exhibits discontinuities of 0.5 [2π] at the nodes of the wavefunction.

REFERENCES FOR APPENDIX D

[202] Katz, R.; Gossiaux, P. B. *Annals of Physics* **2016**, *368*, 267–295.

APPENDIX E

Derivation of the Airy coefficients

Oh! γ, κ ! $\hbar\omega$. C'est null-space
— A. Andoche

We sketch here the procedure used in Ref. [122] to decompose the wavefunction

$$\Psi(x,0) = \frac{1}{(2\pi\zeta^2)^{1/4}} \exp\left[-\frac{(x-h)^2}{4\zeta^2}\right]$$

on the basis of the eigenfunctions of the Hamiltonian (3.31):

$$\chi_n(x) = \Theta(x)\frac{\mathrm{Ai}(x-E_n)}{\mathrm{Ai}'(-E_n)}.$$

Writing $\Psi(x,0) = \sum_n c_n\chi_n(x)$, the problem is reduced to finding an expression of the coefficients

$$c_n = \langle\chi_n|\psi\rangle = \frac{1}{(2\pi\zeta^2)^{\frac{1}{4}}}\int_0^\infty \mathrm{d}x\ \chi_n^*(x)\,\mathrm{e}^{-\frac{(x-h)^2}{4\zeta^2}},$$

where the asterisk denotes complex conjugation.
When the width ζ of the Gaussian is small enough with respect to h, the lower bound of the integral can be replaced by $-\infty$ and the c_n have an analytical expression:

$$\begin{aligned} c_n &= \frac{1}{(2\pi\zeta^2)^{\frac{1}{4}}\mathrm{Ai}'(-E_n)}\int_{-\infty}^{+\infty}\mathrm{d}x\ \mathrm{Ai}(x-E_n)\mathrm{e}^{-\frac{(x-h)^2}{4\zeta^2}} \\ &= \frac{2\zeta}{(2\pi\zeta^2)^{\frac{1}{4}}\mathrm{Ai}'(-E_n)}\int_{-\infty}^{+\infty}\mathrm{d}u\ \mathrm{Ai}(2\zeta u+h-E_n)\mathrm{e}^{-u^2} \\ &= \frac{(8\pi\zeta^2)^{\frac{1}{4}}}{\mathrm{Ai}'(-E_n)}\mathrm{Ai}(h-E_n+\zeta^4)\exp\left\{\zeta^2\left(h-E_n+\frac{2}{3}\zeta^4\right)\right\}, \end{aligned}$$

which is just the expression of Eq. (3.35). Note that we used the following identity:

$$\int_{-\infty}^{+\infty}\mathrm{d}u\ \mathrm{e}^{-u^2}\mathrm{Ai}(2au+b) = \sqrt{\pi}\mathrm{e}^{a^2b+\frac{2}{3}a^6}\mathrm{Ai}(b+a^4).$$

References for Appendix E

[122] Rousselle, O. Statistical Analysis of Classical and Quantum Measurements of Free Fall Acceleration of Antihydrogen for the GBAR Experiment, Theses, Sorbonne Université, 2022.

APPENDIX F

CLASSICAL WORK-OPTIMAL PROTOCOL

> *C'est zéro.*
>
> — J. Polonyi

In order to illustrate the quantum-classical analogy, and to show the importance of adding the functional $G[\bar{\kappa}']$ to the total functional to be minimized, we propose to study a simple and well-documented case: the classical work-optimal protocol developed in [166]. A Brownian particle is trapped in a harmonic potential whose stiffness $\bar{\kappa}(t)$ can vary in time. The particle is immersed in a fluid of damping coefficient γ and thermal diffusion coefficient $D = k_B T/\gamma$, where T is the temperature of the fluid. In Ref. [166], the objective was to find the optimal manner to vary $\bar{\kappa}(t)$ so that both the duration of the transition and the work done on the system are minimal. The position of the Brownian particle follows a Gaussian probability distribution of variance $s(t)$, which obeys Eq. (4.11). Changing the independent variable from the time t to the variance s, we can write the time duration Δt as in Eq. (4.26) and the work done on the system as [166, 179, 244]: $W = \frac{1}{2}\int_{t_\mathrm{i}}^{t_\mathrm{f}} \mathrm{d}t\, \dot{\bar{\kappa}}(t)\langle x^2\rangle = -\frac{1}{2}\int_{s_\mathrm{i}}^{s_\mathrm{f}} \mathrm{d}s\ \bar{\kappa}(s) + \frac{1}{2}(s_\mathrm{f}\bar{\kappa}_\mathrm{f} - s_\mathrm{i}\bar{\kappa}_\mathrm{i})$. Hence, the functional to be minimized is

$$J[\bar{\kappa}] = \int_{s_\mathrm{i}}^{s_\mathrm{f}} \mathrm{d}s\ \frac{\gamma}{D\gamma - s\bar{\kappa}(s)} - \lambda \int_{s_\mathrm{i}}^{s_\mathrm{f}} \mathrm{d}s\ \bar{\kappa}(s), \tag{F.1}$$

with λ a Lagrange multiplier. It is straightforward to find the solution of the associated Euler-Lagrange equation [166]:

$$s\bar{\kappa}(s) = D\gamma \mp \sqrt{\frac{\gamma s}{\lambda}}, \tag{F.2}$$

where the upper and lower signs correspond to the cases of the compression or expansion, respectively. Note that, as the Euler-Lagrange equation is purely algebraic, the boundary conditions cannot be fixed at will. Hence, in the classical case, the solution (F.2) must be supplemented by "jumps" at the initial and final times [166].

The associated quantum protocol is obtained using Eq. (4.27), yielding:

$$\kappa(s) = mD^2/s^2, \tag{F.3}$$

which is independent of λ. Surprisingly, this solution coincides with the equilibrium solution (4.13), which means that it represents an adiabatic process for the quantum oscillator, albeit with a finite duration that can be obtained from Eq. (4.26): $\Delta t = \sqrt{\gamma\lambda}(\sqrt{s_\mathrm{i}} \pm \sqrt{s_\mathrm{f}})$. The variance can be computed solving Eq. (4.11), yielding

$$s(t) = (\sqrt{s_\mathrm{i}} \pm t/\sqrt{\gamma\lambda})^2, \tag{F.4}$$

and the classical and quantum protocols are, respectively,

$$\bar{\kappa}(t) = \frac{D\gamma + \sqrt{\gamma s_{\rm i}/\lambda} \pm t/\lambda}{(\sqrt{s_{\rm i}} \pm t/\sqrt{\gamma\lambda})^2}\,; \quad \kappa(t) = \frac{mD^2}{(\sqrt{s_{\rm i}} \pm t/\sqrt{\gamma\lambda})^4}. \tag{F.5}$$

Note that, if the time is expressed in units of total time duration Δt, then $\kappa(t/\Delta t)$ is indeed independent of the Lagrange multiplier λ.

As mentioned above, the quantum solution is at equilibrium at each instant. However, since the classical equilibrium conditions do not hold, $s_{\rm i,f}\bar{\kappa}_{\rm i,f} \neq D\gamma$, the time derivative of the variance at the initial and final times is not zero. From the point of view of the classical system this is not a problem, because the overdamped dynamics displays no inertia, so that one can change the stiffness abruptly to bring it to the equilibrium value compatible with $s_{\rm f}$ [166]. But for the (inertial) Schrödinger equation, if $\dot{s} \neq 0$ at $t = t_{\rm f}$, then the system will continue to evolve in time after $t_{\rm f}$.

It is therefore necessary to ensure that $D\gamma - s\bar{\kappa} = 0$, both at $t = t_{\rm i}$ and $t = t_{\rm f}$. In order to do that, the Euler-Lagrangian equation should be a second-order differential equation, instead of an algebraic one as was the case for the functional of Eq. (F.1). This is the reason why one needs to add a second functional of the form $G[\bar{\kappa}'] = \int_{s_{\rm i}}^{s_{\rm f}} {\rm d}s\ |\bar{\kappa}'(s)|^2$, associated with the Lagrange multiplier μ, which leads to the following Euler-Lagrange equations

$$2\mu\,\bar{\kappa}''(s) = \frac{\gamma s}{[D\gamma - s\bar{\kappa}(s)]^2} - \lambda. \tag{F.6}$$

This being a second-order differential equation, the boundary conditions at $t_{\rm i}$ and $t_{\rm f}$ can be imposed consistently with the requirement that: $s_{\rm i,f}\bar{\kappa}_{\rm i,f} = D\gamma$.

The various results, both for the analytical solution (F.2)-(F.5) (with jumps) and the smooth numerical solution of Eq. (F.6), are presented in Fig. A1 for the variance $s(t)$ (top panels), the classical protocols $\bar{\kappa}(t)$ (middle panels), and the quantum protocols $\kappa(t)$ (bottom panels). In the left panels, we take $\mu = 0$ (no smoothing) and vary λ from 0.1 to 10, while the right panels keep $\lambda = 1$ fixed, while μ varies from 0.01 to 0.1. It is clear (top left and bottom left panels) that the variance $s(t)$ and the quantum protocol $\kappa(t)$ do not depend on λ, as suggested by Eqs. (F.3) and (F.5). Instead, the classical protocol depends on λ, in accordance with Eq. (F.2). It is also evident that the classical protocol displays discontinuities at the initial and final times (which disappear in the adiabatic limit $\lambda \to \infty$), while the quantum protocol does not.

In the protocols with $\mu > 0$ (right panels of Fig. A1), the variance varies smoothly at the initial and final times, as expected, and the classical protocols display no discontinuities at the boundaries. Hence, the equilibrium conditions are fulfilled and the system's variance will remain at its final value at the end of the transition. Finally, we note that the quantum protocol develops large spikes near $t_{\rm i}$ and $t_{\rm f}$ for small values of μ. Hence, although it must converge to the non-smoothed one for $\mu \to 0$, it appears to do so in a singular way, displaying large positive and negative spikes at the boundaries.

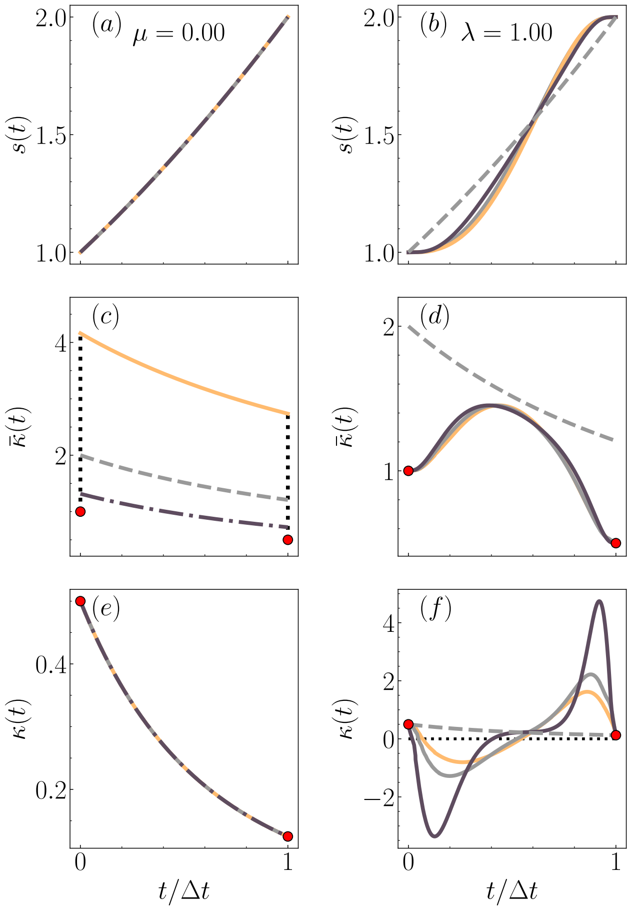

Figure A1: Classical work-optimal protocols. The left panels represent, from top to bottom, the time evolution of the variance (a), the classical protocol (c), and the quantum protocol (e), for the case $\mu = 0$, which displays jumps at the initial and final times (the initial and final conditions are represented by red dots). The different curves are obtained with $\lambda = 0.1$ (orange solid lines), 1.00 (grey dashed lines) and 10.00 (black dash-dotted lines). Note that the variance (a) and the quantum protocol (e) do not depend on λ. The right panels represent, from top to bottom, the time evolution of the variance (b), the classical protocol (d), and the quantum protocol (f), for fixed $\lambda = 1$, and finite values of μ: $\mu = 0.10$ (orange solid lines), 0.05 (grey solid lines) and 0.01 (black solid lines). Note that these finite-μ protocols are continuous and smooth at the initial and final times. For comparison, the dashed grey line represents the classical (discontinuous) protocol with $\mu = 0$.

REFERENCES FOR APPENDIX F

[166] Rosales-Cabara, Y.; Manfredi, G., et al. *Physical Review Research* **2020**, *2*, 012012.

[179] Sekimoto, K. *Progress of Theoretical Physics Supplement* **1998**, *130*, 17–27.

[244] Ciliberto, S. *Physical Review X* **2017**, *7*, 021051.

APPENDIX G

STOCHASTIC LEAPFROG ALGORITHM

Ah non, hein!
— A. Bocci

We use a stochastic version of the leapfrog algorithm to solve the Langevin equation (5.87, 5.88). No demonstration for the forms of the different appearing quantities is given, because it would necessitate a whole report. We just give the procedure that has to be implemented to solve the equations. The time increment is denoted Δt and k_{B} is the Boltzmann constant and T the temperature of the brownian system. All the parameters are those presented in section 5.2. The method is the following:

1· We choose the initial values of q and p. Then, considering step n, we compute $X_{n-1}(\Delta t/2)$ by taking a sample from a normal distribution $\mathcal{N}(0, \sigma_1^2)$, where the width is given by

$$\sigma_1^2 = \frac{k_{\mathrm{B}}T}{m\gamma^2}\, C\left(\frac{\gamma\Delta t}{2}\right) \tag{G.1}$$

with the function C defined as

$$C\left(\frac{\gamma\Delta t}{2}\right) = \gamma\Delta t - 3 + 4\mathrm{e}^{-\gamma\Delta t/2} - \mathrm{e}^{-\gamma\Delta t}. \tag{G.2}$$

2· We compute the force F from the value of the harmonic potential V using

$$F(x) = -\frac{\partial V(x)}{\partial x}. \tag{G.3}$$

3· We then compute Y_v by taking a sample from a normal distribution $\mathcal{N}(0, \sigma_2^2)$, where the width is defined according to

$$\sigma_2^2 = \frac{k_{\mathrm{B}}T}{m}\, B\left(\frac{\gamma\Delta t}{2}\right) C\left(\frac{\gamma\Delta t}{2}\right) \tag{G.4}$$

with the function B defined by

$$B\left(\frac{\gamma\Delta}{2}\right) = \gamma\Delta t\left(\mathrm{e}^{\gamma\Delta t} - 1\right) - 4\left(\mathrm{e}^{\gamma\Delta t/2} - 1\right)^2. \tag{G.5}$$

Then, we can compute

$$V_n\left(-\frac{\gamma\Delta t}{2}\right) = \gamma X_{n-1/2}\left(\frac{\gamma\Delta t}{2}\right)\frac{D\left(\frac{\gamma\Delta t}{2}\right)}{C\left(\frac{\gamma\Delta t}{2}\right)} + Y_v. \tag{G.6}$$

We repeat the same procedure for $V_n(\Delta t/2)$, using this time a normal distribution $\mathcal{N}(0,\rho_1^2)$, where

$$\rho_1^2 = -\frac{k_{\mathrm{B}}T}{m}\left(\mathrm{e}^{-\gamma\Delta t} - 1\right). \tag{G.7}$$

After that, we compute the velocity at step $n+1/2$ using

$$\begin{aligned} &v(t_{n+1/2}) = \\ &v(t_{n-1/2})\mathrm{e}^{-\gamma\Delta t} + \frac{F(x(t_n))}{m\gamma}\left(1-\mathrm{e}^{-\gamma\Delta t}\right) + V_n\left(\frac{\Delta t}{2}\right) - \mathrm{e}^{-\gamma\Delta t}V_n\left(\frac{\Delta t}{2}\right). \end{aligned} \tag{G.8}$$

4\. We take a sample from a normal distribution $\mathcal{N}(0,\rho_2^2)$ to obtain Y_x, where the width of the gaussian is

$$\rho_2^2 = -\frac{k_{\mathrm{B}}T}{m\gamma^2}B\left(-\frac{\gamma\Delta t}{2}\right)\left(\mathrm{e}^{-\gamma\Delta t} - 1\right) \tag{G.9}$$

and then we compute

$$X_{n+1/2}\left(-\frac{\Delta t}{2}\right) = \frac{1}{\gamma}V_n\left(\frac{\Delta t}{2}\right)\frac{D\left(-\frac{\gamma\Delta t}{2}\right)}{\mathrm{e}^{-\gamma\Delta t} - 1} + Y_x. \tag{G.10}$$

Finally, sample $X_{n+1/2}(\Delta t/2)$ using the normal distribution $\mathcal{N}(0,\sigma_1^2)$ and compute

$$\begin{aligned} &x(t_{n+1}) = \\ &x(t_n) + \frac{1}{\gamma}v(t_{n+1/2})\left(\mathrm{e}^{\gamma\Delta t/2} - \mathrm{e}^{\gamma\Delta t/2}\right) + X_{n+1/2}\left(\frac{\Delta t}{2}\right) - X_{n+1/2}\left(\frac{-\Delta t}{2}\right). \end{aligned} \tag{G.11}$$

APPENDIX H

MADELUNG'S STRATEGY

> *La passion et les rêves sont comme le temps, rien ne peut les arrêter, et il en sera ainsi tant qu'il y aura des hommes prêts à donner un sens au mot "Liberté"*
>
> — Gol. D. Roger

FROM MADELUNG'S EQUATIONS TO THE SCHRÖDINGER EQUATION

Change of variable

In this appendix, we will show how to obtain the Schrödinger equation from the Madelung equations,following the method of [229]. This will illustrate the method that can be used to obtain the Schrödinger-Langevin equation from the modified continuity equation. We recall that the continuity equation gives the temporal evolution of the density $\rho(x,t)$ in terms of the spacial derivative of velocity field $v(x,t)$, so that

$$\partial_t \rho(x,t) + \partial_x(\rho(x,t)v(x,t)) = 0. \tag{H.1}$$

Let us suppose that the density and the velocity field can be written in terms of two complex functions $\alpha(x,t)$ and $\beta(x,t)$, so that

$$\rho(x,t) = \alpha(x,t)\beta(x,t) \qquad \text{and} \qquad v(x,t) = C\partial_x \log \frac{\alpha(x,t)}{\beta(x,t)} \tag{H.2}$$

where C is a complex constant. It comes that ρv can be written as $\rho v = C(\beta\partial_x\alpha - \alpha\partial_x\beta)$. We can then rewrite the continuity equation as

$$\alpha\left[\partial_t\beta - C\partial_x^2\beta\right] + \beta\left[\partial_t\alpha - C\partial_x^2\alpha\right] = 0 \tag{H.3}$$

This equation can be rewritten as a fraction equation

$$\frac{\partial_t\alpha + C\partial_x^2\alpha}{\partial_t\beta - C\partial_x^2\beta} = -\frac{\alpha}{\beta}. \tag{H.4}$$

The previous equation is equivalent to equating the numerator and denumerator of both left and righ hand sides, to within a given function f so that

$$\begin{cases} \partial_t\alpha + C\partial_x^2\alpha + \alpha f(x,t) = 0, \\ \partial_t\beta - C\partial_x^2\beta - \beta f(x,t) = 0. \end{cases} \tag{H.5}$$

To go further, we need to express the function f and the constant C.

Schrödinger equation

To express the function f and the constant C, we will first demonstrate a result of Quantum Mechanics that will be useful to us. Consider an observable $\phi(x,t)$ of the system. Its expectation value is given by $\bar{\phi} = \int \mathrm{d}x\ \phi(x,t)\rho(x,t)$. We will prove that the expectation value of the derivative of ϕ is the derivative of the expectation value of ϕ, so that $\overline{\frac{\mathrm{d}\phi}{\mathrm{d}t}} = \frac{\mathrm{d}}{\mathrm{d}t}\bar{\phi}$.

Indeed, we have

$$\begin{aligned}
\frac{\mathrm{d}\bar{\phi}}{\mathrm{d}t} &= \frac{\mathrm{d}}{\mathrm{d}t}\int \mathrm{d}x\ \phi\rho && \text{(H.6)}\\
&= \int \mathrm{d}x\ [\rho\partial_t\phi + \phi\partial_t\rho] && \text{(H.7)}\\
&= \int \mathrm{d}x\ \left[\rho\left(\frac{\mathrm{d}\phi}{\mathrm{d}t} - v\partial_x\phi\right) - \phi\partial_x(\rho v)\right] && \text{(H.8)}\\
&= \int \mathrm{d}x\ \left[\rho\frac{\mathrm{d}\phi}{\mathrm{d}t} - \partial_x(\rho v\phi)\right] && \text{(H.9)}\\
&= \int \mathrm{d}x\ \rho\frac{\mathrm{d}\phi}{\mathrm{d}t} && \text{(H.10)}\\
&= \overline{\frac{\mathrm{d}\phi}{\mathrm{d}t}}. && \text{(H.11)}
\end{aligned}$$

Then, if one take a look at the classical Newton equation, one see that $m\frac{\mathrm{d}\bar{v}}{\mathrm{d}t} = -\partial_x V$, with V the potential energy and m the mass of the particle.

Using the previous relation, one can write the derivative of the mean velocity as

$$\begin{aligned}
\frac{\mathrm{d}\bar{v}}{\mathrm{d}t} &= \overline{\frac{\mathrm{d}v}{\mathrm{d}t}} && \text{(H.12)}\\
&= \frac{\mathrm{d}}{\mathrm{d}t}\int \mathrm{d}x\ v\rho && \text{(H.13)}\\
&= \frac{\mathrm{d}}{\mathrm{d}t}\int \mathrm{d}x\ (\beta\partial_x\alpha - \alpha\partial_x\beta) && \text{(H.14)}\\
&= C\int \mathrm{d}x\ (\partial_t\beta\partial_x\alpha + \beta\partial_x\partial_t\alpha - \partial_t\alpha\partial_x\beta - \alpha\partial_x\partial_t\beta) && \text{(H.15)}\\
&= 2C\int \mathrm{d}x\ (\partial_t\beta\partial_x\alpha - \partial_t\alpha\partial_x\beta) && \text{(H.16)}\\
&= 2C\int \mathrm{d}x\ \big([C\partial_x^2\beta + f\beta]\partial_x\alpha + [C\partial_x^2\alpha + f\alpha]\partial_x\beta\big) && \text{(H.17)}\\
&= 2C\int \mathrm{d}x\ \big(C[\partial_x^2\beta\partial_x\alpha + \partial_x^2\alpha\partial_x\beta] + f[\beta\partial_x\alpha + \alpha\partial_x\beta]\big) && \text{(H.18)}\\
&= 0 + 2C\int \mathrm{d}x\ f\partial_x(\alpha\beta) && \text{(H.19)}\\
&= -2C\int \mathrm{d}x\ \alpha\beta\partial_x f && \text{(H.20)}\\
&= -2C\int \mathrm{d}x\ \rho\partial_x f && \text{(H.21)}\\
&= -2C\overline{\partial_x f}. && \text{(H.22)}
\end{aligned}$$

and this allows to write that $-2mC\overline{\partial_x f} = -\overline{\partial_x V}$, one can finally identify the function f to the potential energy V, so that

$$f(x,t) = \frac{V(x,t)}{2mC}. \tag{H.23}$$

We now need to express the constant C. In fact, it is straighforward to see that if α is taken to be the wavefunction ψ and β its conugate ψ^*, then taking $2mC = \hbar/i$ allows to write the Schrödinger equation. Indeed, under the assumption that $\alpha = \psi$ and $\beta = \psi^*$, one can rewrite (H.5) as

$$\begin{cases} \partial_t\psi + \dfrac{\hbar}{2im}\partial_x^2\psi + \dfrac{i}{\hbar}V\psi = 0, \\ \partial_t\psi^* - \dfrac{\hbar}{2im}\partial_x^2\psi^* - \dfrac{i}{\hbar}V\psi^* = 0. \end{cases} \tag{H.24}$$

Mutliplying the firest line by $i\hbar$ and the second by $i\hbar$, one finally gets

$$\begin{cases} i\hbar\partial_t\psi = -\dfrac{\hbar^2}{2m}\partial_x^2\psi + V\psi, \\ -i\hbar\partial_t\psi^* = -\dfrac{\hbar^2}{2m}\partial_x^2\psi^* + V\psi^*, \end{cases} \tag{H.25}$$

which are the Schrödinger equations for the wavefunction ψ and its conjugate ψ^*.

Hamilton-Jacobi equation

From now, it seems that we did not use the Hamilton-Jacobi equation. However, it is becasue this equation is a direct consequence of the change of variable we made, and we can recover it using (H.5). We recall that $v = C\partial_x \log\frac{\alpha}{\beta}$, and if we note $\mathcal{S} = C\log\frac{\alpha}{\beta}$, we can write that $v = \partial_x\mathcal{S} =$, so $\mathcal{S}$ is proportional to the phase of the wavefunction. We are looking for the time evoltion of $\mathcal{S}$. One can write that

$$\begin{aligned} \partial_t\mathcal{S} &= \partial_t\left(C\log\frac{\alpha}{\beta}\right) && \text{(H.26)} \\ &= C\left(\frac{\partial_t\alpha}{\alpha} - \frac{\partial_t\beta}{\beta}\right) && \text{(H.27)} \\ &= -C\left(\frac{C\partial_x^2\alpha + f\alpha}{\alpha} + \frac{C\partial_x^2\beta + f\beta}{\beta}\right) && \text{(H.28)} \\ &= -C\left(2f + C\left[\frac{\partial_x^2\alpha}{\alpha} + \frac{\partial_x^2\beta}{\beta}\right]\right). && \text{(H.29)} \end{aligned}$$

We know that the Hamilton-Jacobi equation involves the quantum potential $V_\mathrm{Q} = -\frac{\hbar^2}{2m}\frac{\partial_x^2\sqrt{\rho}}{\sqrt{\rho}}$, the square of the derivative of the face $\frac{1}{2m}(\partial_x S)^2$, and the potential energy V. The term $2Cf$ directly gives the potential energy, then the other term should give the quantum potential and the square of the derivative of the phase. Let us write the quantum potential in term of α and β. One gets

$$\begin{aligned} V_\mathrm{Q} &= -\frac{\hbar^2}{2m}\frac{\partial_x^2\sqrt{\rho}}{\sqrt{\rho}} && \text{(H.30)} \\ &= -\frac{\hbar^2}{2m}\frac{\partial_x^2\sqrt{\alpha\beta}}{\sqrt{\alpha\beta}} && \text{(H.31)} \\ & && \text{(H.32)} \end{aligned}$$

and let us compute the first and seconde derivatives of $\sqrt{\alpha\beta}$. One finds

$$\partial_x\sqrt{\alpha\beta} = \frac{1}{2}\left(\sqrt{\frac{\beta}{\alpha}}\partial_x\alpha + \sqrt{\frac{\alpha}{\beta}}\alpha\partial_x\beta\right) \tag{H.33}$$

$$\tag{H.34}$$

and

$$\partial_x^2\sqrt{\alpha\beta} = \frac{1}{2}\sqrt{\frac{\beta}{\alpha}}\partial_x^2\alpha + \frac{1}{2}\sqrt{\frac{\alpha}{\beta}}\partial_x^2\beta - \frac{1}{4}\sqrt{\frac{\beta}{\alpha^2}}(\partial_x\alpha)^2 - \frac{1}{4}\sqrt{\frac{\alpha}{\beta^2}}(\partial_x\beta)^2 + \frac{1}{2}\frac{\partial_x\alpha\partial_x\beta}{\sqrt{\alpha\beta}} \tag{H.35}$$

and then, divinding by $\sqrt{\alpha\beta}$, one gets

$$\frac{\partial_x^2\sqrt{\alpha\beta}}{\sqrt{\alpha\beta}} = \frac{1}{2}\left(\frac{\partial_x^2\alpha}{\alpha} + \frac{\partial_x^2\beta}{\beta}\right) - \frac{1}{4}\left(\frac{(\partial_x\alpha)^2}{\alpha^2} + \frac{(\partial_x\beta)^2}{\beta^2}\right) + \frac{1}{2}\frac{\partial_x\alpha\partial_x\beta}{\alpha\beta}. \tag{H.36}$$

It comes that

$$\frac{\partial_x^2\alpha}{\alpha} + \frac{\partial_x^2\beta}{\beta} = 2\frac{\partial_x^2\sqrt{\alpha\beta}}{\sqrt{\alpha\beta}} + \frac{1}{2}\frac{(\partial_x\alpha)^2}{\alpha^2} + \frac{1}{2}\frac{(\partial_x\beta)^2}{\beta^2} - \frac{\partial_x\alpha\partial_x\beta}{\alpha\beta}. \tag{H.37}$$

$$\tag{H.38}$$

After injecting that in the expression of $\partial_t\mathcal{S}$, one gets, after using $2f = V/mC$ and $C = \hbar/2im$,

$$\partial_t\mathcal{S} = -\frac{V}{m} - C^2\left(2\frac{\partial_x^2\sqrt{\alpha\beta}}{\sqrt{\alpha\beta}} + \frac{1}{2}\frac{(\partial_x\alpha)^2}{\alpha^2} + \frac{1}{2}\frac{(\partial_x\beta)^2}{\beta^2} - \frac{\partial_x\alpha\partial_x\beta}{\alpha\beta}\right) \tag{H.39}$$

$$= -\frac{V+V_{\mathrm{Q}}}{m} - \frac{C^2}{2}\left(\frac{(\partial_x\alpha)^2}{\alpha^2} + \frac{(\partial_x\beta)^2}{\beta^2}\right) + C^2\frac{\partial_x\alpha\partial_x\beta}{\alpha\beta}. \tag{H.40}$$

$$\tag{H.41}$$

The final step consists on expressing $(\partial_x\mathcal{S})^2$ in terms of α and β. One gets

$$\partial_x\mathcal{S} = C\partial_t\log\frac{\alpha}{\beta} \tag{H.42}$$

$$= C\left(\frac{\partial_x\alpha}{\alpha} - \frac{\partial_x\beta}{\beta}\right) \tag{H.43}$$

$$\tag{H.44}$$

and then

$$(\partial_x\mathcal{S})^2 = C^2\left(\frac{(\partial_x\alpha)^2}{\alpha^2} + \frac{(\partial_x\beta)^2}{\beta^2} - 2\frac{\partial_x\alpha\partial_x\beta}{\alpha\beta}\right) \tag{H.45}$$

$$= C^2\left(\frac{(\partial_x\alpha)^2}{\alpha^2} + \frac{(\partial_x\beta)^2}{\beta^2}\right) - 2C^2\frac{\partial_x\alpha\partial_x\beta}{\alpha\beta}. \tag{H.46}$$

which corresponds to the last term that appears in the preivous expression of $\partial_t\mathcal{S}$. It comes that

$$\partial_t\mathcal{S} = -\frac{V}{m} - \frac{V_{\mathrm{Q}}}{m} - \frac{1}{2}(\partial_x\mathcal{S})^2. \tag{H.47}$$

This is an equation that looks very close to the Hamilton-Jacobi equation. To ensure that it is the Hamilton-Jacobi equation, we need to make appear the phase S of the wavefunction. If we write $\alpha = \psi = \sqrt{\rho}\exp(iS/\hbar)$ and $\beta = \psi^* = \sqrt{\rho}\exp(-iS/\hbar)$, we can write that $\mathcal{S} = C\log\frac{\alpha}{\beta} = 2iCS/\hbar = S/m$, so that

$$\partial_t S + \frac{1}{2m}(\partial_x S)^2 + V + V_{\mathrm{Q}} = 0, \tag{H.48}$$

and this is exactly the Hamilton-Jacobi equation, Eq. (5.33).

DERIVATION OF SCHRÖDINGER-LANGEVIN EQUATION

We will employ the same procedure than in the previous appendix, but we will use the modified continuity equation, Eq. (5.38) instead of the continuity equation, Eq. (5.30). We will then obtain a modified Schrödinger equation, the Schrödinger-Langevin equation, and we will see that the Hamilton-Jacobi equation is also modified. We recall the modified continuity equation (Fokker–Planck equation) being

$$\partial_t\rho + \frac{1}{m}\partial_x(\rho\partial_x S) - D\partial_x^2\rho = 0. \tag{H.49}$$

We separate ρ and S as in the previous appendix, so that $\rho = \alpha\beta$ and $S = C\log\frac{\alpha}{\beta}$. Similarly to (H.3), the Fokker-Planck equation can be rewritten as

$$\alpha\big[\partial_t\beta - (C+D)\partial_x^2\beta\big] + \beta\big[\partial_t\alpha - (C+D)\partial_x^2\alpha\big] - D\partial_x\alpha\partial_x\beta = 0. \tag{H.50}$$

but in this case, one can see that the last term couples α and β, and it is no more possible to separate this equation into two independent equation, as we did with (H.5). One should then wonder about a manner to decouple α and β to make it possible to recover the same type of system of equations. It is known that in the case of Gaussian distribution, it is possible to write that $-D\partial_x^2\rho = \gamma(\log\rho - \langle\log\rho\rangle)\rho$ with $\gamma = D/\sigma_x^2$, where σ_x is the variance of the distribution. Then, if one is restricted to the case of Gaussian distribution, it is possible to separate α and β by using this expression. One find that the Fokker-Planck equation can be rewritten as

$$\partial_t\rho + \frac{1}{m}\partial_x(\rho\partial_x S) + \gamma(\log(\rho) - \langle\log\rho\rangle)\rho = 0 \tag{H.51}$$

and this time (H.3) becomes

$$\alpha\big(\partial_t\beta - C\partial_x^2\beta + \gamma\beta[\log\beta - \langle\log\beta\rangle]\big) + \beta\big(\partial_t\alpha - C\partial_x^2\alpha + \gamma\alpha[\log\alpha - \langle\log\alpha\rangle]\big) = 0 \tag{H.52}$$

leading to the system of decoupled equations

$$\begin{cases} \partial_t\alpha + C\partial_x^2\alpha + \gamma\alpha[\log\alpha - \langle\log\alpha\rangle] + f\alpha = 0, \\ \partial_t\beta - C\partial_x^2\beta + \gamma\beta[\log\beta - \langle\log\beta\rangle] - f\beta = 0. \end{cases} \tag{H.53}$$

Using the same values for the different quantities as in the previous appendix, one can write that $f = V/mC$, and $2mC = \hbar/i$, so that the new Schrödinger equations become

$$\begin{cases} i\hbar\partial_t\psi = -\dfrac{\hbar^2}{2m}\partial_x^2\psi + V\psi - i\gamma\hbar[\log\psi - \langle\log\psi\rangle]\psi, \\ -i\hbar\partial_t\psi^* = -\dfrac{\hbar^2}{2m}\partial_x^2\psi^* + V\psi^* + i\gamma\hbar[\log\psi^* - \langle\log\psi^*\rangle]\psi^*, \end{cases} \tag{H.54}$$

they are also called Schrödinger-Langevin equations. The Hamilton-Jacobi equation can be obtained by equaling the real parts of the left and right hand sides, so that

$$\partial_t S + \frac{1}{2m}(\partial_x S)^2 + V + V_{\mathrm{Q}} + \gamma[S - \langle S\rangle] = 0. \tag{H.55}$$

APPENDIX I

ENERGETICS FOR OVERDAMPED DYNAMICS

C'est homéomorphe à un trivia.
— P. Guichard

In this appendix, we derive the expression for the average work expended due to the time-dependent change of the stiffness of a harmonic oscillator, as introduced in Sec. 4.3.1. We consider an overdamped Brownian particle of mass m moving in a viscous medium with drag coefficient γ.

The particle is trapped in a harmonic potential with time-dependent stiffness $\bar{\kappa}(t)$. The overdamped Langevin equation for the particle's position is given by

$$\gamma \dot{x}(t) = -\partial_x V(x(t), t) + \xi(t), \tag{I.1}$$

where $\xi(t)$ is a white noise term representing thermal fluctuations.

We are interested in the stochastic motion of the particle from the energetic viewpoint; that is, we consider the stochastic energetics of the particle.

Let us begin with a time-independent potential $U(x)$. The Langevin equation represents a balance of forces:

$$-\gamma \dot{x} + \xi - \partial_x U = 0, \tag{I.2}$$

where the first two terms represent the interaction between the system and the environment (friction and random force), and the last term is associated with the system's potential energy, its internal energy (in the sense independent of the environement).

If the position changes by $\mathrm{d}x$ in a time interval $\mathrm{d}t$, multiplying the previous equation by $-\mathrm{d}x$, we get

$$-\Big[-\gamma \dot{x} + \xi\Big]\mathrm{d}x + \mathrm{d}U = 0. \tag{I.3}$$

Here, $\mathrm{d}U = \partial_x U \mathrm{d}x$ is the change in the internal energy. The term in brackets represents the energy exchange between the system and the environment due to friction and thermal fluctuations. As mentioned in Ref [179], the the term $\xi \mathrm{d}x$ is the multiplication of two fluctuating quantities and it has to be understood in the sense of the Stratonovich calculus. Since the potential is time-independent, there is no work done on the system by changing the potential. We can identify the term in brackets as the heat exchanged with the environment, leading to the definition of the heat absorbed by the system, δQ, as

$$\delta Q = (-\gamma \dot{x} + \xi)\,\mathrm{d}x. \tag{I.4}$$

This leads to $\mathrm{d}U = \delta Q$, which is a stochastic version of the first law of thermodynamics in the case where no work is done on the system. The heat is the energy lost by the system to the environment.

Now, let us consider the case of a time-dependent potential $U = U(x, t)$. The Langevin equation remains the same, but the change in internal energy now includes a time-dependent term. According to the chain rule, we can write

$$\mathrm{d}U = \partial_x U \mathrm{d}x + \partial_t U \mathrm{d}t. \tag{I.5}$$

Using the definition of heat from (I.4), the Eq. (I.2) is modified as

$$\mathrm{d}U = \delta Q + \partial_t U \mathrm{d}t. \tag{I.6}$$

The last term corresponds to the energy given to the system by changing the potential and can be identified as the work done on the system:

$$\delta W = \partial_t U \mathrm{d}t. \tag{I.7}$$

Thus, the stochastic form of the first law of thermodynamics becomes $\mathrm{d}U = \delta Q + \delta W$. The heat δQ, given by (I.4), is the energy exchanged with the environment, and the work δW, given by (I.7), is the energy supplied to (or extracted from) the system due to the time-dependent potential.

Integrating over time, we obtain the total work done on the system along one trajectory as

$$W = \int \delta W = \int_{t_\mathrm{i}}^{t_\mathrm{f}} \mathrm{d}t\, \partial_t U = \frac{1}{2} \int_{t_\mathrm{i}}^{t_\mathrm{f}} \mathrm{d}t\, \dot{\kappa}(t) x^2(t). \tag{I.8}$$

The macroscopic average of the expended work over the protocol is obtained by averaging (I.8) over all possible trajectories, that is, over all realizations of the noise. We get

$$\Delta W = \frac{1}{2} \int_{t_\mathrm{i}}^{t_\mathrm{f}} \mathrm{d}t\, \dot{\kappa}(t) \left\langle x^2(t) \right\rangle. \tag{I.9}$$

As mentioned in Sec. 4.3.1, the probability distribution of x is Gaussian with variance $\left\langle x^2(t) \right\rangle = s(t)$. The average expended work is finally given by

$$\Delta W = \frac{1}{2} \int_{t_\mathrm{i}}^{t_\mathrm{f}} \mathrm{d}t\, \dot{\kappa}(t) s(t), \tag{I.10}$$

which corresponds to the expression given in Eq. (4.16).

APPENDIX J

OPTICAL TRAPPING OF MICROSCOPIC PARTICLES

Christ on a bike.
— Herr Keiser Hartmann

This appendix provides details on how a (classical) overdamped Brownian particle can be trapped in a harmonic potential. This illustrates how time-dependent stiffness can be generated and how the optimal protocols derived in Chap. 4 can be implemented. Specifically, we will describe how an optical trap is created using optical forces to confine a particle in a harmonic potential.

CONCEPT OF THE EXPERIMENT

The experiments are conducted at the ISIS institute (Institut de Science et d'Ingénierie Supramoléculaires) in Strasbourg. A micro-sphere, referred to as the particle, with a radius of approximately $R \approx 500\,\mathrm{nm}$, is optically trapped using a laser with a wavelength of $\lambda \approx 785\,\mathrm{nm}$. The optical trap is approximated as harmonic (details on how this is achieved will follow). The particle is immersed in water at room temperature, with a drag coefficient of $\gamma \approx 0.4\,\mathrm{\mu m^2/s}$.

The position of the microsphere, $x(t)$, along the optical axis of the trap is recorded at each time using a second laser. For more details, see Ref. [245]. We will show that the trap stiffness, $\bar{\kappa}(t)$, is proportional to the intensity of the trapping laser, $I(t)$. By modulating the laser intensity over time, we can create a time-dependent stiffness protocol, $\bar{\kappa}(t)$. By performing a series of N identical protocols on the trapped microsphere, it is possible to build a statistical ensemble of trajectories that yields a probability density function of the particle's position, x.

HARMONIC POTENTIAL FROM OPTICAL FORCE

Lorentz Force

The sphere used in the experiment is a dielectric sphere. While its total charge is zero, an external electric field $\boldsymbol{E}$, such as the one generated by the laser, displaces the electric charges from their equilibrium positions, causing the sphere to acquire a polarization density $\boldsymbol{P}$. This polarization corresponds to the dipole density induced by the laser, as depicted in Fig. A1.

If the electric field varies with time, the polarization density gives rise to a current density $\boldsymbol{j}$, which is related to the polarization by $\partial_t \boldsymbol{P} = \boldsymbol{j}$. From the continuity equation

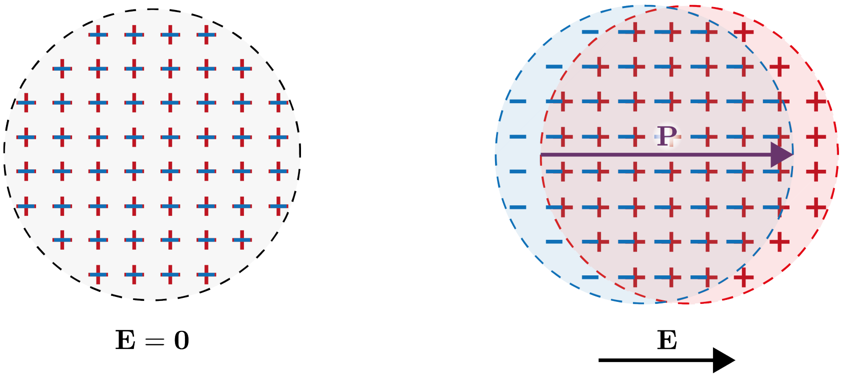

Figure A1: Polarization of a dielectric sphere under an external electric field $\boldsymbol{E}$. The left panel shows the equilibrium state with no external field. The right panel illustrates the situation with an external field applied, resulting in the displacement of charges and the emergence of a polarization vector $\boldsymbol{P}$.

$\partial_t \rho + \boldsymbol{\nabla} \cdot \boldsymbol{j} = 0$, we find that the charge density ρ is given by the divergence of the polarization density

$$\rho = -\boldsymbol{\nabla} \cdot \boldsymbol{P}. \tag{J.1}$$

The sphere is thus sensitive to the electromagnetic fields of the laser through its polarization density and the associated current density. The force exerted on the sphere is the Lorentz force

$$\boldsymbol{F}(\boldsymbol{r}, t) = \int_V \mathrm{d}^3\boldsymbol{r}' \left[\rho(\boldsymbol{r}', t)\boldsymbol{E}(\boldsymbol{r}', t) + \boldsymbol{j}(\boldsymbol{r}', t) \times \boldsymbol{B}(\boldsymbol{r}', t)\right], \tag{J.2}$$

where $\boldsymbol{r}$ is the position of the sphere's center, and the integration is performed over the volume of the sphere. For simplicity, we will omit the arguments of the functions. Using the expressions for $\boldsymbol{P}$ and $\boldsymbol{j}$, we can express the force as

$$\boldsymbol{F} = \int_V \mathrm{d}^3\boldsymbol{r}\, [(\boldsymbol{P} \cdot \nabla)\boldsymbol{E} + \partial_t \boldsymbol{P} \times \boldsymbol{B}] - \int_{\partial V} (\mathrm{d}\boldsymbol{S} \cdot \boldsymbol{P})\boldsymbol{E}. \tag{J.3}$$

Assuming the point dipole approximation, we can write $\boldsymbol{P}(\boldsymbol{r}', t) = \boldsymbol{p}(t)\delta(\boldsymbol{r}' - \boldsymbol{r})$, where $\boldsymbol{p}$ is the dipole moment of the sphere. If the sphere's radius is small compared to the laser wavelength, the surface term can be neglected, as no significant current density is present at the surface. After some vector calculus and using Maxwell's equations, the force simplifies to

$$\boldsymbol{F} = (\boldsymbol{\nabla}\boldsymbol{E})\boldsymbol{p} + \partial_t(\boldsymbol{p} \times \boldsymbol{B}), \tag{J.4}$$

where the μ-th component of the first term is given by $[(\boldsymbol{\nabla}\boldsymbol{E})\boldsymbol{p}]_\mu = (\partial_\mu E_\nu)p^\nu$, using Einstein's summation convention. The second term is a time derivative and cancels out when averaging over time. Denoting the time-averaged force as $\langle \boldsymbol{F} \rangle$ and introducing the complex notation for the electric field $\underline{\boldsymbol{E}} = \boldsymbol{E}_0 e^{i(\boldsymbol{k}\cdot\boldsymbol{x} - \omega t)}$ and the dipole $\underline{\boldsymbol{p}} = \boldsymbol{p} e^{i(\boldsymbol{k}\cdot\boldsymbol{r} - \omega t)}$, where $\boldsymbol{k}$ is the wavevector and ω is the frequency, we obtain

$$\langle \boldsymbol{F} \rangle = \langle (\boldsymbol{\nabla}\boldsymbol{E})\boldsymbol{p} \rangle = \frac{1}{2} \operatorname{Re}\left(\underline{\boldsymbol{p}}^* \cdot \boldsymbol{\nabla}\underline{\boldsymbol{E}}\right). \tag{J.5}$$

In the linear response framework, the dipole moment is proportional to the electric field, $\underline{\boldsymbol{p}} = \alpha \underline{\boldsymbol{E}}$, where $\alpha = \alpha_\mathrm{R} + i\alpha_\mathrm{I}$ is a complex number representing the polarizability of the sphere. After some calculations, we find

$$\langle \boldsymbol{F} \rangle = \frac{\alpha_\mathrm{R}}{4} \boldsymbol{\nabla} |\boldsymbol{E}|^2 + N_1 \alpha_\mathrm{I} \langle \boldsymbol{S} \rangle + N_2 \alpha_\mathrm{I} \boldsymbol{\nabla} \times \langle \boldsymbol{L} \rangle, \tag{J.6}$$

where N_1 and N_2 are constants involving the wavevector $k = |\boldsymbol{k}|$. The first term is a conservative force, as it derives from an optical potential

$$U_{\text{opt}} = -\frac{\alpha_{\text{R}}}{4}|\boldsymbol{E}|^2 = -\frac{\alpha_{\text{R}}}{2c\epsilon_0}I, \tag{J.7}$$

where $I = \frac{c\epsilon_0|\boldsymbol{E}|^2}{2}$ is the intensity of the electric field, and c and ϵ_0 are the speed of light and vacuum permittivity, respectively. The optical force exerted on the sphere is

$$\boldsymbol{F}_{\text{opt}} = -\nabla U_{\text{opt}} = \frac{\alpha_{\text{R}}}{4}\nabla|\boldsymbol{E}|^2 = \frac{\alpha_{\text{R}}}{2c\epsilon_0}\nabla I. \tag{J.8}$$

Its magnitude depends on both the intensity of the electric field and the real part of the polarizability α_{R}. The second and third terms introduce the Poynting vector $\boldsymbol{S} = \boldsymbol{E} \times \boldsymbol{B}$ and the average spin density of the field $\langle \boldsymbol{L} \rangle \propto \text{Im}(\underline{\boldsymbol{E}}^* \cdot \underline{\boldsymbol{B}})$. These two forces are non-conservative, and the last one can usually be neglected compared to the others. The force generated by the Poynting vector is commonly referred to as *radiation pressure*. For a transparent sphere, it can be shown (see Ref. [246]) that the imaginary part of the polarizability is proportional to the square of its real part, $\alpha_{\text{I}} \propto \alpha_{\text{R}}^2$, and $\alpha_{\text{R}} \propto R^3$. This implies that for larger particles (large R), the contribution of radiation pressure to the Lorentz force increases and may dominate over the conservative force. To isolate the contribution of the conservative force, the size of the particle and the intensity of the laser must be optimized. In practice, the laser intensity is adjusted to ensure that the radiation pressure contribution remains negligible.

Optical Trap

When the sphere is trapped at the focus of the laser, it is common to consider a focused beam, typically a Gaussian beam.
This is typically achieved by focusing an incident Gaussian beam of intensity I_{inc} using an optical element, as shown in Fig. A2. The incident beam is Gaussian in the transverse directions, resembling a cylinder of constant radius before focusing. We assume that the wavevector along the optical axis z, denoted k_z, is much larger than those in the transverse directions: $k_z \gg k_x$ and $k_z \gg k_y$. Additionally, we assume that the beam is linearly polarized along the x-axis, meaning the electric field propagates along the optical axis (in the z direction). After focusing, the electric field remains Gaussian in the transverse directions, but the beam radius, denoted $\zeta(z)$, varies with z. Using $r^2 = x^2 + y^2$, and taking $z = 0$ as the point where the beam radius is minimized, the intensity of the field can be written as:

$$I(r, z) = I_0 \left[\frac{\zeta_0}{\zeta(z)}\right]^2 \exp\left(-2\frac{r^2}{\zeta^2(z)}\right), \tag{J.9}$$

which is the well-known equation for a paraxial Gaussian beam (see Ref. [247] for further details). Here, I_0 is the intensity at $z = 0$ and $r = 0$, it is proportional to the intensity I_{inc} of the incident beam. The radius of the beam is given by:

$$\zeta(z) = \zeta_0\sqrt{1 + \left(\frac{z}{z_0}\right)^2}, \tag{J.10}$$

where ζ_0 is the beam radius at $z = 0$, and $z_0 = k\zeta_0^2/2$ is the Rayleigh range [248]. The properties of the Gaussian beam are summarized in Fig. A2.

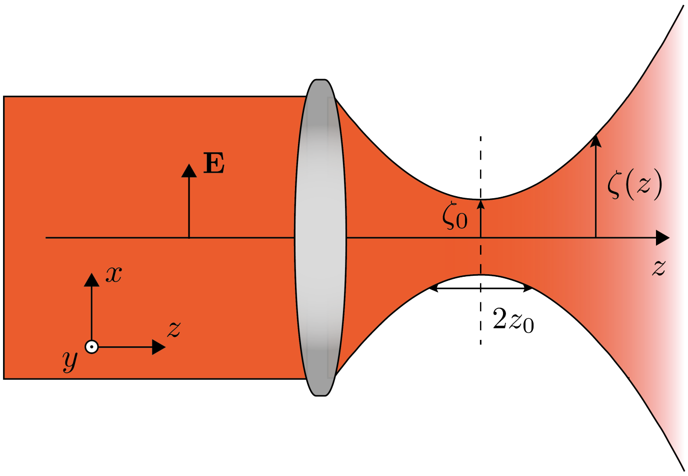

Figure A2: Schematic of a focused Gaussian beam. The incident electric field $\boldsymbol{E}$ is polarized along the x-axis and propagates along the z-axis. It is focussed by an optical element, resulting in a Gaussian beam with a radius $\zeta(z)$ that depends on the position z. At $z = 0$, the beam has a radius ζ_0 that is minimal. For z small as compared the Rayleigh range s_0, the beam can be approximated as harmonic.

By Taylor expanding around $z = 0$, we get $\zeta(z) \approx \zeta_0(1 + z^2/2z_0^2)$, and the intensity of the field becomes:

$$I(r, z) = I_0 \left(1 - \frac{2r^2}{\zeta_0^2} - \frac{z^2}{z_0^2}\right). \tag{J.11}$$

From this expression, we can compute the optical potential generated by the laser using Eq. (J.7), yielding:

$$U_{\text{opt}}(r, z) = -U_0 \left(1 - \frac{2r^2}{\zeta_0^2} - \frac{z^2}{z_0^2}\right), \tag{J.12}$$

where $U_0 = \frac{\alpha_{\text{R}} I_0}{2c\epsilon_0}$. The optical potential can be approximated as harmonic in both the transverse directions and along the optical axis. The stiffness of the harmonic trap along the optical axis is given by:

$$\kappa_z = \frac{U_0}{2z_0^2} = \frac{\alpha_{\text{R}} I_0}{c\epsilon_0 z_0^2}. \tag{J.13}$$

This is the stiffness considered in Chap. 4. To design protocols based on stiffness modulation, the laser intensity must be varied over time. However, this must be done carefully to ensure that the optical force remains the dominant contribution to the Lorentz force.

REFERENCES FOR APPENDIX J

[245] Schnoering, G.; Rosales-Cabara, Y., et al. *Physical Review Applied* **2019**, *11*, 034023.

[246] Jones, P. H.; Maragò, O. M., et al., *Optical Tweezers: Principles and Applications*; Cambridge University Press: Cambridge, 2015.

[247] Raynal, D. Controlled Dynamics of a Levitated Nanoparticle in a Tailored Optical Potential, Ph.D. Thesis, Université Paris-Saclay, 2023.

[248] Siegman, A., *Lasers*; G - Reference,Information and Interdisciplinary Subjects Series; University Science Books: 1986.

APPENDIX K

ITERATIVE METHODS AND THOMAS ALGORITHM

What else?
— G. T. Clooney

CONTEXT

This manuscript aims to elucidate the numerical methodology employed for the resolution of the ensuing differential equation:

$$2\epsilon\frac{\mathrm{d}^2\kappa(s)}{\mathrm{d}s^2} = \frac{s}{[1-s\kappa(s)]^2} - 2\lambda\kappa(s). \tag{K.1}$$

The parameters of significance are designated as ϵ and λ, wherein the former governs the variation of κ, while the latter regulates its magnitude. The function κ is intrinsically contingent upon the independent variable s. Given the second-order nature of Equation (K.1), the imposition of boundary conditions becomes obligatory: we opt to enforce $\kappa_0 = \frac{1}{s_0}$ and $\kappa_\mathrm{f} = \frac{1}{s_\mathrm{f}}$. The inaugural stage of the numerical resolution process entails the specification of the discrete computational lattice: we postulate m discrete values for s, denoted by the integers $i = 1, ..., m$, uniformly segregated at intervals of Δs, resulting in $s_i = s_0 + i\Delta s$. The corresponding values of κ at these discrete junctures are symbolically represented as $\kappa_i = \kappa(s_i)$.

The numerical solution of (K.1) is achieved through an iterative procedure. In the context of the n-th iterative step, the introduction of the parameter $\alpha > 0$ is indispensable to ensure the convergence of the iterative process:

$$-\alpha\kappa_i^{n+1} + \epsilon\left(\frac{\mathrm{d}^2\kappa}{\mathrm{d}s^2}\right)_i^{n+1} = \frac{s_i}{[1-s_i\kappa_i^n]^2} - 2\lambda\kappa_i^n - \alpha\kappa_i^n. \tag{K.2}$$

It is noteworthy that the outcome remains unaffected by the presence of α in (K.2), as it nullifies upon the convergence of $\kappa_i^{n+1} = \kappa_i^n$. The second derivative is then approximated with the standard finite-difference formula

$$\left(\frac{\mathrm{d}^2\kappa}{\mathrm{d}s^2}\right)_i^{n+1} \approx \frac{\kappa_{i+1}^{n+1} - 2\kappa_i^{n+1} + \kappa_{i-1}^{n+1}}{\Delta s^2}. \tag{K.3}$$

Injecting (K.3) in (K.2) and rearranging the terms, one obtains tridiagonal systems of equations

$$-\kappa_{i-1}^{n+1} + \left(2 + \frac{\alpha\Delta s^2}{2\epsilon}\right)\kappa_i^{n+1} - \kappa_{i+1}^{n+1} = -\frac{\Delta s^2}{2\epsilon}\left(\frac{s_i}{[1-s_i\kappa_i^n]^2} - (2\lambda+\alpha)\kappa_i^n\right). \tag{K.4}$$

THOMAS ALGORITHM

A tridiagonal system for n unknowns may be written as

$$a_i x_{i-1} + b_i x_i + c_i x_{i+1} = d_i \tag{K.5}$$

where $a_1 = c_m = 0$, or in matrix form $Mx = d$,

$$\begin{bmatrix} b_1 & c_1 & 0 & \cdots & 0 \\ a_2 & b_2 & c_2 & \cdots & 0 \\ 0 & a_3 & b_3 & \ddots & \vdots \\ \vdots & \ddots & \ddots & \ddots & c_{m-1} \\ 0 & \cdots & 0 & a_m & b_m \end{bmatrix} \begin{bmatrix} x_1 \\ x_2 \\ x_3 \\ \vdots \\ x_m \end{bmatrix} = \begin{bmatrix} d_1 \\ d_2 \\ d_3 \\ \vdots \\ d_m \end{bmatrix} \tag{K.6}$$

where M is a tridiagonal Toeplitz matrix. This system can be solved by using Gaussian elimination, or Thomas algorithm. A first sweep eliminates the a_i's, and then an (abbreviated) backward substitution produces the solution: it is a two-steps procedure. In more details, the first can be called *forward elimination*: we transform the given tridiagonal matrix into an upper triangular matrix by eliminating the off-diagonal elements below the main diagonal. This step involves applying a sequence of row operations to the matrix. The second can be called *backward substitution*: the tridiagonal matrix becomes upper triangular. The next step is to perform backward substitution to solve for the unknown vector. This involves substituting the computed values back into the system of equations.

Thomas' algorithm is not stable in general, but is so in several special cases, such as when the matrix is diagonally dominant (either by rows or columns) or symmetric positive definite.

Forward elimination The forward step consists on creating new coefficients, the primed ones, from the coefficients of the tridiagonal matrix, so that it creates a new matrix where the a_i's coefficients are eliminated. Concretely, we introduce

$$c'_i = \begin{cases} \dfrac{c_i}{b_i}, & i = 1, \\ \dfrac{c_i}{b_i - a_i c'_{i-1}}, & i = 2, 3, \dots, m-1 \end{cases} \tag{K.7}$$

and

$$d'_i = \begin{cases} \dfrac{d_i}{b_i}, & i = 1, \\ \dfrac{d_i - a_i d'_{i-1}}{b_i - a_i c'_{i-1}}, & i = 2, 3, \dots, m. \end{cases} \tag{K.8}$$

Backward substitution The solution is then obtained by back substitution:

$$x_i = \begin{cases} d'_i, & i = m, \\ d'_i - c'_i x_{i+1}, & i = m-1, m-2, \dots, 1. \end{cases} \tag{K.9}$$

CODE

For the case of the equation (K.4), it is clear that a_i, b_i and c_i are independent of the iterative step n while d_i dependent on it, and that

$$a_i = \begin{cases} 0 & i = 1 \\ -1, & i = 2, \dots, m \end{cases}, \qquad c_i = \begin{cases} 0 & i = m \\ -1, & i = 1, \dots, m-1 \end{cases} \tag{K.10}$$

and, for every i between 1 and m,

$$b_i = 2 + \frac{\alpha \Delta s^2}{2\epsilon}, \qquad \text{and} \qquad d_i^n = -\frac{\Delta s^2}{2\epsilon}\left(\frac{s_i}{[1 - s_i \kappa_i^n]^2} - (2\lambda + \alpha)\kappa_i^n\right). \tag{K.11}$$

With all these informations, it is possible to write a script that solves the system.
The following code is a Python implementation of the Thomas algorithm for the resolution of the tridiagonal system of equations (K.4). The code is written in a way that it can be easily adapted to other tridiagonal systems of equations. The code is given in Listing K.1.

LISTING K.1: Iterative methods and Thomas algorithm

```python
import matplotlib.pyplot   as     plt
import numpy               as     np
import matplotlib          as     mpl
from   scipy.integrate     import simpson

""" Define the plotting parameters """
mpl.rcParams.update({'axes.grid'        :  True   ,
                     'grid.color'       : 'black' ,
                     'grid.linestyle'   : '-.'    ,
                     'grid.linewidth'   :  0.3    ,
                     'text.usetex'      :  True   ,
                     'figure.figsize'   : [14,10] ,
                     'figure.dpi'       :  100    ,
                     'font.size'        :  28     ,
                     'lines.linewidth'  :  4      ,
                     'lines.markersize' :  2
                    })


""" Define the parameters """
# Initial value of s
s0      =  1
# Final value of s
sf      =  2
# Initial value of k
k0      =  1/s0
# Final value of k
kf      =  1/sf

# Array of s values
s       =  np.linspace(s0, sf, 1000)
# Step size
ds      =  s[1] - s[0]
# Lagrange multiplier: amplitude
lam     =  0.81
# Lagrange multiplier: variation
eps     = -1e-5
# Assure convergence of the iterative scheme
```

```python
alp     = -10
# ds^2 / (2*epsilon)
dseps   =  ds**2 / (2*eps)

""" Define the tridiagonal matrix elements """
# Lower diagonal
a       = -1
# Diagonal
b       =  2 + alp * dseps
# Upper diagonal
c       = -1
# Initial guess for k(s)
k       =  1/s + 1/(lam*s)**0.5
# Next values for k(s)
knew    =  np.copy(k)


# Right hand side of the linear system
d       =  -dseps * (s/(1-s*k + 1e-10)**2 - 2*lam*k - alp*k)

# New coefficient c' of the Thomas algorithm
cp      =  np.zeros_like(s)
# New coefficient d' of the Thomas algorithm
dp      =  np.zeros_like(s)

# Iteration counter
n       =  0
# Maximum number of iterations
nmax    =  10000

""" Begin iterations: Thomas algorithm """
while True:
    # Initial condition for the Thomas algorithm
    cp[0]   =  0
    # Boundary condition k0
    dp[0]   =  k0

    # Forward sweep of the Thomas algorithm
    for i in range(1,len(s)):
        # c' = c / (b - a*c)
        cp[i]   =  c/(b - a*cp[i-1])
        # d' = (d - a*d') / (b - a*c)
        dp[i]   =  (d[i] - a*dp[i-1])/(b - a*cp[i-1])

    # Boundary condition kf
    knew[-1]   =  kf
    # Backward sweep of the Thomas algorithm
    for i in range(len(s)-2,-1,-1):
        knew[i]   =  dp[i] - cp[i]*knew[i+1]

    # Error of the iteration
    error   =  simpson((k-knew)**2, s)
    # Update k(s)
    k       =  np.copy(knew)
    # Update the right hand side of the linear system
    d       = -dseps * (s/(1-s*k + 1e-10)**2 - 2*lam*k - alp*k)
    # Update the iteration counter
    n      +=  1

    print("Iteration: %i \t Error: %1.5f" %(n, error))
    # Convergence criterion
```

```
    if error < 1e-6   :
        # Break the loop if the error is small enough
        break
    # Break the loop if the maximum number of iterations is reached
    if n > nmax:
        # Print a warning message
        print("Not converging")
        break

""" Plot the results """
plt.plot(s, k, label='k(s)')
plt.plot(s, 1/s + 1/(lam*s)**0.5, ls='--', label='k(s) analytical')
plt.legend()
plt.show()
```

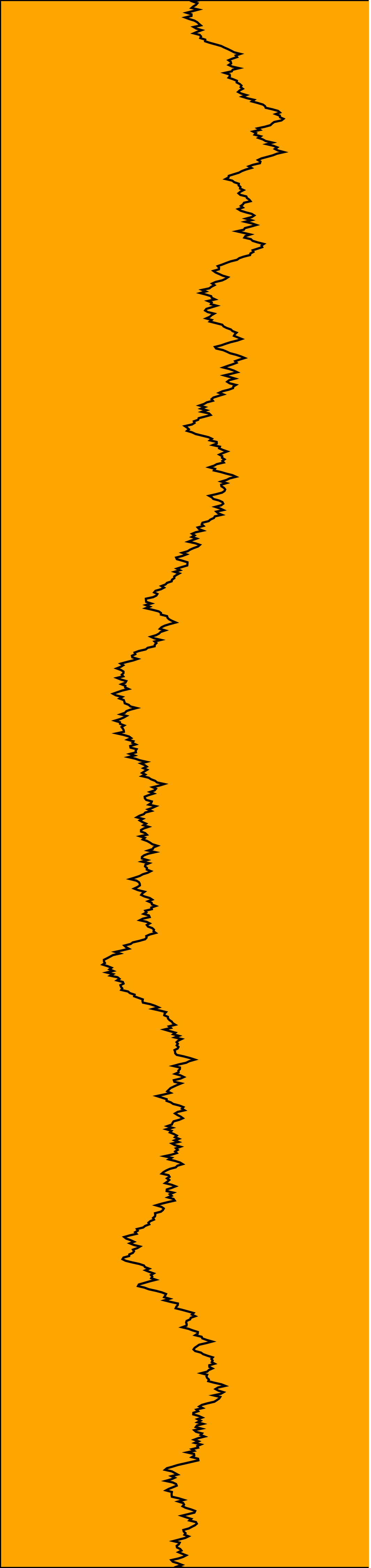

BIBLIOGRAPHY

[1] Benseny, A.; Albareda, G., et al. *The European Physical Journal D* **2014**, *68*, 286.

[2] Libri, G., *Histoire des sciences mathématiques en Italie : depuis la renaissance des lettres jusqu'à la fin du XVIIe siècle*; Renouard: 1838–1841; Vol. 2; 188-189.

[3] Samueli, J.-J., *Une histoire des probabilités: des origines à 1900*; Ellipses: Paris, 2008; 7-8.

[4] Moyer, A. E. *Renaissance Quarterly* **2007**, *60*, 1419–1420.

[5] Smith, D. E. *The American Mathematical Monthly* **1928**, *35*, 280–282.

[6] Ludwig Boltzmann, *Lectures on Gas Theory*; Univ of California Press: 2022; 500 pp.

[7] Brown, R. *The Philosophical Magazine* **1828**, *4*, 161–173.

[8] Paul, W.; Baschnagel, J., *Stochastic Processes*; Springer International Publishing: Heidelberg, 2013.

[9] Bachelier, L. *Annales scientifiques de l'École Normale Supérieure* **1900**, *17*, 21–86.

[10] Einstein, A. *Annalen der physik* **1905**, *17*, 549–560.

[11] Perrin, J. *Le Radium* **1909**, *6*, 353–360.

[12] Langevin *C. R. Hebd. Séances Acad. Sci.* **1908**, *146*, 530.

[13] Wiener *Ann. of Math* **1920**, *22*, 66–72.

[14] Purcell, E. M. *American Journal of Physics* **1977**, *45*, 3–11.

[15] Caldeira, A. O.; Leggett, A. J. *Annals of Physics* **1983**, *149*, 374–456.

[16] Leggett, A. J.; Chakravarty, S., et al. *Reviews of Modern Physics* **1987**, *59*, 1–85.

[17] Lemons, D. S.; Gythiel, A. *American Journal of Physics* **1997**, *65*, 1079–1081.

[18] Uhlenbeck, G. E.; Ornstein, L. S. *Physical Review* **1930**, *36*, 823–841.

[19] Fokker, A. D. *Annalen der Physik* **1914**, *348*, 810–820.

[20] Der Wissenschaften zu Berlin., D. A.; zu Berlin, D. A. d. W., *Sitzungsberichte Der Königlich Preussischen Akademie Der Wissenschaften Zu Berlin*; Deutsche Akademie der Wissenschaften zu Berlin: Berlin, 1917; Vol. Jan-Dec 1917, pp 1–912; 912 pp.

[21] Kramers, H. A. *Physica* **1940**, *7*, 284–304.

[22] Moyal, J. E. *Journal of the Royal Statistical Society: Series B (Methodological)* **1949**, *11*, 150–210.

[23] Smoluchowski *Ann. Phys* **1906**, *21*, 756–780.

[24] Wilemski, G. *Journal of Statistical Physics* **1976**, *14*, 153–169.

[25] Titulaer, U. M. *Physica A: Statistical Mechanics and its Applications* **1978**, *91*, 321–344.

[26] Bocquet, L. *American Journal of Physics* **1997**, *65*, 140–144.

[27] Risken, H., *The Fokker-Planck Equation: Methods of Solution and Applications*; Haken, H., red.; Springer Series in Synergetics, Vol. 18; Springer: Berlin, Heidelberg, 1996.

[28] Ito, K. On Stochastic Differential Equations American Mathematical Society.

[29] Wong, E.; Zakai, M. *The Annals of Mathematical Statistics* **1965**, *36*, 1560–1564.

[30] Schrödinger, E *Sitzungsber. Preuss. Akad. Phys. Math. Klasse* **1931**, 144.

[31] Nelson, E. *Physical Review* **1966**, *150*, 1079–1085.

[32] Bohm, D. *Physical Review* **1952**, *85*, 166–179.

[33] Bohm, D. *Physical Review* **1952**, *85*, 180.

[34] Holland, P. R., *The Quantum Theory of Motion: An Account of the de Broglie-Bohm Causal Interpretation of Quantum Mechanics*; Cambridge University Press: Cambridge, 1993.

[35] Bacciagaluppi, G.; Valentini, A., *Quantum Theory at the Crossroads: Reconsidering the 1927 Solvay Conference*; Cambridge University Press: Cambridge, 2009.

[36] Guerra, F. *Physics Reports* **1981**, *77*, 263–312.

[37] Kyprianidis, A. *Foundations of Physics* **1992**, *22*, 1449–1483.

[38] Nelson, E., *Dynamical Theories of Brownian Motion*; Princeton University Press.: 1967.

[39] De la Peña, L.; Cetto, A. M. *Foundations of Physics* **1982**, *12*, 1017–1037.

[40] Fényes, I. *Zeitschrift für Physik* **1952**, *132*, 81–106.

[41] Davidson, M. *Letters in Mathematical Physics* **1979**, *3*, 271–277.

[42] Kalman, R. E., *The Theory of Optimal Control and the Calculus of Variations*; Research Institute for Advanced Studies: 1960; 31 pp.

[43] Goldstein, H., *Classical Mechanics*; Addison-Wesley Publishing Company: 1980; 696 pp.

[44] Sakurai, J. J.; Napolitano, J., *Modern Quantum Mechanics*; Cambridge University Press: 2017; 569 pp.

[45] Hiley, B. J.; Callaghan, R. E. *Foundations of Physics* **2012**, *42*, 192–208.

[46] Navier, *Mémoire sur les lois du mouvement des fluides*, 1827; Vol. 6; 440 pp.

[47] Stokes, G. G., *On the Theories of the Internal Friction of Fluids in Motion and of the Equilibrium and Motion of Elastic Solids*, 1845; Vol. 8; 305 pp.

[48] Bohm, D.; Hiley, B. J., *The Undivided Universe: An Ontological Interpretation of Quantum Theory*; Routledge: 1995; 347 pp.

[49] Wyatt, R. E.; Bittner, E. R. *The Journal of Chemical Physics* **2000**, *113*, 8898–8907.

[50] Bohm, D. J.; Hiley, B. J. *Foundations of Physics* **1975**, *5*, 93–109.

[51] Philippidis, C.; Dewdney, C., et al. *Il Nuovo Cimento B (1971-1996)* **1979**, *52*, 15–28.

[52] Philippidis, C.; Bohm, D., et al. *Il Nuovo Cimento B (1971-1996)* **1982**, *71*, 75–88.

[53] Hand, L. N.; Finch, J. D., *Analytical Mechanics*; Cambridge University Press: 1998; 598 pp.

[54] Wallstrom, T. C. *Physical Review A* **1994**, *49*, 1613–1617.

[55] McClendon, M.; Rabitz, H. *Physical Review A* **1988**, *37*, 3479–3492.

[56] Kutta; Wilhelm, *Beitrag Zur Naherungsweisen Integration Totaler Differentialgleichungen*; Teubner: 1901.

[57] Runge; König, *Vorlesungen Über Numerisches Rechnen*; Springer: 1924.

[58] Helfand, E. *Bell System Technical Journal* **1979**, *58*, 2289–2299.

[59] Greenside, H. S.; Helfand, E. *The Bell System Technical Journal* **1981**, *60*, 1927–1940.

[60] Crank, J.; Nicolson, P. *Mathematical Proceedings of the Cambridge Philosophical Society* **1947**, *43*, 50–67.

[61] Monahan, J. F. *Mathematics of Computation* **1985**, *45*, 559–568.

[62] Schoenberg, I. J. In *Spline Functions and Approximation Theory: Proceedings of the Symposium Held at the University of Alberta, Edmonton May 29 to June 1, 1972*, Meir, A., Sharma, A., Eds.; Birkhäuser: Basel, 1973, pp 277–327.

[63] Shucker, D. S. *Journal of Functional Analysis* **1980**, *38*, 146–155.

[64] Golin, S. *Journal of Mathematical Physics* **1985**, *26*, 2781–2783.

[65] Büttiker, M.; Landauer, R. *Physical Review Letters* **1982**, *49*, 1739–1742.

[66] Lee, H.-W.; Scully, M. O. *Foundations of Physics* **1983**, *13*, 61–72.

[67] Martinis, J. M.; Devoret, M. H., et al. *Physica B: Condensed Matter* **1988**, *152*, 159–161.

[68] Wigner, E. P. *Physical Review* **1955**, *98*, 145–147.

[69] Büttiker, M. *Physical Review B* **1983**, *27*, 6178–6188.

[70] Sokolovski, D.; Baskin, L. M. *Physical Review A* **1987**, *36*, 4604–4611.

[71] Guerra, M. Electron Optics in Ballistic Graphene Studied by Scanning Gate Microscopy, Ph.D. Thesis, Université Grenoble Alpes, 2021.

[72] Imafuku, K.; Ohba, I., et al. *Physics Letters A* **1995**, *204*, 329–335.

[73] Muga, J. G.; Leavens, C. R. *Physics Reports* **2000**, *338*, 353–438.

[74] Kudo, T.; Nitta, H. *Physics Letters A* **2013**, *377*, 357–361.

[75] Imafuku, K.; Ohba, I., et al. *Physical Review A* **1997**, *56*, 1142–1153.

[76] Hara, K.; Ohba, I. *Physical Review A* **2003**, *67*, 052105.

[77] Glauber, R. J. *Physical Review* **1963**, *131*, 2766–2788.

[78] Pollak, E.; Grabert, H., et al. *The Journal of Chemical Physics* **1989**, *91*, 4073–4087.

[79] Bacciagaluppi, G. In World Scientific, Singapore: 2005, p 367.

[80] Bell, J. S. *Physics Physique Fizika* **1964**, *1*, 195–200.

[81] Dankel, T. G. *Archive for Rational Mechanics and Analysis* **1970**, *37*, 192–221.

[82] Nelson, E. *Journal of Physics: Conference Series* **2012**, *361*, 012011.

[83] Feynman, R. P. *Reviews of Modern Physics* **1948**, *20*, 367–387.

[84] Manfredi, Giovanni *4open* **2022**, *5*, 8.

[85] Born, M. *Zeitschrift für Physik* **1926**, *37*, 863–867.

[86] Einstein, A.; Podolsky, B., et al. *Physical Review* **1935**, *47*, 777–780.

[87] Bell, J. S., *Speakable and Unspeakable in Quantum Mechanics: Collected Papers on Quantum Philosophy*, 2nd ed.; Cambridge University Press: Cambridge, 2004.

[88] Styer, D. F.; Balkin, M. S., et al. *American Journal of Physics* **2002**, *70*, 288–297.

[89] Valentini, A. *Physics Letters A* **1991**, *156*, 5–11.

[90] Valentini, A. *Physical Review D: Particles and Fields* **2010**, *82*, 063513.

[91] Underwood, N. G.; Valentini, A. *Physical Review D: Particles and Fields* **2015**, *92*, 063531.

[92] Lebowitz, J. L. *Physics Today* **1993**, *46*, 32–38.

[93] Lebowitz, J. L. *Physica A: Statistical Mechanics and its Applications* **1999**, *263*, 516–527.

[94] Dürr, D.; Goldstein, S., et al. *Journal of Statistical Physics* **1992**, *67*, 843–907.

[95] Dürr, D.; Struyve, W. In *Do Wave Functions Jump? Perspectives of the Work of GianCarlo Ghirardi*, Allori, V., Bassi, A., et al., Eds.; Springer International Publishing: Cham, 2021, pp 35–43.

[96] Valentini, A.; Westman, H. *Proceedings of the Royal Society A: Mathematical, Physical and Engineering Sciences* **2005**, *461*, 253–272.

[97] Bacciagaluppi, G. *Foundations of Physics Letters* **1999**, *12*, 1–16.

[98] Beyer, M.; Paul, W. *Universe* **2021**, *7*, 166.

[99] Nesvizhevsky, V. V.; al, e. *Nature* **2002**, *415*, 297–299.

[100] Bohm, D.; Hiley, B. J. *Physics Reports* **1989**, *172*, 93–122.

[101] Peruzzi, G.; Rimini, A. *Foundations of Physics Letters* **1996**, *9*, 505–519.

[102] Bohm, D.; Vigier, J. P. *Physical Review* **1954**, *96*, 208–216.

[103] Valentini, A. In *Bohmian Mechanics and Quantum Theory: An Appraisal*, Cushing, J. T., Fine, A., et al., Eds.; Springer Netherlands: Dordrecht, 1996, pp 45–66.

[104] Petroni, N. C.; Guerra, F. *Foundations of Physics* **1995**, *25*, 297–315.

[105] Hatifi, M.; Willox, R., et al. *Entropy. An International and Interdisciplinary Journal of Entropy and Information Studies* **2018**, *20*, 1–32.

[106] Couder, Y.; Protière, S., et al. *Nature* **2005**, *437*, 208–208.

[107] Couder, Y.; Fort, E. *Physical Review Letters* **2006**, *97*, 154101.

[108] Greenside, H. S.; Helfand, E. *Bell System Technical Journal* **1981**, *60*, 1927–1940.

[109] Bayram, M.; Partal, T., et al. *Advances in Difference Equations* **2018**, *2018*, 17.

[110] Valentini, A. *Physics Letters A* **1991**, *158*, 1–8.

[111] Joyce, J. M. In *International Encyclopedia of Statistical Science*, Lovric, M., Ed.; Springer Berlin Heidelberg: Berlin, Heidelberg, 2011, pp 720–722.

[112] Pleinert, M.; von Zanthier, J., et al. *Physical Review Research* **2020**, *2*, 012051.

[113] Cotter, J. P.; Brand, C., et al. *Science Advances* **2017**, *3*, e1602478.

[114] Polyanin, A.; Zaitsev, V., *Handbook of Exact Solutions for Ordinary Differential Equations*; CRC press: New York, 2002.

[115] Tsuru, H. *Journal of the Physical Society of Japan* **1991**, *60*, 3657–3663.

[116] Zhang, L.; Guan, Y. In *Proceedings of the Twenty-Sixth ACM SIGMOD-SIGACT-SIGART Symposium on Principles of Database Systems*; Pods '07; Association for Computing Machinery: Beijing, China, 2007, pp 225–232.

[117] The ALPHA collaboration; Charman, A. E. *Nature Comm.* **2013**, *4*, 1785.

[118] Perez, P.; Sacquin, Y. *Class. Quantum Grav.* **2012**, *29*, 184008.

[119] Dufour, G.; Gérardin, A., et al. *Physical Review A: Atomic, Molecular, and Optical Physics* **2013**, *87*, 012901.

[120] Dufour, G. Quantum Reflection from the Casimir-Polder Potential, Theses, Université Pierre et Marie Curie - Paris VI, 2015.

[121] Crépin, P.-P. Quantum Reflection of a Cold Antihydrogen Wave Packet, Ph.D. Thesis, Sorbonne Université, 2019.

[122] Rousselle, O. Statistical Analysis of Classical and Quantum Measurements of Free Fall Acceleration of Antihydrogen for the GBAR Experiment, Theses, Sorbonne Université, 2022.

[123] Jenke, T.; Geltenbort, P., et al. *Nature Phys.* **2011**, *7*, 468–472.

[124] Jenke, T.; Cronenberg, G., et al. *Physical Review Letters* **2014**, *112*, 151105.

[125] Killian, C.; Burkley, Z., et al. *The European Physical Journal D* **2023**, *77*, 50.

[126] Suda, M.; Faber, M., et al. *Zeitschrift für Naturforschung A* **2022**, *77*, 875–898.

[127] Vallé, O.; Soares, M. In Imperial College Press: London, 2004.

[128] Crépin, P.-P.; Christen, C., et al. *Physical Review A: Atomic, Molecular, and Optical Physics* **2019**, *99*, 042119.

[129] Martínez-Garaot, S.; Torrontegui, E., et al. *Physical Review Letters* **2013**, *111*, 213001.

[130] Wineland, D. J.; Monroe, C., et al. In *Advances in Quantum Chemistry*, Löwdin, P.-O., Ed.; Academic Press: 1998; Vol. 30, pp 41–64.

[131] Marr, C.; Beige, A., et al. *Physical Review A* **2003**, *68*, 033817.

[132] Wendin, G. *Reports on Progress in Physics* **2017**, *80*, 106001.

[133] Khomitsky, D. V.; Gulyaev, L. V., et al. *Physical Review B* **2012**, *85*, 125312.

[134] Song, X.-K.; Zhang, H., et al. *New Journal of Physics* **2016**, *18*, 023001.

[135] Bachmann, S.; De Roeck, W., et al. *Physical Review Letters* **2017**, *119*, 060201.

[136] Pang, S.; Jordan, A. N. *Nature Communications* **2017**, *8*, 14695.

[137] Takahashi, K. *Journal of Physics A: Mathematical and Theoretical* **2013**, *46*, 315304.

[138] Takahashi, K. *Physical Review A* **2015**, *91*, 042115.

[139] Li, J.; Sun, K., et al. *Scientific Reports* **2016**, *6*, 38258.

[140] Li, J.; Fogarty, T., et al. *New Journal of Physics* **2018**, *20*, 015005.

[141] Pinch, E. R.; Pinch, E. R., *Optimal Control and the Calculus of Variations*; Oxford University Press: Oxford, New York, 1995; 242 pp.

[142] Kirk, D. E., *Optimal Control Theory: An Introduction*; Courier Corporation: 2012; 466 pp.

[143] Hegerfeldt, G. C. *Physical Review Letters* **2013**, *111*, 260501.

[144] Sun, C.; Saxena, A., et al. *Journal of Physics B: Atomic, Molecular and Optical Physics* **2017**, *50*, 175501.

[145] Zhou, B. B.; Baksic, A., et al. *Nature Physics* **2017**, *13*, 330–334.

[146] Guéry-Odelin, D.; Ruschhaupt, A., et al. *Reviews of Modern Physics* **2019**, *91*, 045001.

[147] Guéry-Odelin, D.; Jarzynski, C., et al. *Reports on Progress in Physics* **2023**, *86*, 035902.

[148] Berry, M. V. *Journal of Physics A: Mathematical and Theoretical* **2009**, *42*, 365303.

[149] Demirplak, M.; Rice, S. A. *The Journal of Physical Chemistry B* **2005**, *109*, 6838–6844.

[150] Demirplak, M.; Rice, S. A. *The Journal of Chemical Physics* **2008**, *129*, 154111.

[151] Schmiedl, T.; Dieterich, E., et al. *Journal of Statistical Mechanics: Theory and Experiment* **2009**, *2009*, P07013.

[152] Torrontegui, E.; Ibáñez, S., et al. *Physical Review A* **2011**, *83*, 013415.

[153] Muga, J. G.; Chen, X., et al. *Journal of Physics B: Atomic, Molecular and Optical Physics* **2009**, *42*, 241001.

[154] Unanyan, R. G.; Yatsenko, L. P., et al. *Optics Communications* **1997**, *139*, 48–54.

[155] Emmanouilidou, A.; Zhao, X.-G., et al. *Physical Review Letters* **2000**, *85*, 1626–1629.

[156] Couvert, A.; Kawalec, T., et al. *Europhysics Letters* **2008**, *83*, 13001.

[157] Motzoi, F.; Gambetta, J. M., et al. *Physical Review Letters* **2009**, *103*, 110501.

[158] Rezek, Y.; Salamon, P., et al. *Europhysics Letters* **2009**, *85*, 30008.

[159] Salamon, P.; Hoffmann, K. H., et al. *Physical Chemistry Chemical Physics* **2009**, *11*, 1027–1032.

[160] Masuda, S.; Nakamura, K. *Proceedings of the Royal Society A: Mathematical, Physical and Engineering Sciences* **2009**, *466*, 1135–1154.

[161] Demirplak, M.; Rice, S. A. *The Journal of Physical Chemistry A* **2003**, *107*, 9937–9945.

[162] Chen, X.; Ruschhaupt, A., et al. *Physical Review Letters* **2010**, *104*, 063002.

[163] Patra, A.; Jarzynski, C. *New Journal of Physics* **2017**, *19*, 125009.

[164] Plata, C. A.; Prados, A., et al. *Physical Review Letters* **2021**, *127*, 190605.

[165] Raynal, D.; de Guillebon, T., et al. *Physical Review Letters* **2023**, *131*, 087101.

[166] Rosales-Cabara, Y.; Manfredi, G., et al. *Physical Review Research* **2020**, *2*, 012012.

[167] De Broglie, L. *J. Phys. Radium* **1927**, *8*, 225.

[168] Pucci, G.; Harris, D. M., et al. *Journal of Fluid Mechanics* **2018**, *835*, 1136–1156.

[169] Goerlich, R.; Manfredi, G., et al. *Physical Review Research* **2021**, *3*, 033203.

[170] Schmiedl, T.; Seifert, U. *Physical Review Letters* **2007**, *98*, 108301.

[171] Gomez-Marin, A.; Schmiedl, T., et al. *The Journal of Chemical Physics* **2008**, *129*, 024114.

[172] Bulatov, A.; Vugmeister, B., et al. *Physical Review A* **1998**, *58*, 1346–1351.

[173] Feldmann, T.; Kosloff, R. *Physical Review E* **2000**, *61*, 4774–4790.

[174] Hardel, V.; Hervieux, P.-A., et al. *Foundations of Physics* **2023**, *53*, 89.

[175] Lewis, H. R. *Physical Review Letters* **1967**, *18*, 510–512.

[176] Manoliu, A.; Kittel, C. *American Journal of Physics* **1979**, *47*, 678–680.

[177] Gardiner, C., *Stochastic Methods: A Handbook for the Natural and Social Sciences*; Springer Series in Synergetics; Springer Berlin Heidelberg: 2009.

[178] Martínez-Tibaduiza, D.; Pires, L., et al. *Journal of Physics B: Atomic, Molecular and Optical Physics* **2021**, *54*, 205401.

[179] Sekimoto, K. *Progress of Theoretical Physics Supplement* **1998**, *130*, 17–27.

[180] Boltyanski, V. G.; Gamkrelidze, R. V., et al. *IFAC Proceedings Volumes* **1960**, *1*, 464–469.

[181] Lipitakis, A.-D. *Applied Mathematics* **2016**, *7*, 1225–1240.

[182] Albay, J. A. C.; Kwon, C., et al. *New Journal of Physics* **2020**, *22*, 123049.

[183] Wigner, E. *Physical Review* **1932**, *40*, 749–759.

[184] Hudson, R. *Reports on Mathematical Physics* **1974**, *6*, 249–252.

[185] Manfredi, G.; Hervieux, P.-A. *Physical Review Letters* **2008**, *100*, 050405.

[186] Haas, F.; Manfredi, G., et al. *Physical Review B* **2009**, *80*, 073301.

[187] Ruggiero, P.; Zannetti, M. *La Rivista del Nuovo Cimento* **1985**, *8*, 1–47.

[188] Kobayashi, K.; Yamanaka, Y. *Physics Letters A* **2011**, *375*, 3243–3249.

[189] Manzano, D. *AIP Advances* **2020**, *10*, 025106.

[190] Gorini, V.; Kossakowski, A., et al. *Journal of Mathematical Physics* **1976**, *17*, 821–825.

[191] Lindblad, G. *Communications in Mathematical Physics* **1976**, *48*, 119–130.

[192] Redfield, A. G. *IBM Journal of Research and Development* **1957**, *1*, 19–31.

[193] Shibata, F.; Takahashi, Y., et al. *Journal of Statistical Physics* **1977**, *17*, 171–187.

[194] Nakajima, S. *Progress of Theoretical Physics* **1958**, *20*, 948–959.

[195] Zwanzig, R. *The Journal of Chemical Physics* **1960**, *33*, 1338–1341.

[196] Weiss, U., *Quantum Dissipative Systems*; World scientific: 1993.

[197] Schuch, D.; Bonilla-Licea, M. *Entropy* **2023**, *25*, 312.

[198] Caldirola, P. *Il Nuovo Cimento (1924-1942)* **1941**, *18*, 393–400.

[199] Kanai, E. *Progress of Theoretical Physics* **1948**, *3*, 440–442.

[200] Albrecht, K. *Physics Letters B* **1975**, *56*, 127–129.

[201] Kostin, M. D. *The Journal of Chemical Physics* **1972**, *57*, 3589–3591.

[202] Katz, R.; Gossiaux, P. B. *Annals of Physics* **2016**, *368*, 267–295.

[203] Bialynicki-Birula, I.; Mycielski, J. *Annals of Physics* **1976**, *100*, 62–93.

[204] Bateman, H. *Physical Review* **1931**, *38*, 815–819.

[205] Diósi, L.; Halliwell, J. J. *Physical Review Letters* **1998**, *81*, 2846–2849.

[206] Hasse, R. W. *Journal of Mathematical Physics* **1975**, *16*, 2005–2011.

[207] Nassar, A. B. *Journal of Mathematical Physics* **1986**, *27*, 2949–2952.

[208] Nassar, A. B. *International Journal of Theoretical Physics* **2007**, *46*, 548–552.

[209] Chavanis, P.-H. *The European Physical Journal Plus* **2017**, *132*, 286.

[210] Bargueño, P.; Miret-Artés, S. *Annals of Physics* **2014**, *346*, 59–65.

[211] Schuch, D., *Quantum Theory from a Nonlinear Perspective*; Springer International Publishing: 2018.

[212] Ford, G. W.; Kac, M., et al. *Journal of Mathematical Physics* **1965**, *6*, 504–515.

[213] Vargas, A. F.; Morales-Durán, N., et al. *Annals of Physics* **2015**, *356*, 498–504.

[214] Garashchuk, S.; Dixit, V., et al. *The Journal of Chemical Physics* **2013**, *138*, 054107.

[215] Sanin, A. L.; Smirnovsky, A. A. *Materials physics and mechanics* **2014**, *34*, 98–105.

[216] Breuer, H.-P.; Petruccione, F., *The Theory of Open Quantum Systems*; Oxford University Press: 2007.

[217] Weiss, U., *Quantum Dissipative Systems*, 4th ed.; WORLD SCIENTIFIC: 2012.

[218] Messer, J. *Acta Physica Austriaca* **1978**, *50*, 75–91.

[219] Weiner, J. H.; Forman, R. E. *Physical Review B* **1974**, *10*, 325–337.

[220] Li, X. L.; Ford, G. W., et al. *Physical Review E* **1995**, *51*, 5169–5171.

[221] Ford, G. W.; Kac, M., et al. *Journal of Mathematical Physics* **1965**, *6*, 504–515.

[222] Senitzky, I. R. *Physical Review* **1961**, *124*, 642–648.

[223] Gardiner, C.; Zoller, P., *Quantum Noise: A Handbook of Markovian and Non-Markovian Quantum Stochastic Methods with Applications to Quantum Optics*; Springer Science & Business Media: 2004.

[224] Kan, K. .-.; Griffin, J. J. *Physics Letters B* **1974**, *50*, 241–243.

[225] Dekker, H. *Physics Reports* **1981**, *80*, 1–110.

[226] Immele, J. D.; Kan, K.-K., et al. *Nuclear Physics A* **1975**, *241*, 47–60.

[227] Zander, C.; Plastino, A. R., et al. *Annals of Physics* **2015**, *362*, 36–56.

[228] Goerlich, R.; Pires, L. B., et al. *Physical Review E* **2022**, *106*, 054617.

[229] Madelung, E., *Die Mathematischen Hilfsmittel des Physikers*; Springer-Verlag: 1950; 547 pp.

[230] Gisin, N. *Journal of Physics A: Mathematical and General* **1981**, *14*, 2259.

[231] Gisin, N. *Physica A: Statistical Mechanics and its Applications* **1982**, *111*, 364–370.

[232] Schuch, D.; Kaushal, R. S. *Journal of Physics: Conference Series* **2011**, *306*, 012032.

[233] Hillery, M.; Mlodinow, L. D. *Physical Review A* **1984**, *30*, 1860–1865.

[234] Klauder, J.; Skagerstam, B., *Coherent States*; WORLD SCIENTIFIC: 1985.

[235] Schrödinger, E. *Annalen der physik* **1926**, *385*, 437–490.

[236] Steiner, F. *Physica B+C* **1988**, *151*, 323–326.

[237] Heisenberg, W. *Zeitschrift für Physik* **1927**, *43*, 172–198.

[238] Glterra, F.; Loffeedo, M. I. *Lettere al Nuovo Cimento (1971-1985)* **1981**, *30*, 81–87.

[239] Crooks, G. E. *Physical Review E* **1999**, *60*, 2721–2726.

[240] Jarzynski, C. *Physical Review Letters* **1997**, *78*, 2690–2693.

[241] Seifert, U. *Physical Review Letters* **2005**, *95*, 040602.

[242] Seifert, U. *Reports on Progress in Physics* **2012**, *75*, 126001.

[249] Gokler, C. A Local Phase Space Stochastic Quantization? Pre-published.

[243] Nelson, E, *Quantum Fluctuations*; Princeton University Press: Prinston, 1984.

[244] Ciliberto, S. *Physical Review X* **2017**, *7*, 021051.

[245] Schnoering, G.; Rosales-Cabara, Y., et al. *Physical Review Applied* **2019**, *11*, 034023.

[246] Jones, P. H.; Maragò, O. M., et al., *Optical Tweezers: Principles and Applications*; Cambridge University Press: Cambridge, 2015.

[247] Raynal, D. Controlled Dynamics of a Levitated Nanoparticle in a Tailored Optical Potential, Ph.D. Thesis, Université Paris-Saclay, 2023.

[248] Siegman, A., *Lasers*; G - Reference,Information and Interdisciplinary Subjects Series; University Science Books: 1986.

Résumé de thèse

Introduction

Contexte

La frontière entre les systèmes classiques et quantiques a longtemps été un sujet d'intérêt pour les physiciens, offrant des perspectives profondes sur la nature fondamentale de la réalité physique. La mécanique classique, régie par des lois déterministes, comme les lois de Newton, a connu un grand succès dans la description des phénomènes macroscopiques, où les objets suivent des trajectoires prévisibles et bien définies.

Cependant, lorsque l'on étudie des systèmes impliquant un grand nombre de particules, tels que les gaz ou les liquides, l'approche déterministe de la mécanique classique devient inadéquate en raison du nombre extrêmement élevé de particules impliquées, de l'ordre du nombre d'Avogadro.

Par conséquent, les scientifiques ont développé de nouvelles approches pour modéliser ces types de systèmes, où la description n'est plus basée sur le mouvement d'une seule particule mais plutôt sur le comportement statistique d'un grand nombre de particules. Cela a conduit au développement de la physique statistique, qui intègre de l'incertitude dans la description des systèmes physiques. Le système est alors caractérisé par une distribution de probabilité qui donne les chances de trouver une particule dans un état particulier. En théorie, avec un ordinateur infiniment puissant, il serait possible de suivre le mouvement de chaque particule du système et d'obtenir une description déterministe. En pratique, cela n'est pas faisable, ce qui rend la description probabiliste fournie par la physique statistique la plus adaptée pour ces systèmes.

Au début de l'université, la physique statistique est généralement enseignée pour des systèmes à l'équilibre où la distribution de probabilité est stationnaire. Plus tard on explique aux étudiants que le monde n'est pas toujours à l'équilibre et que la distribution de probabilité peut changer au cours du temps. Cela introduit la physique statistique hors d'équilibre, où le but est de décrire le comportement des systèmes qui ne sont pas à l'équilibre. C'est un domaine de recherche très actif, cherchant à comprendre comment les systèmes évoluent dans le temps, comment ils atteignent l'équilibre et même comment contrôler ce processus. Ce domaine est généralement introduit dans le cadre de la physique stochastique, où l'évolution du système est décrite par un processus stochastique, incorporant le hasard. Par conséquent, une seule trajectoire ne suffit pas à décrire le système ; au lieu de cela, il faut considérer une distribution de trajectoires, qui donne la probabilité de trouver le système dans un état donné à un moment donné.

En parallèle à l'université, un autre cours important est la mécnique quantique, la théorie décrivant le comportement de la matière à des échelles microscopiques. Dans ce cours, les étudiants apprennent que la description des particules s'écarte du concept de trajectoires, car l'état d'une particule est entièrement décrit par un objet appelé la fonction d'onde.

Selon Copenhague, la fonction d'onde est un outil mathématique qui donne l'amplitude de probabilité de trouver une particule dans un état particulier (règle de Born). Ainsi, la mécanique quantique est intrinsèquement une théorie probabiliste, où le résultat d'une expérience n'est pas déterministe mais probabiliste.

Bien que le même terme *probabilité* soit utilisé à la fois en physique statistique et en mécanique quantique, l'interprétation est différente. En physique statistique, la probabilité provient de notre manque de connaissance sur l'état du système et sert d'outil pour simplifier la modélisation. En revanche, en mécanique quantique, la probabilité est intrinsèque à la nature des particules. Cette distinction est fondamentale pour les deux théories. La théorie quantique ne donne pas l'origine de cette probabilité ; elle est supposée être une propriété fondamentale des particules.

Malgré ces différences, il existe certaines similitudes dans la manière dont les probabilités sont traitées dans les deux contextes. Dans les deux cas, la probabilité est la solution d'une équation différentielle du premier ordre en temps, l'équation de diffusion en physique statistique et l'équation de Schrödinger en mécanique quantique. Pour une particule libre elles sont données par

$$\frac{\partial P}{\partial t} = D\nabla^2 P \qquad \text{et} \qquad \frac{\partial \psi}{\partial t} = i\frac{\hbar}{2m}\nabla^2\psi.$$

Cependant, une différence clé est qu'en mécanique quantique, le coefficient de diffusion[1] est imaginaire, tandis qu'en physique statistique, il est réel. Cette différence est fondamentale car, en mécanique quantique, la fonction d'onde représente l'amplitude de probabilité, et la probabilité réelle est le carré de cette fonction d'onde. Cette distinction conduit à des effets d'interférence en mécanique quantique, qui sont absents en physique statistique.

Cependant, il existe des formulations de la mécanique quantique qui offrent des interprétations alternatives des probabilités. Notamment, la mécanique bohmienne, développée par Louis de Broglie puis David Bohm, fournit une description déterministe de la mécanique quantique, mais au prix de la rendre non-locale dans l'espace. Cette formulation réintroduit le concept de trajectoires pour les particules quantiques, guidées par la fonction d'onde. Ces trajectoires obéissent à des équations de mouvement déterministes, avec la probabilité provenant de l'incertitude des conditions initiales du système. Les trajectoires des particules sont distribuées aléatoirement selon la distribution de probabilité donnée par le carré de la fonction d'onde. Cette perspective ressemble au point de vue newtonien, où les particules sont décrites par des trajectoires déterministes.

Il existe une autre formulation, similaire dans son concept à la mécanique bohmienne mais avec un ensemble différent d'axiomes, qui introduit la probabilité d'une autre manière. Il s'agit de la formulation nelsonienne, où les particules sont toujours décrites par des trajectoires, mais ces trajectoires sont stochastiques et non plus déterministe. Ici, les probabilités émergent non seulement en raison du manque de connaissance des conditions initiales, mais également de l'aléa intrinsèque des trajectoires elles-mêmes. Cependant, cette formulation ne fournit pas d'origine pour ces fluctuations ; elles sont simplement supposées exister. Nelson a suggéré que, de manière similaire à la description de Langevin du mouvement brownien, la théorie nelsonienne pourrait être une théorie effective d'une théorie sous-jacente plus profonde de la mécanique quantique.

Ces approches ne sont généralement pas les plus utilisées dans la recherche actuelle, car la formulation standard de la mécanique quantique est très efficace et fournit une excellente

---

[1] En réalité, le terme laplacien dans l'équation de Schrödinger est dispersif, car le coefficient de diffusion est imaginaire. Plutôt que d'amortir l'amplitude de la fonction d'onde, comme le ferait un coefficient réel, il induit au contraire une dispersion.

description des phénomènes physiques. Certains auteurs discutent de ces formulations alternatives d'un point de vue philosophique, mais comme elles sont équivalentes à la formulation standard, elles sont rarement appliquées en pratique. Cependant, bien que les questions ontologiques puissent être intéressantes à explorer, nous verrons tout au long de cette thèse que changer de point de vue peut conduire au développeent d' outils puissants pour les contrôle des systèmes quantiques, qui ne pourraient pas naturellement émerger de la formulation standard. La capacité à dériver de nouvelles techniques pour contrôler les systèmes quantiques ajouterait de la valeur à ces formulations alternatives de la mécanique quantique et offrirait des avantages pratiques. Il est clair que cela n'a pas pour but de remplacer la formulation standard, mais de la compléter et de fournir de nouvelles perspectives sur les systèmes quantiques.
Cette thèse explorera spécifiquement de tels développements potentiels en appliquant l'un de ces cadres alternatifs : le formalisme de Nelson.

Objectifs et défis

Le principal objectif de cette thèse est de développer de nouveaux outils pour comprendre, contrôler et manipuler les systèmes quantiques, à la fois pour la recherche fondamentale et les applications pratiques. Nous étudierons des méthodes d'optimisation pour les systèmes classiques et verrons comment elles peuvent être appliquées aux systèmes quantiques grâce à l'élaboration d'analogue classique - quantique, rendue possible par l'utilisation du formalisme nelsonien.

Les problématiques abordée dans cette thèse sont les suivantes :

- Comment est dérivée la mécanique de Nelson et en quoi diffère-t-elle de l'approche standard ?
- Comment sa proximité mathématique avec la physique stochastique peut-elle aider à établir une analogie quantique - classique ?
- Comment cette analogie permet-elle de transférer des méthodes d'optimisation classiques vers le domaine quantique ?
- Comment pouvons-nous étendre ces méthodes pour contrôler les systèmes quantiques ouverts ?

Un défi important de ce travail est de créer une connexion mathématique solide entre les systèmes classiques et quantiques, garantissant que les méthodes développées pour les systèmes classiques puissent être appliquées de manière efficace aux systèmes quantiques. Cela nécessite une compréhension approfondie à la fois de la mécanique classique et de la mécanique quantique, ainsi que des outils mathématiques utilisés pour les décrire.

Nous nous concentrerons principalement sur le contrôle de l'oscillateur harmonique quantique, un système simple et fondamental en mécanique quantique qui peut être facilement manipulé. Les méthodes d'optimisation que nous développerons seront particulièrement utiles pour contrôler de tels systèmes. Nous allons considérer des protocoles sur les paramètres du potentiel harmonique, en particulier sur la raideur du potentiel, afin d'atteindre un état cible plus rapidement que les processus adiabatiques tout en minimisant un certain coût, donné par une fonctioin de coût. L'efficacité de nos méthodes sera démontrée en les comparant à d'autres techniques de contrôle pour différentes

fonctions de coût, illustrant la versatilité et l'efficacité de notre approche. À notre connaissance, aucune autre technique n'a prouvé son optimalité pour une fonction de coût générale.
Le contrôle de la dynamique des systèmes quantiques ouvre de nombreuses applications pratiques. Par exemple, il peut améliorer les performances des ordinateurs quantiques, augmenter l'efficacité des capteurs quantiques et contribuer au développement de nouvelles technologies quantiques. Un tel contrôle est essentiel pour le progrès des technologies quantiques, et les méthodes introduites dans cette thèse pourraient servir d'outils précieux pour atteindre cet objectif.

La dernière étape de ce travail sera d'étendre ces méthodes de contrôle aux systèmes quantiques ouverts, une tâche difficile en raison de leur complexité par rapport aux systèmes fermés. Ces méthodes pourraient poser les bases de nouvelles façons de contrôler les systèmes quantiques ouverts, avec des implications pour une variété d'applications, des machines thermiques au traitement de l'information quantique. À mesure que la technologie avance et que des dispositifs tels que les puces nano-processeurs et les nano-machines thermiques se miniaturisent, la compréhension des relations thermodynamiques à l'échelle microscopique—telles que la dissipation de chaleur et l'efficacité du travail—devient cruciale en raison des effets quantiques. Les machines thermiques quantiques, qui convertissent l'énergie thermique en travail à l'aide de systèmes quantiques tels que des particules uniques ou des qubits, jouent un rôle important en thermodynamique quantique et en nanotechnologie. Une question ouverte clé est de savoir si les effets quantiques peuvent améliorer les performances des machines thermiques, et le développement de nouveaux protocoles de contrôle pour les systèmes quantiques ouverts pourrait fournir des premières pistes de réponse à ce problème.

Structure du Manuscrit

Le manuscrit est structuré en deux parties. La partie 1 fournit les fondements théoriques en présentant les théories de Langevin et de Nelson, qui sont centrales pour comprendre la dynamique des particules classiques et quantiques, respectivement. Dans la partie 2, on applique ensuite ces théories à l'étude des systèmes quantiques dans divers contextes, couvrant à la fois les questions fondamentales et les applications pratiques.

La première partie est organisée en deux chapitres. Dans le chapitre 1, nous introduisons le mouvement brownien classique, en commençant par son contexte historique, de Brown à Einstein et Langevin. Nous développons ensuite le cadre mathématique nécessaire, en nous concentrant sur les équations de Langevin et de Fokker-Planck, qui décrivent la dynamique stochastique des particules. Une analyse détaillée du régime de sur-amortissement du mouvement brownien et du rôle des processus de Wiener, qui sont essentiels dans le calcul stochastique, prépare le terrain pour explorer les analogues quantiques dans la seconde partie.
Dans le chapitre 2, nous nous tournons vers la mécanique quantique et introduisons le formalisme stochastique de Nelson, qui décrit les particules quantiques en termes de trajectoires stochastiques. Nous dérivons le formalisme utilisé pour décrire les systèmes quantiques dans le cadre de Nelson, en soulignant les similarités et les différences avec la formulation standard de la mécanique quantique. Des exemples de systèmes quantiques décrits par le formalisme de Nelson sont ensuite étudiés, démontrant ses avantages, en particulier dans la description des phénomènes de *tunneling*, où il offre une définition naturelle du le temps nécessaire pour qu'une particule traverse une barrière de potentielle.

Une fois ces outils théorique établis, la partie 2, composée de trois chapitres, vise à appliquer la théorie de Nelson sous deux perspectives : une perspective fondamentale et une perspective pratique.

Le troisième chapitre explore l'une des hypothèses fondamentales de la mécanique quantique : la règle de Born. Nous montrons que cette hypothèse n'est pas nécessaire dans le formalisme de Nelson, où la densité de probabilité n'est pas nécessairement liée au carré du module de la fonction d'onde. Nous introduisons ensuite le concept d'équilibre quantique, un état où la règle de Born est satisfaite, et démontrons que si un système n'est initialement pas à l'équilibre quantique, il finira par y parvenir au cours du temps. Nous étudions la convergence d'un système quantique vers l'équilibre quantique et calculons le temps nécessaire pour atteindre cet état pour trois systèmes quantiques différents, en le comparant aux temps caractéristiques de chaque système. L'objectif est d'estimer l'ordre de grandeur du temps de convergence afin de déterminer s'il serait possible d'observer ce processus expérimentalement, en supposant un état initial hors équilibre.

Suite à cette discussion théorique, le chapitre 4 se concentre sur les applications pratiques. En mettant en avant les similarités mathématiques entre l'équation de Nelson et l'équation de Langevin en régime sur-amorti, nous démontrons que le formalisme de Nelson peut être utilisé pour développer une nouvelle technique de contrôle des systèmes quantiques, en exploitant les analogues classiques du système quantique. Plus précisément, cette technique permet de faire passer efficacement un système quantique d'un état stationnaire initial à un état final en moins de temps qu'un processus adiabatique (quasi-statique). Nous appliquons cette méthode pour contrôler la raideur d'un potentiel harmonique et dérivons le protocole optimal pour atteindre une raideur cible, en minimisant à la fois la durée du processus et une fonction de coût arbitraire, qui est maintenue générale dans la dérivation. Nous appliquons ensuite la méthode pour deux fonctions de coût : l'énergie cumulée lors de l'évolution du système, et l'évolution de la phase dynamique de la fonction d'onde au cours du protocole. Enfin, nous comparons nos protocoles à ceux dérivés d'autres techniques pour démontrer l'efficacité de notre approche.

Finalement, dans le cinquième et dernier chapitre, nous explorons l'extension du formalisme de Nelson aux systèmes quantiques ouverts. Notre objectif est d'appliquer les techniques du chapitre précédent pour contrôler les systèmes quantiques ouverts, dans le but de créer des cycles optimaux pour des machines thermiques quantiques. Pour ce faire, nous examinons trois théories effectives différentes des systèmes quantiques ouverts et en dérivons les équations de Nelson correspondantes. Bien qu'aucun résultat final ne soit présenté, nous démontrons que ces approches sont prometteuses et pourraient potentiellement être utilisées pour le contrôle des systèmes quantiques ouverts.

Nous concluons la thèse en résumant les principaux résultats et en discutant des pistes de recherche futures potentielles dans ce domaine.

A Mouvement brownien et équation de Langevin

Ce chapitre a été consacré à l'étude du mouvement brownien, un phénomène stochastique qui a été étudié en détail par Einstein et Langevin au début du XX$^{\text{e}}$ siècle. Nous avons commencé par une introduction historique au mouvement brownien, en expliquant comment Brown a découvert ce phénomène en observant des grains de pollen dans l'eau. Nous avons ensuite discuté des contributions d'Einstein et de Langevin, qui ont fourni une explication théorique du mouvement brownien en introduisant des équations décrivant la dynamique stochastique des particules et leur probabilité de présence, connues sous le nom d'équations de Langevin et de Fokker-Planck.

Le mouvement brownien est un phénomène stochastique découvert par Robert Brown en 1827. Brown, un botaniste écossais, a observé des grains de pollen dans l'eau et a noté qu'ils se déplaçaient de manière aléatoire. Il a observé que les grains de pollen se déplaçaient de manière erratique, changeant de direction de manière imprévisible. Ce mouvement aléatoire a été attribué à l'agitation thermique des molécules d'eau, qui entraîne des collisions aléatoires avec les grains de pollen. Brown a observé que les grains de pollen étaient constamment en mouvement, même s'ils étaient initialement immobiles. Ce mouvement aléatoire a été nommé mouvement brownien en l'honneur de Brown, qui a été le premier à l'observer.

La physique stochastique a été développée pour expliquer le mouvement brownien, en utilisant des équations qui décrivent la dynamique des particules en mouvement. Ces équations, connues sous le nom d'équations de Langevin et de Fokker-Planck, décrivent l'évolution temporelle de la densité de probabilité des particules.

A.1 Description d'Einstein

Einstein a proposé un modèle mathématique pour le mouvement brownien, sans donner une explication directe des observations de Brown. Il a envisagé un ensemble de particules en suspension dans un liquide, soumis à un mouvement irrégulier à cause des collisions avec les molécules du liquide. Il a utilisé une approche probabiliste pour décrire ce phénomène et répondre à deux questions : « jusqu'où une particule brownienne peut-elle se déplacer dans un temps donné ? » et « comment ce mouvement est-il lié à d'autres quantités physiques ? » Son modèle vise à prouver l'existence des atomes et molécules, en reliant les paramètres théoriques à des grandeurs mesurables.

Einstein a démontré que la densité de probabilité $p(x, t)$ de trouver une particule à une position x à un instant t satisfait une équation de diffusion :

$$\partial_t P(x,t) = D\partial_x^2 P(x,t)$$

où D est le coefficient de diffusion. Si toutes les particules sont initialement à x_0, la solution de cette équation est une distribution gaussienne :

$$P(x,t) = \frac{1}{\sqrt{2\pi\sigma^2(t)}} \exp\left(-\frac{(x-x_0)^2}{2\sigma^2(t)}\right)$$

avec une variance $\sigma^2 = 2Dt$, qui montre que les particules se dispersent de manière linéaire dans le temps. Ce résultat relie le mouvement brownien et la diffusion.

Einstein a également cherché à relier le mouvement brownien à des quantités physiques comme la température T, la viscosité η, la masse m et le rayon a des particules. En introduisant le coefficient de friction $\gamma = 6\pi\eta a$, il a établi la relation d'Einstein :

$$D = \frac{k_\mathrm{B}T}{M\gamma} = \frac{RT}{6\pi\eta a\mathcal{N}_\mathrm{a}}$$

où R est la constante des gaz parfaits et $\mathcal{N}_\mathrm{a}$ le nombre d'Avogadro. Cette relation relie les fluctuations dues au mouvement brownien et les forces de friction qui freinent ce mouvement. Elle permet de mesurer des grandeurs comme le nombre d'Avogadro et de mieux comprendre le mouvement erratique des particules browniennes.

A.2 Description de Langevin

En 1908, Paul Langevin a proposé un modèle du mouvement brownien basé sur la dynamique des particules macroscopiques. Les interactions avec les particules du fluide étant microscopiques et nombreuses avant un déplacement visible de la particule brownienne, une approche probabiliste est nécessaire.

Pour modéliser le mouvement d'une particule brownienne (PB) dans un fluide, on suppose que ses degrés de liberté changent lentement comparés aux mouvements rapides des particules du fluide. La force exercée sur la PB est la moyenne des collisions entre la PB et les particules du fluide, un processus appelé *coarse-graining*, qui permet une description simplifiée. Ce lissage temporel se fait sur un intervalle de temps, noté τ_{Bath}, qui doit être suffisamment long pour moyenner les mouvements rapides tout en respectant la dynamique de la PB. Les principales échelles de temps sont :

- τ_{s} : temps des collisions entre les particules du fluide et la PB,
- τ_{B} : temps de relaxation de la vitesse de la PB (inverse du coefficient de friction γ),
- $\tau_{\text{Bath}}^{\text{E}}$: temps utilisé pour décrire uniquement la position (approche d'Einstein),
- $\tau_{\text{Bath}}^{\text{L}}$: temps utilisé pour décrire la position et la vitesse (approche de Langevin).

En pratique, on a $\tau_{\text{s}} \ll \tau_{\text{Bath}}^{\text{L}} \ll \tau_{\text{B}} \ll \tau_{\text{Bath}}^{\text{E}}$. Le choix de τ_{Bath} détermine si l'on modélise uniquement la position (Einstein) ou la position et la vitesse (Langevin).

L'équation de Langevin décrit le mouvement d'une PB en prenant en compte trois forces principales :

- Une force externe $F(x,t)$,
- Une force de friction $-M\gamma v$, proportionnelle à la vitesse et opposée au mouvement,
- Une force aléatoire $F_{\text{L}}(t)$, due aux collisions entre la PB et le fluide.

L'équation de Langevin s'écrit alors :

$$\begin{cases} M\dot{v}(t) = F(x(t),t) - M\gamma v(t) + F_{\text{L}}(t), \\ \quad \dot{x}(t) = v(t), \end{cases}$$

où $\dot{v}(t)$ et $\dot{x}(t)$ représentent les dérivées temporelles de la vitesse et de la position. Les solutions de cette équation sont des processus stochastiques : chaque simulation du mouvement donne un résultat différent. On étudie donc des valeurs moyennes telles que la position et la vitesse moyennes, ou encore le déplacement quadratique moyen.

La force de Langevin $F_{\text{L}}(t)$ suit certaines propriétés statistiques :

- Gaussienneté : la distribution de probabilité de $F_{\text{L}}(t)$ est gaussienne,
- Moyenne nulle : $\langle F_{\text{L}}(t)\rangle = 0$,
- Stationnarité : l'autocorrélation de $F_{\text{L}}(t)$ dépend uniquement de la différence de temps entre deux instants:

  $$\left\langle F_{\text{L}}(t)F_{\text{L}}(t')\right\rangle = 2D\delta(t-t')$$

  où D est l'intensité de la force, et $\delta(t-t')$ est une fonction delta de Dirac, indiquant que la force est non corrélée dans le temps, un processus appelé « bruit blanc ». Si une corrélation temporelle existe, on parle alors de « bruit coloré ».

Nous avons ensuite discuté des propriétés du mouvement brownien dans le cas particulier de la particule libre. En particulier, nous avons étudié le déplacement quadratique moyen (MSD) $\left\langle x^2(t)\right\rangle$ de la particule, qui est une mesure de la distance moyenne parcourue par la particule au carré. Pour une particule libre, le MSD croît linéairement avec le temps, avec une pente donnée par le coefficient de diffusion D :

$$\left\langle x^2(t)\right\rangle = 2Dt.$$

A.3 Régime de sur-amortissement

Nous avons étudié le régime de sur-amortissement, où la force de friction domine le mouvement de la particule. Dans ce régime, l'équation de Langevin se simplifie en une équation de Langevin sur-amortie sur la position de la particule,

$$\dot{x}(t) = \frac{F(x(t),t)}{M\gamma} + F_{\mathrm{E}}(t),$$

où $F_{\mathrm{E}}(t)$ est un bruit blanc gaussien d'intensité $D_{\mathrm{E}} = k_{\mathrm{B}}T/M\gamma$. Cette équation va être fondamental pour le reste de la thèse car c'est l'équation qui servira de base pour le formalisme de Nelson, et le développement des analogues classiques - quantiques.
Pour conclure, nous avons donné l'équation que satisfait la densité de probabilité $P(x,t)$ dans le régime de sur-amortissement, l'équation de Fokker-Planck :

$$\partial_t P(x,t) = -\partial_x \left[\frac{F(x,t)}{M\gamma} P(x,t)\right] + D_{\mathrm{E}}\partial_x^2 P(x,t).$$

A.4 Conclusion

Dans ce chapitre, nous avons exploré le mouvement brownien depuis ses origines historiques jusqu'aux modèles mathématiques qui le décrivent. Ce phénomène joue un rôle fondamental dans plusieurs disciplines scientifiques, telles que la physique, la chimie, la biologie et même la finance.
Nous avons ensuite exploré le concept de régime sur-amorti, où l'inertie de la particule devient négligeable. Cela conduit à l'équation de Langevin sur-amortie, qui se concentre uniquement sur la position de la particule, se rapprochant de l'approche d'Einstein. Enfin, nous avons introduit l'équation de Fokker-Planck, décrivant l'évolution de la densité de probabilité de la position et de la vitesse de la particule. Dans le régime sur-amorti, cette équation se réduit à l'équation de Smoluchowski, simplifiant encore la description du système.
Dans le chapitre suivant, nous étendons ce formalisme mathématique pour décrire les systèmes quantiques, en explorant des modifications permettant de rendre le formalisme réversible dans le temps, contrairement à la nature irréversible du mouvement brownien classique.

B FORMULATION STOCHASTIQUE DE LA MÉCANIQUE QUANTIQUE

Dans ce chapitre, nous présentons le formalisme de Nelson en mécanique quantique, qui propose une approche stochastique pour décrire les systèmes quantiques à l'aide de processus stochastiques réversibles dans le temps. Nous commençons par discuter des défis liés à l'application des méthodes stochastiques aux systèmes quantiques fermés, puis introduisons la notion de processus stochastiques réversibles, menant à la mécanique stochastique de Nelson.
Nous définissons ensuite les processus directs et inverses ainsi que leurs dérivées associées, posant ainsi les bases d'une description stochastique réversible dans le temps. Puis, nous introduisons une loi d'accélération dans l'espace des configurations, analogue à la seconde loi de Newton, intégrant la dynamique dans ce cadre stochastique.
En appliquant ces concepts aux systèmes quantiques, nous dérivons l'équation de Schrödinger à partir de cette loi d'accélération et établissons le lien avec la mécanique quantique standard. Ensuite, nous abordons les méthodes numériques pour résoudre l'équation de

Nelson, en nous concentrant sur la méthode d'Helfand-Greenside de second ordre et en détaillant la méthodologie de calcul.

Nous illustrons l'application du formalisme de Nelson avec des exemples numériques, notamment une gaussienne libre et une particule face à une barrière de potentiel, montrant ainsi que cette approche permet de reproduire des phénomènes quantiques clés tels que l'effet tunnel et le principe d'incertitude de Heisenberg.

Enfin, nous résumons les points essentiels et discutons des implications du formalisme de Nelson en mécanique quantique.

B.1 Equation de Nelson

Comme de Broglie, Nelson supposait qu'il est possible de définir des trajectoires pour les particules quantiques, bien que celles-ci soient cachées à l'observateur. La fonction d'onde seule n'est donc pas suffisante pour décrire complètement le système quantique. La particule quantique suit un mouvement aléatoire, dont l'origine n'est pas débattue ici, car cette approche stochastique est utilisée comme un outil mathématique pour contrôler les systèmes quantiques.

Il a postulé que l'équation de mouvement est donnée par une équation de Langevin sur-amortie,

$$\mathrm{d}x(t) = b(x(t), t)\mathrm{d}t + \mathrm{d}W(t),$$

que l'on appelle l'équation de Nelson. Ici, b peut être vu comme la vitesse moyenne du processus et W est un processus de Wiener, le terme responsable du caractère stochastique des trajectoires. Dans ce chapitre, on a dérivé l'expression de la vitesse moyenne comme étant

$$b(x,t) = \frac{\hbar}{2m}\partial_x S(x,t) + D_{\mathrm{Q}}\partial_x \ln P(x,t)$$

avec S est la phase de la fonction d'onde et P la densité de probabilité. Le terme D_{Q} est le coefficient de diffusion associé au processus de Wiener. Pour déterminer l'amplitude du processus de Wiener W, on suppose que le coefficient de diffusion D_{Q} est inversement proportionnel à la masse m de la particule, ce qui donne :

$$D_{\mathrm{Q}} = \frac{\hbar}{2m},$$

où $\hbar$ est la constante de Planck réduite. Les propriétés statistiques de W sont alors :

$$\langle \mathrm{d}W(t)\rangle = 0 \quad \text{et} \quad \langle \mathrm{d}W(t)\mathrm{d}W(t+\mathrm{d}t)\rangle = 2D_{\mathrm{Q}}\mathrm{d}t.$$

La principale différence entre la mécanique stochastique classique et celle de Nelson est que le terme déterministe b n'est pas imposé par une force extérieure, mais est une quantité intrinsèque du modèle, similaire à l'approche de de Broglie-Bohm.

B.2 Equation de Schrödinger

Nous avons discuté des conditions nécessaires pour obtenir un processus dont la densité de probabilité P satisfait à la fois les équations de Fokker-Planck directe et inverse dans le temps. Si on suppose qu'une force externe $F(x,t)$ dérivée d'un potentiel $V(x,t)$ agit sur le système, et que le champs de vitesse $v(x,t)$ est le fradient de la phase $S(x,t)$ *i.e.*

$$v(x,t) = \frac{\hbar}{m}\partial_x S(x,t),$$

on a pu obtenir l'équation de Hamilton-Jacobi quantique :

$$\hbar\partial_t S(x,t) + \frac{\hbar^2}{2m}(\partial_x S(x,t))^2 + V(x,t) + V_{\mathrm{Q}}(x,t) = 0,$$

où le potentiel quantique V_{Q} est défini par :

$$V_{\mathrm{Q}}(x,t) = -\frac{\hbar^2}{2m}\frac{\partial_x^2\sqrt{P(x,t)}}{\sqrt{P(x,t)}}.$$

Ce potentiel, introduit dans la formulation de de Broglie-Bohm, est responsable des effets quantiques comme les interférences. Lorsque $\hbar \to 0$, ce terme disparaît, et l'équation de Hamilton-Jacobi quantique se réduit à son équivalent classique.

À partir de l'équation de continuité et de l'équation de Hamilton-Jacobi quantique, on peut dériver l'équation de Schrödinger. En combinant la fonction S et la densité de probabilité P sous la forme d'une fonction complexe, la fonction d'onde du système,

$$\psi(x,t) = \sqrt{P(x,t)}\mathrm{e}^{iS(x,t)},$$

on peut montrer que l'équation de Schrödinger

$$i\hbar\partial_t\psi(x,t) = -\frac{\hbar^2}{2m}\partial_x^2\psi(x,t) + V(x,t)\psi(x,t)$$

est satisfaite par cette fonction. Dans la théorie de Nelson, l'équation de Schrödinger découle naturellement, contrairement à l'approche de de Broglie-Bohm où elle est postulée.

Enfin, pour décrire un système quantique avec l'approche de Nelson, il faut résoudre plusieurs fois l'équation de Nelson avec des conditions initiales différentes afin d'obtenir assez de statistiques pour déterminer les propriétés du système. Cela nécessite des méthodes numériques efficaces pour résoudre l'équation de Nelson, comme la méthode d'Helfand-Greenside de second ordre, qui est une méthode de type Runge-Kutta mais généralisée au cas des équations stochastiques.

Le chapitre s'est conclu sur des exemples numériques illustrant l'application du formalisme de Nelson à des systèmes quantiques simples, montrant que cette approche permet de reproduire des phénomènes quantiques clés tels que l'effet tunnel et le principe d'incertitude de Heisenberg.

B.3 Conclusion

Ce chapitre a clos la première partie de la thèse, portant sur les fondements théoriques de la mécanique stochastique. Nous avons introduit le formalisme de Nelson, qui fournit une approche stochastique pour décrire les systèmes quantiques à l'aide de processus stochastiques réversibles dans le temps. Nous avons dérivé l'équation de Nelson, qui décrit le mouvement stochastique des particules quantiques, et montré comment l'équation de Schrödinger peut être obtenue à partir de cette équation. Nous avons également discuté des méthodes numériques pour résoudre l'équation de Nelson et illustré l'application de ce formalisme à des exemples numériques. Ce chapitre a posé les bases pour la deuxième partie de la thèse, qui explore l'application de la mécanique stochastique à la description et au contrôle des systèmes quantiques.

C CONVERGENCE À L'ÉQUILIBRE QUANTIQUE

Dans ce chapitre, nous explorons la relaxation vers l'équilibre quantique dans le cadre de la quantification stochastique de Nelson, en nous concentrant sur l'émergence de la règle de Born en mécanique quantique. En simulant numériquement la dynamique de systèmes quantiques initialisés dans des états hors équilibre, qui violent la règle de Born, nous étudions la convergence vers l'équilibre quantique pour trois systèmes canoniques : l'expérience des doubles fentes, l'oscillateur harmonique et les particules quantiques dans un champ gravitationnel. Nos résultats montrent que, dans les cas de l'expérience des doubles fentes et de l'oscillateur harmonique, la relaxation vers l'équilibre quantique se produit plus rapidement que l'apparition des schémas d'interférence quantique, suggérant que les phénomènes quantiques observables sont des phénomènes d'équilibre. Cependant, pour les particules quantiques dans un champ gravitationnel, nous observons que l'interférence quantique peut apparaître avant que le système n'atteigne l'équilibre quantique, ouvrant la possibilité d'observer des écarts par rapport à la règle de Born dans ces systèmes.

C.1 Equilibre quantique

Dans la formulation standard de la mécanique quantique (MQ), la règle de Born est un postulat essentiel : la densité de probabilité de trouver une particule à une position x à un instant t est donnée par le carré du module de la fonction d'onde $|\psi(x,t)|^2$. Cependant, ce postulat n'est pas nécessaire dans les formalismes de Nelson et Bohm-de Broglie, où la fonction d'onde est considérée comme un champ qui guide la dynamique des particules, sans être nécessairement liée à la probabilité de trouver une particule dans une certaine région de l'espace. Dans ces approches, il est donc parfaitement cohérent d'envisager des situations où $P(x,t) \neq |\psi(x,t)|^2$, ce qui conduirait à des prédictions différentes de celles de la MQ standard.

Comme suggéré par Valentini, la règle de Born pourrait correspondre à une situation d'« équilibre quantique », analogue à l'équilibre thermique en mécanique classique. Selon cette hypothèse, des états hors équilibre, avec $P(x,t) \neq |\psi(x,t)|^2$, peuvent exister, mais ils se relaxeraient vers l'équilibre quantique sur une très courte échelle de temps, rendant ces états difficiles à observer. Valentini a développé ces idées dans le cadre de la mécanique Bohm-de Broglie, qui, étant déterministe, nécessite une forme de *coarse graining* pour observer cette relaxation. Cependant, dans la théorie de Nelson, la relaxation vers l'équilibre devrait se produire plus naturellement, grâce à la nature stochastique du mouvement.

L'objectif de ce travail est d'étudier, par des simulations numériques, si la thermalisation quantique se produit plus rapidement que les effets quantiques typiques, tels que les interférences. Pour cela, il est nécessaire de reconstruire la densité de probabilité $P(x,t)$ des particules à chaque instant. Cela se fait en divisant l'espace $x \in \mathbb{R}$ en intervalles de taille Δx, puis en construisant l'histogramme correspondant. L'équation stochastique de Nelson est résolue en utilisant une méthode de Helfand-Greenside de second ordre. Pour réduire le bruit statistique, les simulations sont répétées plusieurs fois indépendamment et les résultats sont moyennés pour reconstruire la densité de probabilité.

Il est ensuite nécessaire de comparer la densité de probabilité $P(x,t)$ avec le carré du module de la fonction d'onde $|\psi(x,t)|^2 = R^2$. Pour ce faire, on peut définir une distance entre ces deux quantités, comme la distance L_p entre deux fonctions f et g, définie par :

$$L_p[f,g]\,(t) = \sqrt[p]{\int_{-\infty}^{+\infty} \mathrm{d}x\ |f(x,t) - g(x,t)|^p}.$$

En particulier, la distance L_1 a été proposée par Petroni et Guerra comme un outil approprié pour quantifier la relaxation vers l'équilibre quantique. La distance infinie L_∞, qui est la limite lorsque $p \to \infty$, est donnée par :

$$L_\infty[f,g](t) = \max_x |f(x,t) - g(x,t)|.$$

Une autre mesure possible est une fonction de type entropie, utilisée par Valentini, définie par :

$$H \equiv L_H[f,g]\,(t) = \int_{-\infty}^{+\infty} \mathrm{d}x\ f(x,t) \ln\left(\frac{f(x,t)}{g(x,t)}\right),$$

qui est liée à la divergence de Kullback-Leibler, aussi appelée entropie relative.
En prenant $f = P$ et $g = |\psi(x,t)|^2$, ces distances s'annulent lorsque la règle de Born est satisfaite, *i.e.* à l'équilibre quantique. Pour estimer le temps de relaxation, il sera nécessaire de définir un seuil arbitraire en dessous duquel la distance est considérée comme pratiquement nulle.
Enfin, en utilisant la quantité entropique, Hatifi et al. ont pu prouver un théorème H qui assure qu'une distribution de probabilité générique $P(x,t)$ converge vers $|\psi(x,t)|^2$ lorsque $t \to \infty$ (avec certaines réserves, comme le montrera la section suivante).

C.2 Résultats numériques

Dans cette section, nous examinons la question centrale de savoir si la thermalisation quantique se produit plus rapidement que les autres effets quantiques typiques, comme l'apparition des interférences. Si c'était le cas, cela signifierait que tous les phénomènes quantiques sont des phénomènes d'équilibre, donc indiscernables de ceux prédits par la mécanique quantique (MQ) standard. Dans le cas contraire, on pourrait espérer observer des anomalies dans les motifs d'interférence dues à des corrections sous-quantiques, ce qui constituerait une prédiction intéressante pour de futures expériences.
Nous utilisons les distances fonctionnelles définies dans la section précédente pour estimer le temps de relaxation vers l'équilibre quantique, et le comparons avec le temps d'apparition des effets quantiques pour trois systèmes physiques emblématiques : l'expérience des doubles fentes, l'oscillateur harmonique et l'évolution d'un paquet d'ondes dans un potentiel linéaire représentant le champ gravitationnel terrestre.

C.2.1 Expérience des doubles fentes

Nous considérons une expérience classique des doubles fentes, où les deux fentes ont une ouverture de largeur σ et sont séparées par une distance $2a$. Les unités sont choisies de manière à ce que $\hbar = m = a = 1$, et σ représente donc le rapport σ/a. Cela définit une échelle de temps $\tau = ma^2/\hbar$ (qui vaut 1 dans ces unités).
Pour modéliser cette configuration, nous utilisons une fonction d'onde initiale constituée de deux Gaussiennes centrées sur $x = \pm a$, avec une largeur σ. L'évolution libre de cette fonction d'onde peut être calculée analytiquement, tandis que la densité de particules P est obtenue numériquement en résolvant l'équation stochastique de Nelson pour un

grand nombre de trajectoires. Les distances fonctionnelles entre P et $|\psi|^2$ sont ensuite calculées et tracées en fonction du temps.
Les résultats montrent que, quelle que soit la largeur initiale σ, la relaxation vers l'équilibre quantique se produit toujours avant l'apparition des interférences quantiques. Cela signifie que les phénomènes quantiques observés sont des phénomènes d'équilibre.

C.2.2 Oscillateur harmonique

Nous étudions ici l'oscillateur harmonique, un système fondamental en MQ, en nous concentrant sur la convergence vers l'équilibre quantique. L'oscillateur harmonique est décrit par une fonction d'onde gaussienne oscillante, et la relaxation est étudiée en suivant l'évolution de la largeur $\sigma(t)$ de la fonction d'onde.
Les résultats montrent que le temps de relaxation τ_{q} est toujours inférieur à la période d'oscillation de l'oscillateur harmonique. Cela implique que la relaxation vers l'équilibre quantique se produit avant que les oscillations quantiques ne soient pleinement observables.

C.2.3 Champ gravitationnel uniforme

Enfin, nous considérons une particule quantique tombant dans le champ gravitationnel de la Terre, un problème motivé par des expériences récentes sur les neutrons ultrafroids. On suppose que la particule est initialement à une hauteur h au-dessus d'un miroir réfléchissant, et que les particules sont distribuées selon une fonction delta de Dirac à la même hauteur. Les particules tombent ensuite sous l'effet de la gravité, et la densité de probabilité P est reconstruite à chaque instant.
La fonction d'onde initiale est une gaussienne centrée à une hauteur h au-dessus d'un miroir réfléchissant, et de largeur ζ, tel que

$$\psi(x,0) = \Theta(x)\frac{1}{(2\pi\zeta^2)^{\frac{1}{4}}} \exp\left[-\frac{(x-h)^2}{4\zeta^2}\right].$$

Elle est calculée à chaque instant postérieurs en la décomposant sur la base des fonctions de Airy ξ_n,

$$\psi(x,t) = \sum_{n=0} c_n \chi_n(x) \mathrm{e}^{-iE_n t},$$

les coefficients de la décomposition étant connues sous une certine approximation.

$$c_n = \frac{(8\pi\zeta^2)^{\frac{1}{4}}}{\mathrm{Ai}'(-E_n)} \mathrm{Ai}\big(h - E_n + \zeta^4\big) \exp\left\{\zeta^2\left(h - E_n + \frac{2}{3}\zeta^4\right)\right\}.$$

Les résultats des simulations montrent un comportement particulier de la relaxation. Après une phase initiale de convergence, les distances entre P et $|\psi|^2$ augmentent temporairement lorsque des motifs d'interférences apparaissent dans la fonction d'onde. Ce phénomène suggère que, dans ce système, les interférences quantiques peuvent apparaître avant que la relaxation vers l'équilibre quantique soit complète. Ce résultat contraste avec les observations faites pour les deux autres systèmes. S'il est possible de créer des situations où un système quantique est être hors équilibre quantique (par exemple, on peut le suppose lors des premiers instant de la création d'une particule) cela pourrait ouvrir la voie à des vérifications expérimentales de la règle de Born dans des états quantiques gravitationnels.

En conclusion, ces simulations montrent que, dans certains systèmes, les phénomènes d'interférences quantiques peuvent se produire avant la relaxation complète vers l'équilibre quantique, offrant ainsi des perspectives intéressantes pour de futures études expérimentales.

D ANALOGUES CLASSIQUES - QUANTIQUES

Dans ce chapitre, nous proposons une méthode pour optimiser la dynamique d'un oscillateur harmonique quantique en utilisant une analogie quantique-classique basée sur la formulation stochastique de Nelson en mécanique quantique. Notre objectif est de faire passer le système d'un état stationnaire initial à un état stationnaire final en un temps minimal, tout en réduisant un certain coût. En établissant une analogie entre l'oscillateur harmonique quantique et la dynamique classique suramortie d'une particule brownienne dans un potentiel harmonique, nous appliquons un principe variationnel pour dériver des protocoles optimaux pour le paramètre de contrôle, qui est la raideur du potentiel.
Nous considérons deux fonctions de coût : l'énergie cumulée dans le temps et la phase dynamique de la fonction d'onde. Cette dernière nous permet de concevoir des protocoles optimaux du point de vue adiabatique, minimisant les écarts par rapport à un processus adiabatique pour une durée donnée. Nos résultats numériques montrent que les protocoles optimaux proposés surpassent les méthodes existantes, offrant ainsi des raccourcis efficaces vers l'adiabaticité dans des systèmes quantiques fermés.

D.1 Analogie quantique-classique

Une particule unidimensionnelle de masse m piégée dans un potentiel harmonique dépendant du temps obéit à l'équation de Schrödinger :

$$i\hbar\frac{\partial}{\partial t}\psi(x,t) = \hat{H}(t)\psi(x,t) = \left(-\frac{\hbar^2}{2m}\frac{\partial^2}{\partial x^2} + \frac{1}{2}\kappa(t)x^2\right)\psi(x,t),$$

où $\hbar$ est la constante de Planck, $\kappa(t)$ la raideur du potentiel harmonique en fonction du temps, et $\psi(x,t)$ la fonction d'onde du système à l'instant t et à la position x. Le but de cette étude est de concevoir un protocole $\kappa(t)$ qui permet de faire évoluer le système d'un état stationnaire initial $\psi_\mathrm{i}(x)$ à un état stationnaire final $\psi_\mathrm{f}(x)$ en un temps minimal tout en minimisant une fonction de coût donnée.
La dérivation des protocoles optimaux repose sur la formulation stochastique de la mécanique quantique de Nelson. Contrairement aux trajectoires déterministes en mécanique de Bohm-de Broglie, la théorie de Nelson postule que chaque trajectoire suit l'équation différentielle stochastique suivante :

$$\mathrm{d}x(t) = b(x(t),t)\mathrm{d}t + \sqrt{2D}\,\mathrm{d}W(t),$$

où $b(x,t)$ est la vitesse de dérive déterministe, $D = \hbar/2m$ est le coefficient de diffusion, et $\mathrm{d}W(t)$ est une variation de Wiener caractéristique d'un processus de Markov : $\langle \mathrm{d}W(t)\rangle = 0$, $\langle \mathrm{d}W(t)\mathrm{d}W(t')\rangle = \delta(t-t')$.
Le terme de dérive $b(x,t)$ dans l'approche de Nelson est défini comme :

$$b(x,t) = \frac{\hbar}{m}\frac{\partial S(x,t)}{\partial x} + \frac{\hbar}{2m}\frac{\partial \ln\rho(x,t)}{\partial x},$$

où $S(x,t)$ et $\rho(x,t)$ sont respectivement la phase et le module carré de la fonction d'onde $\psi(x,t)$, exprimée sous forme polaire : $\psi(x,t) = \sqrt{\rho(x,t)}\exp(iS(x,t))$. Cette définition de la dérive garantit que la distribution des trajectoires quantiques suit la règle de Born.

Pour l'état fondamental de l'oscillateur harmonique, la fonction d'onde gaussienne implique une forme simple pour le terme de dérive. Si l'état initial $\psi_{\mathrm{i}}(x, t=0)$ est gaussien, il reste gaussien pour tout $t > 0$ et peut s'écrire :

$$\psi(x,t) = \frac{1}{\sqrt[4]{2\pi s(t)}} \exp\left(-\frac{x^2}{4s(t)} + i\alpha(t)x^2 + i\beta(t)\right),$$

où $s(t) = \langle x(t)^2 \rangle$ est la variance dépendant du temps, et $\alpha(t)$ et $\beta(t)$ sont les phases dynamiques et géométriques de la fonction d'onde. Pour que cette fonction soit solution de l'équation de Schrödinger, $\alpha(t)$ et $\beta(t)$ doivent obéir aux relations suivantes :

$$\alpha(t) = \frac{m}{4\hbar}\frac{\dot{s}(t)}{s(t)}, \quad \dot{\beta}(t) = -\frac{\hbar}{4ms(t)},$$

où le point désigne la dérivée par rapport au temps. La variance $s(t)$ doit obéir à l'équation d'Ermakov

$$\ddot{\sigma}(t) + \frac{\kappa(t)}{m}\sigma(t) = \frac{4D^2}{\sigma^3(t)}.$$

On obtient la vitesse que la vitesse moyenne du processus est

$$b(x,t) = \frac{\hbar}{m}\left(2\alpha(t) - \frac{1}{2s(t)}\right)x.$$

L'équation de Nelson devient alors

$$\mathrm{d}x(t) = \frac{\hbar}{m}\left(2\alpha(t) - \frac{1}{2s(t)}\right)x(t)\mathrm{d}t + \sqrt{2D}\,\mathrm{d}W(t).$$

Cette équation est mathématiquement analogue à l'équation de Langevin pour une particule brownienne suramortie dans un potentiel harmonique de raideur $\bar{\kappa}(t)$:

$$\mathrm{d}x(t) = -\frac{\bar{\kappa}(t)}{\gamma}x(t)\mathrm{d}t + \sqrt{2D}\,\mathrm{d}W(t),$$

où γ est le coefficient de friction de Stokes, qui n'apparaît que dans l'équation classique. Les deux équations sont identiques si l'on définit la raideur classique $\bar{\kappa}(t)$ par :

$$\bar{\kappa}(t) = \gamma\frac{\hbar}{m}\left(2\alpha(t) - \frac{1}{2s(t)}\right).$$

Cette relation entre la raideur quantique $\kappa(t)$ et la raideur classique $\bar{\kappa}(t)$ est donnée par :

$$\kappa(t) = \frac{\hbar^2}{2ms^2(t)} + \frac{m}{\gamma}\dot{\bar{\kappa}}(t) - \frac{m}{\gamma^2}\bar{\kappa}^2(t).$$

Enfin, à l'équilibre, la raideur quantique κ_{eq} est :

$$\kappa_{\mathrm{eq}} = \frac{D^2 m}{s_{\mathrm{eq}}^2},$$

ce qui ne dépend pas du paramètre classique γ.

D.2 Protocoles optimaux pour la raideur

Dans cette section, nous développons une méthode pour trouver des protocoles optimaux pour un oscillateur harmonique quantique, afin de passer d'un état initial ψ_{i} à un état final ψ_{f} en minimisant une fonction de coût et en respectant les conditions aux limites. La méthode consiste à minimiser une fonctionnelle $J[\bar{\kappa}] = \Delta t[\bar{\kappa}] + \lambda F[\bar{\kappa}]$, où Δt est la durée du protocol et F la fonctionnelle de coût. Le term λ est un mutliplicateur de Lagrange, utilisé pour déterminer le poids que l'on souhaite donner au coût (vis-à-vis de la durée) dans la procédure de minimisation. En utilisant le principe variationnel, on obtient un protocole optimal $\bar{\kappa}(t)$ qui minimise le coût en fonction de la durée du protocole.

D.2.1 Application à l'oscillateur harmonique quantique

Pour écrire la fonctionnelle à minimiser, on peut re-paramétrer le système en utilisant la variance $s(t)$, supposée monotone dans le temps, à la place de t. On peut montrer qu'elle satisfait à l'équation différentielle

$$\dot{s} = \frac{2}{\gamma}(D\gamma - s\bar{\kappa}).$$

En s'appuyant sur l'analogie entre les systèmes quantiques et classiques, le protocole optimal pour l'oscillateur harmonique quantique est obtenu à partir de la raideur classique $\bar{\kappa}(s)$, via l'équation :

$$\kappa(s) = \frac{\hbar^2}{2ms^2} + \frac{2m}{\gamma^2}[D\gamma - s\bar{\kappa}(s)]\bar{\kappa}'(s) - \frac{m}{\gamma^2}\bar{\kappa}^2(s).$$

La durée du protocole est exprimée comme une fonctionnelle de $\bar{\kappa}(s)$:

$$\Delta t[\bar{\kappa}] = \frac{1}{2}\int_{s_{\mathrm{i}}}^{s_{\mathrm{f}}} \frac{\gamma}{D\gamma - s\bar{\kappa}(s)}\mathrm{d}s.$$

La fonctionnelle de coût peut s'écrire sous forme intégrale comme

$$F[\bar{\kappa}] = \int_{s_{\mathrm{i}}}^{s_{\mathrm{f}}} f(s, \bar{\kappa}(s), \bar{\kappa}'(s))\mathrm{d}s,$$

La fonctionnelle totale à minimiser pour obtenir le protocole optimal est donc

$$J[\bar{\kappa}, \bar{\kappa}'] = \frac{1}{2}\int_{s_{\mathrm{i}}}^{s_{\mathrm{f}}} \left[\frac{\gamma}{D\gamma - s\bar{\kappa}(s)} + \lambda f(s, \bar{\kappa}(s), \bar{\kappa}'(s)) + \mu\left|\bar{\kappa}'(s)\right|^2\right]\mathrm{d}s.$$

Le terme $\mu\left|\bar{\kappa}'(s)\right|^2$ est ajouté pour garantir que les conditions aux limites sur $\kappa(t)$ sont satisfaites tout en s'assurant de la continuité du protocol.

D.2.2 Résolution de l'équation d'Euler-Lagrange

L'équation d'Euler-Lagrange associée au fonctionnel total est une équation différentielle du second ordre :

$$2\mu\bar{\kappa}'' = \frac{\gamma s}{[D\gamma - s\bar{\kappa}(s)]^2} + \lambda\frac{\partial f}{\partial\bar{\kappa}} - \lambda\frac{\mathrm{d}}{\mathrm{d}s}\frac{\partial f}{\partial\bar{\kappa}'}.$$

Cette équation permet de déterminer le protocole optimal $\bar{\kappa}(s)$, qui est ensuite transformé en protocole quantique $\kappa(t)$ grâce à l'analogie quantique-classique.

En résumé, cette approche fournit un cadre pour optimiser la transition entre deux états quantiques stationnaires en minimisant un coût donné, tout en respectant les conditions aux limites et en lissant les variations brusques du protocole. Les résultats numériques montrent que les protocoles optimaux proposés surpassent les méthodes existantes, offrant ainsi des raccourcis efficaces vers l'adiabaticité dans des systèmes quantiques fermés.

D.3 Résultats de l'optimisation

Nous avons exploré plusieurs protocoles dans le cadre de l'oscillateur harmonique quantique en utilisant différentes fonctions de coût. Les résultats obtenus montrent que les protocoles optimaux peuvent être dérivés pour diverses fonctions de coût, avec des performances améliorées par rapport à des protocoles standards, tels que les protocoles polynomiaux précédemment proposés.

D.3.1 Fonction de coût basée sur l'énergie cumulée

Dans cette première étude, la fonction de coût correspond à l'énergie cumulée, qui est physiquement pertinente, notamment dans les applications expérimentales. L'intégrale de l'énergie moyenne sur la durée totale du protocole est exprimée par :

$$E(t) = \langle \psi | \hat{H}(t) | \psi \rangle = \frac{m}{4s(t)} \left(\frac{1}{2}\dot{s}^2(t) + \frac{2s^2(t)\kappa(t)}{m} + 2D^2 \right).$$

Le fonctionnel à minimiser est ensuite donné par :

$$F_E[\bar{\kappa}, \bar{\kappa}'] = \frac{m}{4\gamma} \int_{s_\mathrm{i}}^{s_\mathrm{f}} \mathrm{d}s \, \left[\frac{D\gamma - s\bar{\kappa}(s)}{s} + \frac{3D^2\gamma^2 - s^2\bar{\kappa}^2(s)}{s(D\gamma - s\bar{\kappa}(s))} + 2s\bar{\kappa}'(s) \right].$$

Les solutions de l'équation d'Euler-Lagrange ont été calculées pour différents paramètres de Lagrange. Les protocoles obtenus montrent que les valeurs optimales de la raideur quantique $\kappa(t)$ peuvent être très différentes en fonction de la pondération des termes dans le fonctionnel à minimiser, ce qui permet d'adapter les protocoles pour des durées de transition variées.

D.3.2 Fonction de coût basée sur la phase dynamique

Le second exemple utilise la phase dynamique $\alpha(t)$ comme fonction de coût. La minimisation de cette phase est liée à la distance du protocole par rapport à un processus adiabatique, où $\alpha(t)$ est proportionnelle à la dérivée temporelle de la variance. Le fonctionnel à minimiser est ici :

$$F_\alpha[s, \bar{\kappa}] = \int_{t_\mathrm{i}}^{t_\mathrm{f}} \mathrm{d}t \; \alpha^2(t) = \frac{m^2}{8\gamma\hbar^2} \int_{s_\mathrm{i}}^{s_\mathrm{f}} \mathrm{d}s \; \frac{D\gamma - s\bar{\kappa}(s)}{s^2}.$$

Le protocole optimal obtenu minimise la phase dynamique, se rapprochant ainsi d'un processus adiabatique tout en réduisant la durée de la transition. La représentation des fonctions de Wigner dans l'espace des phases illustre également ce phénomène, montrant que la fonction de Wigner s'incline au cours du processus, mais retrouve une symétrie à la fin du protocole, contrairement à un processus adiabatique standard.

D.3.3 Comparaison avec les protocoles polynomiaux

Nous avons comparé nos résultats avec les protocoles polynomiaux connus dans la litterature, qui minimisent le travail effectué sur le système. Nos protocoles optimaux donnent des coût inférieur que ces derniers pour des durées de transition courtes, en minimisant de manière plus efficace l'énergie cumulée ou la phase dynamique. Ces résultats montrent que nos méthodes peuvent offrir des solutions plus efficaces pour des transitions rapides tout en maintenant un contrôle précis des conditions aux limites.

E SYSTÈMES QUANTIQUES OUVERTS

Ce chapitre vise à étendre les analogies classiques concernant la raideur et la température aux systèmes quantiques ouverts, dans le but d'optimiser des cycles et de potentiellement développer des moteurs thermiques quantiques. Il explore trois approches principales pour modéliser les systèmes quantiques ouverts, ouvrant ainsi la voie à l'extension de ces analogies.

E.1 Approche de Kostin

L'approche de Kostin propose une version stochastique de l'équation de Schrödinger pour décrire les systèmes quantiques ouverts en introduisant la friction et le bruit thermique, similaire au mouvement brownien classique. Cela modifie les équations de Heisenberg en ajoutant un terme de friction et une force aléatoire, aboutissant à l'équation de Schrödinger-Langevin (SLE).
L'équation de Schrödinger est modifiée pour inclure les effets de friction et de bruit aléatoire:

$$i\hbar\partial_t\psi = -\frac{\hbar^2}{2m}\partial_x^2\psi + V\psi - \frac{i\gamma\hbar}{2}\left[\ln\frac{\psi}{\psi^*} - \langle\ln\frac{\psi}{\psi^*}\rangle_\psi\right]\psi - xW_\mathrm{T}\psi$$

où γ est le coefficient de friction et W_T est une force aléatoire avec une diffusion thermique D_T.
Le bruit thermique est caractérisé par le coefficient de diffusion:

$$D_\mathrm{T} = \frac{\hbar\omega}{2}m\gamma\left[\coth\left(\frac{\hbar\omega}{2k_\mathrm{B}T}\right) - 1\right]$$

À haute température, cela se rapproche du cas classique $D_\mathrm{T} \approx m\gamma k_\mathrm{B}T$.
Pour un oscillateur harmonique, la SLE devient:

$$i\hbar\partial_t\psi = -\frac{\hbar^2}{2m}\partial_x^2\psi + \frac{1}{2}m\omega^2x^2\psi - \frac{i\gamma\hbar}{2}\left[\ln\frac{\psi}{\psi^*} - \langle\ln\frac{\psi}{\psi^*}\rangle_\psi\right]\psi - xW_\mathrm{T}\psi$$

L'ansatz de la fonction d'onde gaussienne donne des équations différentielles similaires aux équations de Langevin classiques pour la position $\mu(t)$ et le moment $p(t)$:

$$\partial_t p = -m\omega^2\mu - \gamma p + W_\mathrm{T}, \quad \partial_t\mu = \frac{p}{m}$$

La variance $\sigma(t)$ obéit à une équation d'Ermakov-Milne-Pinney amortie:

$$\partial_t^2\sigma + \gamma\partial_t\sigma + \omega^2\sigma = \frac{\hbar^2}{4m^2\sigma^3}$$

L'équation de Schrödinger-Langevin offre un cadre pour modéliser des systèmes quantiques à température finie, introduisant une dynamique stochastique avec des états thermiques, mais pose des défis pour établir une analogie complète avec la dynamique classique.

E.2 Approche de Schuch

Dans cette approche, Schuch propose de modifier les équations de Madelung, qui décrivent la densité ρ et la phase S de la fonction d'onde $\psi = \sqrt{\rho}e^{iS}$, afin d'introduire l'irréversibilité dans les équations de continuité et de Hamilton-Jacobi. Cette approche permet de dériver une équation de Schrödinger-Langevin modifiée.

E.2.1 Équations non modifiées

L'équation de continuité s'écrit :

$$\partial_t \rho + \frac{\hbar}{m} \partial_x \left(\rho \partial_x S \right) = 0, \tag{1}$$

qui peut aussi s'écrire sous forme d'équation de Fokker-Planck :

$$\partial_t \rho + \partial_x (b\rho) = D_Q \partial_x^2 \rho, \tag{2}$$

avec $D_Q = \frac{\hbar}{2m}$ et $b = \frac{\hbar}{m}\partial_x S + D_Q \partial_x \ln \rho$.
L'équation de Hamilton-Jacobi est :

$$\hbar \partial_t S + \frac{\hbar^2}{2m} (\partial_x S)^2 + \frac{1}{2} m \omega^2 x^2 - \frac{\hbar^2}{2m} \frac{\partial_x^2 \sqrt{\rho}}{\sqrt{\rho}} = 0. \tag{3}$$

E.2.2 Modifications proposées

Modification de l'équation de Hamilton-Jacobi Schuch propose d'ajouter une force de frottement dans l'équation d'Euler dérivée de l'équation de Hamilton-Jacobi :

$$[\partial_t + v\partial_x] v = -\frac{1}{m} \partial_x (V + V_Q) - \gamma v, \tag{4}$$

ce qui modifie l'équation de Hamilton-Jacobi comme suit :

$$\hbar \partial_t S + \frac{\hbar^2}{2m} (\partial_x S)^2 + V + V_Q + \gamma \hbar S = 0. \tag{5}$$

Modification de l'équation de continuité L'irréversibilité est introduite en ajoutant un terme de diffusion thermique dans l'équation de continuité :

$$\partial_t \rho + \partial_x \left(\rho \partial_x S \right) = D_T \partial_x^2 \rho, \tag{6}$$

avec D_T comme coefficient de diffusion thermique.
En combinant ces modifications, on obtient une version déterministe de l'équation de Schrödinger-Langevin :

$$i\hbar \partial_t \psi = -\frac{\hbar^2}{2m} \partial_x^2 \psi + V\psi - i\gamma\hbar \left[\ln \psi - \langle \ln \psi \rangle_\psi \right] \psi. \tag{7}$$

En supposant une solution gaussienne pour la fonction d'onde,

$$\psi(x,t) = \frac{1}{\sqrt{2\pi\sigma^2(t)}} \exp\left(-\frac{x^2}{4\sigma^2(t)} + i \left[\alpha(t) x^2 + \theta(t) \right] \right)$$

, les équations du mouvement pour σ, α, et θ deviennent :

$$\partial_t\sigma = \left[\frac{2\hbar\alpha}{m} + \frac{\gamma}{2}\right]\sigma, \tag{8}$$

$$\partial_t\alpha = \frac{\hbar}{8m\sigma^4} - \frac{2\hbar\alpha^2}{m} - \frac{m\omega^2}{2\hbar} - \gamma\alpha, \tag{9}$$

$$\partial_t\theta = -\frac{\hbar}{4m\sigma^2} + \gamma\alpha\sigma^2. \tag{10}$$

En combinant ces équations, on obtient une équation d'Ermakov modifiée :

$$\partial_t^2\sigma + \Omega^2\sigma = \frac{D_Q^2}{\sigma^3}, \tag{11}$$

avec $\Omega^2 = \omega^2 - \frac{\gamma^2}{4}$.
Le coefficient de diffusion thermique est relié à la température T de l'environnement par la relation :

$$D_T = D_Q\sqrt{\coth^2\left(\frac{\beta\hbar\omega}{2}\right) - 1}, \tag{12}$$

où $\beta = \frac{1}{k_BT}$ est l'inverse de l'énergie thermique.
Cette approche permet d'introduire l'irréversibilité dans la dynamique des systèmes quantiques ouverts, notamment en modifiant les équations de continuité et de Hamilton-Jacobi. L'équation de Schrödinger résultante contient un terme non linéaire et complexe, mais elle permet de maintenir la normalisation de la fonction d'onde et de calculer des analogies classiques.

E.3 Approche de Ruggiero

L'approche de Ruggiero combine la mécanique stochastique de Nelson avec l'équation de Langevin pour décrire les systèmes quantiques ouverts, en particulier pour le cas de l'oscillateur harmonique. L'objectif est d'introduire les effets thermiques dans le formalisme de Nelson en utilisant l'oscillateur harmonique comme système modèle.

E.3.1 Aspects théoriques

Guidage cohérent pour l'oscillateur harmonique Un état cohérent de l'oscillateur harmonique est un état quantique qui se comporte de manière similaire à un oscillateur harmonique classique. Pour chaque solution $q(t)$ et $p(t)$ des équations classiques du mouvement pour un oscillateur harmonique de fréquence ω :

$$\dot{q}(t) = \frac{p(t)}{m} \tag{13}$$

et

$$\dot{p}(t) = -m\omega^2 q(t), \tag{14}$$

il existe un état cohérent correspondant, noté par un nombre complexe α, dont la fonction d'onde est $\psi_\alpha(x,t)$. Ce nombre complexe α est défini par les conditions initiales comme suit :

$$\alpha = \frac{m\omega q_0 + ip_0}{\sqrt{2m\hbar\omega}}. \tag{15}$$

La fonction d'onde $\psi_\alpha(x,t)$ est donnée par :

$$\psi_\alpha(x,t) = \left(\frac{m\omega}{\pi\hbar}\right)^{1/4} \exp\left[-\frac{m\omega}{2\hbar}(x - q_\alpha(t))^2 + i\frac{p_\alpha(t)}{\hbar}(x - q_\alpha(t)) + i\theta(t)\right], \tag{16}$$

où $\theta(t)$ est une phase dépendant du temps.
Le processus stochastique associé à la position x guidé par l'état cohérent est donné par l'équation de Nelson :

$$\mathrm{d}x_\alpha(t) = \left[-\omega(x_\alpha(t) - q_\alpha(t)) + \frac{p_\alpha(t)}{m}\right]\mathrm{d}t + \mathrm{d}W_{\mathrm{Q}}(t), \tag{17}$$

où $W_{\mathrm{Q}}(t)$ est un processus Wiener associé aux fluctuations quantiques.

Mélange thermique d'états cohérents En physique statistique quantique, les états d'équilibre thermodynamique sont représentés par une matrice de densité. Il est possible de décomposer cette matrice de densité dans la base des états cohérents de l'oscillateur harmonique. Le poids de chaque état cohérent α dans le mélange est donné par la distribution de Glauber.
Pour décrire l'état d'équilibre dans le cadre stochastique de Nelson, on construit l'analogue stochastique de la matrice de densité en utilisant une représentation des processus comme une somme de deux composantes indépendantes : une motion classique et une motion quantique dans son état fondamental.

E.3.2 Systèmes ouverts

Nous considérons le cas d'un oscillateur harmonique en contact avec un réservoir thermique. Le mouvement thermique est décrit par une équation de Langevin, alors que la partie quantique est décrite par le processus de Nelson :

$$\mathrm{d}q(t) = \frac{p(t)}{m}\mathrm{d}t, \tag{18}$$

$$\mathrm{d}p(t) = -\big[m\omega^2 q(t) + \gamma p(t)\big]\mathrm{d}t + \mathrm{d}W_{\mathrm{T}}(t), \tag{19}$$

$$\mathrm{d}x_0(t) = -\omega x_0(t)\mathrm{d}t + \mathrm{d}W_{\mathrm{Q}}(t). \tag{20}$$

Le processus total exécuté par l'oscillateur harmonique est donné par :

$$x(t) = q(t) + x_0(t), \tag{21}$$

où $q(t)$ décrit la motion classique, et $x_0(t)$ la motion quantique.

E.3.3 Aspects thermodynamiques et analogies classiques

Cette approche permet d'utiliser des outils de thermodynamique stochastique pour analyser les systèmes quantiques ouverts. On peut ainsi calculer l'entropie, l'énergie moyenne et d'autres grandeurs thermodynamiques.

Entropie et énergie L'entropie associée à une trajectoire $x(t)$ est définie comme :

$$s(t) = -k_B \ln P(x(t),t), \tag{22}$$

et l'entropie moyenne du système est :

$$S(t) = -k_B \int \mathrm{d}x \; P(x,t) \ln P(x,t). \tag{23}$$

On peut également définir l'énergie moyenne en termes de x :

$$E(t) = \frac{1}{2} m\omega^2 \left\langle x^2(t) \right\rangle . \tag{24}$$

Limite suramortie du mouvement thermique Dans la limite suramortie de l'équation de Langevin, il est possible d'obtenir une description complète du mouvement de l'oscillateur harmonique. Le processus total peut être interpolé par un processus de Langevin suramorti.

L'approche de Ruggiero permet de combiner la dynamique de Nelson avec les équations de Langevin pour décrire les systèmes quantiques ouverts. Cependant, la séparation en deux processus indépendants rend difficile le développement d'analogies classiques. Cette approche ouvre néanmoins de nouvelles perspectives pour l'étude des systèmes quantiques ouverts et de leurs propriétés thermodynamiques.

CONCLUSION

Résumé de la thèse

Cette thèse explore les liens entre les systèmes classiques et quantiques, en s'appuyant sur la mécanique stochastique de Nelson pour étudier les particules quantiques à travers des trajectoires stochastiques. En mettant en parallèle des modèles classiques avec des systèmes quantiques, nous avons montré comment ces techniques peuvent simplifier la résolution de problèmes complexes.

Dans les premiers chapitres, nous avons introduit la théorie classique stochastique et la théorie de Nelson, en soulignant leurs différences, telles que la réversibilité des processus. Ensuite, nous avons étudié les systèmes quantiques fermés, à la fois d'un point de vue fondamental en discutant le concept d'équilibre quantique, mais également d'un point de vu pratique, en utilisant cette approche. Un des points forts de la thèse est l'établissement d'analogies classiques pour des systèmes quantiques, notamment l'oscillateur harmonique. Nous avons développé des protocoles optimaux permettant de contrôler ces systèmes tout en minimisant la durée et les coûts énergétiques.

Dans le chapitre final, nous avons exploré des modèles de systèmes quantiques ouverts qui introduit des concepts de thermodynamique stochastique dans le cadre de la théorie de Nelson. Bien que certains modèles permettent des analogies classiques plus facilement, d'autres, comme le modèle de Schuch, nécessitent des investigations supplémentaires.

Perspectives

Les résultats obtenus ouvrent la voie à plusieurs pistes de recherche. Une extension naturelle serait d'appliquer ces méthodes à des systèmes plus complexes, tels que les oscillateurs anharmoniques ou les systèmes à plusieurs corps, comme les condensats de Bose-Einstein. Nous avons également proposé l'idée d'optimiser des cycles thermodynamiques dans des moteurs quantiques, en utilisant à la fois le contrôle de la température et de la raideur du potentiel.

Conclusion

La thèse démontre que la mécanique stochastique de Nelson peut fournir des outils puissants pour le contrôle des systèmes quantiques. Bien qu'il reste encore de nombreux aspects à explorer, cette approche offre des perspectives intéressantes dans les domaines du contrôle quantique et de la thermodynamique quantique.

Demain, dès l'aube...

Demain, dès l'aube, à l'heure où blanchit la campagne,
Je partirai. Vois-tu, je sais que tu m'attends.
J'irai par la forêt, j'irai par la montagne.
Je ne puis demeurer loin de toi plus longtemps.

Je marcherai les yeux fixés sur mes pensées,
Sans rien voir au dehors, sans entendre aucun bruit,
Seul, inconnu, le dos courbé, les mains croisées,
Triste, et le jour pour moi sera comme la nuit.

Je ne regarderai ni l'or du soir qui tombe,
Ni les voiles au loin descendant vers Harfleur,
Et quand j'arriverai, je mettrai sur ta tombe
Un bouquet de houx vert et de bruyère en fleur.

V. Hugo, *Les Contemplations*, 1847

Hiems Viridans

Au milieu des pétales, des roses enneigées
Et des flocons voluptueux,
Des violettes, lilas, et parfums enchantés,
Qui trainent à plis somptueux,
Sous un pi-ano blanc, où comme sous l'hiver
Le son ambitieux est glacial,
Où des fleurs, tombant, dans leurs cercueils de verre,
Nous livrent le soupir final,

Une femme sans corps, épanche comme un fleuve
Sur le blanc d'ouest désaltéré,
Une senteur, dorée, dont la toile s'abreuve,
Essence auburn de la Beauté.

Semblable aux étoiles, lumières de la nuit,
Les yeux clos sous son regard fier,
Dont le rythme, souple, de la profonde harmonie
Se fond dans les souvenirs d'hier.

V. Hardel, 2015

Vincent HARDEL

Classical analog of quantum dynamics

Résumé

Cette thèse se concentre sur une formulation stochastique de la mécanique quantique connue sous le nom de mécanique de Nelson, que l'on a utilisée pour étudier la règle de Born. Cette théorie offre un cadre unique pour comprendre la dynamique quantique à travers des analogies classiques, en établissant notamment des parallèles entre l'évolution stochastique des particules browniennes et les systèmes quantiques. Nous avons appliqué cette approche pour optimiser les transitions des systèmes quantiques, tels que l'oscillateur harmonique quantique, en minimisant les coûts énergétiques et les temps de transition.

À partir de ces résultats, la thèse explore l'extension de ces méthodes à des systèmes quantiques plus complexes, y compris les systèmes ouverts soumis à la décohérence et les systèmes multi-corps tels que les condensats de Bose-Einstein. Ce travail instaure les bases du développement de nouvelles techniques d'optimisation et de stratégies de contrôle pour les systèmes quantiques, pouvant potentiellement conduire à des applications innovantes en thermodynamique quantique et en contrôle de systèmes.

Mots-clés : *fondements de la Mécanique Quantique, mécanique stochastique de Nelson, optimisation, systèmes quantiques ouverts, dynamique de Langevin, méthodes variationnelles.*

Abstract

This thesis focuses on a stochastic formulation of quantum mechanics known as Nelson's mechanics, which we used to study the Born rule. This theory provides a unique framework for understanding quantum dynamics through classical analogies, particularly by drawing parallels between the stochastic evolution of Brownian particles and quantum systems. We applied this approach to optimize the transitions of quantum systems, such as the quantum harmonic oscillator, by minimizing energy costs and transition times.

Building on these results, the thesis explores extending these methods to more complex quantum systems, including open systems subject to decoherence and multi-body systems like Bose-Einstein condensates. This work lays the foundation for developing new optimization techniques and control strategies for quantum systems, potentially leading to innovative applications in quantum thermodynamics and system control.

Key words: *foundations of quantum mechanics, Nelson stochastic quantization, Optimization, Open quantum systems, Langevin dynamics, Variational methods.*